T.C.
FIRAT UNIVERSITY
INSTITUTE OF SCIENCE

DEVELOPMENT OF A SELF-HEALING ASPHALT MIXTURE THROUGH THE USE OF ENCAPSULATED HEALING AGENTS

MSc Erkut YALÇIN

Ph.D. Thesis

Department of Civil Engineering

Program of Transportation

Supervisor : Assoc. Prof. Dr. Mehmet YILMAZ
Co-Supervisor : Assist. Prof. Alvaro Garcia HERNANDEZ

JULY-2018

T.C.

FIRAT UNIVERSITY

INSTITUTE OF SCIENCE

DEVELOPMENT OF A SELF-HEALING ASPHALT MIXTURE THROUGH THE USE OF ENCAPSULATED HEALING AGENTS

Ph.D. Thesis

MSc Erkut YALÇIN

141115201

Date of Submission : 18.06.2018

Date of Defense : 23.07.2018

Department: Civil Engineering

Program: Transportation

Supervisor : Assoc. Prof. Dr. Mehmet YILMAZ

Co-Supervisor : Assist. Prof. Alvaro Garcia HERNANDEZ

Jury Member : Prof. Dr. Necati KULOĞLU

Jury Member : Prof. Dr. Baha Vural KÖK

Jury Member : Assoc. Prof. Dr. Taner ALATAŞ

Jury Member : Assist. Prof. Tacettin GEÇKİL

Jury Member : Assist. Prof. Jose Norambuena CONTRERAS

JULY-2018

ACKNOWLEDGEMENTS

The study titled “Development of a Self-Healıng Asphalt Mixture Through the use of Encapsulated Healİng Agents” was prepared as a Ph.D. thesis in the Transportation Engineering Branch in Civil Engineering Department of Institute of Science in Fırat University during 2014-2018.

I owe a debt of gratitude for many people, without whom this thesis would not be possible. First of all, I would like to express my gratitude to dear Assoc. Prof. Dr. Mehmet YILMAZ, who has always stood with me with his expertise, effort and his approach as a brother, preparing the required environment for my studies and guiding me throughout all the obstacles on the way. His support provided me with the opportunity to conduct my studies at the University of Nottingham and I’ve always seen not only as my supervisor but also my elder brother. I would like to extend my appreciation to my dear co-supervisor, Asst. Prof. Alvaro Garcia HERNANDEZ, who provided me with all the support. I needed for conducting my laboratory experiments in the United Kingdom, solved all my problems and ensured that I collected the knowledge and the experience on the subject. Furthermore, my heartfelt appreciation goes to dear Asst. Prof. Jose NORAMBUENA-CONTRERAS, who extended his help during my studies, guiding me in every way.

I should also take this chance to thank all the academics in our department, Prof. Dr. Necati KULOĞLU, Prof Dr. Baha Vural KÖK and Assoc. Prof. Taner ALATAŞ, all of whom established the foundation of my knowledge with their lectures.

I would like to acknowledge and extend my sincere thanks to the technical staff at the Nottingham Transportation Engineering Centre (NTEC) for their assistance in setting up the laboratory testing machines, specimen preparation, experimental tests and their patience.

I owe a special thanks to Res. Assist. M. Ertuğrul ÇELOĞLU and Res. Assist. Mustafa AKPOLAT, both of whom I deem as my brothers, for never letting me down not only during my thesis but also in my daily life and every time I need them. I would also like to thank M. Gani GENÇER for his language support during writing this thesis in English.

I would like to extend my gratitude to The Scientific and Technological Research Council of Turkey (TÜBİTAK) for the support and the funding for my thesis and the research scholarship (with the application number 1059B141600780).

Finally, I would like to express my endless thanks to my family, who always provided their support and prayers.

Erkut YALÇIN

Elazığ-2018

CONTENTS

Page

ACKNOWLEDGEMENTS .... **II**
CONTENTS .... **III**
ABSTRACT .... **VII**
ÖZET .... **IX**
LIST OF FIGURES .... **XI**
LIST OF TABLES .... **XIX**
LIST OF SYMBOLS .... **XX**
LIST OF ACRONYMS .... **XXI**
1. INTRODUCTION **1**
1.1. Background 1
1.2. Problem Statement 3
1.3. Aim and Objectives 4
1.4. Research Methodology 5
1.5. Thesis Outline 7
2. LITERATURE REVIEW **8**
2.1. Definition of Self-Healing 8
2.2. Self-Healing Technologies for Asphalt Pavements 10
2.2.1 Self-healing by induction heating 12
2.2.2. Self-healing by microwave radiation heating 18
2.2.3. Self-healing by encapsulated rejuvenators 22
2.3. General encapsulation technique 26
3. MATERIALS AND DESIGN **52**
3.1. Introduction 52
3.2. Asphalt mixture 52
3.3.1. Dense asphalt mixture 52
3.3.2. Stone mastic asphalt mixture 53
3.3.3. Procedure for manufacturing the asphalt mixture 54
3.4. Capsule properties 57
3.4.1. Capsule materials 57
3.4.2. Capsules production 58

3.4.3. Characterization of the capsules 62
3.4.4. Effect of the temperature on the properties of capsules 62
3.4.5. Capsules integrity after mixing and compaction processes 63
4. AGING IN HOT MIX ASPHALTS 64
5. TEST METHODS USED IN THE THESIS STUDY 68
5.1 Binder Tests 68
5.1.1. Viscosity of bitumen 68
5.1.2. Rotational Viscometer (RV) Experiment 69
5.1.3. Fourier Transform Infrared Spectroscopy (FTIR) 69
5.2 Tests Conducted on Capsules 71
5.2.1. Thermogravimetric analysis (TGA) 71
5.2.2. Thermomechanical Analyzer (TMA) 72
5.2.3. Density measurement of capsules 73
5.2.4. Compressive Strength 73
5.3. Mixture Tests 74
5.3.1. Indirect Tensile Stiffness Modulus (ITSM) 74
5.3.2. Indirect Tensile Fatigue Test (ITFT) 77
5.3.3. Water sensitivity analysis 82
5.3.4. Preparing Plate-Shaped Samples with Roll Press 84
5.3.5 Wheel tracking test 85
5.3.6. Crack healing 88
5.3.7. Three point bending fatigue test 90
5.3.8. Skid resistance test 92
5.3.9. X-ray computed tomography 93
6. EFFECT OF MIXING AND AGING ON THE MECHANICAL AND SELF-HEALING PROPERTIES OF ASPHALT MIXTURES CONTAINING POLYMERIC CAPSULES 95
6.1. Introductıon 95
6.2. Manufacturing of asphalt mixture samples 96
6.3. Experimental programme description 99
6.4. Effect of temperature on the properties of polymeric capsules 100
6.5. Variation of the physical properties of asphalt mixtures with and without capsules 104

6.6. Influence of mixing and aging time on the mechanical properties of asphalt mixtures 106
6.7. Effect of mixing and aging on the healing properties of asphalt mixtures 113
7. MECHANICAL PROPERTIES AND SELF-HEALING ABILITY OF STONE MASTIC ASPHALT CONTAINING POLYMERIC CAPSULES 116
7.1. Introductıon 116
7.1. Manufacturing of SMA specimen 118
7.2. Tensile strength and water damage of SMA mixtures 119
7.3. Stiffness modulus and resistance to fatigue of SMA mixtures 121
7.4. Crack-healing properties of SMA mixtures with, and without, addition of capsules 127
8. EFFECT OF THE ACTIVATION FORCE ON THE HEALING LEVEL OF ASPHALT MIXTURE WITH EMBEDDED CAPSULES 130
8.1. Introductıon 130
8.2. Manufacturing of asphalt mixture specimens 131
8.3. Influence of loads on the healing properties 131
8.4. Amount of rejuvenator in the bitumen and broken capsules 136
9. SELF-HEALING CAPABILITY OF ASPHALT MIXTURES USING ENCAPSULATED REJUVENATORS: AN EXPERIMENTAL BY FATIGUE AND WHEEL TRACKING TESTS 139
9.1. Introductıon 139
9.2. Manufacturing of asphalt mixture specimens 140
9.3. Influence of capsule contents on the crack-healing properties of asphalt mixtures 141
9.4. Evaluation of rejuvenator diffusion capacity over time and temperature 142
9.5. Effect of capsules on the self-healing properties of asphalt mixtures 144
9.6. Results of Rutting Test 147
10. CONCLUSIONS AND RECOMMENDATIONS 152
10.1. Conclusion 152
10.1.1. Capsule properties 152
10.1.2. Capsules effect on dense asphalt and SMA performance 153
10.1.3. Effect of the capsule on static loads 155
10.1.4. The effect of the capsule on fatigue and wheel tracing experiments 156
10.2. Recommendations for future research 157

REFERENCES 159
BACKGROUND 170

ABSTRACT

The service lives of asphalt pavements can be extended by using encapsulated rejuvenators in asphalt mixtures, improving the natural self-healing ability of asphalt mixtures. When crack damage occurs, the capsules are broken, releasing the rejuvenator substance into the cracks. In this thesis, a novel type of capsule was manufactured. These capsules included sunflower oil as rejuvenators. The size, morphology, mechanical strength and thermal stability of these capsules were investigated. In addition, the effect of the capsules on the chemical composition of bitumen with time of exposure to broken capsules was evaluated by the FTIR test. In order to determine the properties of the capsules and their effect on the chemical components of the asphalt mixture, the capsules were included in the asphalt mixtures, providing an opportunity to observe the mechanical performance of the asphalt mixtures and their self-healing abilities. Physical, thermal and mechanical properties of the capsules were evaluated. The capsules can resist the mixing and compaction conditions and break inside the mixture releasing the encapsulated oil in small volumes. In addition, it was observed that the addition of capsules did not improve the stiffness modulus of asphalt mixtures compared to mixtures without capsules, and that the mixing order and the aging time did not have a significant influence on the flexural strength of the mixtures. Moreover, the healing levels obtained by the mixtures varied depending on the order of addition of capsules, and mixtures with capsules showed higher healing levels than mixtures without capsules. The levels of healing for the mixtures without aging were greater than those of mixtures after the aging process.

The mechanical and self-healing performance of Stone Mastic Asphalt (SMA) mixtures with encapsulated rejuvenators were evaluated. With this purpose, calcium-alginate capsules with encapsulated sunflower oil have been manufactured and added into the SMA mixtures. Physical and mechanical properties of SMA specimens with, and without, calcium-alginate capsules have been evaluated by measuring the stiffness modulus, indirect tensile strength and fatigue tests, and water sensitivity and skid resistance. In addition, self-healing properties of SMA beams with, and without, capsules have been assessed at different healing times, from 5 to 216h. The main results showed that the capsules can resist the mixing and compaction processes without significantly reducing their properties. Additionally, mechanical properties of SMA mixtures with, and without, capsules presented similar results. Moreover, capsules showed a good spatial distribution inside the SMA samples. It was found that capsules with encapsulated oil increase the crack-healing properties of SMA when compared to mixtures without capsules. The capsules with asphalt self-healing purposes can be safely used in the road construction, without affecting its quality.

The self-healing capability of asphalt mixtures containing a new type of capsules with encapsulated sunflower oil as rejuvenating agent. With this purpose, the diffusion capacity of the rejuvenating agent inside of virgin bitumen samples and the healing level of the cracked asphalt mixtures containing of capsules have been evaluated. The main results showed that the rejuvenator concentration inside the bitumen increased with the time and the temperature until the moment where the concentration reached a maximum value that is independent of temperature. In addition, fatigue healing results of asphalt mixture beams with capsules proved that: i) the number of cycles necessary to reach a given percentage of broken capsules reduced when the applied load increased, ii) the results of healing index presented an optimum number of cycles to apply the resting period, at which the obtained life extension was maximum, and iii) the optimum number of cycles to apply the healing treatment decreased when the load increased. CT-Scan results proved that the microstructure of the capsules corresponded to that of a microbead, where the rejuvenating agent can be encapsulated inside of calcium-alginate micropores.

The aim of this study was to develop and characterize a self-healing asphalt pavement that can heal itself and rejuvenate at environmental temperatures. This thesis conducted on self-healing provided answers to a lot of questions regarding the subject. However, unsolved problems, such as capsules homogeneous dispersion or capsules service lives, still remain. Further studies could be conducted on these points.

Keywords: Encapsulated rejuvenator, Aged asphalt, Mechanical performance, Thermal performance, Self-healing.

ÖZET

İyileştirici Maddeler İçeren Kapsüller Kullanılarak Kendini Onarabilen Bitümlü Sıcak Karışımların Geliştirilmesi

Asfalt karışımların servis ömrü kapsüllenmiş iyileştiricilerin asfalt karışımlarına eklenmesiyle uzatılabilir ki bu durum asfalt karışımlarının doğal kendini iyileştirme yeteneklerini geliştirmektedir. Çatlak hasarı meydana geldiğinde, kapsüller kırılır ve içlerindeki gençleştiriciler çatlak içine akar. Bu çalışmada yeni bir tip kapsül üretilmiştir. Bu kapsüller iyileştirici olarak ayçiçeği yağı içermektedir. Kapsüllerin, boyut, morfoloji, mekanik mukavemet ve termal stabiliteleri araştırılmıştır. İlaveten, kapsüllerin bitümün kimyasal bileşenleri üzerindeki etkisi kırılan kapsüllere maruz kalma zamanları ile birlikte FTIR testi kullanılarak değerlendirilmiştir. Kapsüllerin, özelliklerini ve asfalt karışımların kimyasal bileşenleri üzerindeki etkilerini belirlemek için, kapsüller asfalt karışımlarına eklenmiştir ve bu durum asfalt karışımlarının mekanik performanslarını ve kendini iyileştirme yeteneklerini gözlemleme olanağı sağlamıştır. Kapsüllerin fiziksel, termal ve mekanik özellikleri değerlendirilmiştir. Kapsüller karıştırma ve sıkıştırma şartlarına dayanabilmektedir ve karışımlar içinde kırılarak kapsüllenmiş yağları küçük hacimlerle serbest bırakmaktadır. Ayrıca, kapsül içermeyen karışımlar ile karşılaştırıldığında, kapsüllerin asfalt karışımlarına eklenmesinin sertlik modülünü arttırmadığı ve karıştırma sırası ve yaşlanma süresinin karışımların esneme mukavemetleri üzerinde önemli bir etkiye sahip olmadığı gözlemlenmiştir. Ek olarak, karışımlardan elde edilen iyileşme seviyeleri, kapsüllerin eklenme sıralarına göre değişmiştir ve kapsül içeren karışımların, kapsül içermeyen karışımlara göre daha yüksek iyileştirme seviyelerine sahip olduğu gözlemlenmiştir. Yaşlanmaya tabi tutulmamış karışımların iyileşme seviyeleri, yaşlanmaya tabi tutulmuş karışımlarla karşılaştırıldığında, daha yüksek bulunmuştur.

Kapsül içeren Taş Mastik Asfalt (TMA) karışımlarının mekanik ve kendini iyileştirme performansları incelenmiştir. Bu amaç için, kalsiyum-alginat ve gençleştirici olarak ayçiçeği yağı içeren kapsüller üretilmiş ve TMA karışımlara ilave edilmiştir. TMA karışımlarının hem kapsüllü hem de kapsülsüz numunelerinin fiziksel ve mekanik özellikleri, sertlik modülü, indirekt çekme mukavemeti, yorulma testi, su hassasiyeti ve kayma testleri kullanılarak ölçülmüştür. İlaveten, kapsüllü ve kapsülsüz TMA kirişlerinin özellikleri, farklı

iyileştirme zamanlarında, 5 ila 216 saat arasında, kendini iyileştirme özellikleri açısından incelenmiştir. Başlıca sonuçlar kapsüllerin, özelliklerini önemli bir derecede kaybetmeden, karıştırma ve sıkıştırma süreçlerine dayanabildiğini göstermiştir. Ayrıca, kapsüllü ve kapsülsüz TMA karışımlarının mekanik özellikleri benzer sonuçlar göstermiştir. Kapsüller, TMA karışımların içerisinde de iyi bir boşluksal dağılım göstermiştir. Yağ içeren kapsüllerin, kapsülsüz karışımlarla karşılaştırıldığında, TMA karışımlarının çatlak iyileştirme özelliklerini arttırdığı tespit edilmiştir. Kendini iyileştirme amaçlı kapsüller yol yapımında, yolun kalitesini etkilemeden, güvenle kullanılabilir.

İçinde gençleştirici olarak kapsüllenmiş ayçiçeği yağı içeren yeni tip kapsüllerin ilave edildiği asfalt karışımlarının kendini iyileştirme yetenekleri incelenmiştir. Bu amaç için saf bitüm numuneleri içindeki gençleştirici maddenin yayılma kapasitesi ve çatlak içeren kapsüllü asfalt karışımlarının iyileşme seviyeleri değerlendirilmiştir. Başlıca sonuçlar bitüm içindeki gençleştirici konsantrasyonunun zamanla ve sıcaklıkla, konsantrasyonun sıcaklıktan bağımsız bir şekilde maksimum değerine ulaşıncaya kadar arttığını göstermiştir. Ayrıca, kapsüllü asfalt karışımı kirişlerinin yorulma iyileşmesi sonuçları i) uygulanan yük arttığında belirli bir yüzdede kırılmış kapsüllere ulaşmak için gerekli olan döngü sayısın azaldığını, ii) iyileştirme endeksinin dinlenme sürecinde, elde edilen ömür uzamasının maksimum olduğunda, uygulanacak olan optimum döngü sayısını ortaya koyduğunu ve iii) yük arttığında, iyileştirme için gereken optimum döngü sayısının azaldığını göstermiştir. Bilgisayarlı tomografi taraması sonuçlarının, gençleştirici maddelerin kalsiyum-alginat mikro gözenekleri içinde kapsüllenebilen, bir mikro kapsüle karşılık geldiğini göstermiştir.

Bu çalışmada çevre sıcaklıklarında iyileşebilen ve gençleştirilebilen kendi kendini iyileştiren bir asfalt kaplama geliştirmek ve karakterize etmektir. Kendi kendini iyileştirme konusunda bu tez çalışması birçok bu konudaki soru işaretini gidermiştir. Fakat hala asfalt karışımlardaki kapsüllerin homojen dağılımı veya kapsüllerin yaşam ömrü gibi çözülmemiş soru işaretleri bulunmaktadır. Gelecekteki çalışmalar bu eksikliklerin giderilmesi üzerine yürütülebilir.

Anahtar Kelimeler: Kapsüllenmiş İyileştirici, Yaşlandırılmış Asfalt, Mekanik Performans, Termal Performans, Kendini İyileştirme

LIST OF FIGURES

Page

Figure 1.1. Examples of deteriorations in asphalt pavements: (a) fatigue cracks, and (b) low-temperature cracks. 2
Figure 1.2. The performance-time curve in different types of material 5
Figure 2.1. The concept of self-healing with microcapsules 9
Figure 2.2. Natural self-healing in asphalt pavements 11
Figure 2.3. The mechanism of induction heating 13
Figure 2.4. Induction heating device, (a) laboratory induction heating device used by and (b) induction heating generator installed in a test truck 14
Figure 2.5. Induction heating process in asphalt mixtures 14
Figure 2.6. (a) Sample without clusters of fibers (4% of fibers and 3.5 min mixing). (b) Sample with clusters of fibers (4% of fibers and 3.5 min mixing) 16
Figure 2.7. Examples of CT-Scan 3D model of fiber clusters existence inside dense asphalt mixture samples with: (a) 4% fibers, and (b) 8% fibers 19
Figure 2.8. Schematic diagram of the measurement of the crack size before and after microwave heating 19
Figure 2.9. Measuring the surface temperature of the specimen 20
Figure 2.10. The conceptual framework of retrofitting conventional, distressed asphalt pavements into a novel sustainable asphalt pavement with crack-healing properties 22
Figure 2.11. Encapsulated rejuvenator healing mechanism 23
Figure 2.12. Section of the capsules embedded in asphalt concrete 24
Figure 2.13. The external shape of an epoxy-cement capsule and its internal configuration 25
Figure 2.14. Interface morphology of bitumen/microcapsule sample 25
Figure 2.15. Optical micrograph of the core materials of the capsules: (a) porous stone used; (b) porous stone with the rejuvenators embedded 26
Figure 2.16. Broken capsule after an ITT test 27
Figure 2.17. Fluorescent microscope observation of the crack healing at various periods (0, 1, 3 and 18 hours) 28

Figure 2.18. Capillary flow experiment **29**
Figure 2.19. Morphologies of MF-shell microcapsules, (a) optical microscope morphology of microcapsules fabricated with core/shell ratio of 1/1 under core material stirring rate of4000rmin_1, (b)SEMmorphologyofwithcore/shellratioof1/1undercorematerialstirringrateof4000rmin _1, (c)thecross-sectionSEMmorphologyofasingle microcapsule embedded in epoxy, and (d) the measurement method of shell thickness by SEM **30**
Figure 2.20. Morphologies of microcapsules containing rejuvenator, (a) optical morphology of microcapsules in emulsion, (b) SEM morphology of dried microcapsules, (c) smooth surface of single microcapsule, (d) SEM morphology of dried microcapsules with larger size, (e, f) optical morphology of microcapsules embedded in epoxy resin, and (g) cross-section SEM morphology of microcapsules **31**
Figure 2.21. (a) Test sample before testing. (b) Test sample after testing, with capsules broken **32**
Figure 2.22. The required resting periods for mixtures with healing agent **33**
Figure 2.23. The examination of micro WCO samples' morphology under temperatures between -10 ºC and 50 ºC and repeated changes with a fluorescent microscope **34**
Figure 2.24. The capillarity behaviors of rejuvenator in self-healing bitumen by microcapsules, (a–c) a micro crack was generated by liquid N2 with the width about 10–15 lm, the micro crack propagates and pierce the shells of microcapsules, (d and e) the liquid of rejuvenator leaked out from microcapsules and flowed into the microcapsules, and (f) movement trace and direction of rejuvenator during the capillarity **35**
Figure 2.25. (a) Porous sand. (b) Oil contained in the porous sand. (c) Detail of the shell. (d) Capsule **36**
Figure 2.26. CT images of asphalt specimens with capsules type (a) II and (b) III [69]. **37**
Figure 2.27. Images of microcapsule (diameter 16.5 _m) during compression and after rupture by nanomanipulation in chamber of environmental scanning electron microscope under high vacuum (5 kV, spot size 4): (a) microcapsule being compressed and (b) microcapsule being ruptured **38**
Figure 2.28. Effects of temperature on the prepared microcapsules at (a) 50°C; (b) 60°C **39**
Figure 2.29. Illustration of the self-healing process of aged bitumen by microcapsules containing rejuvenator: (a) the structure of asphalt consisting of bitumen and aggregates;

(b) microcrack generation and microcapsules broken; and (c) the self-healing of aged bitumen by leaked rejuvenator with the help of diffusion **40**
Figure 2.30. XCT visualization process of microcapsules' embedded cement paste cylinder including (a) volume construction; (b) surface generation; and (c) transparent adjusting. The scale bar is 2 mm for all three images **41**
Figure 2.31. ESEM morphologies of microcapsules with 10% nano-CaCO3 composite shells **42**
Figure 2.32. Fluorescence microscope morphologies of rejuvenator movement in aged bitumen, (a) microcrack in microcapsule/bitumen composite, (b) the shells of microcapsules broken by microcracking, and (c and d) the movement traces and direction of rejuvenator induced by capillarity **43**
Figure 2.33. SEM and OM images of (a) surface morphology of a microcapsule, (b) a ruptured microcapsule and the wall thickness, (c) a single microcapsule, and (d) broken microcapsules compressed by two parallel glass sheets **44**
Figure 2.34. Image of a capsule exposed to the air after particle loss testing **45**
Figure 2.35. Morphologies of microcapsules in a microcrack in asphalt, (a) ESEM morphology of a microcrack, (b) fluorescence microscope morphology of microcapsules in a microcrack, and (c) fluorescence microscope morphology of microcapsules in a microcrack after 60 min **46**
Figure 2.36. Morphology of microcapsules... **48**
Figure 2.37. Synthetic principle of self-healing microcapsules **49**
Figure 2.38. (a) Spherical capsule produced in this study. (b) SEM image of the internal structure of capsule **50**
Figure 2.39. (a) Spherical polymeric (calcium-alginate) capsule type C1 produced in this study. (b) SEM image of the calcium-alginate structure in core of capsules type C4.... **50**
Figure 3.1. a)Inclined b) normal horizontal mixer. **54**
Figure 3.2. a)Inclined b) normal horizontal schematic of mixers....................................... **55**
Figure 3.3. Slab roller compactor. **56**
Figure 3.4. Asphalt mixture slab and the produced beam for the healing test. **56**
Figure 3.5. Cooper Gyratory Compactor. **57**
Figure 3.6. Schematic diagram of the manufacturing process of capsules by ionotropic gelation of alginate. **59**

Figure 3.7. (a) Individual polymer capsule, and (b) SEM image of calcium-alginate internal structure of capsules. **59**
Figure 3.8. Flowchart of the capsule fabrication process: (a) polymeric (calcium-alginate) capsules. **61**
Figure 3.9. Samples of capsule produced in this research, a) dry capsules, b) wet capsules. **61**
Figure 3.10. (a) Embedded capsule inside the asphalt mixture and example of an extracted individual capsule, (b) 2D cross-section image of a sample with capsules, and (c) 3D cutting reconstruction of the capsule spatial distribution inside the asphalt sample. **63**
Figure 4.1. The relationship between the aging index and time [94]. **65**
Figure 4.2. Long-term aging of the HMA samples. **67**
Figure 5.1. The DSR machine. **68**
Figure 5.2. FTIR machine. **70**
Figure 5.3. FTIR curves for asphalt mixture samples with and without oil. **71**
Figure 5.4. TGA machine. **72**
Figure 5.5. TMA machine. **72**
Figure 5.6. Density measurement of capsules using a Gas Pycnometer AccuPyc II 1330 equipment. **73**
Figure 5.7. (a) Compressive strength test of capsules, and (b) example of a broken capsule after test at 20˚C. **74**
Figure 5.8. ITSM Test configuration in the NAT. **75**
Figure 5.9. a) ITSM test equipment and its side view's cross-section, b) the deformation induced by the ITSM test **75**
Figure 5.10. Typical result sheet of ITSM test. **76**
Figure 5.11. Stress distribution along diameter of the specimen in Indirect Tensile Test model **80**
Figure 5.12. ITFT test set up in NAT machine. **82**
Figure 5.13. ITS test equipment. **83**
Figure 5.14. Roll press and sample preparation. **85**
Figure 5.15. a) Immersion wheel tracker for wet condition b) wheel tracking test (WTT) device in an insulated temperature control cabinet for dry condition. **88**

Figure 5.16. Schematic diagram of the asphalt mixture crack-healing test: Step 1. crack generation in the asphalt beam, Step 2. capsules activation to begin the oil release, and Step 3. healing process. **89**

Figure 5.17. Scheme of how the number of cycles with 50% probability of breaking can be obtained based on Weibull probability distribution (left) and how service life extension can be evaluated (right). **91**

Figure 5.18. a) 3PB fatigue testing configuration.b) broken specimen after 3PB fatigue test. **92**

Figure 5.19. Skid test configuration. **93**

Figure 5.20. CT scans analysis and an example of an image of results. **94**

Figure 6.1. Images of (a-b) pre-heating and mixing process for the asphalt mixture types 1 and 4, (c) embedded capsules in mixture, and (d) individual capsule extracted after mixing process. **98**

Figure 6.2. (a) Asphalt beam used in the crack-healing tests, and (b) asphalt core cylinder used in the CT scan tests. **99**

Figure 6.3. Diagram of the experimental program followed in this section. **100**

Figure 6.4. (a) TGA test result of a capsule and its components, and (b) thermal expansion curve of a capsule. **101**

Figure 6.5. (a) Mechanical strength, and (b) statistical values of maximum compressive load. **103**

Figure 6.6. (a) Individual polymer capsule, and (b) SEM image of calcium-alginate internal structure of capsules. **104**

Figure 6.7. Results of the (a) bulk density and (b) air void content of the asphalt mixtures with and without capsules (WO/C). **105**

Figure 6.8. ITSM test samples. **106**

Figure 6.9. (a) Results of stiffness modulus for asphalt mixture samples with and without capsules (WO/C), and (b) stiffness modulus results of all test specimens versus air voids content. **108**

Figure 6.10. Relationship between stiffness modulus of the test specimens measured in longitudinal (Y) and cross (X) directions. **109**

Figure 6.11. CT-Scans reconstructions of the asphalt mixture M4 with capsules highlighted in green color: (a) 2D cross-section image of sample with capsules, (b) 3D reconstruction of the embedded capsules in asphalt, and (c) 3D reconstruction of the capsule spatial distribution inside of the asphalt sample. **110**

Figure 6.12. Variation of the maximum flexural forces versus aging times for all the asphalt test samples measured under (a) stage 2@140ºC, and (b) stage 2@160ºC. **111**

Figure 6.13. (a) Relation between the maximum flexural forces resisted by samples without capsules versus viscosity variation of bitumen with the aging time. (b) Normal probability-probability plot of the ratio between the flexural force of the test samples with (W/C) and without (WO/C) capsules at different aging times. **112**

Figure 6.14. 3PB post-test appearance of aged samples. **113**

Figure 6.15. Results of the (a) healing levels for the different asphalt mixture types, and (b) percentage of broken capsules inside the different asphalt mixtures evaluated at healing time of 120h. **115**

Figure 7.1. Experimental programme used in this study. **118**

Figure 7.2. Average values and standard deviation bars of the: (a) Indirect Tensile Strength (ITS) of the SMA specimens with (W/C), and without (WO/C), capsules after dry and wet conditioning evaluated at two different test temperatures, and (b) Indirect Tensile Strength Ratio (ITSR). **121**

Figure 7.3. Appearance of SMA ITSM test specimens. **122**

Figure 7.4. Average values and standard deviation bars of the: (a) stiffness modulus of SMA specimens with (W/C), and without (WO/C), capsules versus test temperature, and (b) relationship between stiffness modulus of the SMA specimens measured in longitudinal (Y) and cross (X) directions. **123**

Figure 7.5. Maximum horizontal tensile strain average results versus the number of cycles to failure reached by the SMA specimens with, and without, capsules measured by indirect tensile fatigue tests. **124**

Figure 7.6. Appearance of samples after fatigue test. **124**

Figure 7.7. CT-Scans reconstructions of the SMA mixture with 0.5% of capsules: (a) SMA mixture core extracted from a cylindrical Marshall specimen, (b) 2D cross-section images of the sample with embedded capsules inside, (c-d) 3D reconstruction of the capsule spatial distribution inside the SMA sample, capsules have been highlighted in yellow color. **126**

Figure 7.8. Crack healing test samples. **127**

Figure 7.9. Results of the: (a) healing levels for the SMA specimens with (W/C), and without (WO/C), capsules versus healing period, and (b) percentage of broken capsules inside the different SMA mixtures before, and after, healing process. **128**

Figure 8.1. Compressive load-displacement different healing loads for a sample with capsules. **133**

Figure 8.2. Healing level results of asphalt mixture a) without and b) with capsules different healing loads. **133**

Figure 8.3. Self-healing results for asphalt mixture samples with capsules: a) healing level with healing time and b) box plots of the maximum healing range. **134**

Figure 8.4. Comparison of healing rates of asphalt mixtures with and without capsules under different loads. **135**

Figure 8.5. Force Effect Ratio results for all asphalt mixture beams (a) without and (b) with capsules tested at different healing loads. **136**

Figure 8.6. Percentage of broken capsules for asphalt mixture samples with different loads after compression at 20ºC. **137**

Figure 8.7. Broken capsules for maximum healing ratio. **138**

Fıgure 9.1. (a) CT Scan 3D image of the capsule spatial distribution inside a cylindrical sample of mixture with 0.5% capsule content, (b) healing level depending on healing time. **142**

Figure 9.2. (a) Relationship between the dimensionless absorbance index of rejuvenator and the time inside bitumen at two different temperatures, and (b) representative scheme of the diffusion of the rejuvenator (into capsule and test) as a function of time and temperature. **143**

Figure 9.3. (a) Percentage of broken capsules over loading cycles, and (b) healing index obtained when applying a resting time at different number of cycles. The shown values represent the percentage of broken capsules at the number of cycles when the healing is optimum. **145**

Figure 9.4. Results of healing indexes for the different loads. **145**

Figure 9.5. CT-Scans reconstructions of the (a) asphalt mixture with capsules highlighted in green colour (modified from Norambuena-Contreras et al., 2018), and (b) 3D reconstruction of an individual polymeric (calcium-alginate) capsule. **146**

Figure 9.6. 3PB fatigue test samples. **147**

Figure 9.7. The relationship between deformation-number of load repetition obtained from the rutting test conducted at 60 ˚C in a dry environment. **148**
Figure 9.8. Results of the rutting test conducted in a dry environment. **148**
Figure 9.9. The relationship between deformation-number of load repetition obtained from the rutting test conducted at 60 ˚C temperature inside water. **149**
Figure 9.10. Percentage of broken capsules for mixture samples with capsules after wheel tracking tests at different healing temperatures. **151**
Figure 9.11. Samples after wheel tracking test. **151**

LIST OF TABLES

Page

Table 3.1. Design properties of asphalt mixture AC 20 base 40/60. .... **53**

Table 3.2. Design properties of Stone Mastic Asphalt SMA 14 surf 40/60. .... **53**

Table 3.3. Average physical and mechanical properties of the capsules at different temperatures. **62**

Table 4.1. Factors that cause aging in bituminous binders **64**

Table 5.1. Comparison of the load and deformation-controlled fatigue tests..................... **79**

Table 6.1. Average viscosity and aging indices for the bitumen and sunflower oil at different aging times. **114**

Table 6.2. Average viscosity values and viscosity reduction indices of the oil-release asphalt samples with and without aging... **115**

Table 7.1. Physical properties of the SMA mixtures with, and without, capsules: Average (Std. deviation) values. **126**

Table 7.2. Physical properties of the SMA mixtures with, and without, capsules: Average (Std. deviation) values. **129**

Table 9.1. Number of cycles with 0.5 probability of breaking the material depending on the applied load by using fatigue tests. **146**

LIST OF SYMBOLS

AI	: Aging index
η_{unaged}	: Without aging process
η_{t-aged}	: Different aging times
BC	: Broken capsules
Sm	: Indirect tensile stiffness modulus
F	: Maximum vertical load
H	: Horizontal deformation
L	: Sample height
R	: Poisson ratio
N_f	: Number of load repetition
k_1, k_2	: Characteristics of the material
σ	: Applied tensile
σ_{vx}	: Vertical compressive stress
σ_{hx}	: Horizontal tensile stress
P	: Vertical load
d	: Diameter
t, L	: Thickness
$\varepsilon_{x,max}$	: Maximum tensile strain
υ	: Poisson ratio
G_{mm}	: Maximum theoretical specific weight
V_a	: Void of the sample
HL	: Healing level
$F_{initial}$	: Initially force
F_{healed}	: After the healing process force

LIST OF ACRONYMS

EU : European Union
USA : United States of America
SEM : Scanning Electron Microscopy
FTIR : Fourier Transform Infrared Spectroscopy
CT : Computer Tomography
SMA : Stone Mastic Asphalt
SWF : Steel Wool Fibers
RAP : Reclaimed Asphalt Pavement
WCO : Waste Cooking Oil
ESEM : Environmental Scanning Electron Microscopy
XCT : X-Ray Computerized Tomography
PF : Phenol-Formaldehyde
HMA : Hot Mix Asphalt
DMP : Dimethylphenol
MMF : Methanol Melamine Formaldehyde
EMA : Ethyl Methyl Acrylate
PG : Performance Grade
MF : Melamine-Formaldehyde
EDS : Energy Dispersive Spectroscopy
BOEF : Beam on Elastic Foundation
DCPD : Dicyclopentadiene
TGA : Thermo-Gravimetric Analysis
OM : Optical Microscope
MUF : Melamine Urea Formaldehyde
SDS : Sodium Dodecyl Sulfate
FM : Fluorescent Microscope
UK : United Kingdom
CO : Cooking Oil

G : Guluronic

M : Manuronic

PAV : Pressured Aging Vessel

RTFO : Rolling Thin Film Oven Test

DSR : Dynamic Shear Rheometer

RV : Rotational Viscometer

TMA : Thermomechanical Analyzer

ITSM : Indirect Tensile Stiffness Modulus

NAT : Nottingham Asphalt Testing

LVDT : Linear Variable Differential Transformers Differential Transformers

ITFT : Indirect Tensile Fatigue Test

ITS : Indirect Tensile Strength

ITSR : Indirect Tensile Strength Ratio

WTT : Wheel Tracking Test

3PB : Three-Point Bending

UTM : Universal Testing Machine

BPN : British Pendulum Number

FER : Force Effect Ratio

1. INTRODUCTION

1.1. Background

Highway transportation is the most common type of cargo and passenger transportation all over the world since it provides flexible and quick transportation in short and medium distances, door to door transportation without needing any other transportation type and convenience in vehicle planning and obtainment. Highway transportation has a significant part in our daily lives. Highway transportation, with its simplifying properties in both passenger and cargo transportation, preserved its importance from old times until today. The global road network spans 16.3 million kilometers [1], of which 5 million kilometers is in the EU, 4.4 million kilometers in the USA and 3.1 million kilometers in China [2]. The governments invest heavily in the development and maintenance of national and regional road networks. In 2015, EU government invested 23% (€2.8 billion) of the EU roads and motorways transport network fund (€12.43 billion) into the development and maintenance of EU road networks [2]. The development and maintenance of the EU road network are crucial for the growth and competitiveness of the EU economy.

In order to sustain the desired performance of highways during their service life, it is necessary to use quality material, and maintenance and repair works are needed to be carried out on time, which imply expensive investments. Incorrect planning of maintenances and repairs or inability to have funds on time arose a need to search for alternative methods in order to sustain the expected performance of highway pavements for a long time. Moreover, due to traffic and environmental conditions, deteriorations such as rutting, moisture damage, low temperature and fatigue cracks, and aging occur in hot mix asphalts [3], see Figure 1.1. Additives are used with the aim to extend the service life of pavements by increasing the performance and resistance of bitumen and hot mix asphalts to temperature and traffic loads [4]. When deteriorations occur in highway pavements, various improvement works can be carried out to ensure that the serviceability of the pavement is increased. In highway pavements, the properties of materials are improved to extend maintenance and repair works.

Lately, the use of additives has become a common practice, however, even though additives can extend the service life this method is based on extending the maintenance and repair works only for several years.

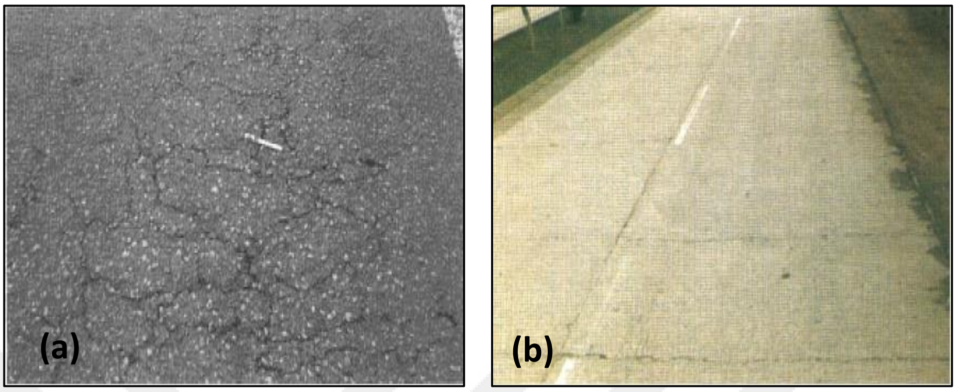

Figure 1.1. Examples of deteriorations in asphalt pavements: (a) fatigue cracks, and (b) low-temperature cracks.

Another method to repair deteriorations is the use of self-healing materials. The point of self-healing materials is to implement the self-healing mechanisms of nature and its additional processes into construction materials, such as self-healing of injuries on the human body. In hot mix asphalts, three different options stand out as self-healing methods. The first one is the manufacturing of mixtures with capsules that contain a crack filling or rejuvenating material inside. In the second and third methods, heat is used in the elimination process of the cracks.

Self-healing can be defined as the built-in ability of a material to automatically heal (repair) the damage occurred during its service life [5]. The properties of a material degrade over time due to damage at the microscopic scale, such as micro-cracks. These cracks can grow and lead to full-scale failure. Usually, cracks are repaired by hand, which is difficult because micro-cracks are often hard to detect. In the field of materials science, researchers are now trying to introduce self-healing components to common materials to obtain self-healing systems which can improve their service life, and consequently, reduce production costs of several different industrial processes, reduce inefficiency over time caused by degradation, as well as prevent costs incurred by material failure.

Asphalt pavement is a self-healing material [6]. When subjected to rest periods, asphalt pavement has the potential to restore its stiffness and strength by closing the micro-cracks caused in the material because of traffic loads and severe environmental conditions. Crack repair in asphalt pavement systems occurs because of the wetting and inter-diffusion of material between the two faces of a micro-crack, to regain the properties of the original material [7]. Little and Bhasin [8] proposed a 3 steps model to describe the healing process of asphalt materials: i) wetting of the two faces of a nano-crack, ii) diffusion of the molecules from one face to the other, and iii) randomization of the diffused molecules to attempt to reach the original strength of the material. Wetting is of significance by the mechanical and viscoelastic properties and the material constant of the bitumen. The subsequent recovery of strength is determined by the surface free energy of the asphalt binder and the self-diffusion of asphalt cement molecules across the crack interface [9].

1.2. Problem Statement

The role of road transport in the fields of economic activity and investment is very important. When compared to different transportation systems, the importance of road transportation is evident in a developing world. Therefore, the road development is of great economic and social importance.

No studies have been found in our country regarding the asphalt that improves itself in the literature studies. In the literature reviews, it is seen that there is no study conducted in our country regarding the self-healing asphalt. Bituminous materials have a self-healing characteristic during the day. In areas with excessive traffic, the microscopic cracks increasing during the day slowly heal at low traffic density at night. However, a chemical change called aging occurs in the structure of bituminous binder because of the reasons such as high temperature and sunlight. This effect increases over time. Because of aging, a bitumen hardening occurs, and microcracks rapidly increase in a short time because of this hardening. The resulting cracks adversely affect the performance of the superstructure during the expected service period. Therefore, studies on the use of additives have been increased and successful results have been obtained to increase the strength of superstructure. However, although the use of additives is effective in the short term, it cannot prevent deteriorations in the long term. Although bitumen used in asphalt mixtures has the self-healing property, the healing period takes a long time, and it cannot repair all the deteriorations that have occurred. The aged bitumen is restored using rejuvenators to regain the original bitumen properties. In addition, these rejuvenators used to reduce the bitumen viscosity. Therefore, a new approach is to ensure the self-healing of the material. One of the methods used is to add capsules to the hot mixture of bitumen during the production process. Sunflower oil is used as the rejuvenator in these capsules. Health problems and cost are the reasons for the use of chemical rejuvenators. When the crack formed in the bitumen material expands with the effect of aging, the capsule on the crack path cracks and the deterioration is eliminated by the healing effect of the substance in the capsule. In addition, its effect on the mechanical properties of asphalt mixtures has been investigated.

1.3. Aim and Objectives

Flexible superstructures become unavailable over time due to traffic and environmental loads. As can be seen in Figure 1.2, relatively earlier deteriorations occur in pure mixtures, while the service life is longer in mixtures containing additives. Although the service life increases with the use of additives, an inevitable end waits for the superstructure. This is a major problem particularly in roads that are difficult to maintain or in those that cannot be maintained economically on time. Because every 1 cent spent on time for the maintenance of the road superstructures prevents a cost of 6 cents of major repair to be made in the next periods. With these thoughts in mind, the number of studies on the self-healing asphalt mixtures continues to increase each passing day. The most important objective of this study is to suggest a capsule containing a new rejuvenator to enhance the healing properties of asphalt mixtures. Compared to those in other studies, this capsule should be easy to produce, low cost, but not have a health problem. In addition, these capsules should not disrupt the mechanical properties of asphalt mixtures while healing them. Another objective of this study is to develop an asphalt mixture which can heal at ambient temperature by using the healing agents provided by these capsules produced.

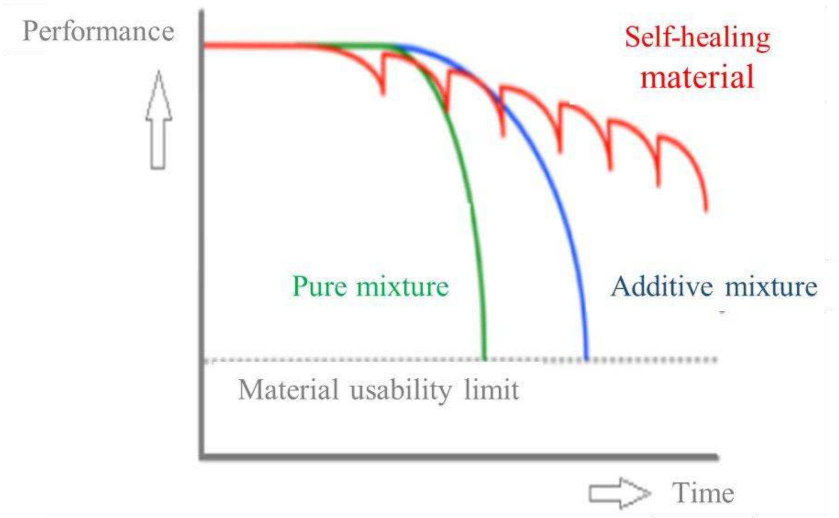

Figure 1.2. The performance-time curve in different types of material [10].

To accomplish these objectives, the following research targets are introduced:

- A new capsulation method or capsules with different properties can be developed considering the methods in the literature.
- The physical, thermal and mechanical properties of these capsules are determined.
- The properties of the capsules produced are evaluated during the mixing and compression processes.
- The effect of capsules on the mechanical properties of asphalt mixtures can be evaluated. Standard test methods are applied to evaluate the mechanical properties such as fatigue, sensitivity to water, hardness, frictional resistance and wheel tracking. The effect of capsules on the self-healing properties of the asphalt mixtures is evaluated. The self-healing process is visualized using computerized tomography scans. The effects of capsules on the capsule containing asphalt mixtures are evaluated with mechanical tests performed before and after healing. In addition, these results are evaluated by being compared to the results of the asphalt mixtures without capsules. Then the resting time in the maximum healing ratio is determined.

1.4. Research Methodology

The research methodology begins with the determination of the production mechanism of capsules. Then the mechanism and materials to be used are purchased. This is followed by the determination of the optimum number of capsules to be used in an asphalt mixture.

Capsules are tested for physical, thermal and mechanical properties following the production process. The Scanning Electron Microscopy (SEM) analyses are used to determine the morphology and the structural properties of the capsules. For example, SEM is used in determining the change in the structure of the capsule with the changing amount of oil used or the interaction between the core and the shell of a capsule. Then the asphalt mixtures are prepared, capsules are added, and the emission of the oil within an asphalt mixture is observed. The oil-dependent chemical changes of the samples are measured by the fourier transform infrared spectroscopy (FTIR) test at different times. This test gives the percental amounts breaking of the capsules in asphalt mixtures under any load.

Capsules are added to asphalt mixtures at different percentages according to total weights of mixtures. Capsules should also be added at a rate of 0.5% based on previous studies. Capsules added to a mixture can resist the mechanical properties depending on the mixture temperature and the breaking capability when a crack occurs in an asphalt mixture. Computer tomography (CT) scans are used to evaluate the vitality and distribution of capsules in asphalt samples. Then asphalt samples are prepared to evaluate the mechanical effect of the capsules. These samples are subjected to different loadings and resting durations to consider the time needed for the dispersion of oil into asphalt mixtures. The first point of the test is to evaluate whether capsules will reduce the hardness of the bitumen or not. Because this is an important assumption for the rejuvenation of an aged bitumen. The second point is to analyze the effect of capsules on the mechanical properties of asphalt mixtures such as durability, rutting, fatigue, wheel tracking, particle loss, and moisture. Capsules are strongly bound to an asphalt mixture and the mechanical performances of asphalt mixtures with and without capsules are evaluated. The capsule containing asphalt samples are compared to those without capsules to evaluate the effect of capsules on asphalt mixtures accurately. So, the effect of capsules on asphalt mixtures can clearly be understood.

The capsules have been analyzed in two asphalt samples to evaluate the self-healing potential. The first mixture was added to dense asphalts. A healing test is applied to asphalt mixture beams with and without capsules at ambient temperature. These asphalt beams are produced in the laboratory. Different static loads are applied to evaluate healing at different resting periods. In this way, the best healing rate is determined at optimum load. In addition, the effects wheel tracks on dense asphalt mixtures are determined. Static and dynamic loads were applied to create cracks in asphalt mixtures. The effect of these loads on the breaking of capsules was also evaluated. The capsules were added to the stone mastic asphalt (SMA) in the second phase. The effects of the capsules on the mechanical properties of SMA mixtures were investigated. In this way, the effects of the capsules on two different asphalt mixtures were determined.

1.5. Thesis Outline

Chapter	Description
Chapter 1	An overview and general background information about the asphalt self-healing. This chapter also includes the problem statement, the aims and objectives as well as the research methodology.
Chapter 2	This chapter provides an overview, background of self-healing materials, the general concept of encapsulated rejuvenators, diffusion of rejuvenators inside an asphalt pavement, asphalt self-healing by induction heating and asphalt self-healing by encapsulated rejuvenators.
Chapter 3	This chapter presents the materials and methods involved in capsule design, asphalt mixture preparation and types, types of asphalt samples used in the research, methods of incorporating the capsules into the asphalt mixtures, performed in the research. In addition, it gives the physical and thermal properties of the capsules.
Chapter 4	The properties of aging in asphalt mixtures are given in this chapter.
Chapter 5	The test methods applied to capsules, bitumen and asphalt mixtures are described in this chapter.
Chapter 6	The effect of capsules on the asphalt behavior are investigated in this chapter. The order of mixing, the effect of aging duration on the mechanical stability and self-healing properties of the asphalt mixtures with and without capsules, hardness module, and bending strength are evaluated in this chapter.
Chapter 7	This chapter provides the effect of capsules on the mechanical properties of stone mastic asphalt mixtures.
Chapter 8	The investigation of crack healing with the proposed capsules is the main topic of this chapter. The chapter describes the effects of different static loads on the self-healing properties of asphalt mixtures.
Chapter 9	Two test methods applied for the first time to asphalt mixtures with capsules are investigated in this chapter. These are the fatigue and wheel tracking tests.
Chapter 10	In this chapter, the main conclusions and recommendations for future research are presented.

2. LITERATURE REVIEW

Recently, researchers have started to investigate alternative maintenance methods due to economic and environmental reasons. One of these alternative methods is the self-healing of the bituminous materials technique. This method is known for approximately 40 years; today's researchers started to investigate the natural healing method in asphalt pavements. This method reduces the maintenance cost of asphalt pavements while improving the service lives of the pavements. In order to better understand the self-healing method in asphalt pavements, it is vital to consider and investigate all the factors that can contribute to this method.

The aim of this section is to establish the basis of a literature review that presents the subject of self-healing in asphalt pavements in order to provide a background according to the subject of the study. Details of natural self-healing methods, self-healing techniques by using various materials, and weak aspects of this method were evaluated. Lastly, studies were conducted on three different self-healing methods (heath induction, microwave heating and encapsulated rejuvenators) that were recently investigated and developed in order to improve the self-healing level.

2.1. Definition of Self-Healing

Self-healing materials

Generally, deformations occur in asphalt pavements following the initiation of the damages that are inclined to grow at a microscopic scale and cause the materials' properties to degrade. Self-healing materials are the materials that have the ability to partially or completely repair the damage occurred during the service life [11]. The materials that can self-repair the degradations occurring in the normally used asphalt pavements prevents both the performance reduction that results from these degradations and the increase in the repair cost of the asphalt pavements [11].

Major studies on the self-healing materials were conducted in the field of polymers. The first patent study in this field dates back to 1966. Various groups of polymers were produced [12]. These polymers can return to their cross-linked states following the cracking. However, the potential routes of these polymers were not determined.

The first synthetic self-healing material was developed by White et al.. This healing concept was presented in Figure 2.1. A microcapsuled healing agent is buried inside a structural matrix that has a catalyst that can be polymerized. The crack occurring in the asphalt pavement cracks the buried microcapsules, releases the rejuvenating agent onto the crack surface by brittle movements.

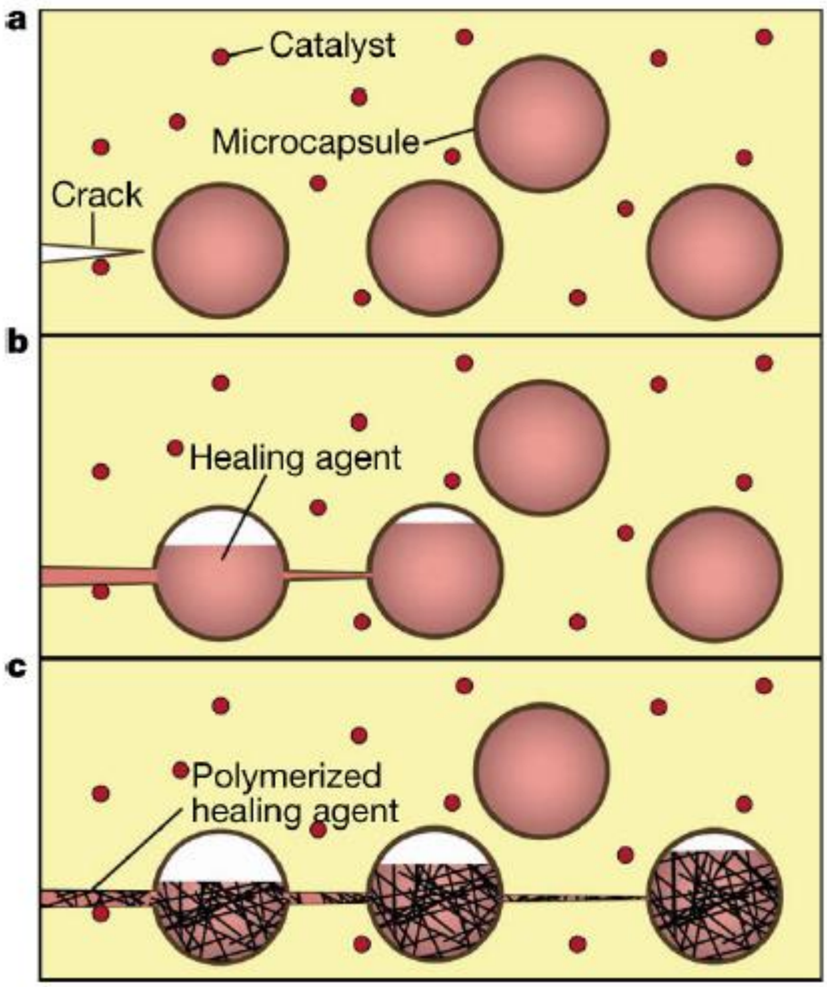

Figure 2.1. The concept of self-healing with microcapsules [5].

Self-healing of bituminous materials

The stiffness and the strength of the bituminous materials decrease when they are exposed to repetitive loads. The micro crack initiation and their later transformation into macro crack during cyclic loading is investigated by a number of researchers [13-15]. The recovery of the materials' stiffness and strength and extension of fatigue life were first identified in the 1960s by fatigue test with resting times.

Novel self-healing materials

In the biological world, organisms' self-healing mechanisms and constant detecting and repairing of damages are well known. For example, trees have the ability to self-heal the damage occurred in the branches or the trunk, and humans have the ability to self-heal the damages in bones or wounds on the skin. Researchers are now trying to transfer and develop these self-healing behaviors into man-made materials. Scientists aim to introduce the self-healing components to normal materials and improve the service life of normal materials in order to build a self-healing system. This method was first studied by White. Up to now, self-healing materials, such as concrete, polymers, composites, asphalt pavements and metals, which can be used in various fields, have been investigated. Successful self-healing systems involve systems such as encapsulation, polymer diffusion, thermos-reversible polymers and etc.

2.2. Self-Healing Technologies for Asphalt Pavements

The concept of self-healing materials was used by Romans 2000 years ago. The remaining lime following the evaporation of the rainwater that flows into the cracks in the asphalt pavements provides the healing of the crack. With self-healing materials, pavements are expected to remain durable and reliable during their service lives. Long-term use of asphalt pavements leads to fatigue cracks. Increased fatigue cracks cause the pavements to degrade. Self-healing materials have the properties to self-heal themselves in time [16].

According to Van der Zwaag, the process of self-healing is a combination of detecting and repairing the damage for the material to self-heal. Molecules of these type of self-healing materials fill the crack by moving towards them. In the construction industry, due to the need for reliable and durable structures, appropriate self-healing materials to be used in areas where maintenance and repair are difficult were sought [11].

In asphalt pavements, natural self-healing concept is suggested in the study conducted by [17], in which they examined the self-healing process of asphalts by investigating the fatigue cracks and the recovery process during the resting period. This study was one of the first studies that were conducted in a laboratory environment. Regarding the recovery of the properties of materials, healing concept following the resting period was investigated by a number of researchers [17]. Raithby and Sterling [18] conducted a study in order to identify the self-healing mechanisms at a molecular level on all pavement levels and model the self-healing behaviors of asphalt pavements based on experimental studies. However, this mechanism was not fully comprehended [18]. Figure 2.2 demonstrated how the natural self-healing phenomenon takes place in an asphalt sample.

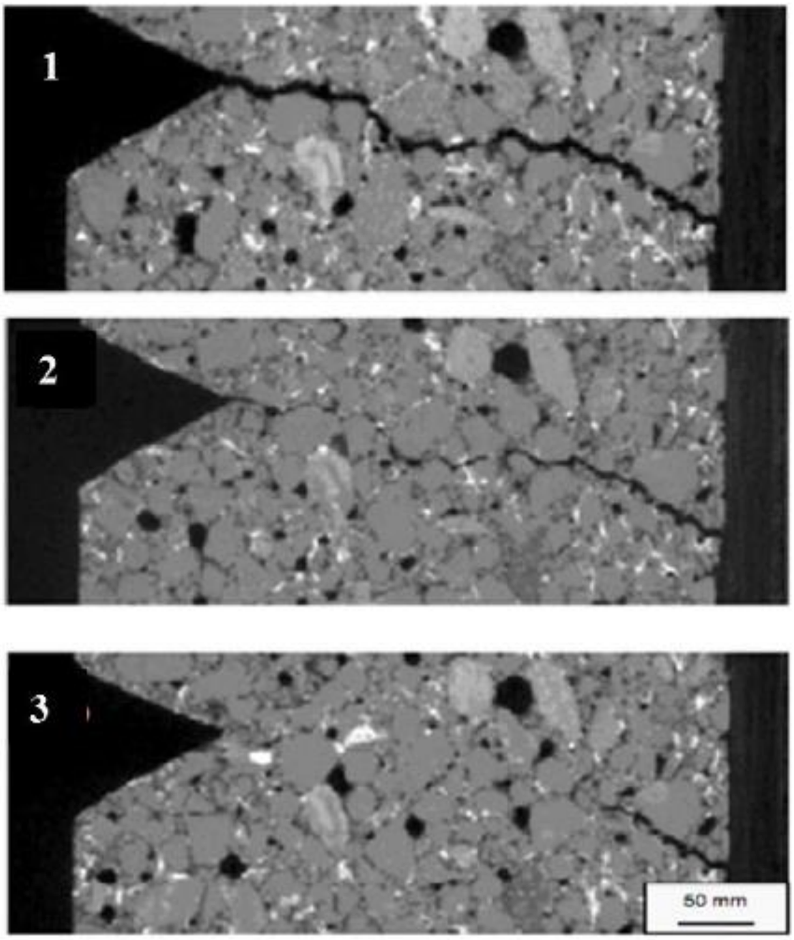

Figure 2.2. Natural self-healing in asphalt pavements [19].

Boyer (2000) investigated the use of rejuvenators in order to eliminate the fatigue cracks occurring in asphalt pavements. As it was previously mentioned, rejuvenators improve the service lives of pavements for several years upon their implementation on the pavement surface. However, these rejuvenators do not affect the cracks occurring in the depths of the pavement but a few centimeters from the surface [20]. Chiu and Lee, conducted experiments with rejuvenators at three distinct amounts on a 12-years-old pavement in order to evaluate the effects of the rejuvenator. Even though the pavement contained high amounts of air voids, it was determined that, for the three rejuvenators, approximately 10% did not penetrate more than 2 cm into the pavement [21].

Recently, three inventory techniques were developed to improve the healing rate of asphalt pavements without the side effects that have been discussed above of using the rejuvenators or sealants, the three techniques were a passive self-healing mechanism as rejuvenators are encapsulated and embedded within the asphalt mix, an active self-healing mechanism where heat induction is used to stimulate the healing process and microwave radiation heating.

2.2.1 Self-healing by induction heating

The process of producing electrical currents in a conductor by placing it in an alternating magnetic area is called Faraday electromagnetic induction. The induced currents flow against the electrical resistivity of the conductor, producing heat in the conductor due to the "Joule effect". This heating method is often called induction heating [22]. In order to heat materials with electrical conductivity, induction heating that uses high-frequency electricity has more advantages compared to other heating methods. First, 90% of the electricity used during the induction heating can be transformed into beneficial heating. Second, induction heating is a contactless heating method. Third, problems such as product warpage, distortion and rejection rates can be minimized because the heat is triggered by Joule heating. Fourth, induction heating works very quickly because the heat is generated directly and instantly inside of the heated material, so there is no cooling cycle in the system. Finally, induction heating also eliminates the inconsistencies and quality issues associated with an open flame, torch heating and other methods [22]. Induction heating has already found wide applications in modern manufacturing processes like bond hardening or other conductive materials. The existing induction heating techniques offer the possibility to apply induction heating on pavements to increase their temperature and close the cracks by high-temperature self-healing of bitumen [22]. This process is supposed to increase the level of self-healing, and melt the cracks. Figure 2.3 shows how the cracks close by the use of fibers and induction heating.

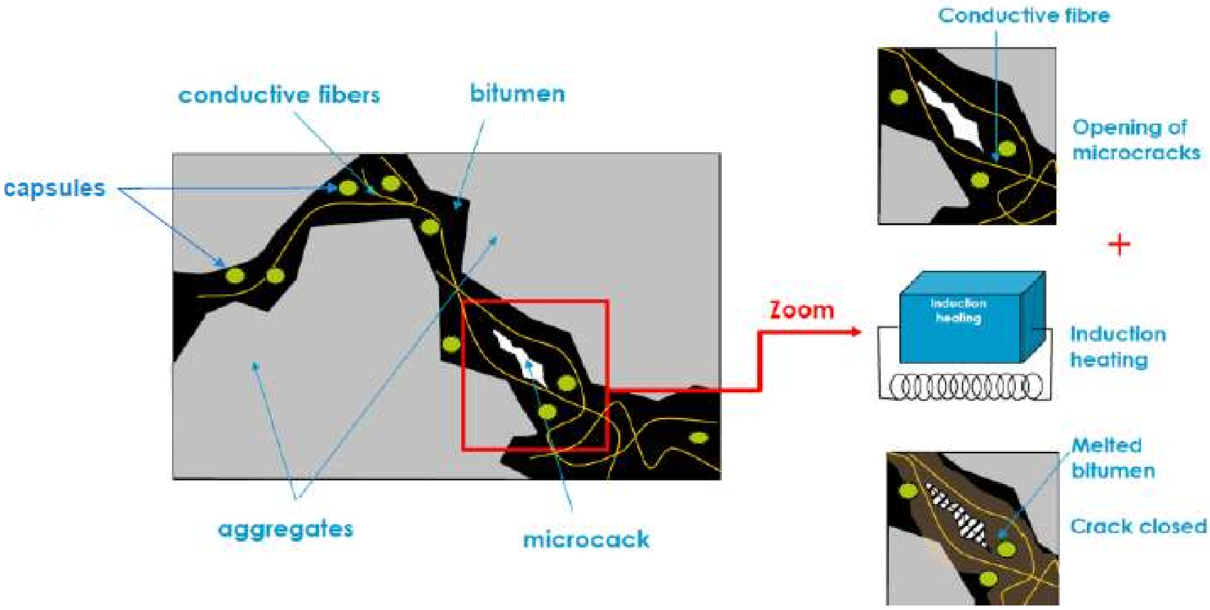

Figure 2.3. The mechanism of induction heating [23].

Electrically conductive asphalt pavement is a functional material developed to achieve good electrical conductivity. For this property, conductive components like graphite or fibers should be added to the mixture. The pioneered of making electrically conductive asphalt test plots for control of snow and ice accumulation dates back to the 1960s [24]. Currently, induction heating in the self-healing of asphalt pavements regained its popularity. Electrically conductive fibers and fillers (carbon fibers, graphite, steel slag, steel fibers, steel wool and the conductive polymer polyaniline) were added to asphalt pavements to study their electrical conductivity. Results indicated that the electrical resistivity varied with the type, shape, and size of fibers and fillers [7].

Even though this self-healing method seems simple and effective, induction heating possesses several problems to be solved before it becomes an industrial process worldwide. Because the test samples in laboratories are small in size, the induction heating device should be small as well, which contradicts with the situation in the field. This is because fieldwork requires larger devices. This state is not economical and cancels out one of the advantages of self-healing due to causing degradation of roads when implemented. The movement speed of the induction heating device should be adjusted according to the heating and cooling of the asphalt pavements [25]. An image of the induction heating devices that are used in the laboratory and in the field was presented in Figure 2.4.

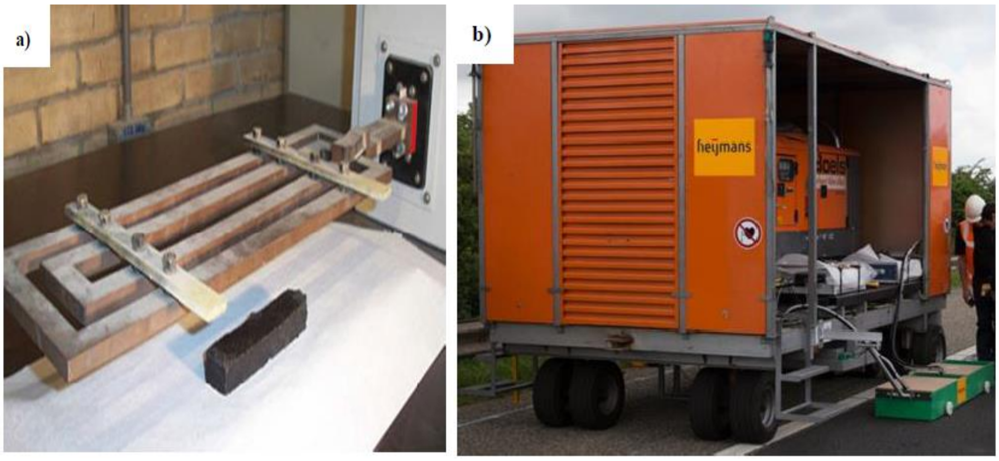

Figure 2.4. Induction heating device, (a) laboratory induction heating device used by and (b) induction heating generator installed in a test truck [26].

Previous studies outlined the influence of induction heating on the self-healing of asphalt mixtures. Representative examples include a study conducted by Liu et al. [27], where the mixing procedure was optimized to disperse steel wool into asphalt mixture. The induction heating potential of porous asphalt concrete containing steel wool was measured, and Rotating Surface Abrasion Test with rest periods to apply induction heating was employed to study the raveling resistance improvement of porous asphalt concrete. It was found that porous asphalt concrete containing steel wool can be heated with induction energy and induction heating can greatly reduce its stone loss (Figure 2.5).

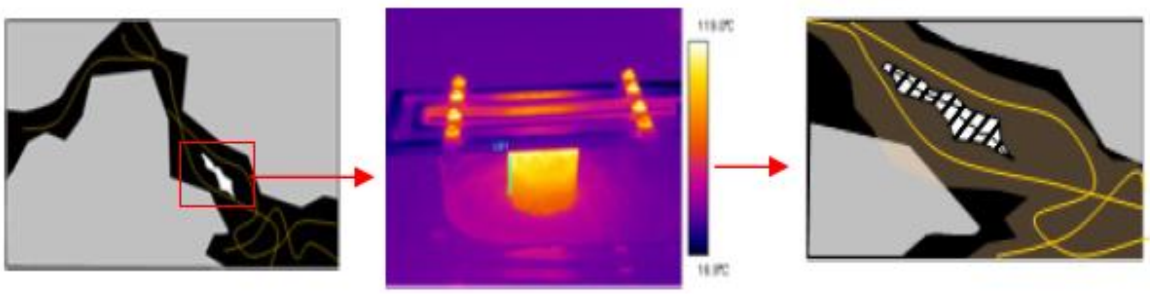

Figure 2.5. Induction heating process in asphalt mixtures [22].

In another study, Obaidi et al. [28] suggested a new method for the maintenance and repair of the potholes in asphalt pavements. To use this technology, the potholes should be: i) previously cleaned, ii) filled with an asphalt tile (with a bottom bonding layer made of bitumen, and steel fibers), and iii) exposed to high-frequency electromagnetic fields to heat the fibers up and melt the bitumen in the bonding layer. Liu et al. [29] investigated the ways of improving the asphalt mastic self- healing properties. For this purpose, they used several additives (steel wool and steel fibers) in order to improve the conductivity of asphalt mastics. Finally, with various additives, properties such as induction heating speed, bending strength and induction healing rate were investigated.

The size and shell thickness were two main influencing factors of micromechanical properties of the microcapsules containing rejuvenator [30].

Moreover, since the factors affecting the induction healing of dense asphalt mixture are not well-known, Garcia et al. [19], considered different mixtures, with different lengths, quantities, and diameters of steel wool fibers in their study. In addition, they developed a semi-empirical model describing asphalt recovery. Furthermore, Gómez-Meijide et al. [31], induced asphalt self-healing in cracked asphalt beams with three air void contents: 4.5%, 13% and 21%, by exposing them at various times under infrared radiation and induction heating. Main results showed that cracks in asphalt mixture can be completely repaired by infrared and induction heating, but the last one is more efficient since the effect is concentrated only on the binder instead of heating the whole asphalt mixture. Moreover, it has been observed that dense mixtures obtained better healing with low energy but their maximum healing ratios were lower than those obtained by semi-dense and porous mixtures.

In studies investigating how to heath the mastic asphalt with induction heating, steel fibers were included with the aim of improving the conductivity. It was determined that using fibers more than 6% did not have a positive effect. When the steel fiber amount is less than 2%, it demonstrated an insulating property and only local heating was achieved. Following the implementation of the first induction heating, it was reported that strength was achieved at a 90% and 70% following the fifth heating. It was suggested that, in order to benefit from the healing, this process should be conducted prior to extreme conditions, such as winter [32].

In the A58 highway in the Netherlands, the first test road regarding the self-healing asphalt with induction heating was implemented. With this aim, steel wool fibers were included in the asphalt mixture. Here, the purpose of using conductive particles was to ensure the heating of the pavement with the induction energy. With the impact of this heating, the amount of healing improves and the closure of the potential cracks is provided. Laboratory studies were conducted in order to determine the amount of steel wool. In order for the steel wool to have a long life in the mixture, they should not cluster or rust with the effects of water and they should not lose their mechanical properties in the meantime. To that end, the mixing time of the hot mix asphalts should not exceed 3.5 minutes. Accordingly, mixtures including 5% steel wool fibers were mixed for 1.5 minutes. The clusters of steel wool fibers in the asphalt mixture were demonstrated in Figure 2.6. Following this process, the mixtures were implemented to the A58 highway in the Netherlands and the gathered samples were subjected to performance tests. The obtained results were determined to be better compared to the regular porous asphalts [33].

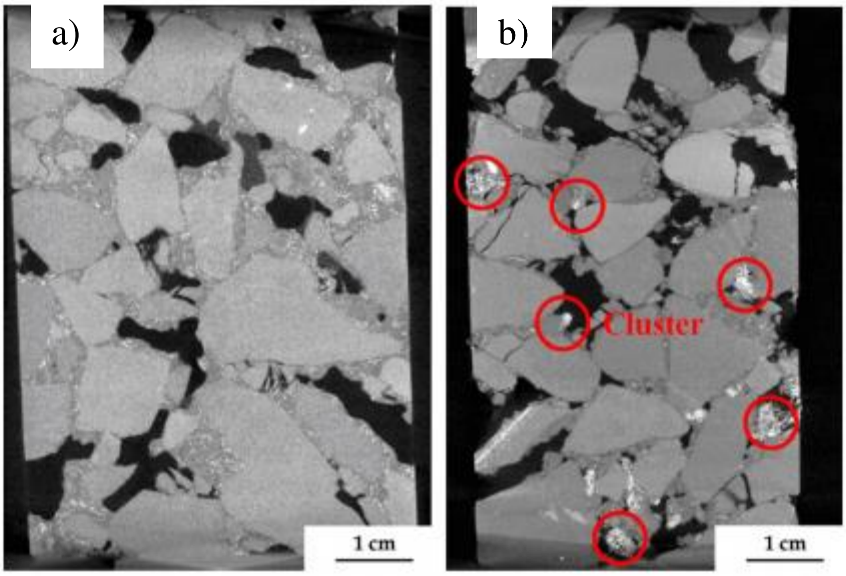

Figure 2.6. (a) Sample without clusters of fibers (4% of fibers and 3.5 min mixing). (b) Sample with clusters of fibers (4% of fibers and 3.5 min mixing) [33].

In the study conducted by Liu et al., the healing with induction heating on hot mix asphalts including steel wool fibers was investigated. In the study, 4-point bending fatigue tests were conducted on beam samples. The obtained results indicated that mixtures with steel wool fibers provided better results compared to pure mixtures. In order to determine the amount of improvement with the use of these materials, the rate of increase in the fatigue life and rigidity values were used. It was determined that the temperature should be 85 °C for the best steel wool induction heating. Higher temperatures caused the sample to swell and decreased the strength. It was also reported that the healing improved with more than one induction implementation [34].

In a study conducted by Garcia et al., the usability of induction heating in the repair of the cracks in the asphalt concrete was investigated. For this purpose, electrically conductive particles were included in the asphalt mixture and then, they were heated by using the induction-heating device. Because the factors affecting the healing of the asphalt concrete with induction heating are not well known, steel wool fibers in different mixtures with different lengths, amounts and diameters were investigated in this paper. As a result, it was determined that the minimum temperature for the healing of the asphalt concrete was 50 ºC. Additionally, a semi-empirical method that explains the healing of the asphalt with the brittle behavior theory was developed and its parallelism was established with the results [19].

In the study conducted by Menozzi et al., hot mix asphalt samples were subjected to indirect tensile fatigue test, causing damages on them. Following this process, it was attempted to heal the samples with induction heating implementation. The occurred damage and healing were determined by using a computerized tomography scan. It was determined that there was an optimum damage level for the healing. As a result of the healing with induction heating, the service lives of the asphalt were improved by 30%, however, the bitumen was subjected to aging due to the heating during this time [35].

In another study conducted by Menozzi et al., hot mix asphalt samples were heated with the induction method in order to determine whether heating was beneficial in the self-healing of the asphalt. Because hot mix asphalts are insulating, the improvement in the conductivity was provided by including steel fibers in order to ensure that not only the surface is heated but also the material in the deep. Following that process, the heating of the pavement was provided with the induction device. When the temperature of the asphalt mixture exceeds a certain temperature (between 30 ºC and 70 ºC, depending on the type of the bitumen), the micro cracks starts to self-heal. Induction healing was previously used in the repair of split half hot mix asphalt samples; however, it was not used in the micro crack repair caused by the fatigue damage. In this study, the optimum time and temperature to repair the asphalt mixture under the fatigue damage were determined by using the scientific method. For this purpose, Marshall test samples were subjected to damages with indirect tensile fatigue test and were healed with the induction heating method. Finally, the quantitative amounts of the damage and healing were determined by computerized tomography scan tests. From the obtained results, it was determined that the lives of the Marshall test samples were improved by 31% and the healings occurred in the cracks of the samples [35].

Inductive heating has been reported as the most promising self-healing technology for asphalt pavements. A problem that has not been addressed by research is the loss of conductivity due to the oxidation of the steel wool fibers, although they lead to aging in pavements [36-38]. Self-healing induction technology should be developed to get better results because of all these positive features.

2.2.2. Self-healing by microwave radiation heating

Microwave energy received significant attention from researchers for a wide spectrum of appeals [39]. The present interest in industrial applications of heating by microwave radiation, such as melting, smelting, sintering, drying and joining, was prompted a good deal of research aimed at formulating mathematical models able to simulate accurately the microwave phenomena [40]. Several studies were conducted comparing the microwave heating and the conventional heating of materials, providing beneficial information for the application of this methodology and demonstrating its great advantages [41,42]. Nowadays, microwave technology is considered as a promising technique to promote self-healing of new composite materials with metallic fibers, because they can be used to increase the heating rates of the composite materials [43].

On the other hand, previous studies have outlined the influence of microwave heating on asphalt mixtures. Benedetto et al. [44]. compared the data with conventional heating and used numerical simulation for calibrating and validating a model for further applications. Their objective was to check the possibility of including microwave-heating technology in the manufacturing and recycling processes of asphalt to reduce environmental and health risks with an increase in the efficiency of the whole process. The obtained results were consequent with several literature findings regarding the advantages of microwave heating compared to conventional heating and validate a numerical simulation model that can be applied for designing a prototype of microwave heating plant.

Moreover, the potential of using steel slag asphalt mixture as a self-healing material by means of microwave heating was studied by Sun et al. [45]. The microwave-heating rate and thermal conductivity of asphalt mixtures were tested. The results showed that steel slag asphalt mixtures can be used to promote self-healing, because of the heating rate of steel slag asphalt mixtures was approximately two times faster than that of limestone asphalt mixtures, while its thermal conductivity was slightly lower. Furthermore, Norambuena-Contreras et al. [46], studied the steel wool fibers spatial distribution and their influence on the physical and mechanical properties of asphalt mixtures with self-healing purposes via microwave heating. Additionally, samples of these mixtures were examined by X-ray micro computed tomography to study the distribution of fibers within the bitumen matrix, demonstrating that the presence of fiber clusters more than double of the average fiber content of the mixture. The fiber clusters existence in samples of dense asphalt mixtures is shown in Figure 2.7.

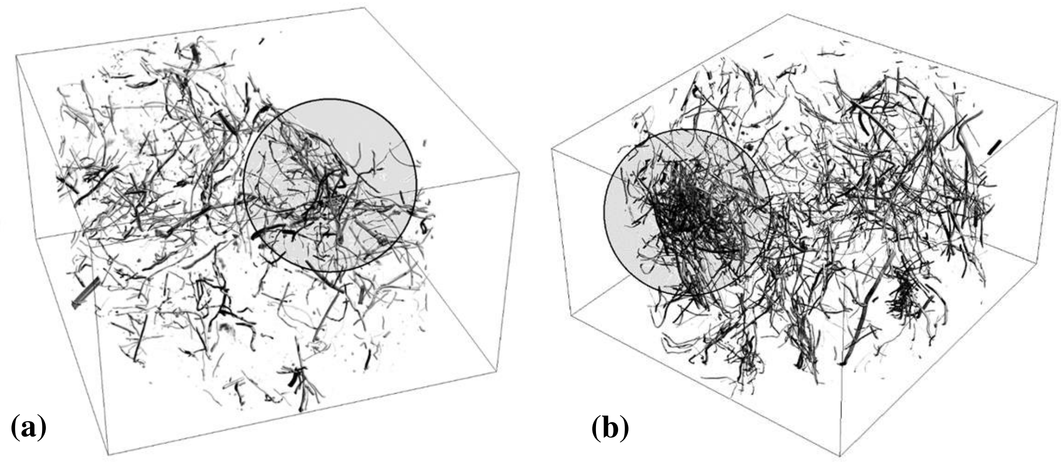

Figure 2.7. Examples of CT-Scan 3D model of fiber clusters existence inside dense asphalt mixture samples with: (a) 4% fibers, and (b) 8% fibers [46].

Besides, Norambuena-Contreras and Garcia [47], studied the effect of microwave and induction heating on the self-healing of dense asphalt mixtures with steel wool fibers added in four different percentages. As a result, they found that microwave technology is more effective than induction heating for crack repair in asphalt roads. Recently, Norambuena-Contreras and Gonzalez-Torre [48], investigated the influence of the microwave heating time on the self-healing properties of four different asphalt mixtures with steel fibers. They concluded that 40s was the optimum heating time to reach the highest healing levels with the lowest damage on the asphalt samples, and that heating times over 30s can also seal the cracks, thus achieving the self-healing of asphalt mixtures via microwave heating, see Figure 2.8.

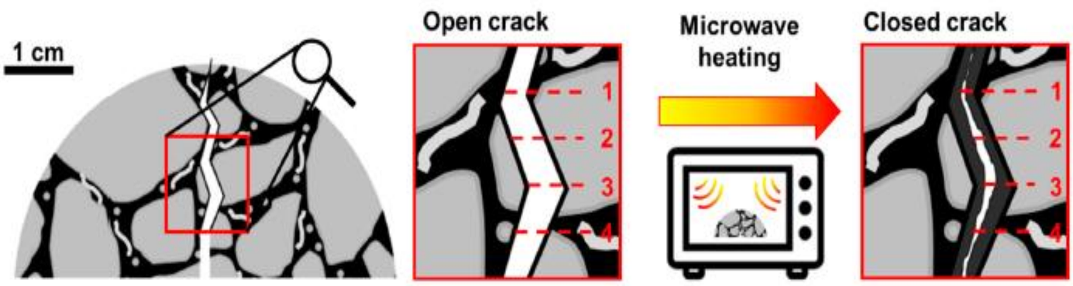

Figure 2.8. Schematic diagram of the measurement of the crack size before and after microwave heating [48].

In the study conducted by Gallego et al., the effects of the microwave heating of the hot mix asphalts on the self-healing of the mixtures were investigated. In some of the previous studies, it was determined that applying high-temperature on the asphalt during times when there is no load applied on the asphalt improved the properties of the asphalt. Additionally, recent studies reported that the use of graphite and steel wool fibers improved the electromagnetic conductive and facilitated the heating of the pavement. In this study, the heating of the asphalt with microwave was investigated. As a result of the conducted studies, it was determined that 10 times less steel fiber was required for the heating with microwave compared to induction heating. Furthermore, it was reported that the tools used for microwave were less than those used for induction [49]. The measurement of the surface temperature of the asphalt samples was presented in Figure 2.9.

Figure 2.9. Measuring the surface temperature of the specimen [49].

In the study conducted by Yihan et al., the effects of steel slag use on the microwave heating of the hot mix asphalts were investigated. The rate of heating of the asphalt materials in the microwave and their thermal conductivity were examined. It was reported that the heating rate of the samples with steel slag was twice as high compared to the samples with limestone. In the obtained results, it was reported that steel slag could be used instead of steel wool fibers in facilitating the heating in self-healing mixtures [45].

As a binder-based modifier, activated carbon is added to asphalt concrete to enhance electromagnetic radiation absorption. The provided microwave power causes the modified asphalt binder to heat up into the asphalt concrete by swirling flow and bipolar molecular mechanisms at high speed rotation. Raising the internal temperature causes the asphalt binder to pass through microfractures. The flowing asphalt binder moistens the microcracked surfaces and partially heals the damage. The results obtained confirm that AC is a potentially suitable and robust binder-based conductive component for the induced heating and remediation of asphalt concrete [50].

The concept of self-healing asphalt with increasing temperature was used by the researches in order to create an asphalt mixture that has the properties of healing the cracks with microwave or induction heating. Metals, regularly steel wool fibers (SWF), are included in the asphalt mixtures, which were not prepared with materials that can absorb or conduct the thermal energy. Metal chips, which are waste materials obtained in the metal industry, can be used in the place of SWF. Additionally, reclaimed asphalt pavement (RAP) can be included in these mixtures in order to create a more sustainable road material. In this study, it was aimed to investigate the effects of the microwave heating of asphalt mixtures with metal chips and RAP on the properties of crack healing (Figure 2.10). In the study, it was reported that metal chips had an irregular shape with larger width compared to a typical SWF used in for the self-healing of asphalts. The general effect of metal chip inclusion is an improvement in the crack healing of asphalt mixtures while RAP inclusion in mixtures with metal chips decreased the improvement. Following the microwave heating, the mean surface temperatures of the asphalt samples were higher than those obtained following the induction heating and this situation indicated the chips were more efficient when heated with microwave radiation. Computerized tomography scan indicated that the chips were disturbed homogenously in the mixture and inclusion of metal chips increased the air voids. Generally, it was concluded that asphalt mixtures with RAP and waste metal chips had the potential of crack healing with microwave heating [51].

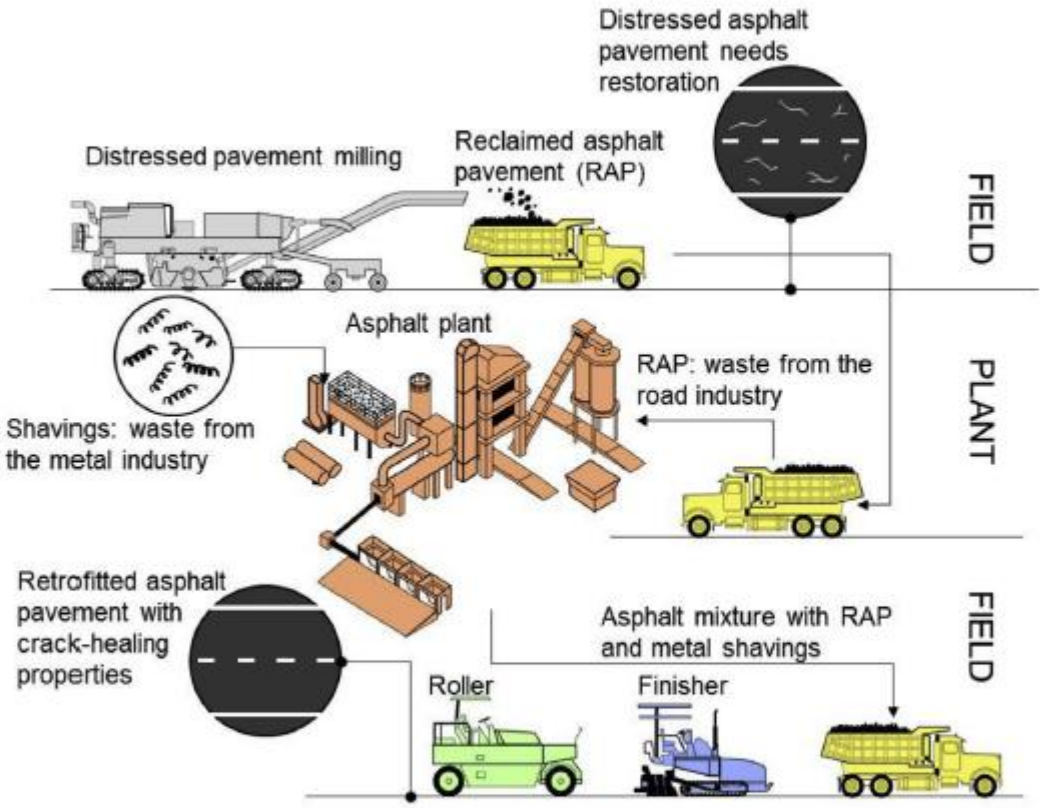

Figure 2.10. The conceptual framework of retrofitting conventional, distressed asphalt pavements into a novel sustainable asphalt pavement with crack-healing properties [51].

For all the above-mentioned reasons, microwave heating technology has shown potential for healing asphalt mixture, although it has not been deeply explored. Hence, self-healing microwave heating technology should be developed to get better results.

2.2.3. Self-healing by encapsulated rejuvenators

Rejuvenators on the asphalt surface can be encapsulated to eliminate the degradations and can be included in the asphalt mixture in the manufacturing process. This study covers the encapsulation of rejuvenators and their inclusion in the asphalt mixture.

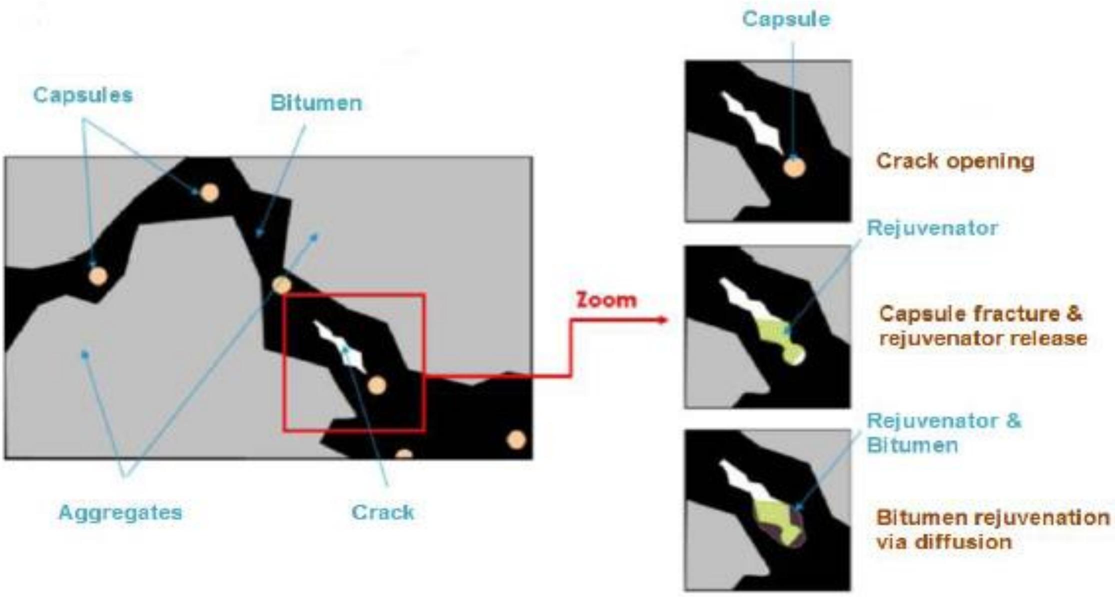

Figure 2.11. Encapsulated rejuvenator healing mechanism [52].

The idea here is to improve the healing capacities of cracks, which upon formation crack the capsules that they are in contact with, as presented in Figure 2.11 and 2.12, and the oils inside the broken capsules contact with the bitumen in the crack, recovering the properties of the bitumen. It is believed that this process repairs the cracks, minimalizes them significantly and prevents further crack propagation. The basic assumption is that the capsules will be broken when fatigue and thermal cracks exert a high stress on them. The rejuvenator penetrates the bitumen, reducing its stiffness and facilitating it to recover its chemical balance. According to Garcia et al., the capsules with mechanical strength ranges from 11N to 18N, or as an average of 14N have survived the mixing process. This means that capsules within this range of mechanical strength are the preferred ones to survive the mixing process and break under loading [53].

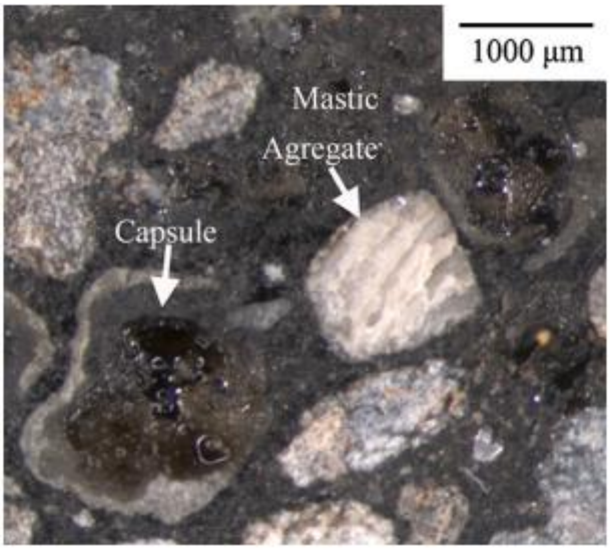

Figure 2.12. Section of the capsules embedded in asphalt concrete [53].

The results obtained in the study conducted by White et al., led to numerous possibilities to conduct studies regarding the capsule use for self-healing of asphalt pavements and other materials [13]. In this manner, two types of capsules were manufactured to be used in the self-healing of asphalt pavements. The first of these is the capsules with epoxy-cement shells that measure around 1-1.5 mm in diameter (Figure 2.13) [54]. The second type is the capsules with methanol-melamine-formaldehyde (MMF) polymer shells that measure approximately 23.5 μm in diameter. The sizes of the capsules depend on the amount of the rejuvenator agent included inside them. Thus, epoxy-cement shelled capsules contain higher amounts of rejuvenators. Epoxy-cement shelled capsules are manufactured by manually combining the materials in an easy way while the manufacturing of MMF prepolymer microcapsules require complex polymerization techniques in the preparation of the chemical structures of the polymers, which includes two steps of cross-linking the polymer to contain the rejuvenator inside then making the microstructure of the microcapsules [55].

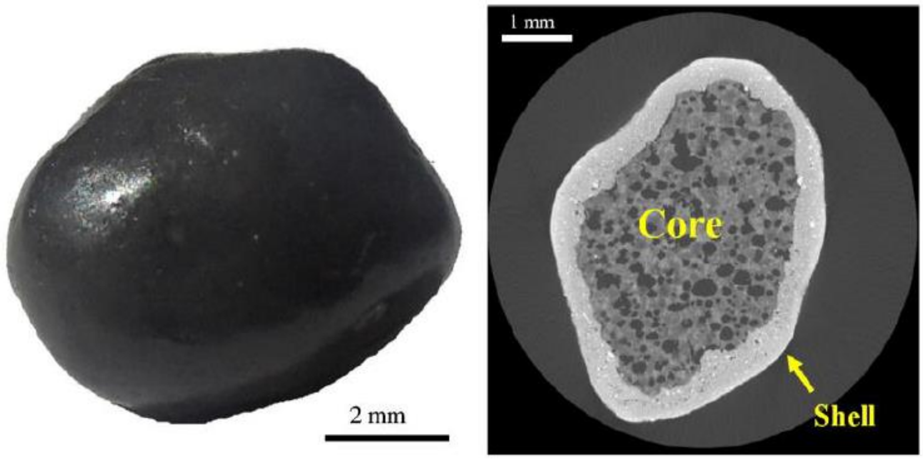

Figure 2.13. The external shape of an epoxy-cement capsule and its internal configuration [54].

Su et al. stated that in order to penetrate to the rejuvenator inside the microcapsule shell and allow it to spread, the stress required to crack the shell of the microcapsule should be determined. Following the cracking of the microcapsule shell, the rejuvenator contacts with the bitumen in the crack and improves the healing capacity of the cracks by recovering the properties of the bitumen [56]. However, the formation of a fatigue crack or a thermal crack in close proximity cannot be guaranteed, thus, it means that the self-healing process cannot occur every time [57]. In addition, Su et al. found out that some microcapsules do not break because of their high plastic deformation. They suggested that this plastic deformation might result from the combination of heat and applied load [58]. Figure 2.14 presents the SEM of the microcapsules in bitumen with their plastic deformation.

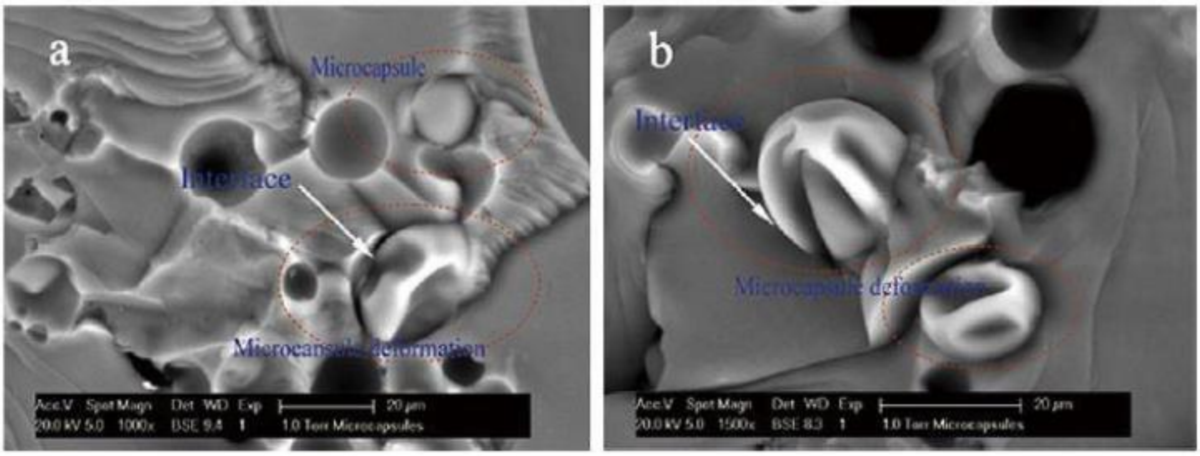

Figure 2.14. Interface morphology of bitumen/microcapsule sample [58].

The two methods of encapsulating rejuvenators described above have several advantages over the traditional rejuvenation system; these advantages can be summarized as the whole volumetric penetration of the rejuvenator inside the asphalt mix, no negative side effects on the pavement surface friction, and a better environmental performance. In addition, it can be considered as one of the pioneer steps towards producing clever roads.

2.3. General encapsulation technique

Oxidation forms in hot mix asphalts in time and causes them to lose their properties. Traditionally, rejuvenators are implemented on asphalt pavements to recover their original properties. However, the problem at this point is the fact that the rejuvenator is required to penetrate into the pavement surface in order to be successful. Furthermore, the implementation of the rejuvenator decreases the shear resistance of the pavement. Rejuvenators also include numerous aromatic components that can damage the environment. In order to solve this problem, a new concept was introduced in the road construction: encapsulated rejuvenators. The main principle here is the explosion of the embedded capsules inside the asphalt when a certain pressure value is exceeded and release of a certain amount of rejuvenator that can recover the original properties of the pavement. Figure 2.15 shows an experiment conducted by García et al., to produce capsules by immersing the porous sand in the rejuvenator (the cooking oil). It was suggested that this step is one of the initial steps in building smart road pavements [53].

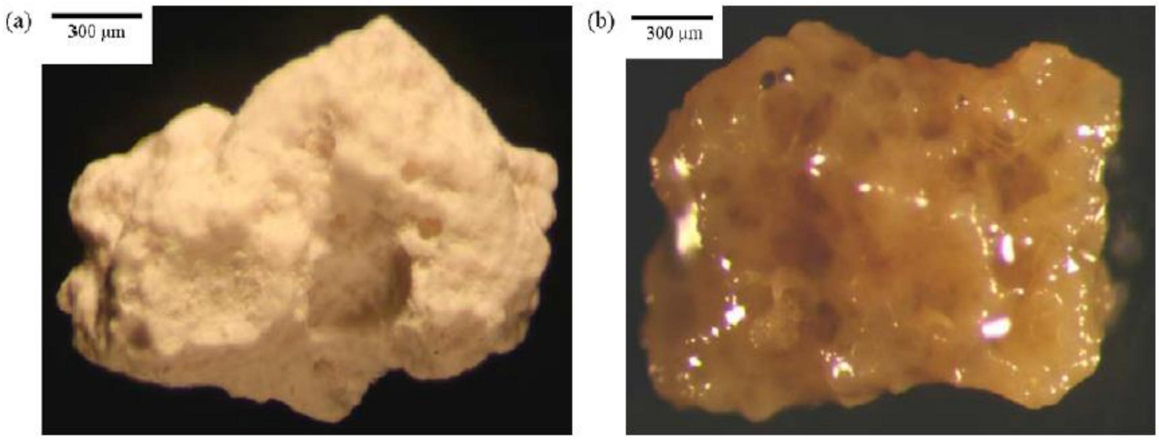

Figure 2.15. Optical micrograph of the core materials of the capsules: (a) porous stone used; (b) porous stone with the rejuvenators embedded [53].

In the study conducted by Garcia et al., the rate of asphaltenes to maltenes was determined in aged binders. In the aged bituminous binder samples, rejuvenators were used in order to provide the asphaltene/maltene rate prior to aging. These materials were used with the aim of reducing the loss of thin particles on the surface and reduce possible cracks. However, because the rejuvenators are required to penetrate from the surface towards the bottom in order to become effective and because they reduce the shear resistance, these rejuvenators were encapsulated and mixed into the asphalt cement. The idea behind this implementation was the fact that capsules crack upon the pressure inside them exceeds a certain value, releasing the rejuvenators. In the study conducted by Garcia et al., the properties of these capsules were emphasized. Four different types of rejuvenators were encapsulated and the effects of the capsules were investigated. On the other hand, the releasing mechanisms of the capsules were attempted to be discovered. Finally, the capsules were included in a porous asphalt mixture and when the asphalt sample was cracked by the indirect tensile test, the images of cracks were examined by microscopes (Figure 2.16). According to the obtained results, the rejuvenating effects of the microcapsules on bitumen and the optimum shell thickness of the microcapsules were determined [59].

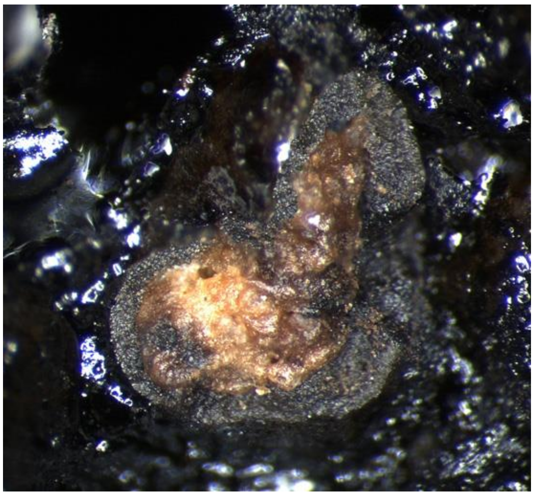

Figure 2.16. Broken capsule after an ITT test [59].

In the study conducted by Qui et al., it was suggested that the self-healing property of bituminous binders are known for a long time. Researches who previously studied the rheology of bituminous materials generally focused on self-healing following load implementations (such as elastic behavior). Because these tests are complex and take a long time, a simpler self-healing test was presented in this study. In this method, cracking –

repairing - re-cracking and image processing were used in combination. Initially, a 100-200 µm crack formation was caused by rapid loading. Then, the sample was placed in a silicon mold, causing it to self-heal. Various repairing periods, temperatures and additives were tested. The change in the repairing process was observed by using a fluorescent microscope (Figure 2.17). Following this process, the sample was cracked under the same conditions. In the obtained results, it was determined that with the increased self-healing period and ambient temperature, the load-carrying capacity increased in the second crack. With strength values and microscope images, it was also determined that the healing consisted of two stages, the first one being the closure of the crack and the second one being the improvement of the strength. Additionally, in the study, it was determined that the self-healing abilities of the mixtures prepared with SBS additive were lower compared to the mixtures prepared with B 70/100 class pure binder. The obtained results indicated that the suggested method was simpler and more effective in terms of the self-healing of bituminous binders [60].

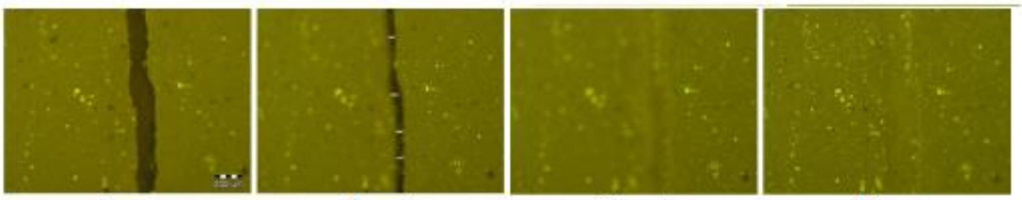

Figure 2.17. Fluorescent microscope observation of the crack healing at various periods (0, 1, 3 and 18 hours) [60].

The main problem of using reclaimed asphalt pavement (RAP) material in hot mix asphalts (HMA) is the bitumen's aging which limits the percentage of RAP used in HMA. Within this scope, the rejuvenation of bituminous binders is the most significant yet the most costly part of recycling. In this study, the use of waste cooking oil (WCO), which is obtained from the food industry and usually considered as a waste material that pollutes the dumpsites and rivers, was investigated as a novel method of rejuvenating bituminous binders. The original bitumen, aged bitumen and rejuvenated bitumen were measured for their physical properties and were analyzed with traditional bituminous binder tests such as softening point, penetration and Brookfield viscosity and statistical analyses were conducted to evaluate the results. Generally, the results indicated that the aged bitumen was rejuvenated by WCO depending on a change that occurred in the physical properties, which were similar to the physical properties of the original bitumen (80/100). The optimum waste cooking oil percentages for 50/60, 40/50 and 30/40 rejuvenated aged bitumen groups were determined to be 1%, 3-4% and 4-5% WOC, respectively. Additionally, the statistical analyses indicated that there was no significant difference between the original bitumen and the rejuvenated bitumen [61].

Mastic asphalt is a self-healing material. As a result of various factors such as repeating traffic loads or freezing-thawing cycles, cracks may form in the asphalt mixture. However, when a crack in a pavement becomes plain, it starts healing and if there is enough time to complete the process, it can completely close. Because the self-healing property of mastic asphalt directly depends on the temperature and resting period, it can be classified as a thermally induced material. Additionally, it is well known that the speed of occurrence of this phenomenon directly increases with increased temperature (Figure 2.18). In this study, it was suggested that the changes in the self-healing rate with temperature could be related to the Arrhenius equation. Thus, a certain activation energy is required for the healing. In order to calculate that, a series of mastic asphalt beams were broken and healed at different temperatures, and the completion time of the healing was used to calculate the activation energy. Furthermore, the brittle flow from the cracks was determined to be the main reason for the healing. Finally, the healing process of one of the asphalt beams was observed with CT-scan tests, providing a visual proof [62].

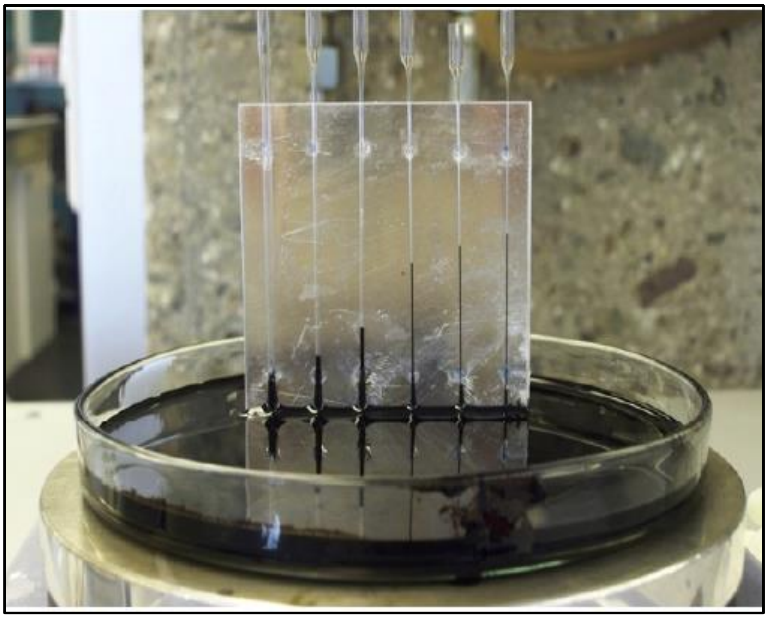

Figure 2.18. Capillary flow experiment [62].

Self-healing cemented materials that contain a microcapsuled rejuvenator material are attractive due to their great potential of improving the serviceability and durability of concrete structures. In this study, poly (phenol-formaldehyde) (PF) microcapsules, which aim to provide a self-healing function for cemented materials, were manufactured with an in situ polymerization reaction. The size gradation of the synthesized microcapsules was determined by a series of eliminating processes. Shell thickness and the diameter of a single microcapsule were accurately measured by using environmental scanning electron microscopy (ESEM). The relationship between the physical and micromechanical properties of the synthesized microcapsules was examined by the nanoindentation method. The results of the mechanic tests indicated that with the increase in the average size of the microcapsules and the decrease in the shell thickness, the mechanical strength required for triggering the self-healing correspondingly increased between 68,5 _ 41,6 mN and 198,5 _ 31,6 mN, which indicates a very sensitive triggering process. Finally, the rupture behavior and crack surface of the cement mixture with embedded microcapsules were observed and analyzed by using X-ray computerized tomography (XCT). Synthesized PF microcapsules can have a potential area of implementation in self-healing cemented materials. The morphology of the manufactured microcapsules was presented in Figure 2.19 [63].

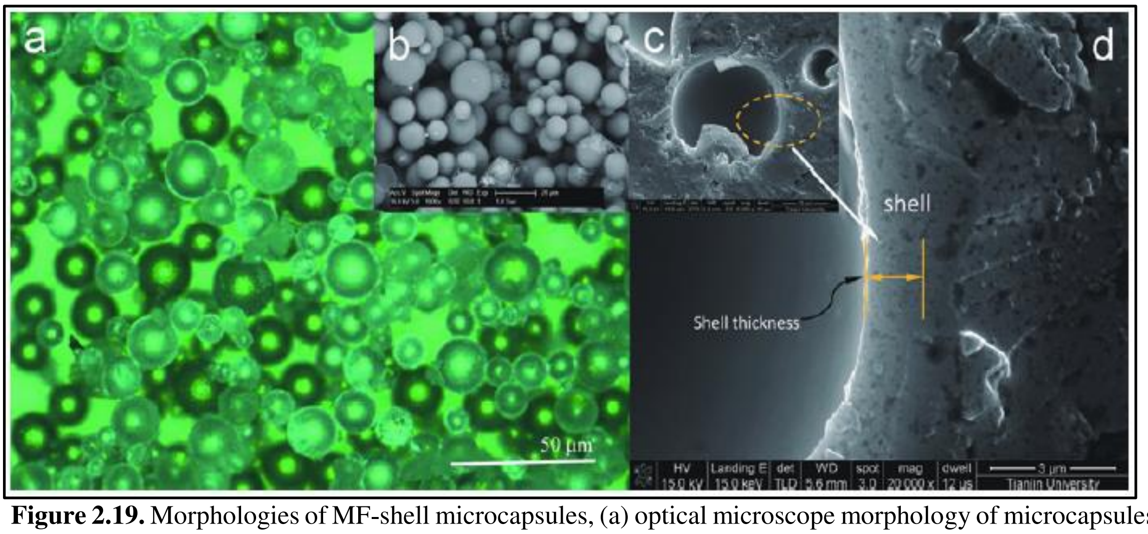

Figure 2.19. Morphologies of MF-shell microcapsules, (a) optical microscope morphology of microcapsules fabricated with core/shell ratio of 1/1 under core material stirring rate of4000rmin_1, (b)SEMmorphologyofwithcore/shellratioof1/1undercorematerialstirringrateof4000rmin_1, (c)thecross-sectionSEMmorphologyofasingle microcapsule embedded in epoxy, and (d) the measurement method of shell thickness by SEM [63].

In the study conducted by Feng Su et al., based on their previous study, the thermal stability, mechanical stability and interface stability of microcapsules included in bitumen were investigated. The results indicated that these microcapsules with rejuvenators endured the melted bitumen and repetitive temperature changes. Because microcapsules have the ability of elastoplastic deformation, it was observed that they resisted the temperature changes and mixing pressure. Additionally, chemical bonds improved the interface stability between the bitumen and the shell. The authors believed that the microcapsules containing rejuvenators are promising materials in actualizing smart pavements [10]. SEM images of microcapsules were presented in Figure 2.20 [58].

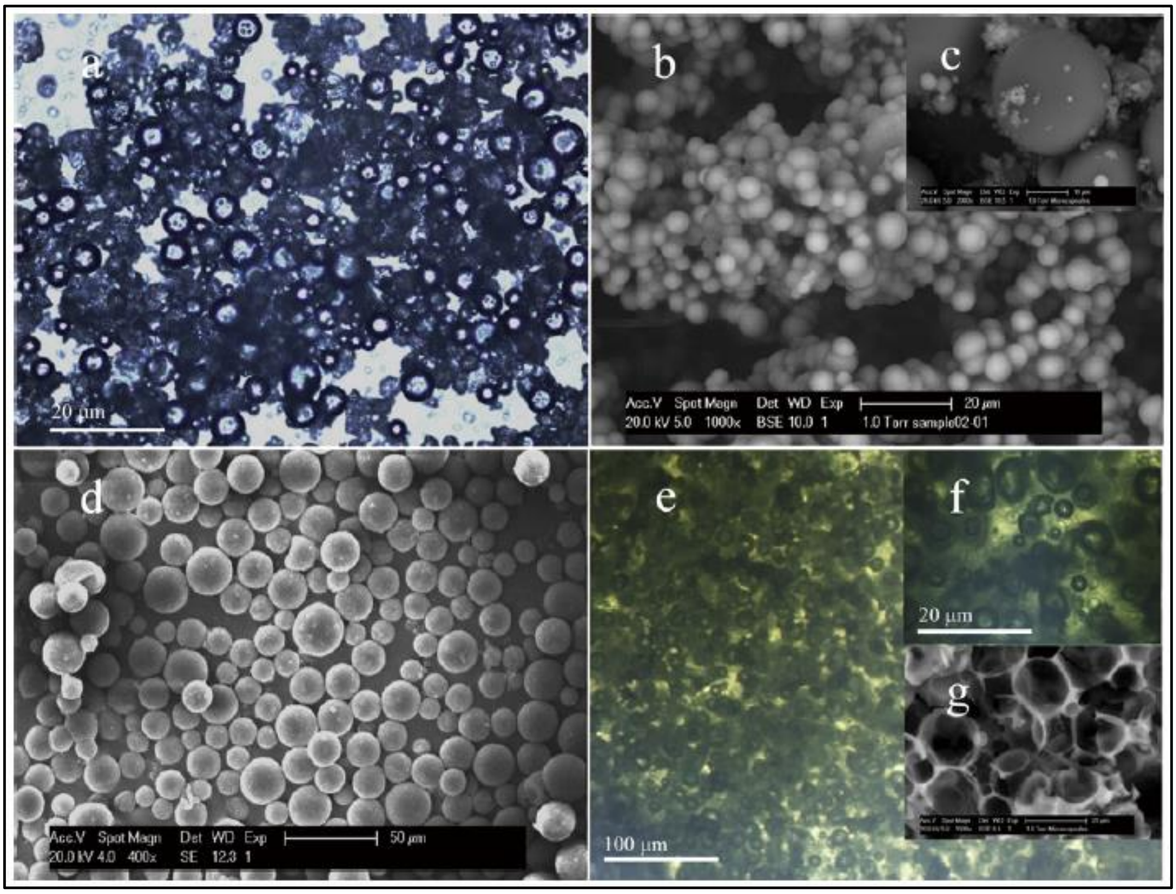

Figure 2.20. Morphologies of microcapsules containing rejuvenator, (a) optical morphology of microcapsules in emulsion, (b) SEM morphology of dried microcapsules, (c) smooth surface of single microcapsule, (d) SEM morphology of dried microcapsules with larger size, (e, f) optical morphology of microcapsules embedded in epoxy resin, and (g) cross-section SEM morphology of microcapsules [58].

In the study conducted by Garcia et al., the effects of the capsules with viscous oil included in the asphalt mixture (low viscosity) upon breaking under simulated traffic load were investigated (Figure 2.21). For this purpose, capsules containing sunflower oil were manufactured and the mechanical composition and strength were characterized. Later, the capsules were included in hot mix asphalts as aggregates and compacted. In order to determine the effects of the capsules included in the hot mix asphalt, the samples were subjected to periodic loading, rested and re-tested. The magnitude and differences between the loadings before the test and following the resting period provided an opportunity to determine the effects of the capsules inside the asphalt mixture. Additionally, the opening and healing processes of the cracks were observed before the test, after period loading and following the resting period by using computerized tomography scan. As a result, it was observed that capsules were gradually cracked during the exertion of the period pressure and the released oil from the capsules during the resting period softened (healed) the bitumen (Figure 2.21) [54].

(a) (b)

Figure 2.21. (a) Test sample before testing. (b) Test sample after testing, with capsules broken [54].

Li et al. investigated the microcapsule use to repair the cracks formed in how mix asphalts due to traffic and environmental loads. These microcapsules were manufactured by using the in situ polymerization method with urea formaldehyde resin. It was aimed to trigger the release of the healing agent upon the cracking of the microcapsules, joining the damaged parts. The shell thickness and shell density were increased by adding more pre-polymers in the manufacturing process. The optimum conditions were carefully studied in order to examine the synthetic microcapsule. The results of thermal stability indicated that the breaking temperature of the microcapsule was higher than the melting temperature of the bituminous binder. The optimum microcapsule rate was determined to be 0.3%. With the use of microcapsules at an optimum rate, the healing effect was improved by 38.67%. It was determined that microcapsules healed the cracks in hot mix asphalt (HMA) pavements in a way that provides savings in the maintenance costs and improves the performances of HMA pavements [65].

In the study conducted by Chung et al., the capsules, which were used to heal the cracks formed in hot mix asphalts, were manufactured with dimethylphenol (DMP) or SBS/DMP while the shells were manufactured with urea/formaldehyde resin. The samples of hot mix asphalts with microcapsules demonstrated better mechanical properties compared to the samples of hot mix asphalt without capsules. The impact resistance of hot mix asphalts with microcapsules improved in time. While the samples of DMP including hot mix asphalts with microcapsules required a 7-day resting period in order to regain the resistance of the samples without microcapsules, this period was determined to be only 3 days for SBS/DMP including microcapsules HMA samples (Figure 2.22). This result indicated that the microcapsules (including DMP or SBS/DMP) had a flawless self-healing potential. SEM and X-ray images demonstrated that the DMP that is released from the microcapsules upon crack formation fills the cracks on the HMA surface and repairs the damage [65].

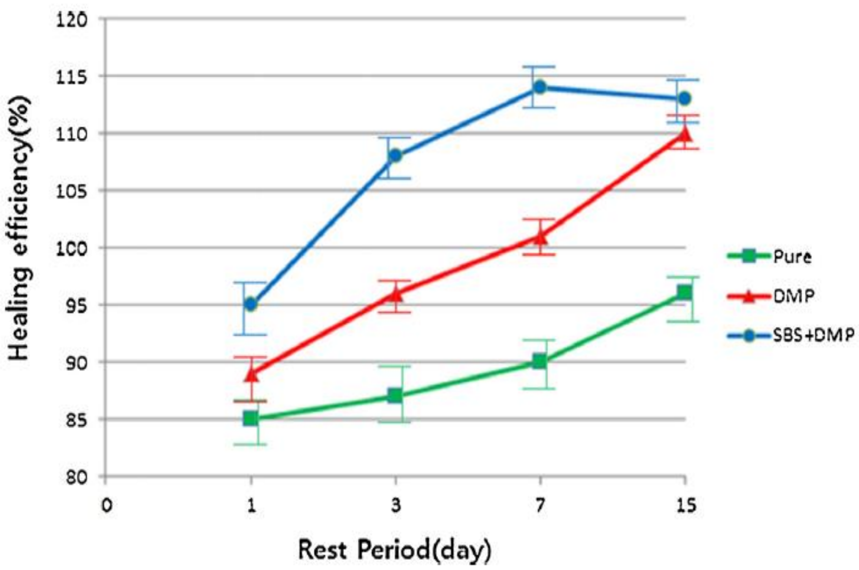

Figure 2.22. The required resting periods for mixtures with healing agents [65].

In the study conducted by Feng Su et al., the properties of the hot mix asphalts with microcapsules, which contained waste cooking oil (micro WCOs), were investigated in order to heal aged bitumen in situ. Micro WCOs were successfully manufactured by using the in situ polymerization method with methanol melamine formaldehyde (MMF) pre-polymer as the shell material. Properties such as morphology, size, shell thickness and mechanical properties were adjusted by emulsion speed and core/shell rate. The thermal stabilities of the micro WCOs inside bitumen and their resistance to repeating temperature changes were presented in Figure 2.23. The obtained results indicated that WCOs can easily penetrate aged bitumen as a healing agent. Following the healing, the aged bitumen's initial properties, which include penetration rate, softening point value and viscosity value, were observed to be improved [66].

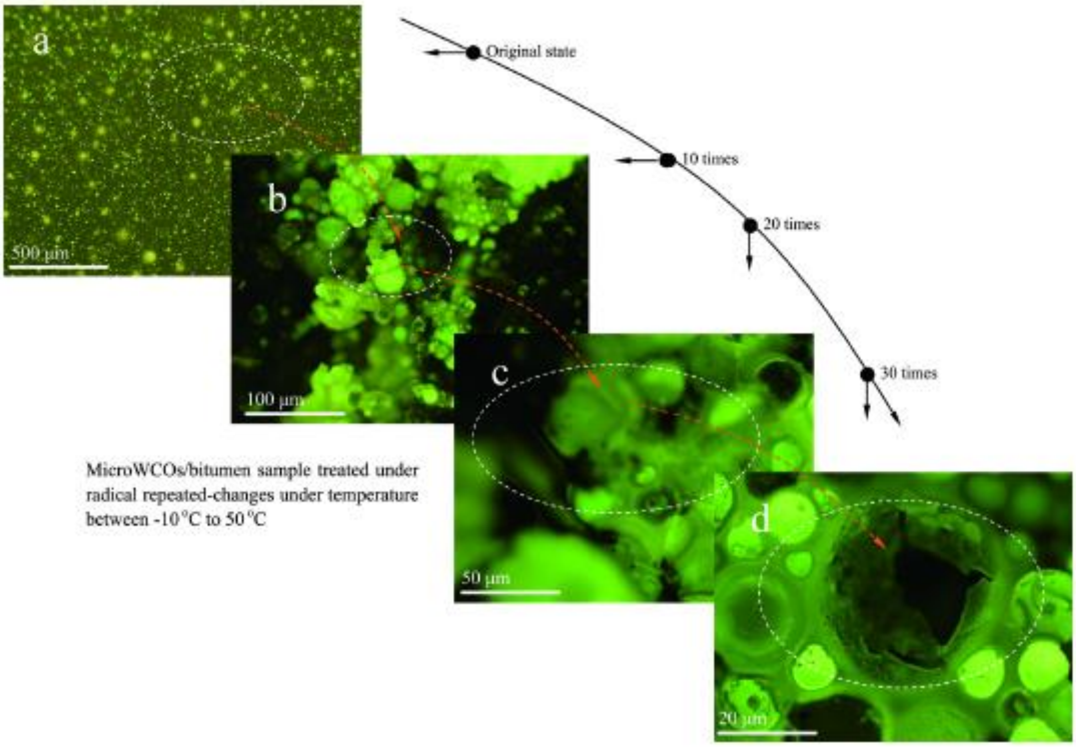

Figure 2.23. The examination of micro WCO samples' morphology under temperatures between -10 ºC and 50 ºC and repeated changes with a fluorescent microscope [66].

In the study conducted by Feng Su et al., the self-healing mechanism of aged bitumen depending on the use of microcapsules with healing agents. Various capsule samples were successfully manufactured and the average size and shell thickness were adjusted. It was determined that the shell thickness is not significantly affected by the core/shell rate and emulsion mixing rate. These microcapsules were determined to demonstrate a resistance by having a sound thermal stability inside melted bitumen. According to this data, a typical microcapsule sample, which has a 2/1 core/shell rate and manufactured with 300 r.min-1, was chosen to examine the self-healing mechanism. The whole self-healing process was observed in a way that covers crack formation, brittle behavior and diffusion behavior. The results indicated that with crack propagation, the microcapsule was broken and the oily-liquid was released into the micro crack (Figure 2.24). With capillarity behavior, the rejuvenator filled the cracked by having a movement speed that is basically determined by the volume of the microcapsule inside the bitumen. Additionally, a diffusion case was also observed in the fluorescent microscope images. The measurement of initial and healed bitumen properties proved that aged bitumen could be partially healed by using microcapsules with rejuvenators [67].

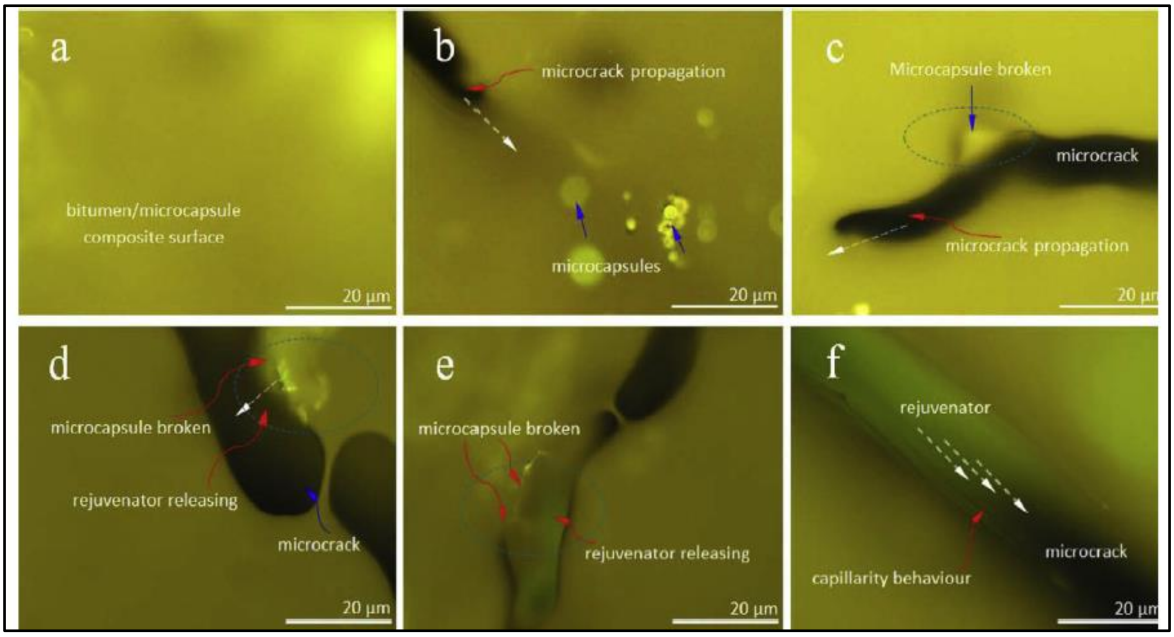

Figure 2.24. The capillarity behaviors of rejuvenator in self-healing bitumen by microcapsules, (a–c) a micro crack was generated by liquid N2 with the width about 10–15 lm, the micro crack propagates and pierce the shells of microcapsules, (d and e) the liquid of rejuvenator leaked out from microcapsules and flowed into the microcapsules, and (f) movement trace and direction of rejuvenator during the capillarity [67].

In the study conducted by Garica et al., it was aimed to extend the lives of pavements and reduce the negative effects of not meeting the current maintenance processes by including rejuvenator capsules in hot mix asphalts. In this study, the use of capsules with oil as rejuvenators in hot mix asphalts was examined. The implemented capsule material was presented in Figure 2.25. For this purpose, capsules with 5 different diameters were manufactured and their mechanical strengths and components were characterized. Then, they were mixed into the hot mix asphalts and their mixing and compacting resistances were observed. Finally, the capsules' effects on the fatigue lives, indirect tensile strength and rigidity of hot mix asphalts were investigated. According to the results, capsules with larger diameters had lower strengths compared to capsules with smaller diameters and capsules with more oil content. Additionally, it was determined that capsules resisted the mixing and compaction processes and they reduced the indirect tensile strength and rigidity of the mixture. It was determined that this situation was due to the fact that capsules demonstrated less strength than necessary. It was also determined that capsules did not affect the fatigue lives of the asphalt mixtures [68].

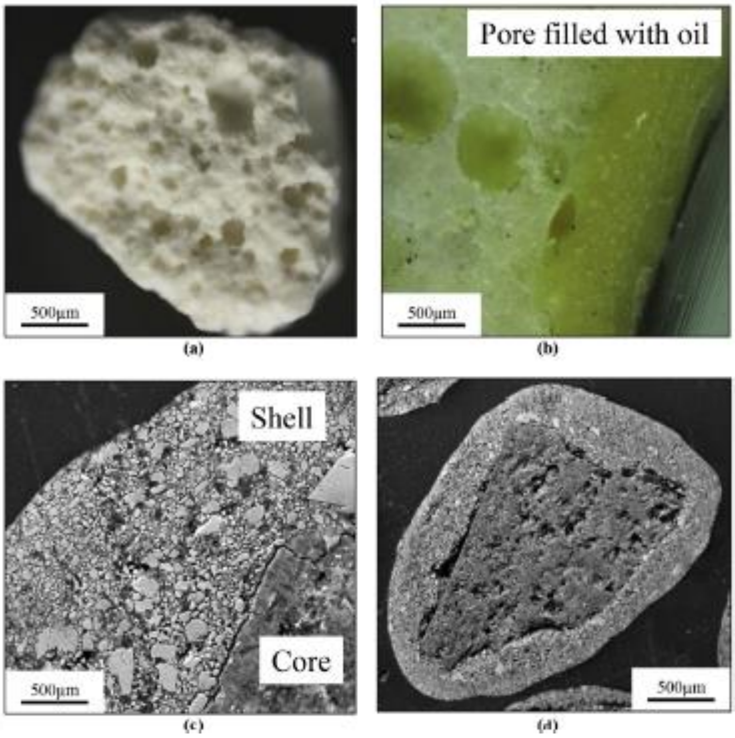

Figure 2.25. (a) Porous sand. (b) Oil contained in the porous sand. (c) Detail of the shell. (d) Capsule [68].

The natural self-healing properties of asphalt mixtures can be improved by encapsulated rejuvenators; when a crack damage occurs, capsules release the rejuvenator material that melts the bitumen and fills inside the cracks. In this study, the effects of a novel capsule on the mechanical properties and the self-healing ability of asphalt mixtures were investigated. Sunflower oil was encapsulated inside a calcium-alginate and protected with a thick shell made from epoxy-cement composite. The results indicated that these capsules did not require a thick shell in order to resist to the mixing and compaction processes. The capsules were deformed and broken with loading and released the oil that spread into the bitumen earlier in a period less than 24 hours. The healing of the cracks in the asphalt mixture caused the stiffness to increase. However, asphalt samples with capsules had lower deformation resistance. The computerized tomography scan of the samples indicated a significant reduction in the cracks surrounding the capsules after a resting period of 4 days at 20 °C. The CT scan images were presented in Figure 2.26 [69].

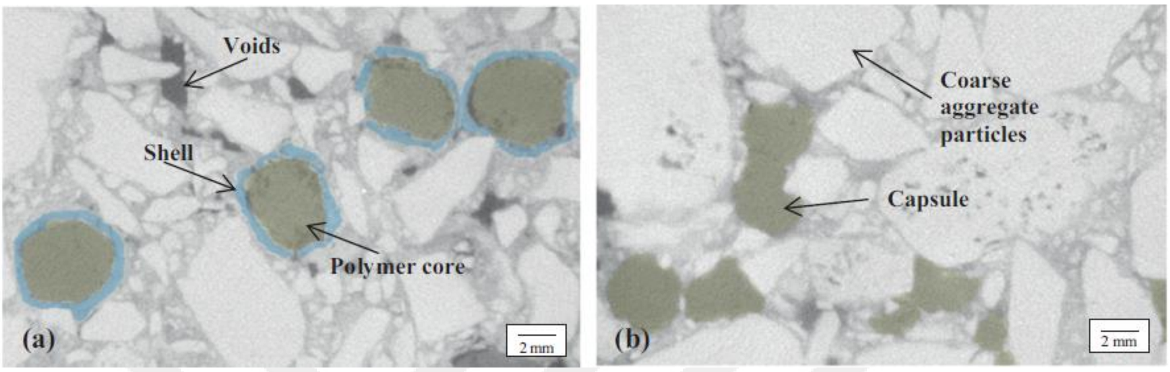

Figure 2.26. CT images of asphalt specimens with capsules type (a) II and (b) III [69].

The investigation of the basic properties of microcapsules and the results' use in developing various materials in industries such as fast moving consumer goods, pharmacy products and agricultural chemicals are dynamic and ever-developing fields of study. In order for the microcapsules to provide protection in a difficult environment and become effective in carrying large loads, the properties should be successfully understood to provide quality control during formulation, storage and implementation. In this study, the common techniques used to determine the physiochemical, structural and mechanical properties of microcapsules were aimed to be presented in general terms and the interconnected nature of these three fields' final uses were emphasized in terms of industrial implementations. The study provides information regarding the supported techniques in the literature and also investigates microcapsule analytic techniques, which can be more common by technological developments or the extents of other fields of study. The changes in the microcapsules during the applied loading were presented in Figure 2.27 [70].

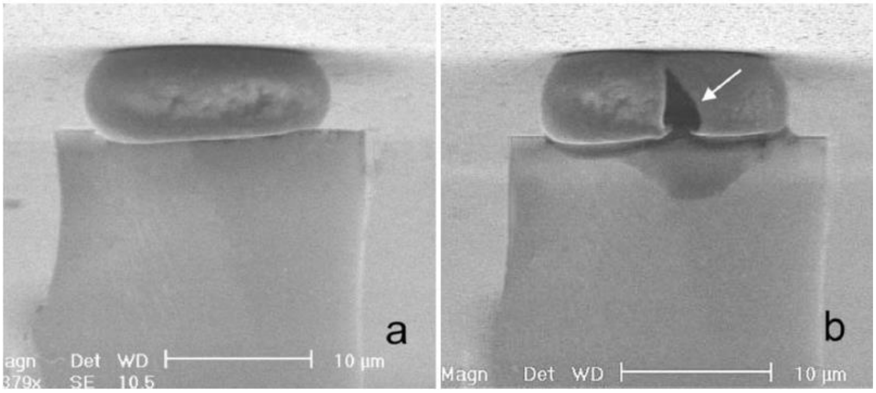

Figure 2.27. Images of microcapsule (diameter 16.5 _m) during compression and after rupture by nanomanipulation in chamber of environmental scanning electron microscope under high vacuum (5 kV, spot size 4): (a) microcapsule being compressed and (b) microcapsule being ruptured [70].

Self-healing microcapsulation in asphalt cement is a novel technology that provides this special material with resistance to cracking damage, which results from vehicle and environmental loads. The aim of this study is to investigate the effects of the asphalt rejuvenators on asphalt binders, choosing a suitable rejuvenator for materials with asphalt and develop a synthesis procedure for the microcapsulation of the asphalt rejuvenators. The manufactured microcapsules were characterized by using scanning electron microscopy (SEM) in order to evaluate the effects of preparation parameters on the microcapsules' sizes and morphologies (Figure 2.28). As a result of the test program, it was determined that using sunflower oil as a rejuvenator was effective in reversing the aging of the asphalt binder and affected the binder positively at both very high and very low temperatures. However, using Pennz Suppress as a rejuvenator is not effective in reversing the aging of the asphalt binder and did not marginally affect the degrees of binders aged and extracted at very high and very low temperatures. According to these results, the microcapsulation of sunflower oil was chosen considering its effectiveness in reversing the aging of the asphalt binder. A synthesis procedure was developed in order to characterize the properties of the microcapsules such as diameter and morphology for the preparation of sunflower microcapsulation [71].

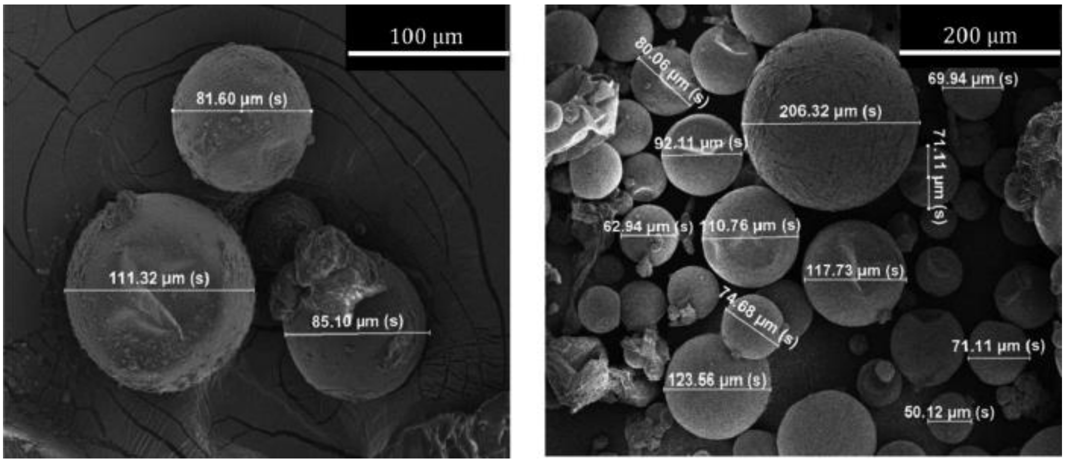

Figure 2.28. Effects of temperature on the prepared microcapsules at (a) 50°C; (b) 60°C [71].

The aim of this study is to evaluate the self-healing behavior of bitumen through the repeated tensile test with modified crack healing-refractor method by using microcapsules containing rejuvenators (Figure 2.29). Microcapsules had 1/1 core/shell ratio and 10, 20 and 30 _m average size values. Various microcapsule/bitumen specimens were manufactured with 1.0%, 3.0% and 5.0% microcapsule content by weight. Microcapsule/bitumen specimens were measured with tensile strength values and a reparative cracking-healing process at various temperatures. These specimens were observed to have higher tensile strengths following four tensile cracking-healing cycles compared to pure bitumen specimens under the same conditions. Crack morphology examination and mechanism analysis demonstrated that the self-healing process consists of cracked, penetrated and spread microcapsules. Additionally, bitumen's crack healing process can be evaluated a viscosity-focused process. The ability of self-healing partially repaired the bitumen damage during the service life, according to the comparison made between untreated and rejuvenated bitumen properties [72].

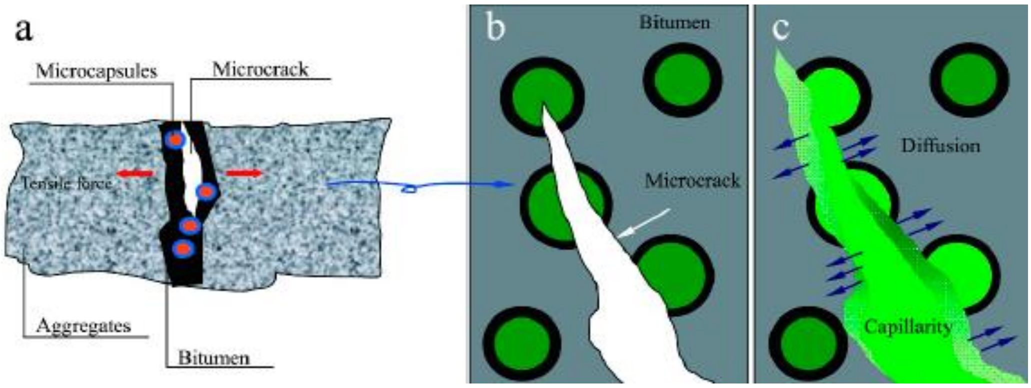

Figure 2.29. Illustration of the self-healing process of aged bitumen by microcapsules containing rejuvenator: (a) the structure of asphalt consisting of bitumen and aggregates; (b) microcrack generation and microcapsules broken; and (c) the self-healing of aged bitumen by leaked rejuvenator with the help of diffusion [72].

Asphalt pavement roads are exposed to natural elements such as rain, sun light and oxidation in addition to traffic load that reduces its comfort capability and crack formation. Novel maintenance techniques such as developing rejuvenating microcapsules have emerged in order to reverse the aging process of asphalt binders. The aim of this study is to evaluate the effectiveness of asphalt rejuvenators in reversing the aging process in asphalt binders and develop a microcapsulation process for the tested asphalt rejuvenator. The properties of the manufactured microcapsules such as size, shell thickness and morphology were evaluated by changing manufacturing parameters, namely the mixing rate, heating temperature and the concentration of Ethyl Methyl Acrylate (EMA). In the test program, three binders were evaluated: two binders that were aged in laboratory and not used and Reclaimed Asphalt Pavement (RAP). According to the results of the test program, it was concluded that the Performance Grade (PG) 70-22 of the binder was partially regained at both high and low temperature by using rejuvenators. Contrarily, binder PG 76-22's low temperature and RAP binder's high temperature were recovered by using the tested rejuvenator material. The microcapsules with rejuvenators were synthesized and characterization processes for the microcapsule properties of the prepared microcapsules such as diameter, shell thickness and morphology were conducted [73].

Melamine-formaldehyde (MF) microcapsules were implemented in a number of functional materials at a wide scale. Micromechanical properties are significant properties that determine whether the microcapsules could resist the manufacturing and implementation processes. In this study, the nanoindentation method was successfully implemented as an effective method to measure the micromechanical properties of microcapsules containing paraffin. The manufacturing of a series of MF-shell microcapsule in various sizes and thicknesses by controlling the core material mixing rates (1000-8000rmin_1) and load-displacement curves, indicated that MF shells had elastic-plastic deformation. Both stiffness and Young's modules were based on size and shell thickness parameters. The results confirmed that larger microcapsules' larger modules and thicker shells could increase the microcapsules' abilities to resist deformations and increase core/shell weight rates (1/1, 1/2 and 1/3). Load-displacement curves indicated the MF shells had the elastic-plastic deformation abilities. Both stiffness and Young's modules were based on size and shell thickness parameters. The results confirmed that larger microcapsules had higher modules and thicker shells could improve the microcapsules' ability to resist deformation. The XCT images of microcapsules were presented in Figure 2.30 [74].

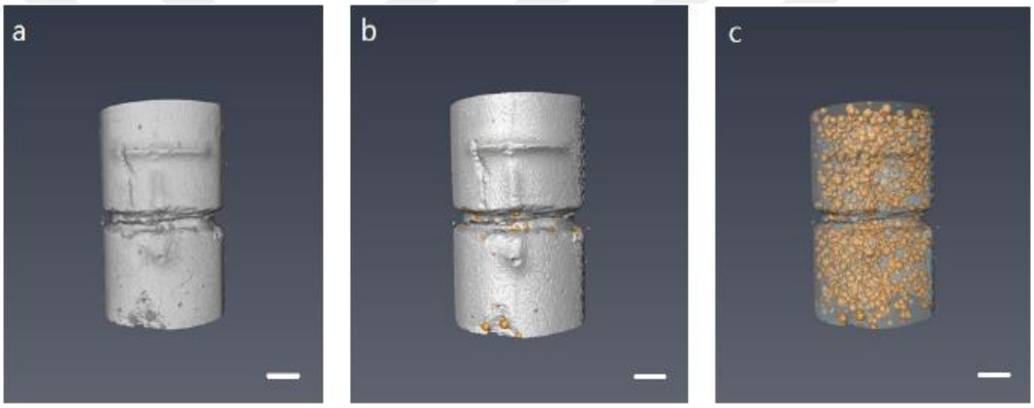

Figure 2.30. XCT visualization process of microcapsules' embedded cement paste cylinder including (a) volume construction; (b) surface generation; and (c) transparent adjusting. The scale bar is 2 mm for all three images [74].

The aging problem of bitumen causes the pavement to degrade after years of use. Microcapsules containing rejuvenators are promising chemical products that are used for improving the self-healing ability of bitumen. The aim of this study is to manufacture self-healing microcapsules that contain bitumen rejuvenator with nano-inorganic/organic hybrid shells and determine their characteristics. The shell had a two-layered structure: the inner layer material is crosslinked methanol modified melamine-formaldehyde (MMF) resin and the outer layer contained methanol modified MMF resin and nano-calcium carbonate particles (nano-CaCO3). The manufacturing mechanism of the two-layered structure was identified based on two-layered consolidation process. The results of fourier transform infrared spectroscopy (FTIR) and Energy Dispersive Spectroscopy (EDS) confirmed the shells' inorganic/organic hybrid structure. The ideal content of nano-CaCO3 particles was optimized by observing the morphology. The inclusion of nano-CaCO3 particles did not affect the average sizes of microcapsules greatly. Contrarily, nano-CaCO3 particles increased the shell thicknesses of microcapsules due to the loose composite structure of the shells. Thermal stability tests indicated that microcapsules could endure 200 ºC temperatures inside bitumen. Additionally, the microcapsules resisted a severe temperature changing process regardless of a demolition based on the protection of the particles. The nano-particles on the microcapsules decreased the deformation possibility of shells that were tested with nanoindentation method (Figure 2.31) [75].

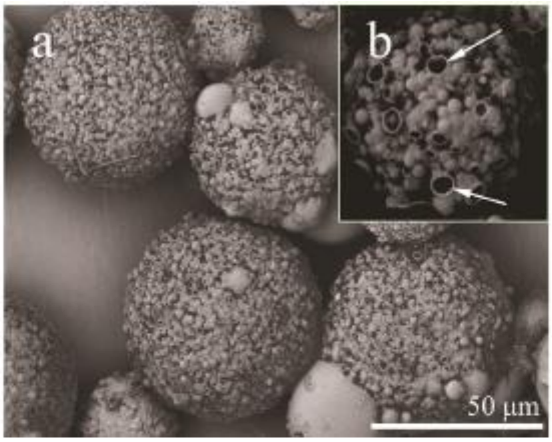

Figure 2.31. ESEM morphologies of microcapsules with 10% nano-CaCO3 composite shells [75].

The aging problem of bitumen causes the pavement to degrade after years of use. It was determined that the microcapsules rejuvenators could be an alternative approach to improve the self-healing ability. The aim of this study is to investigate the bitumen’s self-healing behavior by using microcapsules with rejuvenators, which have various shell thicknesses and various size distributions. The microcapsule specimens consist of three types of microcapsules that have different average sizes and shell thickness values. In order to examine the mechanical properties of the bitumen/microcapsule materials, beam on elastic foundation (BOEF) method was adopted. The results indicated that these microcapsules were broken by micro cracks under different circumstances with a normal distribution. The microcapsules that left around the micro cracks had the ability to release the rejuvenator with a later-formed micro crack that has a higher crack tip strain. Following the loading-unloading cycles, microcapsule/bitumen composite’s multiple self-healing abilities were softened by rejuvenator’s release into the bitumen. The properties of unused and rejuvenated bitumen confirmed that microcapsules with rejuvenators had multiple healing abilities. In order to analyze the mechanism of multiple self-healing processes, both mechanical healing and physical-chemical healing model were implemented. A number of times more healing ability was possessed by regulating microstructure, viscosity and bitumen's thixotropy with a stable change. The rejuvenator's movement in aged bitumen was presented in Figure 2.32 [76].

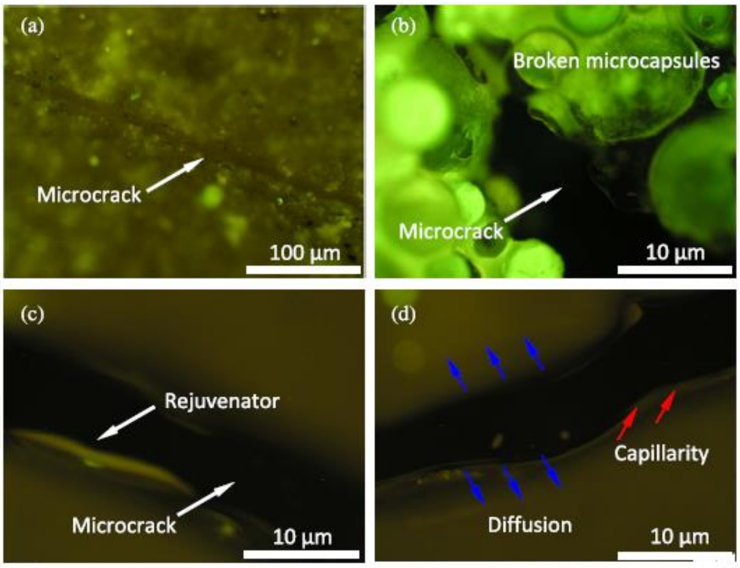

Figure 2.32. Fluorescence microscope morphologies of rejuvenator movement in aged bitumen, (a) microcrack in microcapsule/bitumen composite, (b) the shells of microcapsules broken by microcracking, and (c and d) the movement traces and direction of rejuvenator induced by capillarity [76].

In this paper, studies were aimed at developing a novel type of polymeric microcapsule with phenol- formaldehyde (PF) resin as the shell and dicyclopentadiene (DCPD) as the rejuvenator for self-healing micro cracks in cement based materials. PF/DCPD microcapsules were synthesized by in situ polymerization and they were characterized by optical microscope (OM), scanning electron microscope (SEM) and thermal analysis (TGA) (Figure 2.33). The chemical stability and trigger performance of the synthesized microcapsules were examined in simulated concrete pored solution and hardened cement mixture samples, respectively. The results revealed that the synthesized microcapsules had perfect stability in both simulated porous solution and real cement environments. In order to observe the state of the microcapsules inside cement mixture and crack behavior, X-ray computerized tomography (XCT) scan was conducted. Further segmentation of the restructured data obtained from XCT and 3 dimensional restructured data indicated that the microcapsules had the desired trigger sensitivity and a sound distribution. An OM research of a cracked surface in a cement mixture combined with microcapsules confirmed that the self-healing function of the microcapsules can be triggered by cracking and the rejuvenating material can be released at the same time in order to heal the cracks [77].

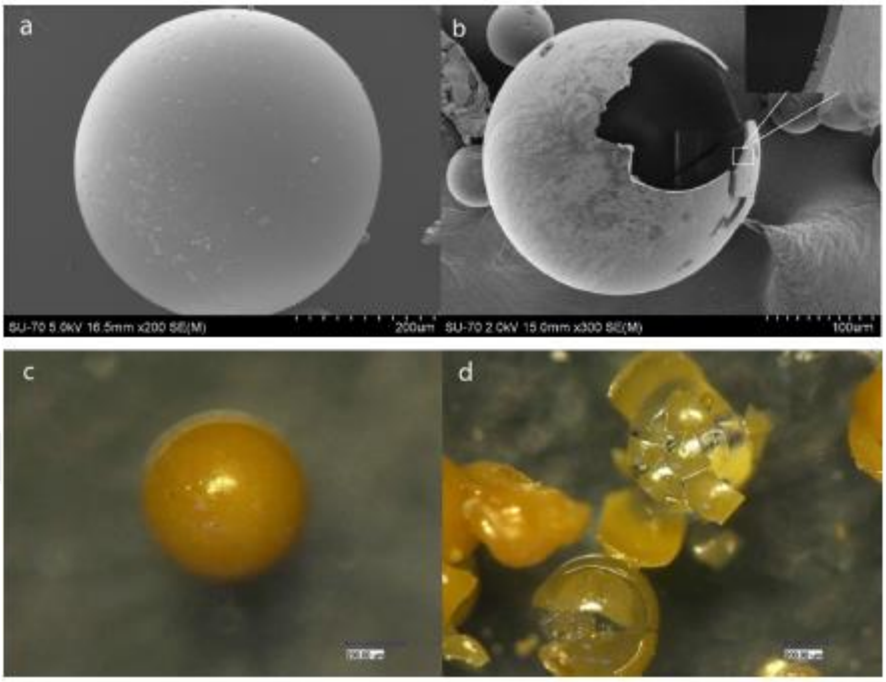

Figure 2.33. SEM and OM images of (a) surface morphology of a microcapsule, (b) a ruptured microcapsule and the wall thickness, (c) a single microcapsule, and (d) broken microcapsules compressed by two parallel glass sheets [77].

In this study, calcium-alginate capsules, which could release their vegetable oil contents with a mechanical trigger, were manufactured and they were included in asphalt mixtures in order to improve the natural self-healing properties. The physical, mechanical and self-healing properties of the asphalt mixtures with those capsules were investigated for the first time. An image of a capsule exposed to the air after particle loss testing was presented in Figure 2.34. Three different capsule contents with oil-bitumen rates of 1.1, 2.8 and 5.5, respectively, were used. The capsules strongly bonded with the asphalt mixture and the results of water sensitivity, particle loss and permanent deformation indicated a similar mechanical performance to asphalt with and without capsules. This indicates that capsules used for the self-healing of asphalt could be used safely on the roads without affecting the quality. The asphalts with capsules had a slightly lower stiffness and this can be solved by the reducing the capsule size in the future. Additionally, a new method was designed and tested to analyze the asphalts with capsules. It was observed that cracked asphalts with capsules were improved by 52.9% compared to their initial strength at 20°C while this rate was 14.0% for asphalts without capsules [78].

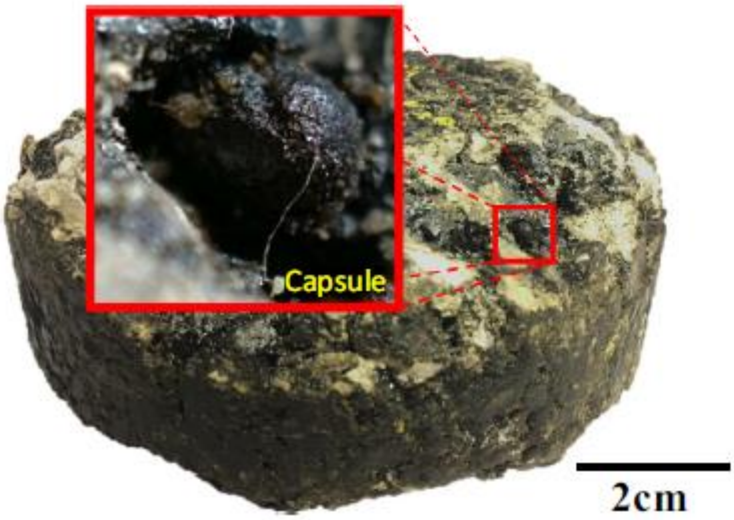

Figure 2.34. Image of a capsule exposed to the air after particle loss testing [78].

Asphalt materials are inevitably exposed to aging, temperature and load-based cracking problems, however, recently microcapsules containing rejuvenators provide a promising way to solve these problems. In this study, microcapsules were prepared by in situ polymerization method and their optimum manufacturing conditions were carefully analyzed. Then, the morphologies, particle sizes, pavement speeds, thermal stabilities and molecular structures of the microcapsules were extensively investigated. Additionally, the self-healing capabilities of the asphalts with mixtures were completely investigated under low temperature and fatigue loading conditions. The results revealed that microcapsules could stay intact during the asphalt melting process and demonstrated a fine healing performance under lower temperature and fatigue loading conditions, however, it was also observed that the healing efficiency was initially improved and then with additional microcapsule content, it decreased and the most suitable amount of additional microcapsule amount was 0.3-0.5% of the asphalt weight [79].

Microcapsules with rejuvenators are particles used for improving the self-healing capacity of asphalts. Until today, no report focused on their behavior in asphalt binders between aggregates. The aim of this study was to directly observe the status of microcapsules included in self-healing asphalt binders. The morphology is presented in Figure 2.35. Asphalt samples were prepared by mixing bitumen and microcapsules at various amounts.

The asphalt binders were subjected to experimental tests in order to determine their morphology, integrity, dispersion, thermal stability, interface connection and the triggered rupture of microcapsules. Fluorescent microscope morphologies and x-ray computerized tomography images indicated that microcapsules kept their durability without any damages against the high temperature and strong agitation in asphalt. Additionally, microcapsules were homogenously dispersed in the asphalt, which inhibits particle aggregation and adhesion. In order to simulate the temperature changes of a natural environment, circular heating-cooling process was used. Even after extreme temperature changes, the microcapsules were observed to be stable. Furthermore, there was no reduction in adhesion in the interface [80].

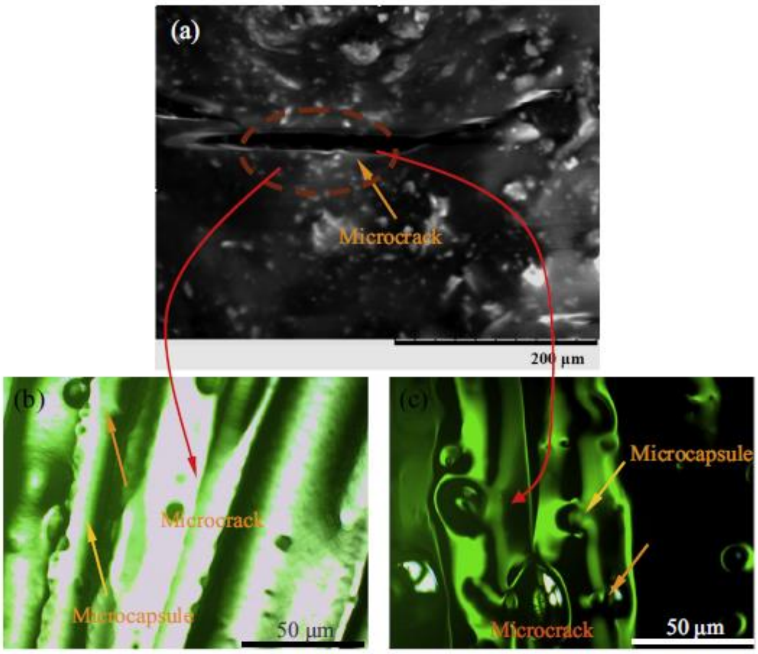

Figure 2.35. Morphologies of microcapsules in a microcrack in asphalt, (a) ESEM morphology of a microcrack, (b) fluorescence microscope morphology of microcapsules in a microcrack, and (c) fluorescence microscope morphology of microcapsules in a microcrack after 60 min [80].

Self-healing materials such as microcapsules filled with asphalt rejuvenators are present a new technology that enables asphalt mixtures to resist to cracking damage caused by vehicle and environment loads. The aim of this study is to determine properties of microcapsules prepared in laboratories in order to evaluate the microcapsules' self-healing effect as well as asphalt mixtures' thermal stability. In order to evaluate the healing efficiency and strength regain of asphalt mixtures under two healing circumstances, which are at room temperature and high temperature, three-point bending test was used. In order to measure the healing process of the samples as a time function, an optic microscope was used. It was observed that microcapsules manufactured based on microscopic characterization had a sufficient thermal stability and this was because microcapsules had not demonstrated a cracking indication when exposed to high temperature. The analysis of the microscopic images revealed a reduction in the sizes of the cracks under both healing conditions within a 0 to 6 days period. When the mixing with microcapsules was compared with the control, a lower healing efficiency was observed and this was because not all the microcapsules were broken during the tests and they were designed to be broken at different times rather than at once. The results also indicated that there was an improvement in the stiffness of the mixtures and this was because the healed stiffness was higher than the damaged stiffness while being lower than the undamaged stiffness. A higher stiffness healing was observed at high temperatures and this state could be explained by the binder aging during the 5-day healing period [81].

Asphalt has a self-healing property in its nature. However, the rate of damage occurrence is higher than the damage healing rate. In order to improve the self-healing capability of asphalt materials, microcapsulation technique was considered as a potential method. In order to demonstrate the benefits of the microcapsules technique for the pavement engineering, the fatigue behavior of asphalt cement that self-heals based on microcapsules was investigated. Firstly, melamine urea formaldehyde (MUF) containing microcapsules with rejuvenators were manufactured by in situ polymerization method. The surface morphology, diameter and shell thickness of microcapsules were observed by scanning electron microscopy (Figure 2.36). In order to investigate the components of the microcapsule material, infrared spectroscopy analysis technology was used. Later, in order to investigate the effects of the microcapsule on the asphalt mixture's fatigue life, a four-point bending fatigue-healing-healing test was designed. The test results suggested that 3% microcapsule addition by weight could double the AC-10 asphalt mixture's fatigue life [82].

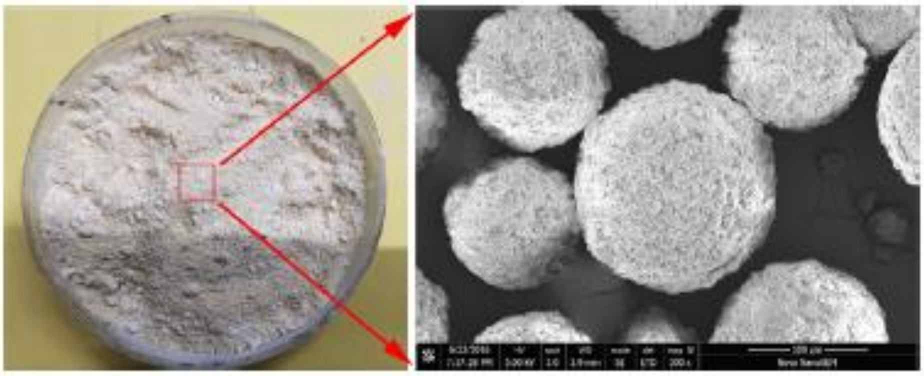

Figure 2.36. Morphology of microcapsules [82].

Microcapsules are considered as a potential method to improve the self-healing abilities of asphalt materials. This study aims to investigate the optimization of the self-healing microcapsule synthesis technology. According to prepolymer synthesis test results, melamine-urea-formaldehyde (MUF) terpolymer containing 20% urea by weight was chosen as the shell material. In order to observe the rejuvenator emulsion and the prepared microcapsules, fluorescent microscope (FM) was used. The results revealed that Sodium Dodecyl Sulfate (SDS) had the best emulsion result and it was determined as the emulsifier material for the core material. FM and by calculating microcapsule size, 16 sets of microcapsules prepared under different circumstances were investigated to determine the optimization of the reaction condition (Figure 2.37). The optimum MUF microcapsule was synthesized under the conditions of 2:1 core/shell rate, peak reaction temperature of 65 °C, emulsifier speed of 1500r/min, emulsifying agent content of 0.7% and peak pH of 3. Scanning electronic microscope (SEM) results indicated that microcapsules were undamaged, spherical and unspoiled. Fourier transform infrared spectroscopy (FTIR) results indicated that with increasing core/shell ratio, the shell material in microcapsules was decreased. Thermo-gravimetric analysis (TGA) results indicated that the amount of loss mass of microcapsules was not noticeable after being kept at 180 °C for 1 hour and optimal microcapsules could meet the requirements of asphalt's mixing and compaction process. Finally, it was observed that microcapsules in asphalts improved the self-healing process [83].

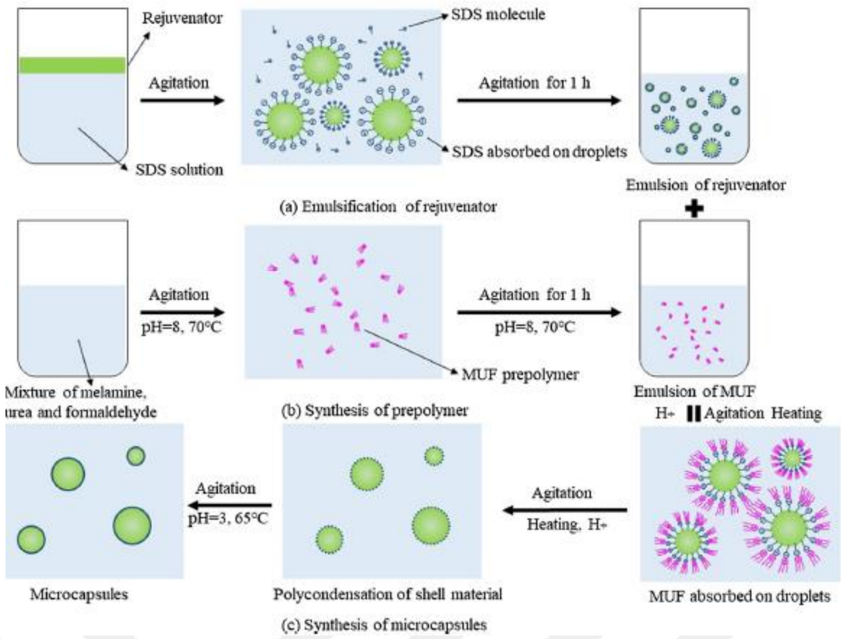

Figure 2.37. Synthetic principle of self-healing microcapsules [83].

In this study, the effects of calcium-alginate capsules, which include sunflower oil as encapsulated rejuvenators, and asphalt mixtures' self-healing results were presented. The samples were included with 3 different capsule contents, 0.10%, 0.25% and 0.50% by the total weight of the mixture. The mechanical and thermal properties of the capsules were evaluated. Additionally, the effects of capsule inclusion and healing temperature on the self-healing properties of the asphalt mixtures were evaluated on cracked asphalt beams with capsules and without capsules by using three-point bending tests. It was reported that capsules could resist the compaction process, were broken with mechanical loads in mastic asphalts and the encapsulated oils were released. The capsule content in the asphalt mixture, with increasing capsule content, providing higher levels of healing, has a significant effect on the healing. Finally, it was proved that the asphalt mixtures that healed below 40 ºC had a greater effect on the healing level. The SEM images of the capsules used in this study were presented in Figure 2.38 [84].

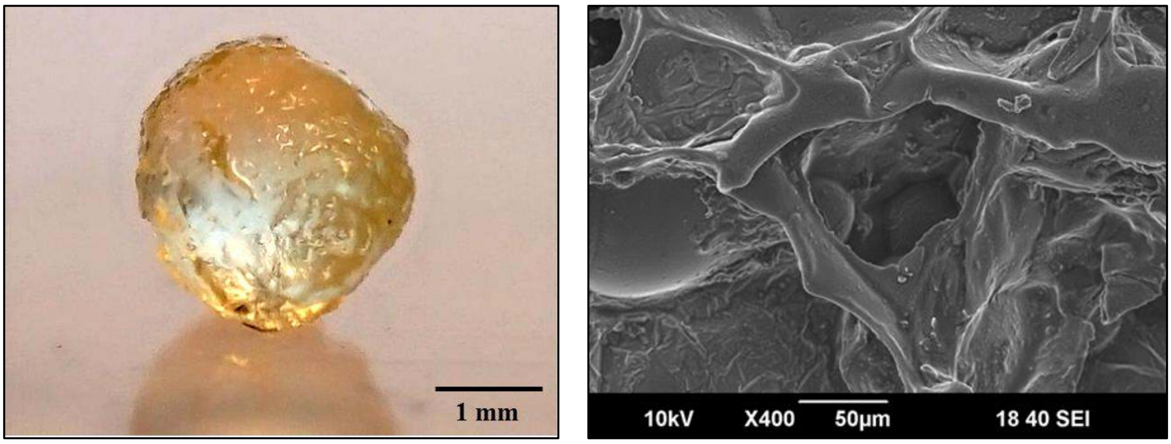

(a) **(b)**

Figure 2.38. (a) Spherical capsule produced in this study. (b) SEM image of the internal structure of capsule [84].

In this study, the results of the self-healing mastic asphalts with the activity of calcium-alginate capsules containing sunflower oil were presented. The morphological, physical, thermal and mechanical properties of the capsules were evaluated (Figure 2.39). Additionally, the effects of capsule oil content and healing temperature on the mastic asphalt's self-healing properties were evaluated. It was proven that capsules could resist the mixing and compaction processes and they were broken inside the mastic asphalt with mechanical loading, releasing the oil. The healing level observed in the mastic asphalt samples with capsules were higher compared to samples without capsules. The healing level depended on the oil content of the capsules and the temperature [85].

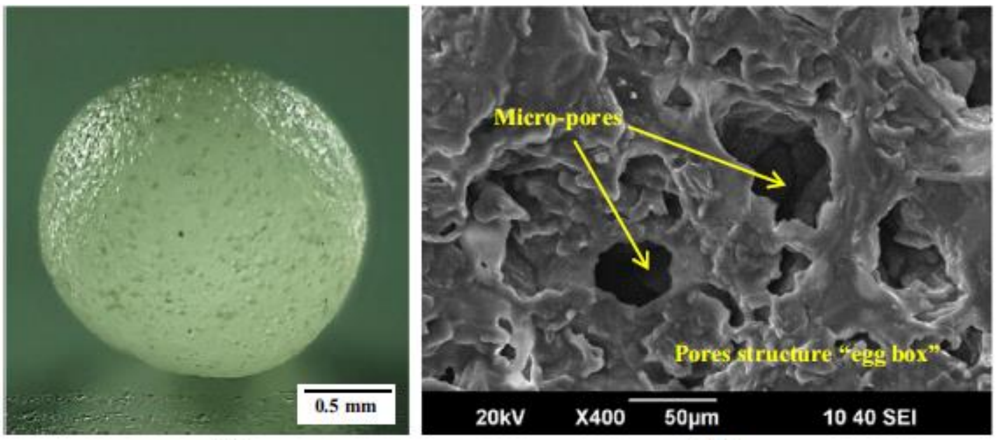

(a) **(b)**

Figure 2.39. (a) Spherical polymeric (calcium-alginate) capsule type C1 produced in this study. (b) SEM image of the calcium-alginate structure in core of capsules type C4 [85].

The capsule behavior was successful for asphalt self-healing in that it allows the rejuvenation of aged binder. However, this approach presented one disadvantage, which is the inability to reuse the capsules after they are cracked. Nevertheless, the use of capsules in asphalt mixtures is still in a start-up phase and it can be improved more in future years. A reasonable amount of microcapsules should be added to the asphalt mixture to ensure their proper dispersion. Additionally, the improvement of the multiphase self-healing process in asphalt mixtures needs to be the focus of future research works in this field.

3. MATERIALS AND DESIGN

3.1. Introduction

This chapter presents the materials generally used in this research. These include the capsule materials, stone mastic asphalt materials and asphalt materials. The manufacturing procedure of the capsules is also presented in this chapter. The asphalt mixtures are generally classified as mixtures with capsules and mixtures without capsules. Standard mixture design that comprises a dense-grade asphalt skeleton with 4.5% air voids is used for both asphalt slabs and asphalt cylinders (gyros). To evaluate the variation of the physical and mechanical properties of polymeric (calcium-alginate) capsules with the temperature by using several experimental tests. Likewise, the integrity of the capsules inside the asphalt mixture samples was also evaluated using X-ray computed tomography.

3.2. Asphalt mixture

Different asphalt mixtures were used in this research. Other asphalt mixtures ranged from cylindrical samples to asphalt slabs depending on the purpose they were produced to achieve. The bitumen used in all the tests of the research was virgin bitumen 40/60 pen, with softening point 49.8ºC and density of 1.03g/cm^3.The aggregate was a crushed limestone aggregate from Tunstead quarry, UK.

3.3.1. Dense asphalt mixture

A dense asphalt concrete mixture, AC 20 base (EN 13108-1) [86], was selected for this research and Table 3.1 presents the aggregate gradation and volumetric properties of the asphalt mixture. The bitumen used in all the tests of the research was virgin bitumen 40/60 pen. The aggregates and binder were pre-heated at general 160ºC for 12h and 4h, respectively, while the capsules were left to defrost for two hours at 20ºC before mixing. The materials were mixed for 2min at 125revs/min at 160ºC, for adequate dispersion. The capsules were added to the asphalt mixture just 20sec before the end of the mixing process.

Table 3.1. Design properties of asphalt mixture AC 20 base 40/60.

Aggregate gradation	% passing
20 mm	100.0
10 mm	80.2
6.3 mm	60.3
4 mm	45.3
2 mm	29.7
0.5 mm	15.5
0.125 mm	9.9
0.063 mm	8.0
Property	**Value**
Binder content ($\%_M$)	4.5
Bulk density (g/cm^3)	2.384
Air voids (%)	4.5
Voids in mineral aggregate (%)	14.9
Voids filled with bitumen (%)	69.8

3.3.2. Stone mastic asphalt mixture

A dense asphalt concrete mixture, AC 20 base (EN 13108-5) [87]. The SMA mixture consists of virgin bitumen 40/60 pen with a density of 1.030 g/cm^3 and graded Tunstead limestone aggregate with a density of 2.700 g/cm^3. Table 3.12 shows the aggregate gradation and design properties of the SMA mixture.

Table 3.2. Design properties of Stone Mastic Asphalt SMA 14 surf 40/60.

Aggregate gradation	% passing
20 mm	100.0
14 mm	98.64
10 mm	96.15
6.3 mm	61.16
2 mm	19.78
0.063 mm	7.29
Property	**Value**
Binder content ($\%_M$)	5.9
Bulk density (g/cm^3)	2.243
Maximum density (g/cm^3)	2.370
Air void content (%)	5.5
Voids in mineral aggregate (%)	14
Voids filled with bitumen (%)	75

3.3.3. Procedure for manufacturing the asphalt mixture

The procedure for preparing and manufacturing asphalt mixtures is very important in the mix design process as this ensures that mixtures produced are consistent and homogenous. Mixing mechanism was investigated by using two different types of mixers: a normal and an inclined mixer. Figure 3.1 shows photos of both mixers, while Figure 3.2 depicts schematic diagrams for both mixers to illustrate how they work.

Figure 3.1. a)Inclined b) normal horizontal mixer.

Inclined mixer

Figure 3.2 (a) illustrates how the inclined mixer works. Four mixing paddles are used to steer and blend the admixture inside the bowl. Since the rotating axis of the mixer is not vertical, but inclined with 60° (compared to ground plane), the collision between the materials within the mixing bowl consists of not only horizontal but also vertical movement. Moreover, the mixer allows reverse rotation. The heat supplied to the mixer is controlled by a thermocouple that measures the temperature of air inside the mixer.

Normal mixer

The normal or horizontal mixer is sketched in Figure 3.2(b). There are two mixing paddles moving with different orbits that help to drive and blend materials in the mixing bowl. Providing heat to the mixer is done by heating the oil which moves between the external and internal walls of the mixing bowl. There is a thermocouple in the oil to control the heat supply; hence the mixer can be maintained at the required temperature.

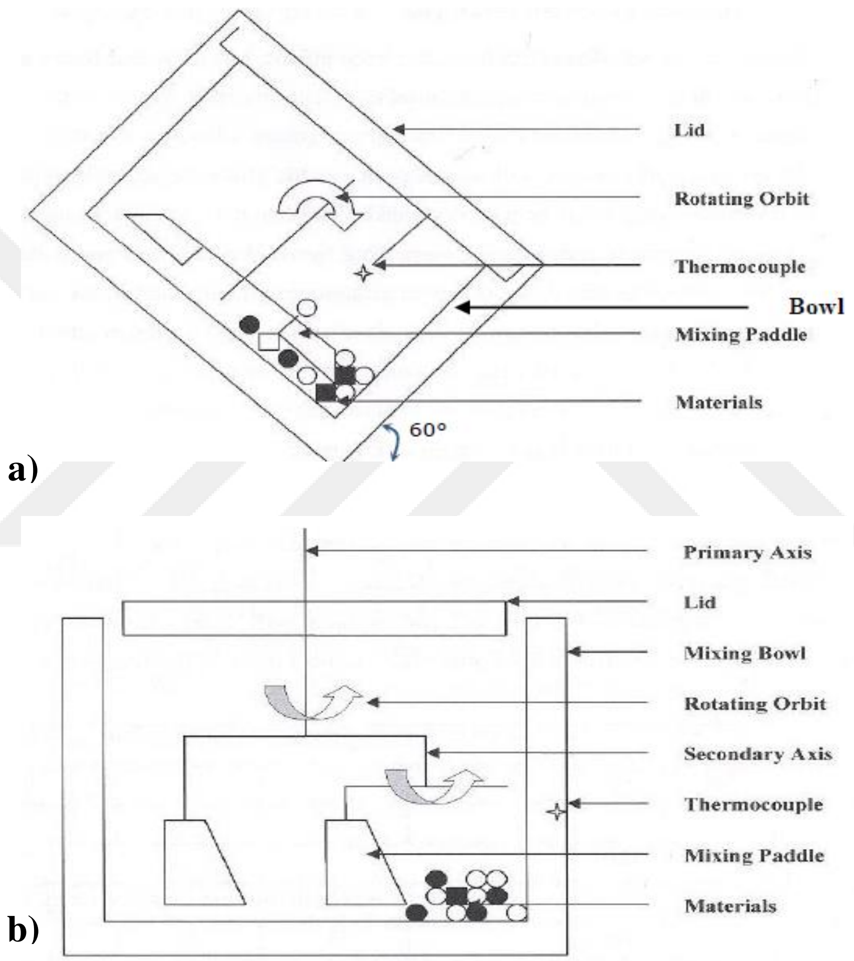

Figure 3.2. a)Inclined b) normal horizontal schematic of mixers [88].

The prismatic specimens (approximate 150*100*60mm^3 and 150×75×60 mm^3) were cut from (306*306*60mm) asphalt slabs compacted using a laboratory roller compactor (Figure 3.3) to reach an air voids content of 4.5%. Prismatic samples obtained in different sizes are shown in Figure 3.4. The purpose of a roller compactor of asphalt mixtures is to ensure that the compaction is representing the compaction in the field. Although the roller compactor simulates the field compaction, the use of it is limited due to several reasons: the size of the compactor is relatively large, the compactor is not portable, and it is expensive. Moreover, there are some difficulties in controlling the air voids of the sample, and the compaction process is time consuming.

Figure 3.3. Slab roller compactor.

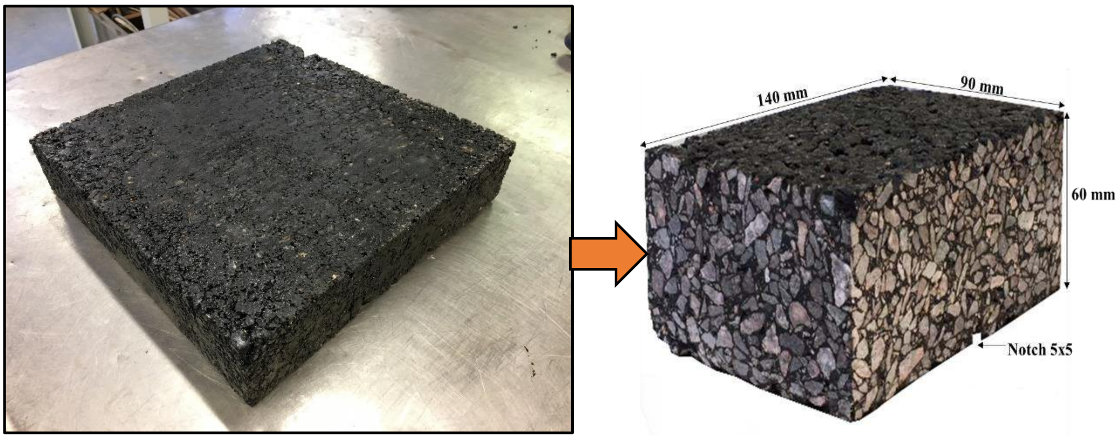

Figure 3.4. Asphalt mixture slab and the produced beam for the healing test.

100mm cylindrical molds were utilized as this provided an avenue for producing cylindrical specimens in an easy, convenient manner. Compaction was done using a Cooper gyratory compactor as seen below in Figure 3.5. This compactor was well suited for producing the asphalt mixtures used in this study. Density and compaction shear stress values are generated automatically by the compactor, providing a good basis for comparison during use. Previous studies on various modes of compaction and degree/level of compaction to simulate field conditions have positively recommended the use of the Cooper gyratory compactor.

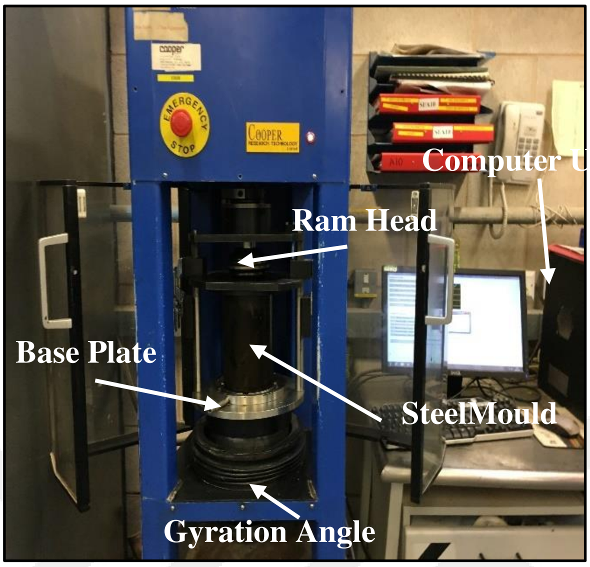

Figure 3.5. Cooper Gyratory Compactor.

3.4. Capsule properties

Different materials are used to manufacture the capsules, they range from cheap and safe such as sunflower cooking oil. This section presents these materials and the capsules manufacturing process.

3.4.1. Capsule materials

The capsules mainly consist of the rejuvenator and calcium-alginate polymer that encapsulates the rejuvenator, which is trapped in the core of the capsule. The rejuvenator material used in the capsules was sunflower cooking oil (CO), which is a commercial sunflower oil supplied by East End (UK).The rejuvenator used in the capsules was sunflower oil, with a density, smoke point and flash point of 0.92 g/cm^3, 227ºC and 315ºC, respectively [69]. Sunflower oil was selected because of its low cost, thermal stability, and the fact that extra health and safety procedures are not required in the laboratory [89]. Similar oil has been used before as a rejuvenator [59,89]. Nevertheless, other rejuvenating agents can be encapsulated using the same method.

The polymeric material in the inner core of the capsules was composed of (1) sodium alginate ($C6H7O6Na$), provided by Sigma-Aldrich, which is an anionic polysaccharide widely distributed in the cell walls of brown algae. The name alginate is given to a family of linear polysaccharides consisting of guluronic (G) and manuronic (M) units [91]. It is sold in filamentous, granular or powdered forms, and mixing it with water creates a viscous white to yellowish-brown gum; (2) a calcium source, provided by Sigma-Aldrich as anhydrous, granular pellets of calcium chloride ($CaCl2$), of 7mm diameter, and 93% purity.

3.4.2. Capsules production

Calcium-alginate capsules with a water and oil ratio of 0.1 were prepared at 20ºC by ionotropic gelation of alginate in the presence of calcium [78]. A scheme of the manufacturing process of the capsules is illustrated in Figure 3.6. To prepare the capsules, first, 150 ml of sunflower oil and 1500 ml of deionized water were introduced into a 2000 ml glass container and stirred to produce a stable emulsion. Sunflower oil and water were mixed using a laboratory gear drive mixer for 1 minute at 400 rpm. Then, 55 g of sodium alginate were added to the glass container and stirred until complete solution at 400 rpm for 10 minutes, see Figure 3.6. The amount of the sodium alginate used to produce the polymer capsules (see Figure 3.7(a)) was defined so as to obtain a structure of calcium-alginate (see Figure 3.7(b)) strong enough to hold the oil and hence with a strength higher than the capsules developed by Micaelo et al. [69] and Al-Mansoori et al. [78].

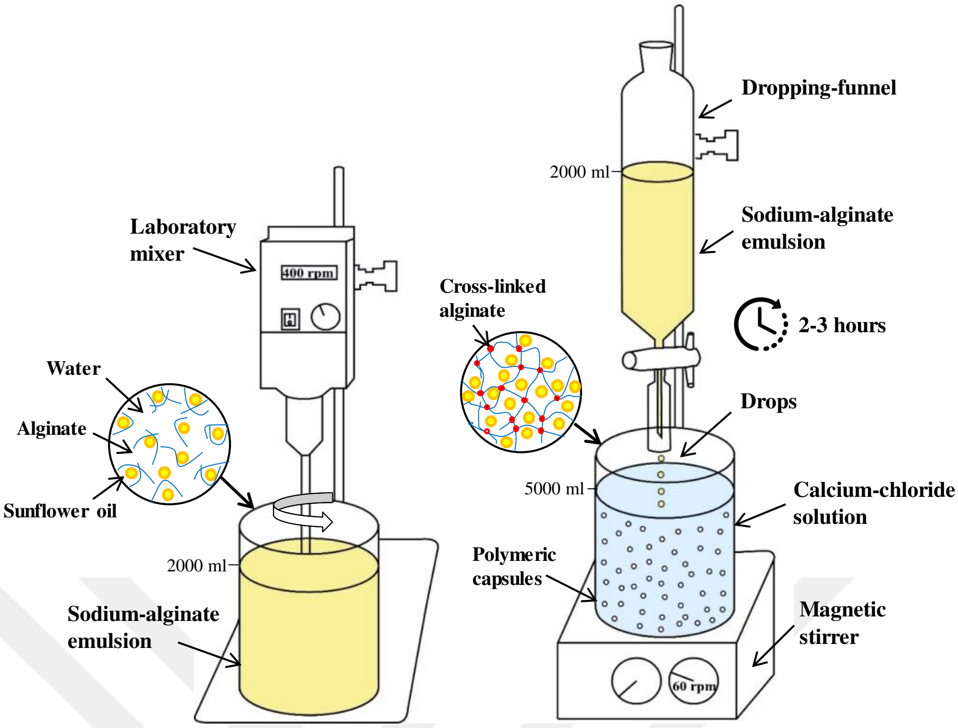

Figure 3.6. Schematic diagram of the manufacturing process of capsules by ionotropic gelation of alginate.

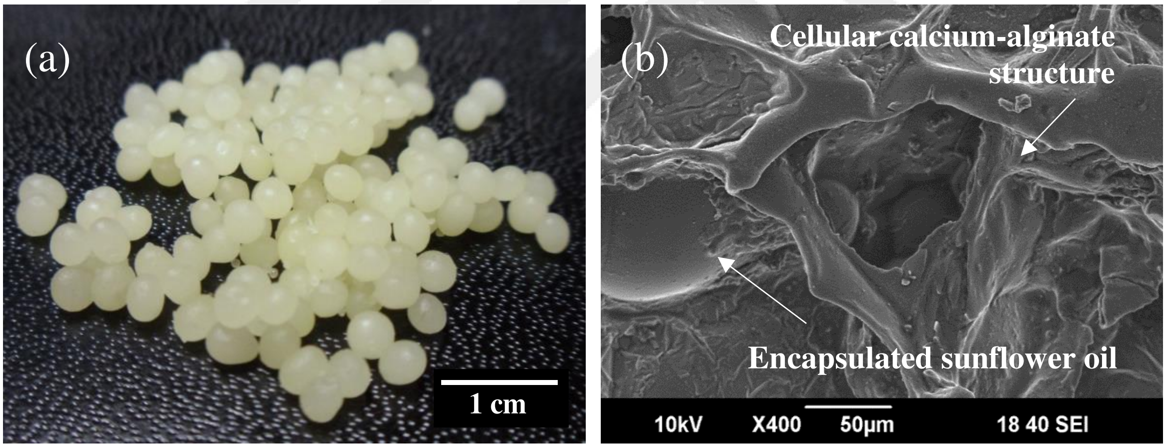

Figure 3.7. (a) Individual polymer capsule, and (b) SEM image of calcium-alginate internal structure of capsules.

Simultaneously, a calcium chloride solution at 2%$_w$ was prepared by mixing 1800 ml of deionized water with 36 g of calcium chloride in a 5000 ml glass container, see Figure 3.6. Capsules were formed by letting the oil-in-water emulsion drop into the calcium chloride solution from a 2000 ml pressure-equalizing dropping funnel with 3 mm socket size. The process is called a cross-link of calcium-alginate via ionotropic gelation of sodium alginate in the presence of calcium ions [90]. During the capsule formation process, the calcium-chloride solution was gently agitated using a magnetic stirrer at 60 rpm. Capsules were allowed to stay in the solution until the end of the encapsulation process. In this study, the capsules' manufacturing process was of 2-3 hours, approximately. After this time, the capsules were decanted and washed with deionized water and then dried in an electric dryer at 40ºC for 36 hours. Then, the capsules were stored in a freezer at -18ºC to avoid the release and oxidation of the oil at room temperature. The alginate molecular weight and the concentration of the calcium chloride (CaCl2) can affect the mixture and possibly the properties of the capsules [91]. The process can be defined as producing capsules by ionotropic gelation of alginate in the presence of calcium, as shown in scheme (3.1) [92]. The encapsulated procedure allowed the manufacture of capsules with an average diameter of 2.5 mm and composed of a 75% vol. of sunflower oil and a 25% vol. of calcium-alginate polymer. A total of 3 kg of capsules were manufactured in this study.

$$ {}^{ww}COO^{-}\ {}^{+}Na + {}^{ww}COO^{-}\ {}^{+}Na \xrightarrow{Ca^{2+}} {}^{ww}COO^{-}\text{- - }Ca^{2+}\text{--}{}^{-}OOC^{ww} + 2Na^{+} \qquad (3.1) $$

The flowchart in Figure 3.8 presents the fabrication process in more detail, shows the procedure to fabricate the polymeric capsules. All tasks were performed at room temperature. Figure 3.9 shows sample of capsule at the three stages: directly after production, dry and ready to use capsules shell.

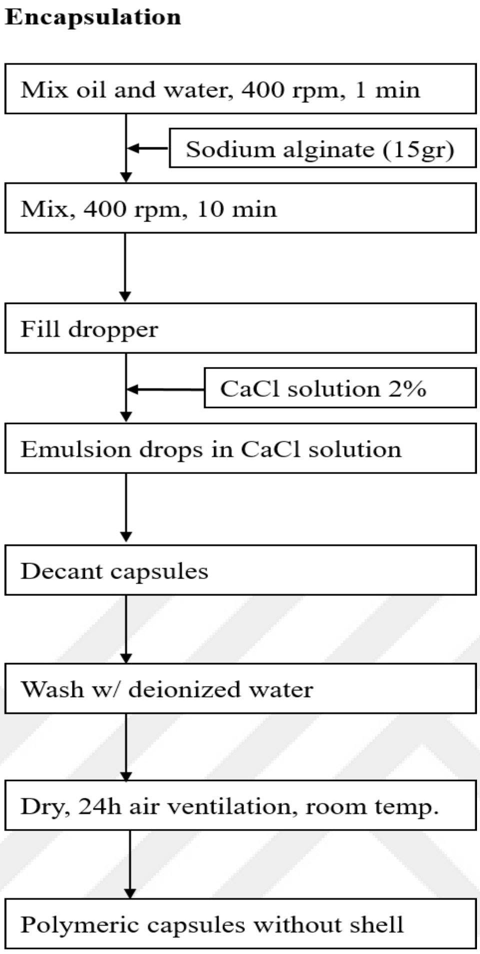

Figure 3.8. Flowchart of the capsule fabrication process: (a) polymeric (calcium-alginate) capsules.

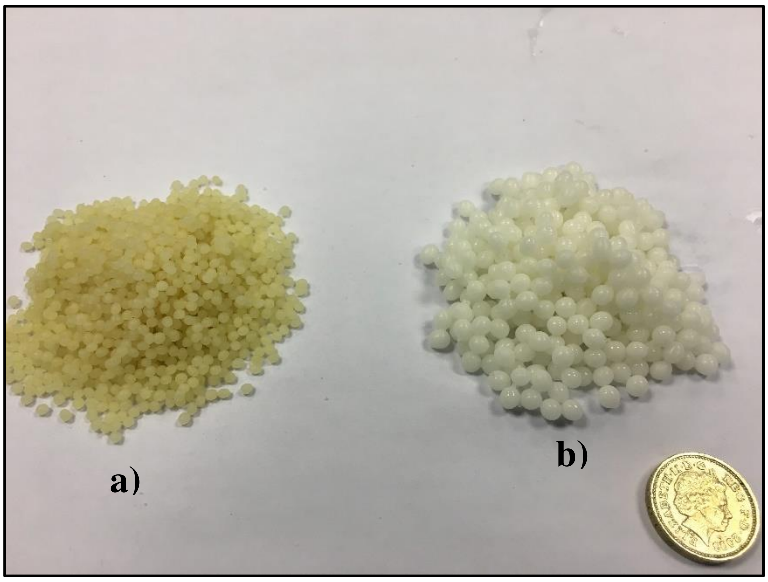

Figure 3.9. Samples of capsule produced in this research, a) dry capsules, b) wet capsules.

3.4.3. Characterization of the capsules

The bulk density and compressive strength of dry capsules were measured at 20ºC, 40ºC, 80ºC, 120ºC, 160ºC and 180ºC. For the tests, the capsules were pre-conditioned for 4h at the test temperature. The density was measured using a helium pycnometer. The mechanical strength was measured by uniaxial compression testing of 10 individual capsules. To do that, individual capsules were loaded until failure at a loading rate of 0.2 mm/min.

3.4.4. Effect of the temperature on the properties of capsules

The effect of the temperature on the physical and mechanical properties of the capsules was studied by means of density and compressive strength tests, see results in Table 3.3. Table, it can be observed that the density of the capsules reduced with the increase of temperature, which was mainly due to the loss of mass experienced by the capsules when exposed to increasing temperature.

Table 3.3. Average physical and mechanical properties of the capsules at different temperatures.

Property measured	Unit	Temperature value					
		@20ºC	@40ºC	@80ºC	@120ºC	@160ºC	@180ºC
Bulk density	g/cm3	1.116	1.115	1.097	1.083	1.021	0.766
Compressive strength	N	45.5	43.5	35.4	27.6	19.4	5.5

On the other hand, Table 3.3 also shows the results of compressive strength of the polymeric capsules tested at different temperatures, from 20ºC to 180ºC. The results proved that the capsules reduced their compressive strength with the increase of temperature. This was because the exposure to high temperatures degraded the calcium-alginate polymeric structure of the capsules making them more brittle, and hence less flexible to mechanical loads. Nevertheless, based on the study of Al-Mansoori et al. [85], the obtained results proved that the capsules designed in this study can satisfactorily resist the mixing and compaction processes.

3.4.5. Capsules integrity after mixing and compaction processes

In this chapter, the integrity of the calcium-alginate capsules into the asphalt mixture was evaluated by developing mixing tests and scanning asphalt samples via X-ray computed tomography. An example image of the embedded capsules inside the asphalt mixture and CT-Scans reconstructions are shown in Figure 3.10. It can be observed that the capsules resisted the mixing processes and presented a good thermal stability and adherence to the mixture matrix, see Figure 3.10(a). Additionally, from CT-Scans results shown in Figure 3.10(b) and (c), it was concluded that the calcium-alginate capsules presented good distribution inside the asphalt mixture, with some damaged capsules due to mixing and compaction processes.

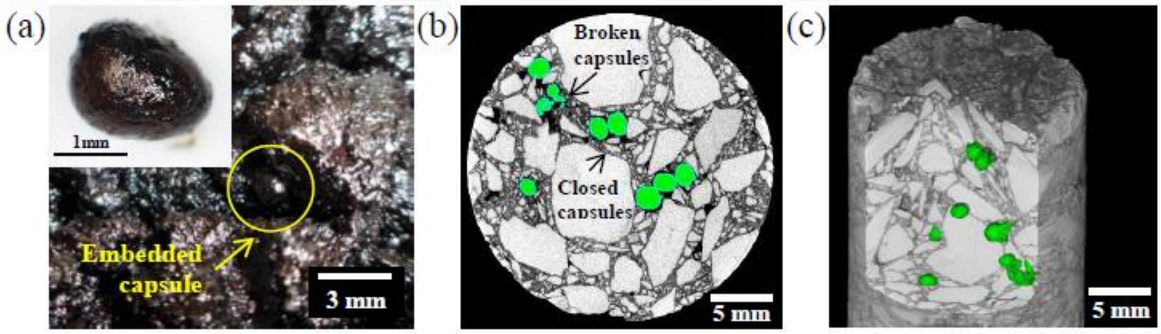

Figure 3.10. (a) Embedded capsule inside the asphalt mixture and example of an extracted individual capsule, (b) 2D cross-section image of a sample with capsules, and (c) 3D cutting reconstruction of the capsule spatial distribution inside the asphalt sample.

4. AGING IN HOT MIX ASPHALTS

The asphalt cement's durability is a function of aging, temperature and the amount of loading. The process of bituminous binders' stiffening due to various reasons is called aging [93]. The two major factors for HMAs to age during their manufacturing process and service life are the oxidation and the evaporation of the light elements included in the binder. Oxidation is defined as the process of losing a part of hydrogen and carbon found in the bituminous binder as a result of the combination of hydrocarbon components with the oxygen in the air [94]. A wide variety of information regarding the factors that cause aging in bituminous binders is presented in Table 4.1. The viscosity of the binders increases due to aging, increasing the stiffness of the mixture. Due to the aging, the brittleness of the mixtures increase and their resistance to crack propagation decreases [95].

Table 4.1. Factors that cause aging in bituminous binders [96].

The effects causing aging	Reason of Occurrence				Location of Occurrence	
	Time	Temperature	Oxygen	Sun Light	Surface	Body
1. Oxidation	X	X	X		X	-
2. Photo-oxidation (Direct light)	X	X	X	X	X	
3. Evaporation	X	X	-	-	X	X
4. Photo-oxidation (Reflected light)	X	X	X	X	X	-
5. Photo Chemical (Direct light)	X	X		X	X	-
6. Photo Chemical (Reflected light)	X	X		X	X	X
7. Polymerization	X	X			X	X
8. Aging occurring in the structure (Thixotropy)	X	-	-	-	X	X
9. Oil expulsion (Syneresis)	X	X	-	-	X	-
10. Changes in Nuclear Energy	X	X	-	-	X	X
11. Effect of Water	X	X	X	X	X	
12. Absorption by Aggregate	X	X	-	-	X	X
13. Absorption of the Components on the Surface of Aggregate	X	X	-	-	X	
14. Chemical Reactions Occurring in the Interface or Catalyst Effect	X	X	-	-	X	X
15. Microbiologic Degradation	X	X	X		X	X

The aging in bituminous binders is evaluated in two parts based on their occurrence period as the short and long term. Short-term aging occurs during storing the bitumen, transporting to plant, mixing with aggregate, transporting to the application area, laying and compaction while long-term aging occurs during the service life of the road. Aging index is used to determine the degree of aging. The relationship between the aging index and time is presented in Figure 4.1 [94].

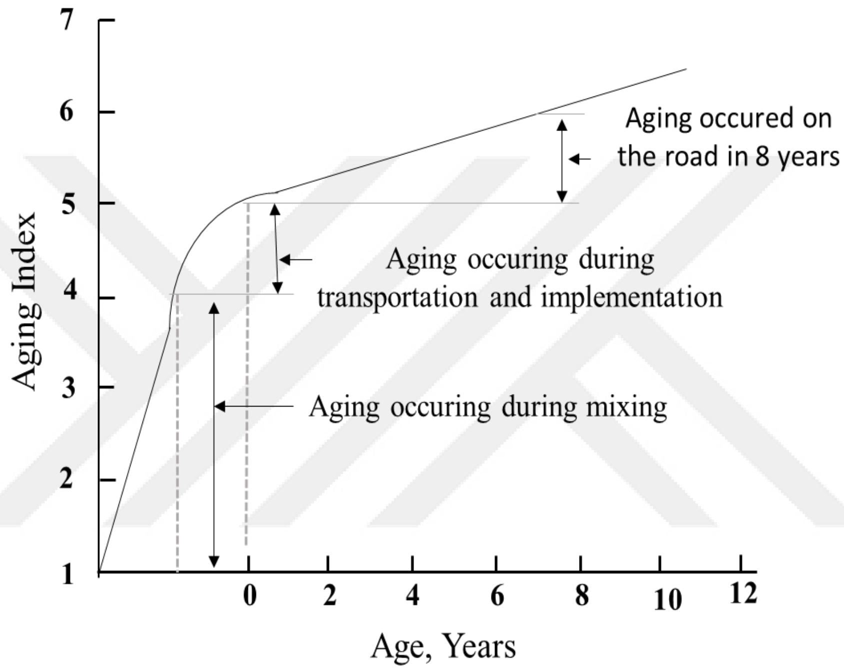

Figure 4.1. The relationship between the aging index and time [94].

As it can be observed in Figure 4.1, most of the aging occurs until the road is opened for service. The aging occurring during the service life covers the 30% of the total amount of aging. Most of the aging also occurs during the mixing process [94]. Studies conducted on the subject of aging occurring in HMAs are divided into two groups as studies on binders and mixing. Even though it is believed that aging occurs only in binders, certain types the chemical bond formation between certain types of aggregate and bitumen, and changes in the properties of certain types of aggregates over time reveals the fact that it is necessary to evaluate the mixture samples in terms of long-term aging [97].

The effect of short-term aging can be reflected in the laboratory environment by RTFO test while the effect of long-term aging can be reflected by pressured aging vessel (PAV) test. In the short-term aging of mixtures, according to the Superpave method, it is advised to keep the mixtures loosely at 135 °C for 4 hours before compaction. The long-term aging occurring in HMAs is not covered in the Superpave method. In SHRP, according to the field and laboratory studies conducted by Bell et al, to reflect the long-term aging in the laboratory in the most suitable way, it was determined that the most suitable method for HMAs' long-term aging was keeping the short-term aged mixtures (4 hours at 135 °C), following compaction, at 85 °C in a drying oven with air circulation for 120 hours (5 days) [97-99]. With the long-term aging of HMAs as stated in the standards, keeping them at 85 °C in a drying oven with air circulation for 120 hours (5 days), it is provided to reflect a field aging of 7-10 years on the laboratory environment [100]. The method regarding the long-term aging of HMAs was first defined with the AASHTO PP2 temporary standard and the latest version was determined in the AASHTO R30-02 "Standard Practice for Mixture Conditioning of Hot-Mix Asphalt (HMA)". The aging occurring in the hot mix asphalt is a vital subject to be focused because it directly affects the behavior of HMAs in the field. Studies regarding the short and long-term aging occurring in bituminous binders have been conducted since 1903 [101] and the studies on these subjects are still in practice. In today's agreements regarding the short-term aging of bituminous binders, rolling thin film oven (RTFOT) test is suggested. This method, which is suitable for original binders in various conducted studies, is reported to be unsuitable for modified bitumen due to increasing the viscosity of the bitumen and immobility of the bitumen film. Thus, the modified-RTFOT method was developed and studies regarding this still continue [102]. Additionally, several studies suggested that the method used for the long-term aging of HMAs is not a suitable one [103]. Because the most detailed study conducted regarding the aging of HMAs to date is reported in AASHTO R30-02 standard, this standard was adopted in the aging of HMAs in this study. For the short-term aging of the hot mix asphalts, the non-compacted samples were kept at 135 °C in a drying oven for 4 hours and then compacted while for long-term aging, the compacted samples were kept at 85 °C in a drying oven with air circulation for 120 hours (5 days) (Figure 4.2). At the end of the process, the oven door was opened and the samples were kept for 24 hours without any movement, and they were subjected to tests after these processes.

Figure 4.2. Long-term aging of the HMA samples.

5. TEST METHODS USED IN THE THESIS STUDY

5.1 Binder Tests

5.1.1. Viscosity of bitumen

To evaluate the variation of the physical properties of the bitumen and sunflower oil used in the asphalt mixtures and capsules manufacturing, viscosity measurements were performed on test samples of bitumen and oil at different aging times. The bitumen viscosity test was performed by means of a Dynamic Shear Rheometer (DSR) supplied by Malvern Instruments Ltd. Before tests, bitumen samples were pre-conditioned in an oven at 85ºC for 9 different aging times: 2, 24, 48, 72, 96, 144, 180, 210 and 240 h (Figure 5.1). The aged bitumen samples were tested at 20ºC with an oscillatory sweep frequency of 0.1-10 Hz. A parallel-plate geometry of 8 mm diameter was used with a gap of 2 mm between the spindle and the sample to allow the shearing movement as required by the standards. Moreover, the viscosity of bitumen was also measured on the bitumen samples pre-conditioned in an oven at 140 and 160ºC for 4 h.

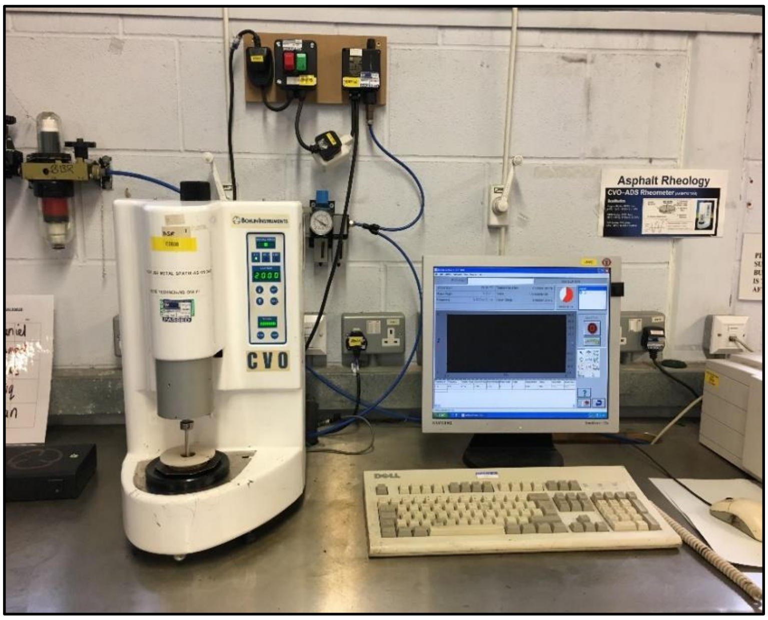

Figure 5.1. The DSR machine.

5.1.2. Rotational Viscometer (RV) Experiment

The viscosity of sunflower oil was measured under the same aging conditions of bitumen samples but using a different test. With this purpose, a simple laboratory tool using a Brookfield Rotational Viscometer at low shear rate was used. Samples of 10 g of each aged oil were transferred into separate Brookfield viscometer tubes. After that, a rotational spindle (SC4-27) was lowered into the oil tube and rotated at a constant speed of 200 rpm. Viscosity was recorded after reaching the constant value at 200 rpm. The test temperature was of 20ºC in all the measurements.

Likewise, based on the viscosity results of the bitumen and sunflower oil, an aging index (AI) was defined as follows:

$$AI(\%) = \frac{\eta_{unaged} - \eta_{t-aged}}{\eta_{unaged}} \times 100 \tag{5.1}$$

where, η_{unaged} is the viscosity of the bitumen or sunflower oil at 20ºC (Pa·s) without aging process, and η_{t-aged} is the viscosity of the bitumen or sunflower oil measured at 20ºC (Pa·s) for the different aging times (h).

5.1.3. Fourier Transform Infrared Spectroscopy (FTIR)

To quantify the oil release from the capsules into the asphalt mixture beams, several asphalt samples were chemically analyzed by using Fourier Transform Infrared Spectroscopy (FTIR) spectrum model Bruker Tensor 27 (Figure 5.2). Samples were randomly taken from the asphalt beams with, and without, capsules after healing tests and were tested by using FTIR spectroscopy tests. Furthermore, samples of virgin and aged bitumen with the same amount of oil contained in the capsules were prepared to simulate the same amount of oil in asphalt if all the capsules had released their content. The oil-bitumen samples group were aged in an oven at 85ºC for 240 h. FTIR tests on the oil-bitumen samples with, and without, aging process were set in the absorption mode, in the wavenumber band range of 400 to 4000 cm-1 at a resolution of 4 cm-1. The oil effect on the bitumen was evaluated from changes in the absorbance peak between the wavenumbers 1700 to 1800 cm-1. This range was adopted based on the methodology proposed by Micaelo et al. [69] and

Al-Mansoori et al. [78] to determine the amount of oil released in the asphalt mixture with capsules. These works are based on the fact that vegetable oils have a distinct peak at ~1745 cm-1 (C-O stretch), while the bitumen has zero index in this range [104].

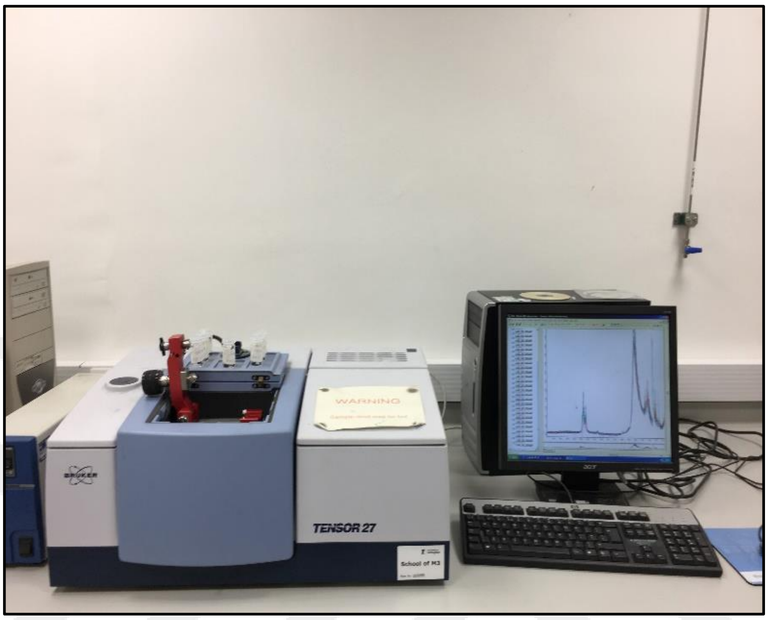

Figure 5.2. FTIR machine.

Thus, FTIR absorbance spectrum was normalized in the selected wave length range and the absorbance area under the spectrum was measured using the trapezoidal rule of numerical integration [105]. Figure 5.3 shows an example of the results of FTIR absorbance spectrums for asphalt samples with, and without, oil and an explanation of the absorbance area. Finally, the percentage of broken capsules, BC, inside the asphalt beams after healing tests was defined as follows:

$$BC\ (\%) = \left[\frac{A_{1745-Mi}}{A_{1745-Ref}}\right]_j \times 100 \quad (5.2)$$

where, $A_{1745-Mi}$ is the absorbance area at the peak 1745 cm-1 for the different types of asphalt with capsules (M1-M4), and $A_{1745-Ref}$ is the absorbance area at the peak 1745 cm-1 for the asphalt samples with the 100% of capsules broken, and where j indicates the state of the asphalt beams, i.e., with or without the aging process.

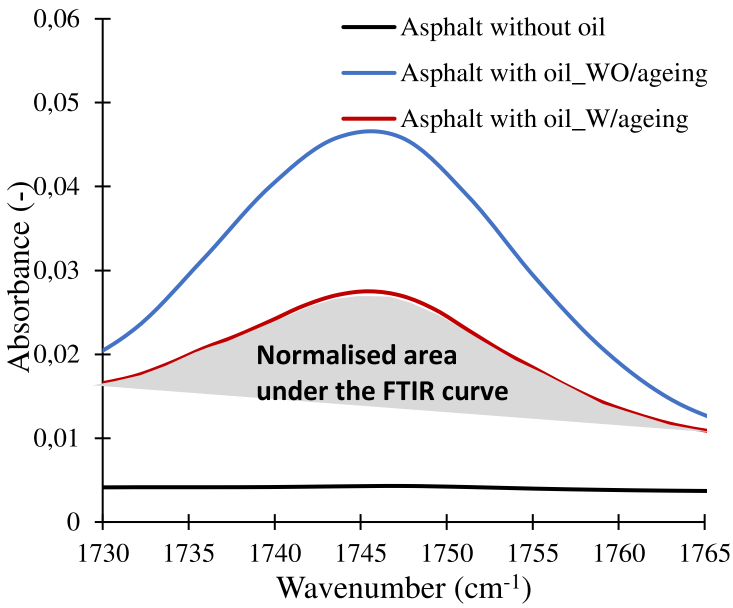

Figure 5.3. FTIR curves for asphalt mixture samples with and without oil.

5.2 Tests Conducted on Capsules

5.2.1. Thermogravimetric analysis (TGA)

During the manufacturing of the slabs, the capsules face high temperatures of up to 160ºC. Therefore, to validate if the capsules and its components (calcium-alginate and oil) survive this process and how different temperatures influence the mass loss of the capsules, a thermal stability test was performed. The investigation for the thermal stability test will be achieved by using a thermogravimetric analysis (TGA) test, performed on an NETZSCH, TG 449 F3 Jupiter Thermo-Microbalance using nitrogen atmosphere and a heating rate of 10ºC/min (Figure 5.4). The mold used for the measurement of all samples was an aluminum crucibles mold. The profile that the test will be performed is at a temperature of 0-1000°C. However, the machine can only start the test at the room temperature – i.e., 20 °C.

Figure 5.4. TGA machine.

5.2.2. Thermomechanical Analyzer (TMA)

Thermomechanical Analyzer (TMA) equipment model Q400 (Figure 5.5). Thermal expansion tests were applied on individual capsule samples to measure the dimension change of the capsule as it is heated, while simultaneously subjected to mechanical loading. The tests were conducted at a heating rate of 5ºC/min.

Figure 5.5. TMA machine.

5.2.3. Density measurement of capsules

The effect of the temperature on the density of the polymeric capsules was measured by non-invasive tests. The tests were performed at temperatures of 20ºC, 140ºC and 160ºC by using a Helium Pycnometer AccuPyc II 1340 (Figure 5.6).

Before tests, capsules were pre-conditioned in an oven for 4 h. The mass of capsules in each sample test was 5 g. The test temperature values were selected with the aim of evaluating the physical behavior of capsules under environmental, and mixing conditions, respectively.

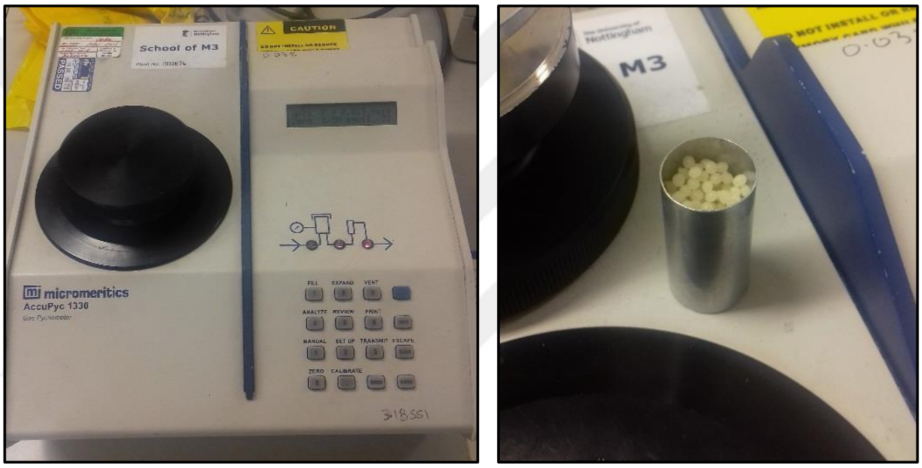

Figure 5.6. Density measurement of capsules using a Gas Pycnometer AccuPyc II 1330 equipment.

5.2.4. Compressive Strength

The mechanical strength of capsules was measured through uniaxial compression tests on a total of 20 capsules for each temperature value. Capsules were loaded until failure at a loading rate of 0.2 mm/min, see Figure 5.7(a). The tests were performed at 20ºC, 140ºC and 160ºC, using an Instron Model 5969 with a 5 kN load cell and an environmental chamber with temperature control. Capsules were pre-conditioned in the chamber for 4 h before each test. Figure 5.7(b) shows an example of the type of failure that an individual broken capsule presented after test at 20ºC.

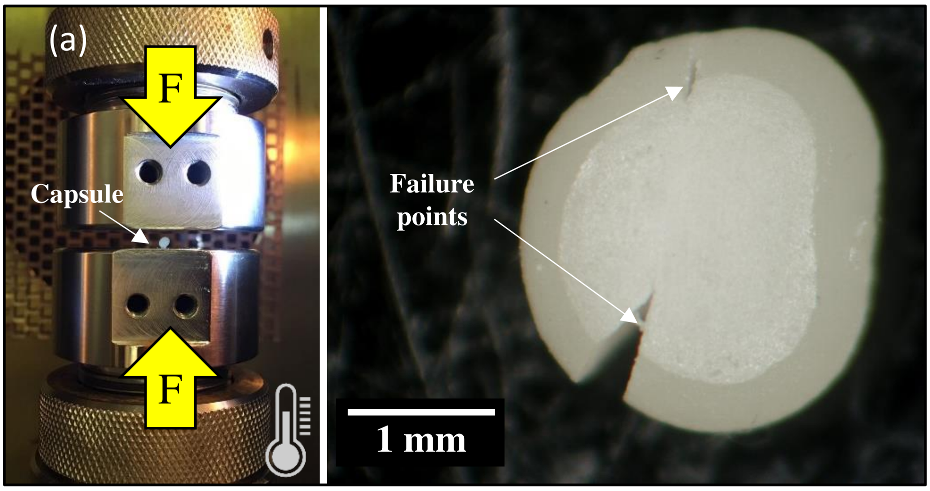

Figure 5.7. (a) Compressive strength test of capsules, and (b) example of a broken capsule after test at 20°C.

5.3. Mixture Tests

5.3.1. Indirect Tensile Stiffness Modulus (ITSM)

In the experimental determination of the rigidity modulus of HMAs, direct pressure, indirect tensile and torsion tests could be implemented. All of the testing methods are based on the acceptance that a viscoelastic material behaves elastically with short-term loading. The test methods include the periodically applied loads and instant deformations occurring during these processes. The rigidity modulus is calculated by applied stress and regained unit of deformation. Diametral (applying load in line with the diameter) tests are used more commonly due to being more sensitive to the effect of the binder in the mixture, compared to direct pressure tests [106]. The rigidity modulus, which is a measure for the load dispersion ability of bituminous layers, is one of the most important performance characteristics of hot mix asphalts [107].

The indirect tensile stiffness modulus (ITSM) test, which is a non-damaging and deformation-controlled tests defined by BS EN 12697-26 standard [108], was conducted by using the Cooper's Nottingham Asphalt Testing (NAT) Machine testing equipment.

The ITSM is the most common test for determining the stiffness modulus of asphaltic samples via the NAT machine; Figure 5.8. The dimensions of specimens were 100±2 mm diameter and 40±2 mm thickness. The test was carried out under the standard conditions of 5μm target horizontal deformation, 124 ms rise time, 20 °C test temperature. The horizontal deformation is induced by the loads and measured by external Linear Variable Differential

Transformers Differential Transformers (LVDT) lined up wşth the specimen's diameter as shown in Figure 5.9. The samples were initially conditioned in a cabinet at 20 °C for at least 3 hrs before testing.

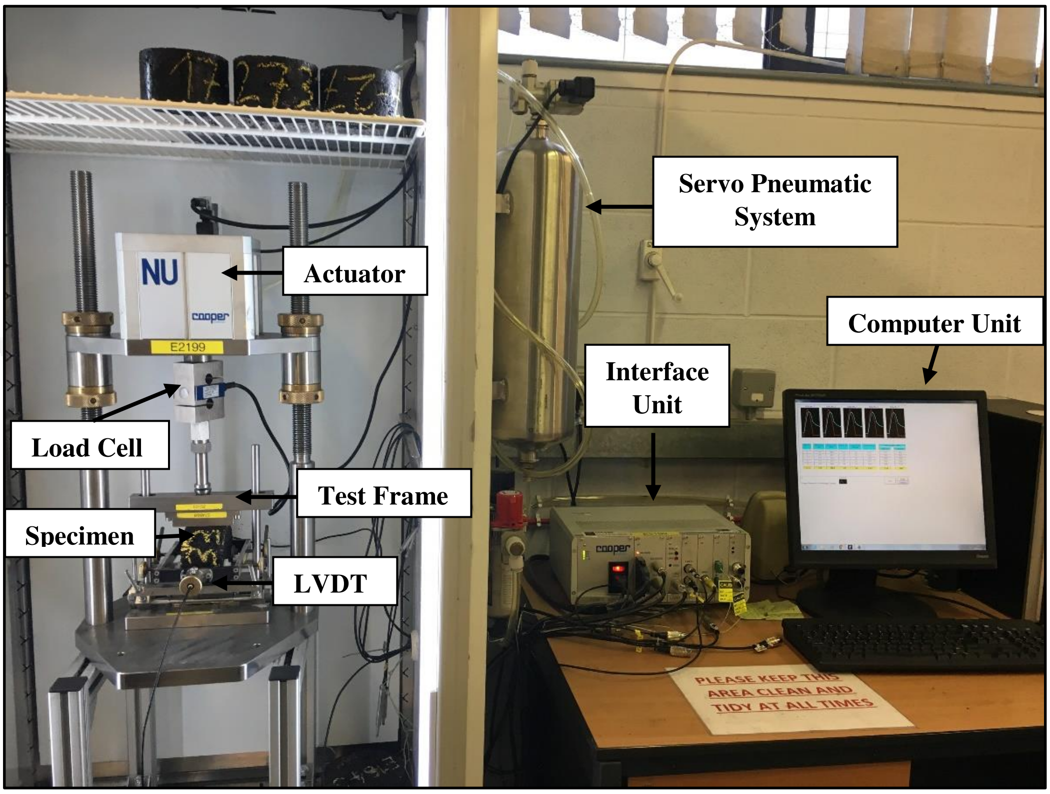

Figure 5.8. ITSM Test configuration in the NAT.

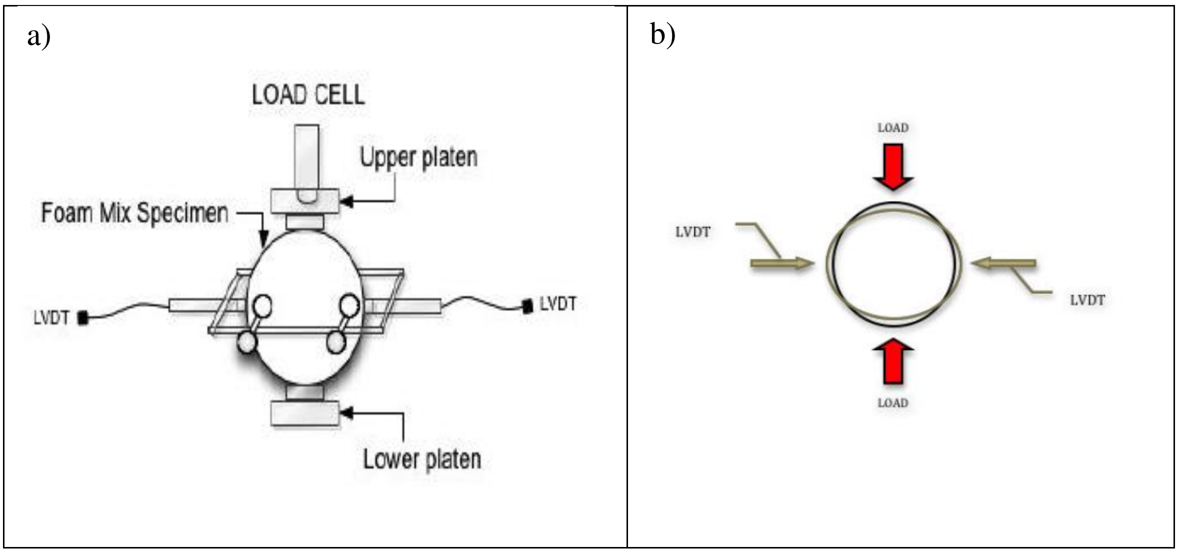

Figure 5.9. a) ITSM test equipment and its side view's cross-section, b) the deformation induced by the ITSM test [109].

Five conditioning pulses are applied before starting the test to make any adaptation for the load needed to produce the target horizontal deformation, and to embed the loading plates correctly over the sample. The system then applies five load pulses to generate the horizontal deformation. Then the specimens were calculated for their ITSM values by using the equation below following 5 impacts applied to the sample at the loads determined (Equation 5.3). A typical test result is shown in Figure 5.10.

$$S_m = \frac{F(R + 0.27)}{LH} \tag{5.3}$$

Here, Sm is the indirect tensile stiffness modulus (MPa) while F is the maximum vertical load (N), H is the horizontal deformation occurring after 5 load repetitions (mm), L is the mean sample height (mm) and R is the poisson ratio (3.35). Following the test, the samples were turned for 90° and the test was repeated. The ITSM value of the sample is calculated by averaging the two values with less than 10% deviation.

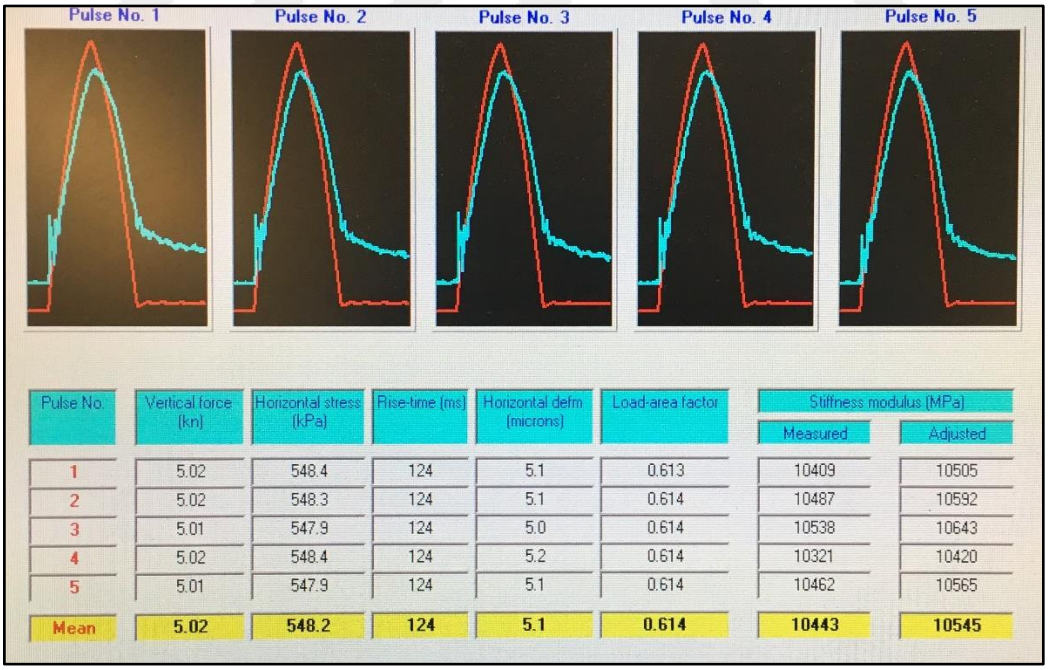

Pulse No.	Vertical force (kn)	Horizontal stress (kPa)	Rise-time (ms)	Horizontal defm (microns)	Load-area factor	Stiffness modulus (MPa) Measured	Stiffness modulus (MPa) Adjusted
1	5.02	548.4	124	5.1	0.613	10409	10505
2	5.02	548.3	124	5.1	0.614	10487	10592
3	5.01	547.9	124	5.0	0.614	10538	10643
4	5.02	548.4	124	5.2	0.614	10321	10420
5	5.01	547.9	124	5.1	0.614	10462	10565
Mean	5.02	548.2	124	5.1	0.614	10443	10545

Figure 5.10. Typical result sheet of ITSM test.

5.3.2. Indirect Tensile Fatigue Test (ITFT)

Bituminous materials used in highways are exposed to a short-term load each time a vehicle passes on them. These loads cause micro damages that lead to the reduction in the rigidity of the material. These micro damages lead to pavement deformations called fatigue cracks in the long term [110]. Fatigue cracks are the most common type of deformation caused by loading. Fatigue cracks gradually increase following the crack formation due to repeating loads [106]. In practice, the deformation caused by fatigue is defined as the coverage of the pavement by fatigue cracks at a certain rate.

In the laboratory environment, there are a number of tests developed to determine the fatigue resistance of hot mix asphalt mixtures. These tests can be conducted under both tensile and deformation-controlled conditions. Because the loading type, sample geometry and increase in tensile depend on the test type, fatigue lives in these tests may vary. As a result of the studies conducted on the fatigue life, it was determined that fatigue lives obtained from deformation-controlled tests were higher compared to tensile-controlled tests. It was also observed that the fatigue lives observed in the laboratory were rather shorter compared to those obtained in the field. This situation is due to the fact that fatigue life is a function of tensile distribution and the pavement's limit conditions [111]. Nevertheless, fatigue tests provide an opportunity to compare the fatigue performances of different mixtures.

In the indirect tensile fatigue test (ITFT), fatigue life is determined as the load repetition number until the sample is broken. Each type of sample is subjected to fatigue tests at different tensile levels, determining the load repetition number that causes the cracking at different tensile levels (N_f). Thus, the classical fatigue relationship between N_f and tensile (σ) can be calculated on the graph drawn on a logarithmic scale or the Wöhler formula presented below.

$$N_f = k_1 * (\frac{1}{\sigma})^{k_2} \qquad (5.4)$$

Here, N_f is the number of load repetition, representing the fatigue life, k_1 and k_2 are the characteristics of the material and σ is the applied tensile (kPa) [112]. The k_1 and k_2 coefficients obtained from the fatigue equation can be used to determine the effects of additives on the fatigue characteristics of mixtures. The high k_2**,** which is an exponential coefficient, indicates that the trend of the fatigue line is more leaning. In the condition of equal k_1 values for both mixtures, the fatigue life of the mixture with higher k_2 value is the longer one. On the other hand, equal k_2 values indicate that the fatigue lives of the samples are parallel to each other and the mixture with lower k_1 value has a lower fatigue life [113].

With decreasing tensile or unit of deformation in asphalt mixtures, just like many other materials, the fatigue life gradually increases. Reductions in the tensile deformation cause the materials to demonstrate an elastic behavior (at very low temperatures or rapid loadings), thus, preventing the formation of fatigue cracks. Generally, the tensile under the fatigue limit causes only elastic deformations. In the indirect tensile fatigue test, plastic deformations cause fatigue deformations and thus, forming fatigue cracks based on this.

The tests conducted in order to determine the fatigue resistance of hot mix asphalts could be implemented as bending tests and direct or indirect tensile tests. In these tests, various types of controlled-loading, such as sinusoidal and haversine, can be used on samples with different geometries. The fatigue tests that are included in the BS DD ABF [114] standard and depended on the sample geometry, type of loading and test apparatus are two-point bending tests conducted on the sample with trapezoid geometries, two-point bending test conducted on the prismatic samples, four-point bending test conducted on prismatic samples and indirect tensile test conducted on cylindrical samples. The tests can be conducted in both a deformation-controlled way and a load-controlled way. The differences between the load and deformation-controlled fatigue tests were presented in Table 5.1 [110].

Table 5.1. Comparison of the load and deformation-controlled fatigue tests [110].

	Load-controlled test	**Deformation-controlled test**
Changes during test period	Increasing displacement	Decreasing load
General cracking criterion	Sample's cracking	Reduction in the half of the initial rigidity
Distribution of results	Low	High
Increase in temperature (> 0 ^oC)	Decrease in fatigue life	Increase in fatigue life
Increase in rigidity modulus	Increase in fatigue life	Decrease in fatigue life
Effect of waiting time	High	Low
Crack formation time	Short	Long
Increase in test frequency	Increase	Decrease
Damage progress	Fast	Medium

The facts that indirect tensile fatigue test is easy to conduct and the samples could be comfortably collected in both laboratory and field environments due to their geometries has made this test one of the most commonly preferred ones. Indirect tensile fatigue test is used to characterize the fatigue resistance of bituminous mixtures under repetitive loading in both tensile and deformation-controlled ways. Cylindrical shaped testing samples are subjected to repetitive pressure loadings on a vertical diametric surface in a haversine way. This loading causes a tensile stress that is perpendicular to the applied load and relatively uniform in the horizontal diametric direction. The formed tensile stresses cause the sample to split vertically from the middle.

Diametral ındirect tensile fatigue test

In diametral indirect tensile test mode (both ITFT and ITSM), a compressive load is applied across the vertical diameter of a cylindrical specimen and this results in a biaxial stress distribution in the specimen as shown in Figure 5.11. As found in the figure the magnitude of both vertical compressive stress (σ_{vx}) and horizontal tensile stress (σ_{hx}) induced on the horizontal diameter of the specimen varies along the diameter. Both σ_{vx} and σ_{hx} reach a maximum value at the center of the specimen. By measuring the horizontal deformation, the values of both the maximum strain and the stiffness modulus of the specimen can be calculated. However, these calculations are based on following assumptions [115].

- The specimen is subjected to plane stress conditions (σ_Z=0)
- The material is linear elastic
- The material is homogeneous and behaves in an isotropic manner
- Poisson's ratio for the material is known
- The vertical load (P) is applied as a line loading

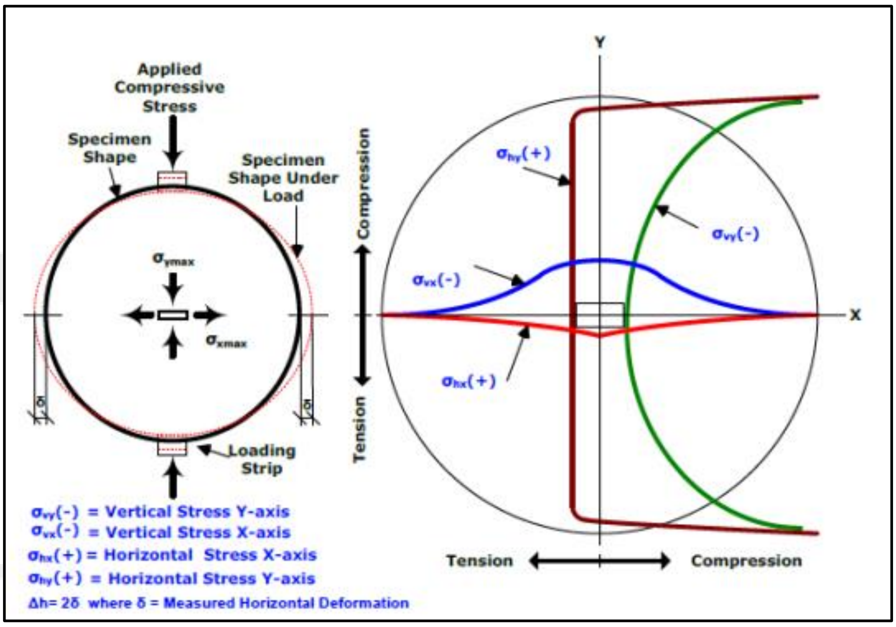

Figure 5.11. Stress distribution along diameter of the specimen in Indirect Tensile Test model [115].

ITFT set up

The Diametral Indirect Tensile Fatigue Test (ITFT) was conducted using the Nottingham Asphalt Tester (NAT), performed in accordance with BS DD ABF: 2003 [114]. Similarly to the ITSM test, the experiment consists of the air-conditioning cabin, loading frame, software and computer. Although the standard test temperature 25^{o}C, the test can be conducted at various temperature thanks to the air-conditioning cabin. Prior to the test, the specimens should be kept at testing temperature for at least 3 hours. The test was performed at various stress levels (initial strain levels) at a rate of 40 pulses/minute. Each specimen was repeatedly loaded until it failed by cracking or a total vertical deformation of 9 mm had been achieved (as larger permanent deformation would likely compromise reliable measurement of the fatigue behavior). The target test stress levels were selected to give as wide a range of lives as possible.

Configuration of the test frame and specimen position in ITFT mode is similar to that in ITSM mode, but without the mounting frame and the alignment jig for LVDT instalment (Figure 5.12). The cylindrical specimen is positioned in between the loading platens. Prior to the ITFT test, an ITSM test in stress controlled mode was conducted on specimens at the required test stress level for the ITFT to determine the horizontal deformation and corresponding ITSM values. Once these tests were done, Eq. 5.5 and Eq. 5.6 were used to determine the maximum stress and maximum strain at the center of the specimen as recommended by the standard. The initial maximum tensile strain at the center of the specimen for each respective stress level as determined for each specimen using Eq. 5.6 was subsequently plotted against corresponding number of cycles to failure (Nf). Linear regression analysis using the least square method was then applied to the data to obtain the fatigue relation in the form of Eq. 5.7.

$$\sigma_{x,max} = \frac{2 * P_L}{n * d * t} \tag{5.5}$$

$\sigma_{x,max}$ is the maximum tensile stress at the centre of the specimen; P_L is the applied vertical load in kN; d is the diameter of the specimen in m; t is the thickness of the specimen in m.

$$\varepsilon_{x,max} = \frac{\sigma_{x,max}}{S_m} * (1 + 3\upsilon) * 1000 \tag{5.6}$$

$\varepsilon_{x,max}$ is maximum tensile strain at the centre of the specimen; υ is poisson's ratio which was assumed as 0.35; S_m is the indirect tensile stiffness modulus at $\sigma_{x,max}$ in Mpa.

$$N_f = \mathrm{C} * (\frac{1}{\varepsilon_{x,max}})^m \tag{5.7}$$

N_f is number of cycles to failure; C is antilog of the intercept of the logarithmic relationship between fatigue life and tensile stress and m is stope of the logarithmic relationship between fatigue life and tensile stress.

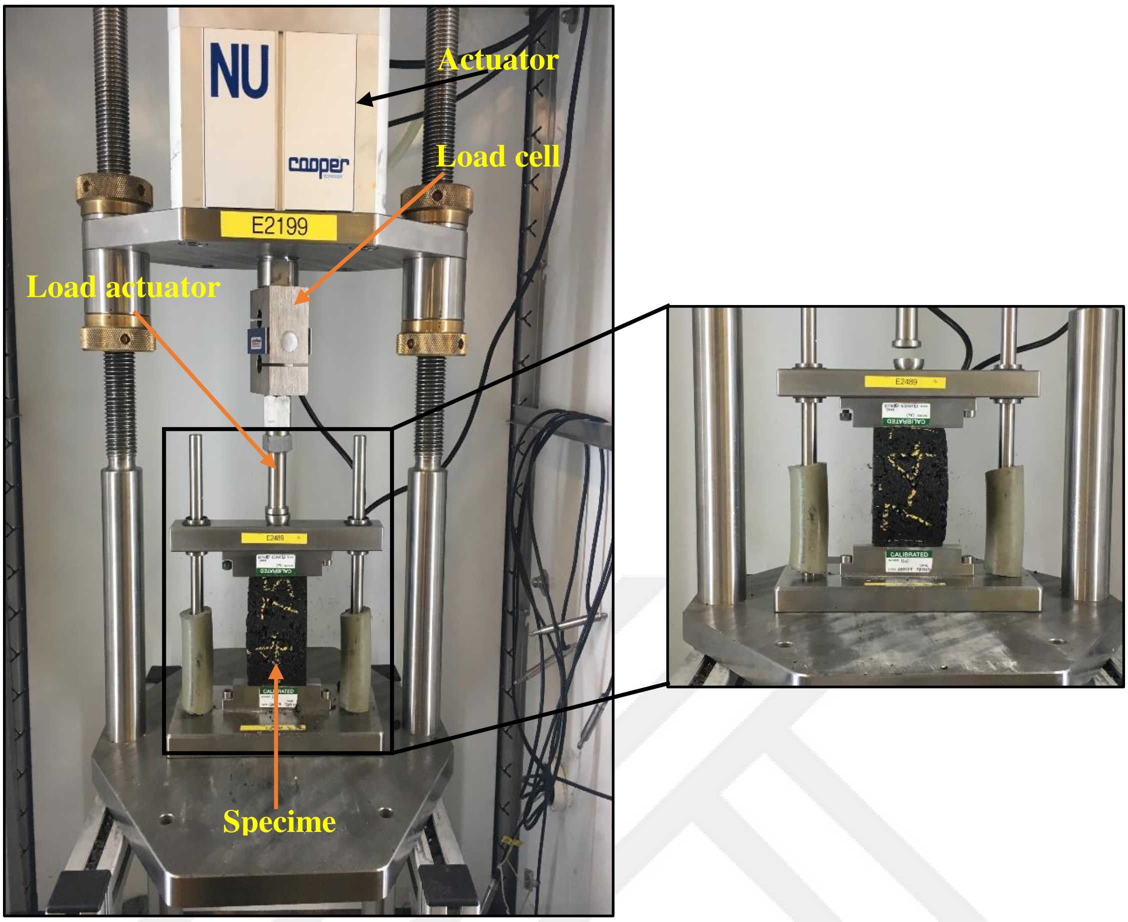

Figure 5.12. ITFT test set up in NAT machine.

5.3.3. Water sensitivity analysis

Based on previous studies, the rehydration of the capsules may affect the preservation of the encapsulated sunflower oil [116]. Likewise, swelling of capsules may affect the capsule/mastic bonding. The A-method defined in standard EN 12697-12 [117] was adopted to assess the effect of saturation and accelerated water conditioning of asphalt mixture specimens with, and without, capsules. A typical test result is shown in Figure 5.13. With this purpose, two subsets of test specimens were conditioned as follows:

(1) Dry group of asphalt specimens: cylindrical asphalt specimens with, and without, capsules were conditioned in a temperature controlled room at 20ºC during 72 h.
(2) Wet group of asphalt specimens: cylindrical SMA specimens with, and without, capsules were conditioned in a water bath at 40ºC during 72 h. Before placing the specimens in the

water bath, they were saturated in a vacuum container for 30 min, using a residual pressure of 6.7 kPa, as defined in the Standard [117].

Figure 5.13. ITS test equipment.

Water sensitivity of the SMA mixtures was measured using the Indirect Tensile Strength (ITS) method of the cylindrical asphalt specimens, following the methodology defined in the EN 12697-23 [118], at the test temperatures of 20ºC and 25ºC. The Indirect Tensile Strength (ITS) in units of kPa was calculated by applying the following equation:

$$\mathrm{ITS} = \frac{2 \cdot \mathrm{F}}{\pi \cdot \mathrm{L} \cdot \mathrm{D}} \qquad (5.8)$$

where, F is the peak value of the applied vertical load in kN, L is the mean thickness of the test specimen in m, and D is the specimen diameter in m.

Furthermore, to quantify the effect of the accelerated water conditioning on the ITS values with respect to the ITS reached for the asphalt specimens tested in dry conditions, the Indirect Tensile Strength Ratio (ITSR) was determined by the following equation:

$$\text{ITSR} = \frac{\text{ITS}_{\text{wet}}}{\text{ITS}_{\text{dry}}} \tag{5.9}$$

where ITS_{dry} and ITS_{wet} are the ITS values calculated for the dry and wet conditioned specimens in kPa, respectively.

5.3.4. Preparing Plate-Shaped Samples with Roll Press

In the compaction of the plate-shaped hot mix asphalt samples prepared in order to subject the samples to tests directly or obtaining the test sample by cutting, the methods defined in BS EN 12697-33 [120] standard are used. In the methods stated in this standard, a bituminous mixture sample at a certain weight is compacted by using a controlled compaction energy or until a determined volume, thus, a void rate, is reached. Standard pneumatic method, steel cylinder (roll press) method and sliding plate method explain the three different methods.

The device providing the compaction of the sample contains forward and backward control, self-advancing rolling cylinder that compacts the sample or hand-controlled cylinder or the cylinder piece that simulates the effect of the cylinder and applies static loads to the sample. If the samples are to be prepared at a certain volume or a certain amount of air voids, a vibrating compactor or a table could be used. The vehicle can apply the F static load presented below.

$$\frac{\text{F}}{\text{l} * 2\text{D}} \geq 10^{-5} \tag{5.10}$$

Here, F is the static load applied to the cylinder or the rubber (kN), l is the inner width of the mold (mm) and D is the diameter of the cylinder or the rubber (mm). The steel cylinder's diameter should be between 400 and 1100 mm. The desired density or the air void could be achieved after 10-50 steel cylinder passes. If the plate-shaped samples are prepared by using a steel cylinder with controlled-compaction energy, the width of the cylinder should be lower (10±5 mm) than the inner width of the mold. The amount of the material to be used is calculated by using the formula presented below that covers maximum theoretical specific weight (G_{mm}), inner sizes of the mold (L and l), the thickness of the sample (e) and void content (V_a).

$$M = 10^{-6} * L * l * e * G_{mm} * \left(\frac{100 - V_a}{100}\right) \quad (5.11)$$

Here, M is the weight of the sample (kg), L is the length of the mold (mm), l is the inner width of the mold (mm), e is the last height of the sample, G_{mm} is the maximum theoretical specific weight of the bituminous mixture (gr/cm^3) and V_a is the amount of void of the sample (%). The mold is filled with M ± % 0.1 gr material. If possible, the material inside the mold is spread with a shovel, preventing segregation. The materials in the corners should be removed by pressing before the compaction.

A soapy solution is slowly sprayed to the cylinder and a film plate is placed between the material and the cylinder. The compaction process is conducted restlessly until a smooth surface is achieved. The compaction is maintained until the required number of passes are completed. The plate-shaped samples prepared and the roll press are presented in Figure 5.14.

Figure 5.14. Roll press and sample preparation.

5.3.5 Wheel tracking test

The wheel tracking test is conducted by the passing of the rubber wheel that applies a certain amount of load at a stable temperature. The rut depth formed as a result of the test indicates the HMAs' resistance to deformation. The wheel tracking test device used in this thesis study is classified as a small-size type of device stated in the standard.

According to the standard, the outer diameter of the wheel should be between 200-205 mm. The wheel should not be textured and its width should be 50±5. The thickness of the rubber on the type should be 20±2. Under normal test conditions, the load (P) to be applied on the wheel, which is measured from the surface of the sample, is calculated in Newton by using the formula below.

$$P = \left[\left(700\frac{w}{50}\right) \pm 10\right] \tag{5.12}$$

The movement distance of the wheel should be 230 ± 10 and load repetition frequency for every 60 seconds should be 26.5 ± 1. The device can provide the set temperature with a sensitivity of ± 1 ºC. The test samples should be prepared in their own molds and according to the EN 12697-32 [119] or EN 12697-33 [120] standards. The difference between the volume specific weights of two test samples from the same series should be 1% different from the mean volume specific weight. The height of the samples to be used in small devices should be prepared in a way that is suitable for field implementation or the approximate thickness presented below should be taken into account according to the size of the aggregate.

- 25 mm for the mixtures with the largest grain size lower than 8mm
- 40 mm for the mixtures with the grain size between 8-16 mm
- 60 mm for the mixtures with the grain size between 16-22 mm
- 80 mm for the mixtures with the grain size between 22-32 mm

The height of each sample should be measured from the middle of each corner. If the nominal thickness is 50 mm or less, the difference between the four measurements should not be more than 2.5 mm. If the nominal thickness is more than 50 mm, the difference between the four measurements should not be more than 5%. The movement area of the wheel should be gauged and the samples with a height difference of more than 2mm should not be used in tests.

Rutting was developed using a wheel tracking machine on the slabs to study the mechanical effects of the capsules on the asphalt. The device uses a loaded wheel to apply a moving load on the slab specimens to simulate traffic load applied on the asphalt pavement.

The standards followed in this test were British Standard BS EN12697-22:2003 [121]. In the Immersion Wheel Tracker, a mechanical re-circulating water bath controls the temperature to within ± 0.5ºC, in a range of 20-70ºC. Also, the device can test two slabs simultaneously for the same temperature. However, in the dry condition test, the device can only test one sample at a time. Moreover, the test will be running in a cabinet with a double-glazed door to control the temperature.

Asphalt mixture slab with and without capsules were manufactured. In asphalt mixture with capsules, three different capsule contents as a percentage of the total mixture were used, 0.5%, 0.75% and 1%. The asphalt slabs have tested by using wheel tracking equipment/s at two different environmental conditions (dry and wet) and at five different temperatures, between 20, 30, 40, 50 and 60 ^{0}C. First, slabs were tested in an Immersion Wheel Tracker at 20 and 60ºC, see Figure 5.15(a). After placing the samples in the moulds and positioning them in the device, the machine will fill with water. The temperature was set one day before the test, to allow the device to reach the desired temperature. On the next day, the test was started and the wheel started passing through the samples. The wheel passed 10,000 cycles (20,000 passes) before stopping, otherwise it will stop if the rut depth reaches 15mm - the maximum depth that the device can measure. The ruts are measured using two displacement transducers attached to the wheel support arms. When the test is finished, the slabs are removed from the mould and water is discharged from the bath; to repeat the test for each slab, one must only change the temperature. However, the slab will test each one individually, since there is only one slab at each temperature; each test will take around 6 to 6.5 hours.

In the dry condition, the British Standard BS EN12697-22:2003 method is also followed. As shown in Figure 5.15(b), it has a solid aluminium frame and a cabinet made of stainless steel to control the temperature with a double-glazed window. The traffic simulation is carried out by rolling a rubber wheel thickness of 20 mm. The rut depth in this device by LVDT transducer is at the centre of the slab along the longitudinal profile. Also, the test will stop after 10,000 cycles (20,000 passes), or the rut depth reaches the maximum rut depth 15mm. The temperature setting and the sample preparation will be the same as the Immersion Wheel Tracker machine.

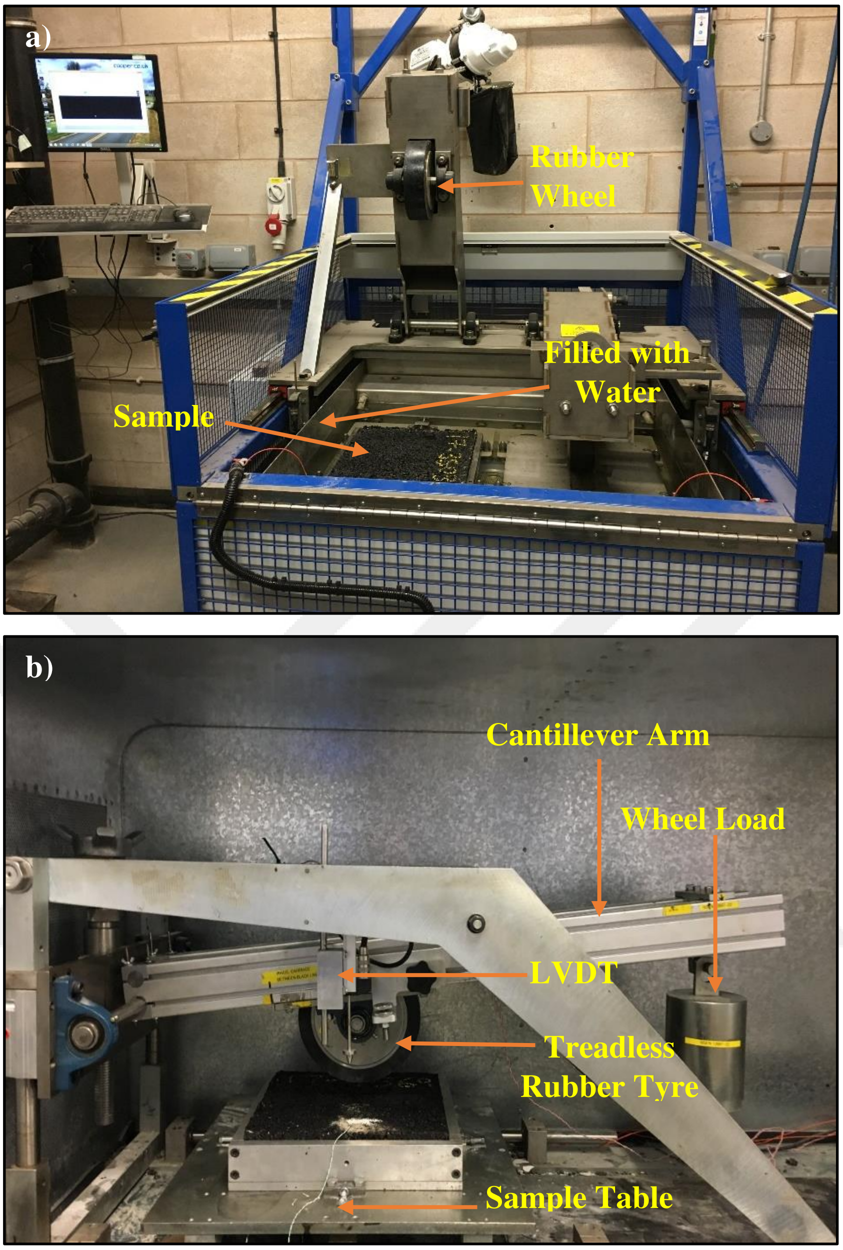

Figure 5.15. a) Immersion wheel tracker for wet condition b) wheel tracking test (WTT) device in an insulated temperature control cabinet for dry condition.

5.3.6. Crack healing

To evaluate the effect of mixing method and aging time on the self-healing properties of asphalt under real conditions, an experimental crack-healing methodology was used [78]. Self-healing of asphalt mixtures with, and without, capsules was quantified as the healing level reached from the flexural strength recovery of cracked asphalt mixture beam tested under a three-point bending (3PB) test after a rest healing time. The crack-healing test was implemented according to the following steps, which were applied for both mastic and asphalt beams with slight changes, see Figure 5.16:

- Step 1 - Crack generation: asphalt mixture beams with, and without, capsules were conditioned at -20ºC for 4 h and 3PB tests were carried out at a loading rate of 2 mm/min until the beams were broken in two pieces.
- Step 2 – Capsules' activation: after the 3PB test, a plastic membrane adaptable to the faces of the crack, was placed between the two broken pieces of the beam. Then, the two pieces were put back together and placed in a steel mould. To break the embedded capsules, a strain controlled compressive load was applied at a rate of 2 mm/min on the top surface of the beam, at 20ºC, until the vertical deformation reached 5 mm. Later, the plastic sheet was removed, and finally the two pieces of the beam were put back together into the steel mould.
- Step 3 – Healing process: to start the healing process of the broken beam, the asphalt beam in the steel mould was placed into a temperature-controlled chamber at 20ºC for 120h. Once the healing (rest) time was reached, the healed beam was removed from the chamber and steel mould, and Step 1 was repeated thus completing a damage-healing cycle.

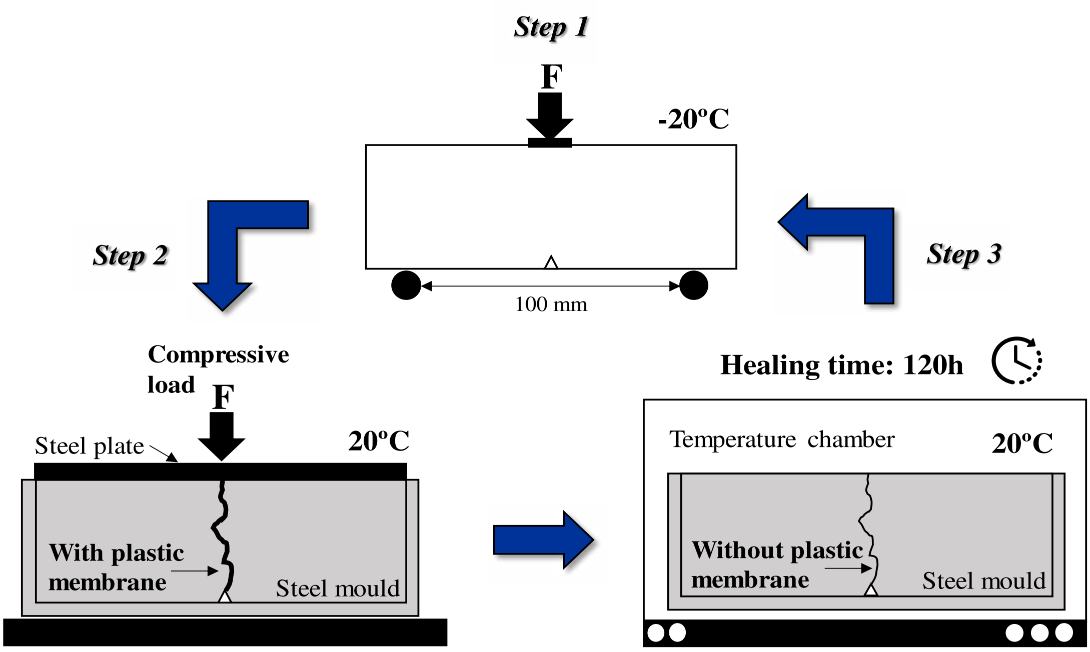

Figure 5.16. Schematic diagram of the asphalt mixture crack-healing test: Step 1. crack generation in the asphalt beam, Step 2. capsules activation to begin the oil release, and Step 3. healing process.

The healing level, HL, reached for each cracked asphalt mixture beam after the healing time was defined as the relationship between the maximum load of the beam initially tested, $F_{initial}$, and the maximum load measured in the same beam after the healing process, F_{healed}:

$$P = \frac{F_{healed}}{F_{initial}} \tag{5.13}$$

5.3.7. Three point bending fatigue test

The fatigue healing capacity of asphalt containing capsules was studied by subjecting prismatic beams to 3-point dynamic cyclic bending. A Universal Testing Machine (UTM) was used to perform the fatigue tests. To avoid the production of permanent deformations during the fatigue test, a flexible pad was placed under the sample. Each loading wave lasted 0.10s and it was followed by a resting period of 0.15s before the following loading pulse. Hence, the loading frequency was 4Hz. A minimum load of 0.15 kN was selected to ensure that actuator and sample are in contact at every moment. Four different maximum loads were selected to study the effect of this parameter on the healing performance of asphalt mixes: 1.75, 2.75, 3.75 and 4.75 kN. The tests were carried out at 20ºC. The test samples were previously painted in white and continuously monitored during the test by a static camera with an f/2.8 aperture and a 12Mpx resolution taking a picture every 40 loading cycles. The length of the crack was determined at every moment by processing the images by ImageJ® software. It was considered that the asphalt samples failed when the crack length reached 10% of total crack length at the end of the test (samples completely split). The 3PB fatigue test was implemented according to the following steps:

- **Step 1.** Asphalt mixture beams with, and without, capsules were conditioned at 20ºC for 4 h before starting 3PB fatigue tests. The test continued until the sample broke in two pieces.
- **Step 2.** The average lifetime of the samples was estimated as the number of cycles whose Weibull probability of breakage is 50% ($N_{0.5}$). Such number of cycles will be referred hereafter as $N_{0.5}$ (Fig. 5.17–left). The cycle number at which cracks reach an approximate length of 1 cm from the beginning of the tests will be referred hereafter as $N_{0.5}$ (Fig. 5.17–right).

Besides, the healing test was implemented according to the following steps:

- **Step 1**. In order to evaluate the capacity of the asphalt mixture to extend its service life, series of 10 samples of each type of mixture were manufactured. Asphalt mixture beams with, and without, capsules were conditioned at 20ºC for 4 h and 3PB fatigue tests were carried out at different loadings (1.75, 2.75, 3.75 and 4.75 kN) until the beams were broken in two pieces (Figure 5.18).
- **Step 2.** In this case, each fatigue test was paused at different number of cycles depending on the calculated $N_{0.5}$. Then, the samples were placed into a temperature-controlled chamber at 20 ± 2ºC for 48 h. Once the healing (rest) time was reached, the healed beam was removed from the chamber and returned to the test until the failure was reached.
- **Step 3.** The extension of the service life was assessed for each sample through the concept of Healing Index (HI), which compares the total number of cycles resisted (Nf) and the reference ($N_{0.5}$) explained above as follows:

$$\mathrm{HI} = \frac{F_f - N_{0.5}}{N_{0.5}} \tag{5.14}$$

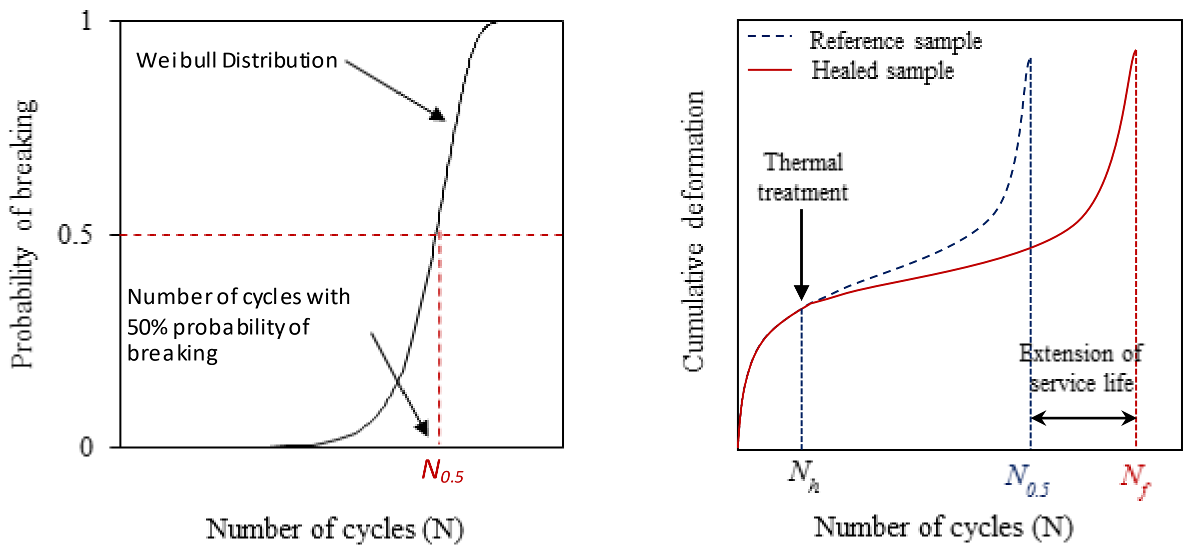

Figure 5.17. Scheme of how the number of cycles with 50% probability of breaking can be obtained based on Weibull probability distribution (left) and how service life extension can be evaluated (right).

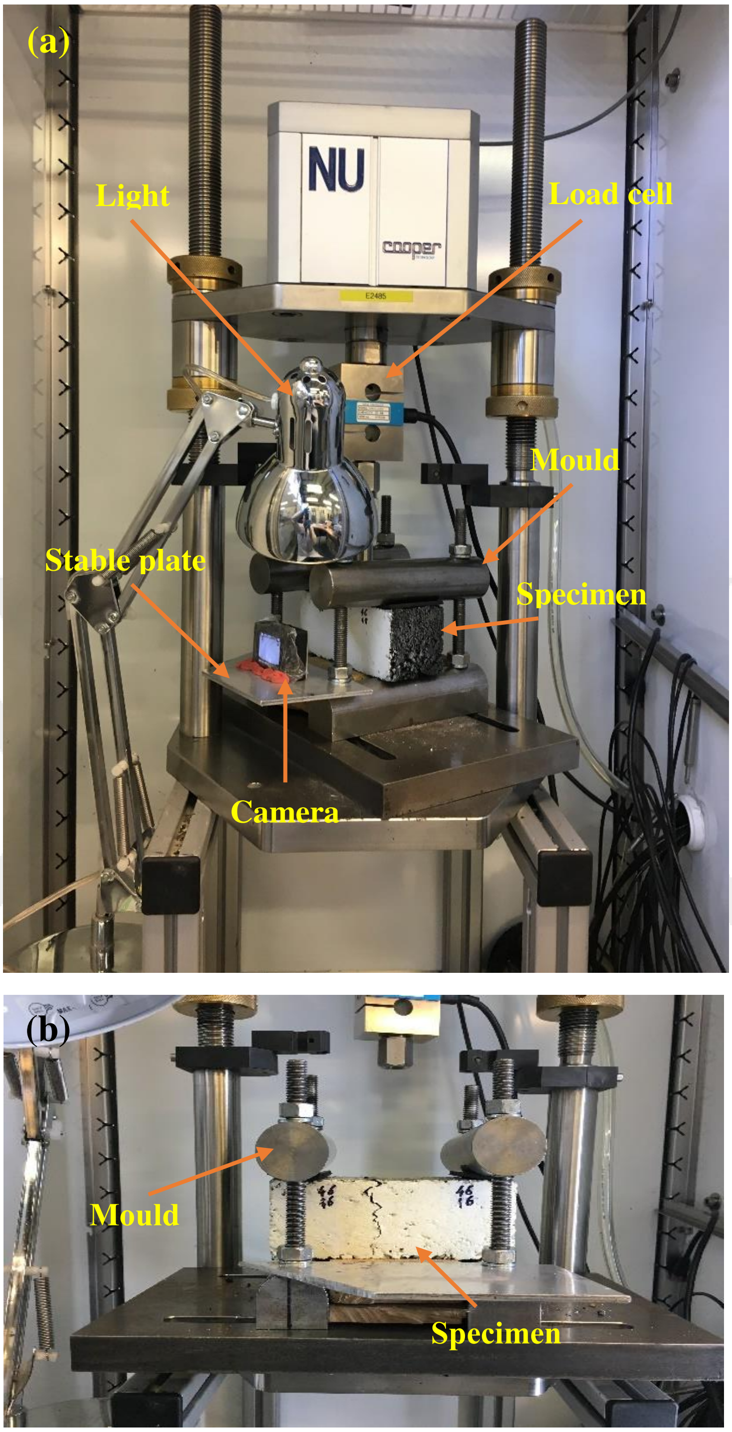

Figure 5.18. a) 3PB fatigue testing configuration.b) broken specimen after 3PB fatigue test.

5.3.8. Skid resistance test

It was proven that the capsules can release small amounts of rejuvenator during the mixing and compaction processes [78]. With the aim of evaluating the effect of the oil release on the skid resistance of the asphalt slabs, dynamic pendulum test measurements on the asphalt slabs with, and without, capsules were carried out following the protocol defined in the standard BS EN 13036-4 [122]. In this test, the measured values represent the friction properties of the surface given by the British Pendulum Number (BPN) (Figure 5.19). The test consists of applying water on the surface of the slabs and re-wetting it every time after swinging the pendulum. Then, the pendulum is raised to a fixed height and it is released to make contact with the surface of the slab. A drag marker shows the BPN value. With increasing friction between the pendulum and the test surface, the BPN value increases. All the tests were measured at 20ºC and the BPN value was calculated as the average of five repetitions.

Figure 5.19. Skid test configuration.

5.3.9. X-ray computed tomography

To evaluate the capsule distribution and their integrity inside the asphalt mixtures described, X-ray computed tomography (CT scan) was employed. To do that, asphalt cylindrical samples of 3.5 cm diameter and 60 mm height were extracted from asphalt mixture beams with capsules, see Figure 5.20. The X-ray tomography scans were developed using a GE Sensing and Inspection Technologies GMBH Phoenix VTomeX M operated at 200 kV and 180 µA. Thus, each tested sample was mounted on a rotational table at distance of 163.74 mm (FOD) from the X-ray source and the distance between the X-ray source and the X-ray detector was 818.698 mm (FDD). A spatial resolution of 40 µm was achieved. Scan settings were 200 ms per radiograph capture with 2520 projections captured on a 360º rotation using an average of four images and skip of one. Detector panel sensitivity was set at 2. Reconstruction of radiographs was performed using Phoenix Datos X2 Reconstruction software. Radiographs were uploaded into the software and corrections were applied for: movement using a scan optimiser algorithm; beam hardening; cone beam ROI; and air observation ROI. Once reconstructed into 3D volume 2D image slices were exported in TIFF format along the XY axis. Image processing of the capsule distribution was prepared by segmenting the materials found in a specific volume, based on simple thresholding to separate the asphalt mixture of the capsules. The software used for 3D volume and 2D image processing was VGStudio MAX version 2.2.

Figure 5.20. CT scans analysis and an example of an image of results.

6. EFFECT OF MIXING AND AGING ON THE MECHANICAL AND SELF-HEALING PROPERTIES OF ASPHALT MIXTURES CONTAINING POLYMERIC CAPSULES

6.1. Introductıon

An asphalt mixture is composed of aggregates and bitumen, and it is the most used material to build road pavements worldwide. Aggregates usually give strength and structural stability, while bitumen works as a binder. The capacity of pavements to carry loads depends on the bond between aggregate particles provided by the bitumen [123]. However, this bond degrades over time due to the most significant issue that bitumen faces, which is the damage by aging [124]. The damage by aging results from oxidation and loss of the volatiles from bitumen composition, which causes stiffness and an increase in viscosity. This leads to the appearance of microcracks which evolve to form cracks and the detachment or raveling of aggregates in asphalt pavements, reducing their mechanical performance over time [125].
Hence, to maintain pavements in good condition during their lifetime, external maintenance is usually required by the road agencies of each country [126]. The most common solution to restore the original properties of aged pavements and reconstitute the bitumen chemical composition is to use rejuvenators, which are low viscosity oils with high maltenes content, on the surface of asphalt roads [127]. However, spreading rejuvenators over the surface of roads has side effects, such as reducing the skid resistance of the pavement surface because they penetrate only for the first few centimetres. Additionally, roads must be closed for some time after the application of rejuvenators [67].

To overcome the disadvantages of using rejuvenators on the pavement surface, researchers have proposed the use of encapsulated rejuvenators to restore the original properties of the bitumen via self-healing processes [53,55,67,69,85]. This technique is supported by the fact that bitumen is a self-healing material with the ability to close microcracks by itself [128]. The principle behind this approach is that these capsules containing rejuvenators will remain inactive in the asphalt road for several years until external damage happens to the asphalt pavement [68]. Consequently, cracks will break the shell of the capsules in a timely manner, leading them to release the rejuvenator into the asphalt medium, which will diffuse and reduce the bitumen viscosity so it can easily flow into the cracks [53].

Different methods have been used to manufacture microcapsules, or capsules, with encapsulated rejuvenators for asphalt self-healing purposes. For example, Su et al. [55] prepared microcapsules containing rejuvenator droplets by in-situ polymerisation of urea-formaldehyde, making a Methanol-Melamine-Formaldehyde (MMF) prepolymer as a shell. Garcia et al. [53] prepared capsules of a larger size by saturating porous sand with sunflower oil as rejuvenator material, protected by a hard shell of cement and epoxy resin. Details of another type of polymeric capsule were published by Micaelo et al. [69] and Al-Mansoori et al. [78,85]. These capsules were made by the ionotropic gelation of sodium alginate in the presence of calcium chloride solution. In these capsules, the encapsulated material was also sunflower oil and their size was a few millimetres. Broadly, these studies proved that the capsules are resistant to asphalt fabrication and release the rejuvenators only when broken due to external loading, and they have a positive effect on the durability and safety of asphalt mixtures [69]. Additionally, these capsules proved the self-healing ability of aged bitumen and rejuvenated aged asphalt mixture; although these studies did not evaluate the effect of the mixing method of the capsules and aging conditions of the asphalt on the mechanical stability and self-healing properties of asphalt mixtures with capsules.

For all these reasons, in this study calcium-alginate capsules for asphalt self-healing have been designed and tested using different mixing orders and aging conditions to investigate the effect of mixing and aging conditions on the mechanical stability and self-healing properties of asphalt mixtures with, and without, capsules. The manufacturing process of the polymeric capsules and their thermal and mechanical characteristics are firstly presented in this study. The mechanical tests implemented in this study to evaluate asphalt mixtures were stiffness modulus and flexural strength. Moreover, self-healing properties of the studied asphalt mixtures were quantified through three-point bending tests on cracked asphalt beams with, and without, capsules. Finally, an X-ray computed tomography analysis was carried out to evaluate the capsules' distribution and their integrity inside the asphalt mixture.

6.2. Manufacturing of asphalt mixture samples

Prismatic and cylindrical asphalt mixture samples with, and without, capsules were manufactured in this study. A capsule content of 0.5% by total mass of the mixture was added in the asphalt mixtures. This amount provides an approximate oil-to-bitumen content of 6.97% by mass in bitumen which is set with the oil-to-bitumen content (6 to 8%) recommended by Ji et al. [129] in order to recover the aged bitumen and improve its physical and chemical properties. Furthermore, asphalt mixtures were produced in the laboratory in batches of approximately 14 kg, using a lab mixer equipped with a helical horizontal mixing shaft. Capsules were pre-heated and mixed in four different conditions with the aim of evaluating the effect of the mixing order on the mechanical and self-healing properties of asphalt mixtures. The pre-heating and mixing methods for the asphalt mixtures with, and without, capsules were as follows:

- Mixture 1: the aggregates were pre-heated at 160ºC for 12 h, while the bitumen and the capsules were pre-heated at 160ºC for 4 h. The capsules were mixed at the beginning of the mixing process with the aggregates, see 6.1(a).
- Mixture 2: the aggregates were pre-heated at 160ºC for 12 h, while the bitumen and the capsules were pre-heated at 160ºC for 4 h. The capsules were mixed at the end of the mixing process with the asphalt mixture.
- Mixture 3: the aggregates and bitumen were pre-heated at 160ºC for 12 h and 4 h, respectively, while the capsules were left to defrost for two hours at 20ºC before mixing. The capsules were mixed at the beginning of the mixing process with the aggregates.
- Mixture 4: the aggregates and bitumen were pre-heated at 160ºC for 12 h and 4 h, respectively, while the capsules were left to defrost for two hours at 20ºC before mixing. The capsules were mixed at the end of the mixing process with the asphalt mixture, see 6.1(b).
- Reference mixture: the aggregates and bitumen were pre-heated at 160ºC for 12 h and 4 h, respectively. The materials were mixed without capsules (WO/C).

For all the asphalt mixture types, the materials were mixed for 2 minutes at 125 rpm at 160ºC, ensuring an adequate dispersion. Likewise, depending on the type of mixture, the capsules were added to the drum at the beginning or at the end, and mixed for 20 additional seconds to obtain their uniform dispersion, see 6.1. Then, the mixture was transferred to the moulds for their compaction. Simultaneously, some capsules embedded in the mixtures,

Figure 6.1(c), were randomly extracted with the aim of evaluating their damage condition, see Figure 6.1(d), before the compaction process.

Prismatic samples of approximately 150×100×60 mm, see Figure 6.2(a), were cut from 306×306×60 mm asphalt slabs compacted by using a roller slab compactor to reach the design for air voids, see Table 3.1. Likewise, to facilitate the creation of a single crack surface on the prismatic samples during crack-healing tests, a transverse notch of 5×5 mm was made at the mid-point on the bottom surface of the beams. Additionally, cylindrical test specimens, with 100 mm diameter and approximately 50 mm height, were compacted by using a gyratory compactor, with an inclination angle of 2.0º and 650 kPa of static pressure. A maximum of 250 gyrations were applied during compaction.

Furthermore, some semi-circular samples were cut from the cylindrical specimens. On the semi-circular samples, a notch of 5×5 mm was cut at the midpoint in the direction of the loading from the central axis of the sample. Finally, a total of 300 prismatic and cylindrical test specimens with, and without, capsules were manufactured in this study.

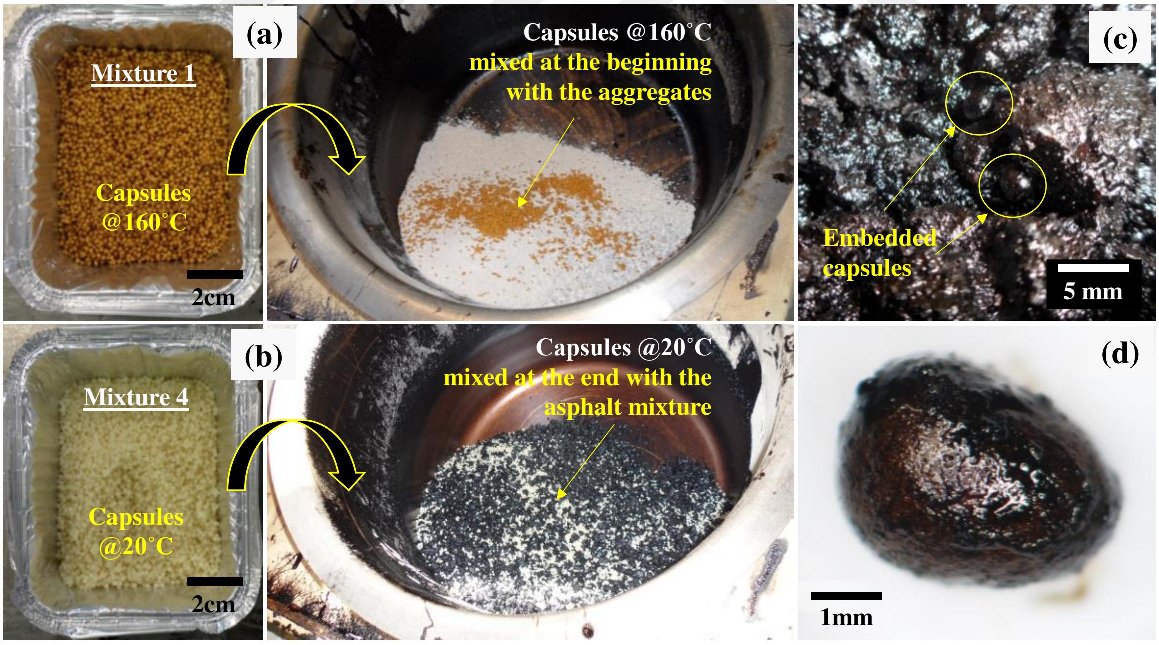

Figure 6.1. Images of (a-b) pre-heating and mixing process for the asphalt mixture types 1 and 4, (c) embedded capsules in mixture, and (d) individual capsule extracted after mixing process.

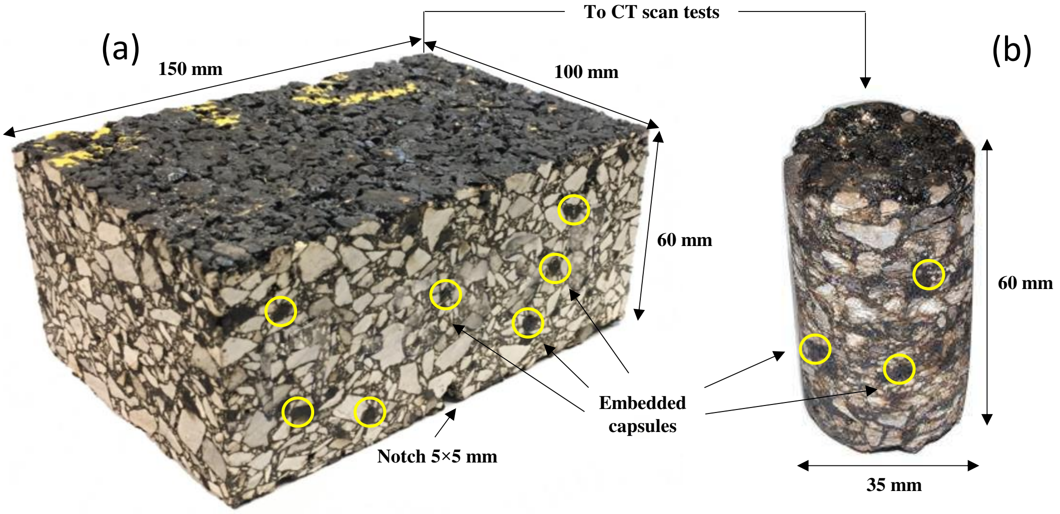

Figure 6.2. (a) Asphalt beam used in the crack-healing tests, and (b) asphalt core cylinder used in the CT scan tests.

6.3. Experimental programme description

6.3 describes the experimental programme followed in this study. Basically, in this research two different experimental stages were defined depending on their objective, as follows:

- Stage 1: to evaluate the effect of the mixing order and the aging times on the mechanical and self-healing properties of asphalt mixtures. In this stage, all asphalt mixture types described in section 6.2 were evaluated using tests of stiffness modulus at 20ºC, flexural strength and crack-healing. In the flexural strength and crack-healing tests the asphalt mixture samples were tested under different aging times, see Figure 6.3.
- Stage 2: to evaluate the effect of compaction waiting time and aging process on the mechanical stability of asphalt mixtures. The waiting time of un-compacted asphalt mixture under in-situ conditions was simulated by pre-conditioning all asphalt mixture types described in section 6.2, as follows: first, batches of un-compacted asphalt mixtures were stored in an oven at 140ºC and 160ºC for 4 h. Then, asphalt mixtures were compacted in asphalt cylinders following the process described in section 6.2. In this stage, pre-conditioned asphalt mixtures at 140ºC and 160ºC were evaluated using tests of stiffness modulus at 20ºC and flexural strength under different aging times, see Figure 6.3.

Finally, the aging process on the asphalt test samples was simulated in laboratory conditions by using an oven according to Garcia et al. [130]. For flexural strength tests, semi-circular asphalt samples were placed in an oven at 85ºC for 9 different aging times: 2, 24, 48, 72, 96, 144, 180, 210 and 240 h. While for crack-healing tests, asphalt beam samples were placed in an oven for a single aging time of 240 h at 85ºC.

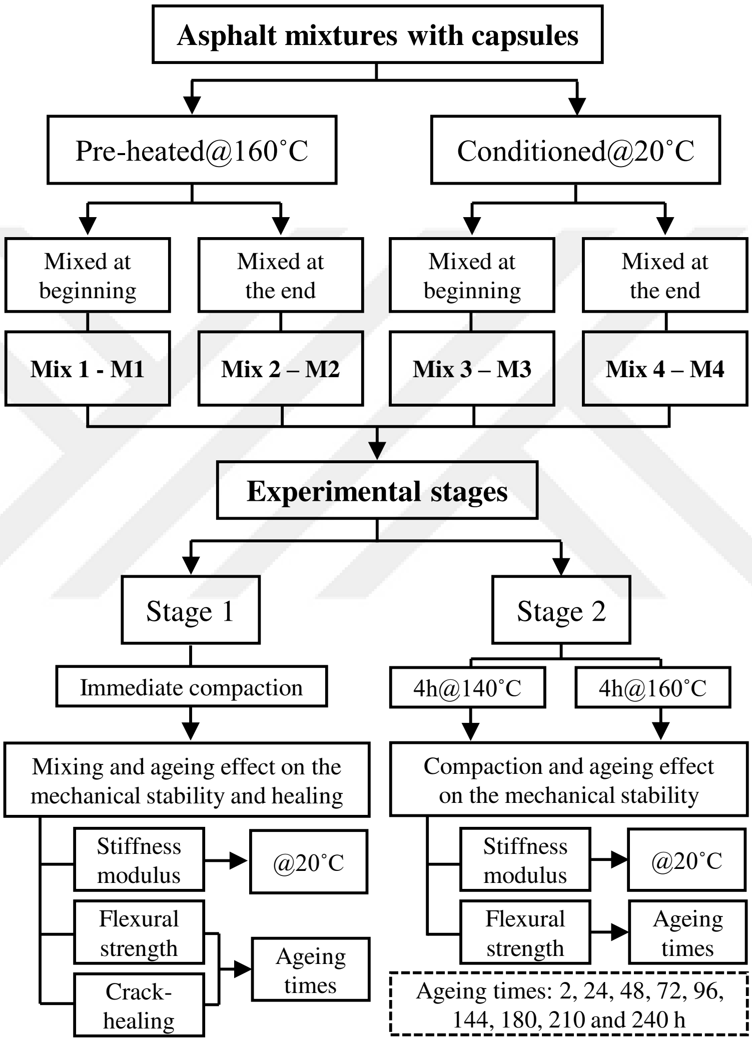

Figure 6.3. Diagram of the experimental program followed in this section.

6.4. Effect of temperature on the properties of polymeric capsules

Polymeric capsules with encapsulated sunflower oil were added to the asphalt mixtures to improve their self-healing properties. However, the mixing and compaction processes of the asphalt mixtures may possibly affect their physical, thermal and mechanical properties [78]. This section presents and discusses the characterization results of the capsules.

The effect of the temperature on the density of the capsules was studied. The capsules registered average density values of 1.116 g/cm^3, 1.059 g/cm^3 and 1.021 g/cm^3, at temperatures of 20ºC, 140ºC and 160ºC, respectively. This demonstrated that the density of the polymeric capsules reduced with the increase of temperature, which was due to the loss of mass experienced by the capsules when exposed to increasing temperature, as evidenced in the TGA profiles, see results shown in Figure 6.4(a). It can be observed in Figure 6.4(a) that the capsules designed in this study reduced their mass with the increase of temperature, registering mass loss values of 3% and 4%, at 140ºC and 160ºC, respectively. This mass loss registered by the capsules at high temperatures is mainly attributed to the degradation of the calcium-alginate polymer structure and water evaporation.

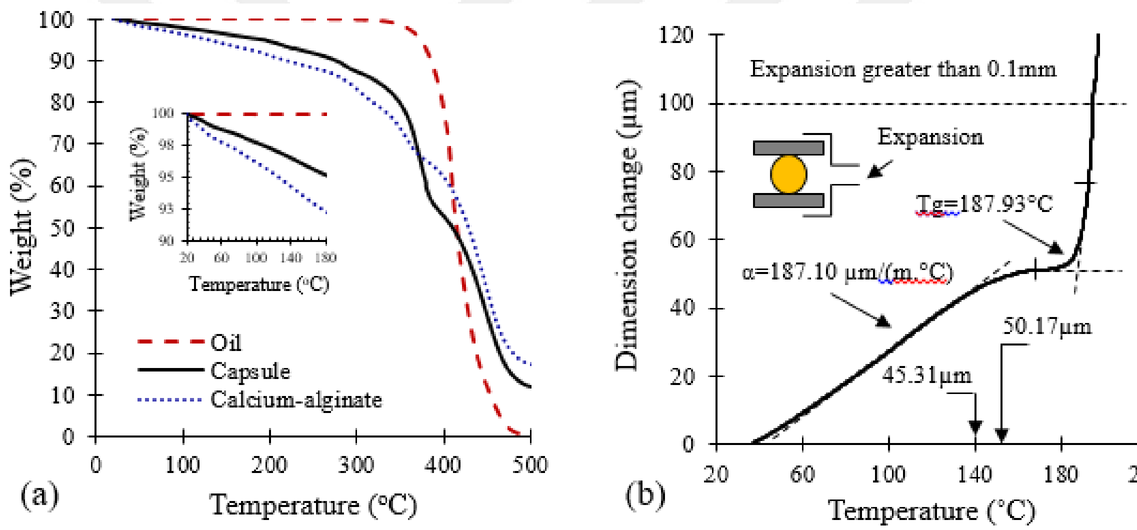

Figure 6.4. (a) TGA test result of a capsule and its components, and (b) thermal expansion curve of a capsule.

Furthermore, their change in color to a darker one at high temperatures, see Figure 6.1(a), was due to the partial peroxidation of the encapsulated oil [131]. This chemical phenomenon occurs when the sunflower oil is exposed to high temperatures (160-200ºC), causing the hydrogen atoms to separate from the oxygen and carbon bonds. As a result, peroxides are formed in the bonds that oxidize the oil thus making it a darker color with a more viscous texture.

Moreover, the reduction of the capsules' density with the temperature could also be due to the variations in their volume caused by thermal expansion. In this context, Figure 6.4(b) shows the average curve obtained from the thermal expansion test carried out on the capsules. In this Figure, it can be observed that the size of the capsules linearly increased with the temperature, from 20ºC to 170ºC, registering changes on the diameter of 45.31 µm and 50.17 µm, at mixing temperatures of 140ºC and 160ºC, respectively. Thus, the variation of the capsules' diameter at mixtures manufacturing temperatures (~140ºC) was apparently not significant.

To prove this hypothesis, the average diameter of 20 individual polymeric capsules before, and after, the mixing process was measured by taking photographs under an optical microscope. After-mixing capsules were randomly taken by hand from a blend batch of un-compacted hot mixture asphalt, see Figure 6.1(c). As a result, the average values of the capsules diameter before, and after, the mixing process were, respectively, 2.572 mm and 2.895 mm. Likewise, after-mixing capsules were surrounded by a bitumen membrane with an average thickness of 0.271 mm, see Figure 6.1(d). Therefore, the increase of the diameter of capsules after mixing was not significant (<53 µm), and can be considered as thermally stable at the mixing temperatures (140-160ºC) used to manufacture asphalt mixtures. Additionally, Figure 6.4(b) shows that the capsules presented a thermal expansion coefficient of 187.10 µm/m.ºC, with changes in the diameter over 100 µm at temperatures over 200ºC, which can be translated into capsules' mass loss close to 10%, see Figure(a).

On the other hand, Figure 6.5 shows the results of compressive strength of the polymeric capsules tested at 20ºC, 140ºC and 160ºC. The stress-strain curves of the compressive tests showed a ductile behavior where the peak load was reached at deformation levels between 0.6 mm and 0.2 mm at, respectively, 20ºC and 160ºC, see Figure 6.5(a). This result proves that the capsules reduced their strength and strain with the increase of temperature. This was because the exposure to high temperatures degrades the calcium-alginate polymeric structure of the capsules making them more brittle, and hence less flexible to mechanical loads. Similar results were also recently published by Micaelo et al. [69].

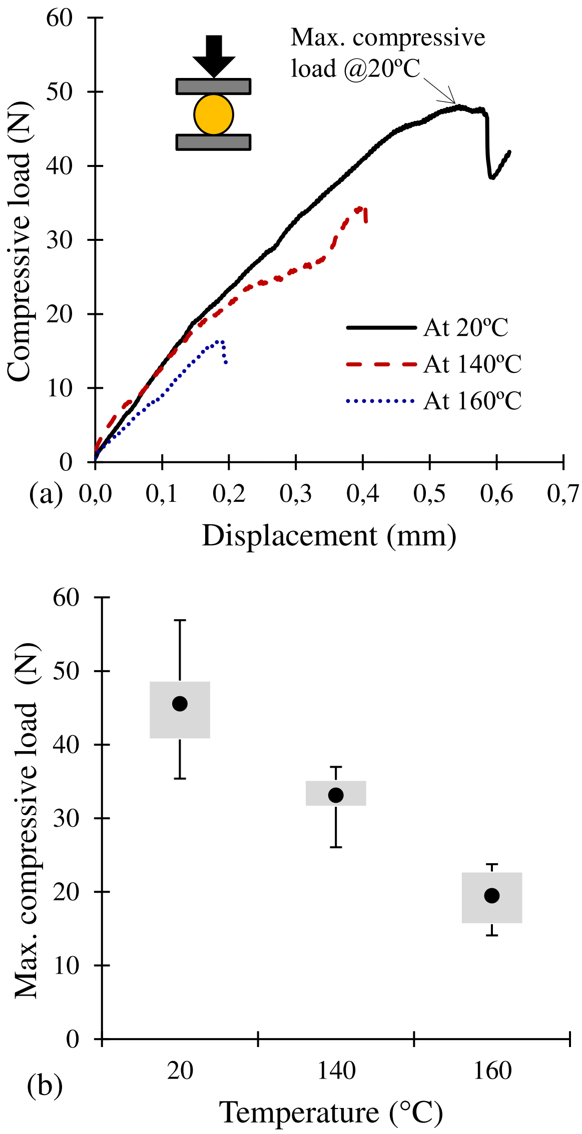

Figure 6.5. (a) Mechanical strength, and (b) statistical values of maximum compressive load.

Otherwise, Garcia et al. [53] in their study about characterization of capsules containing rejuvenators had shown that the minimum compressive strength of capsules required to resist the mixing and compaction processes was 10 N. Consequently, the measured compressive strength of the polymeric capsules at 20ºC, 140ºC and 160ºC, was 46 N, 33 N, and 19 N, respectively (see Figure 6.5(b)), which proved that the designed capsules can resist the mixing and compaction processes. Likewise, compressive strength reached by calcium-alginate capsules at low and high temperatures, was two times greater than that of the capsules presented by Al-Mansoori et al. [53]. This proved that the addition of a higher amount of sodium alginate to the capsules' composition helped to increase their mechanical strength, because the calcium-alginate capsules present a denser internal structure, see SEM image in Figure 6.6(b).

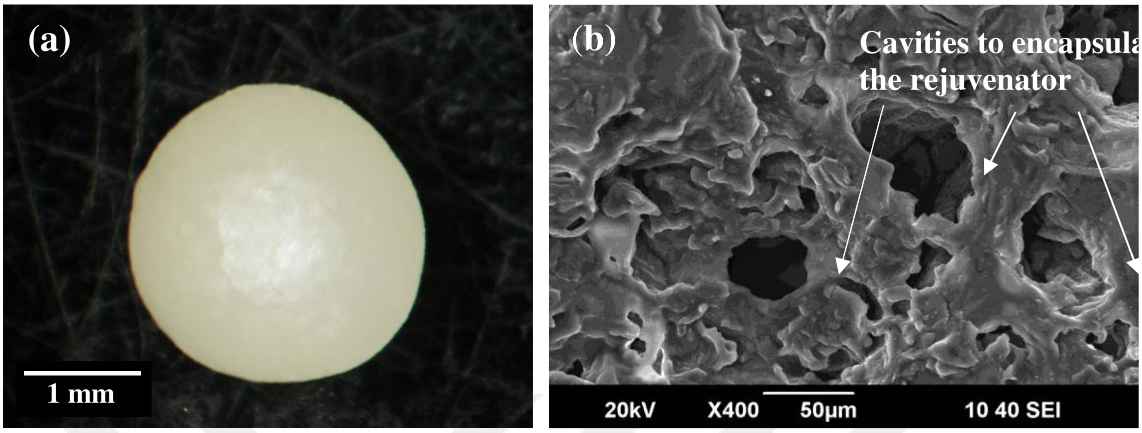

Figure 6.6. (a) Individual polymer capsule, and (b) SEM image of calcium-alginate internal structure of capsules.

6.5. Variation of the physical properties of asphalt mixtures with and without capsules

Figure 6.7 shows the average results of the bulk density and air voids content of the asphalt mixtures with, and without, capsules evaluated after different mixing and aging conditions. In Figure 6.7(a), it can be observed that the average density values of the mixtures with, and without, capsules evaluated after the usual compaction conditions, Stage 1, were similarly regardless of the pre-conditioning temperature of the capsules and the mixing order. In general, average results of the mixtures density were similar to the bulk density of the design mixture (2.383 g/cm^3), asphalt mixtures without capsules (WO/C) and M2-mixture with capsules being those which registered the highest and lowest densities, with average values of 2.420 g/cm^3 and 2.404 g/cm^3, respectively. Additionally, it was observed that M4-mixture with capsules added at the end of the mixing process at 20ºC, presented the average bulk density most similar to that of the reference mixture, which was 2.416 g/cm^3.

Moreover, Figure 6.7(a) shows that the average density of asphalt mixtures evaluated according to Stage 2 was lower than that of the mixtures evaluated according to Stage 1. In general, mixtures according to Stage 2 presented higher average density values at 140ºC than at 160ºC. It can be deduced from the results that the mixtures without capsules (WO/C) presented the highest reduction of density with the temperature, registering values of 2.363

g/cm^3 and 2.337 g/cm^3 at 140ºC and 160ºC, respectively, equivalent to an average density reduction of 2.35% and 3.43% respectively, with respect to the density measured in Stage 1.

In contrast, the average air voids content of mixtures evaluated according to Stage 2 at 140ºC and 160ºC was higher than that of mixtures evaluated according Stage 1, see Figure 6.7(b). This was due to the reduction of the mixtures density with the temperature, produced by the reduction on the mass of the capsules at the temperatures evaluated, see Figure 6.4(a). Another reason of the increase in the air voids content of the Stage 2-mixtures was the aging of the bitumen caused by the aging time, which hardened the bitumen thus making the mixture less workable. It was proven that aging times of 4 h in the oven at 140ºC and 160ºC, resulted in aging indices of 7.57% and 28.46%, respectively. Finally, results shown in Figure 6.7 demonstrated that the 4h-waiting time (aging time) before compaction at high temperatures can affect the physical properties of mixtures with, and without, capsules. And that this phenomenon can be due to the mixing order and to the aging damage of bitumen.

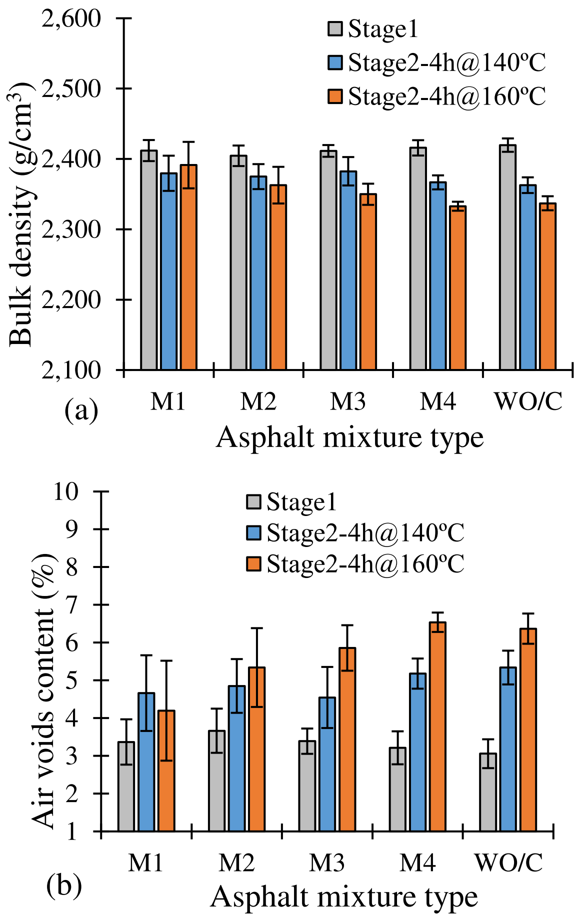

Figure 6.7. Results of the (a) bulk density and (b) air void content of the asphalt mixtures with and without capsules (WO/C).

6.6. Influence of mixing and aging time on the mechanical properties of asphalt mixtures

Examples of ITSM are shown in Figure 6.8. The results of the stiffness modulus depending on the asphalt mixtures evaluated and air voids content can be observed in Figure 6.9(a) and Figure 6.9(b), respectively. Figure 6.9(a) shows that depending on the mixing order (i.e., mixture type) and the aging temperature (4 h in oven at 140ºC or 160ºC), the stiffness modulus was different. In the case of mixtures evaluated according to Stage 1 conditions, the average values of stiffness modulus of mixtures with capsules were lower than that of mixtures without capsules (WO/C). Thus, the reference mixture without capsules presented the highest stiffness modulus, with an average value of 7880 MPa, followed by the mixtures with capsules of types M4, M1, M2 and M3, with average values of 6423 MPa, 5946 MPa, 5861 MPa, and 5474 MPa, respectively. This result demonstrated that the mixing order and the pre-conditioning temperature of the capsules had an influence on the stiffness modulus values. An increase in the porosity was another factor that could have had an influence on the reduction of the modulus in the asphalt mixtures with capsules evaluated according to Stage1. In Figure 6.9(b), it can be observed that, regardless of the evaluation state, Stage 1 or Stage 2, the stiffness modulus of mixtures with capsules decreased with the increase of the air voids content.

Figure 6.8. ITSM test samples.

Furthermore, it can be seen in Figure 6.9(a) that the mixtures evaluated according to Stage 2 at 140ºC and 160ºC, presented stiffness modulus values different to that of mixtures evaluated according to Stage 1 conditions. These modulus values were different depending on the mixture type evaluated. Therefore, mixture types M1, M2 and M3, presented stiffness modulus higher than in Stage 1, with values 6964 MPa, 6993 MPa and 6445 MPa, respectively. However, M4-mixture presented an average stiffness modulus lower than that obtained according to Stage 1. The same behavior was observed in the mixture without capsules, registering average values lower than those of Stage 1, such as: 4759 MPa and 5342 MPa at 140ºC and 160ºC, respectively.

Additionally, in Figure 6.9(a) it can be observed that mixtures with capsules, evaluated according to Stage 2 conditions at 160ºC, presented lower values of stiffness modulus than at 140ºC, this difference being larger or smaller depending on the mixing order. For example, in the case of M3-mixture, where the capsules were mixed with the aggregates at 20ºC at the beginning of the mixing process, the stiffness modulus presented a higher reduction compared with M4-mixture, where the capsules were mixed with the asphalt mixture, at 20ºC, but at the end of the mixing process, see Figure 6.9(a). As in the case of mixtures evaluated according to Stage 1 condition, the reduction of stiffness in mixtures evaluated according to Stage 2 at 140ºC and 160ºC, can be attributed to the increase of the air void content, Figure 6.9 (b), and the effect of the capsule distribution inside the tested specimens.

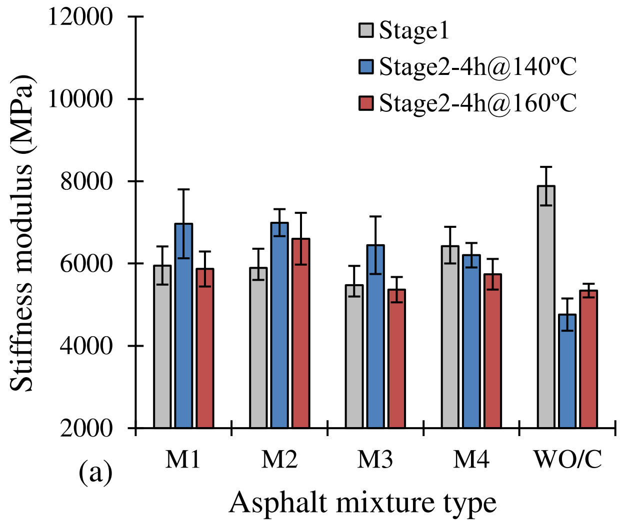

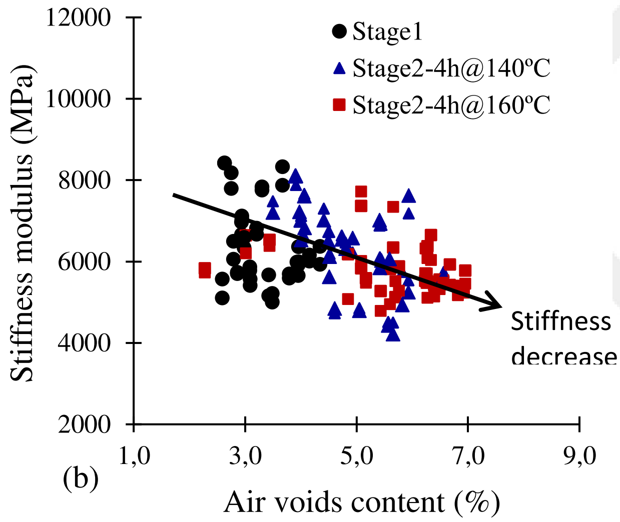

Figure 6.9. (a) Results of stiffness modulus for asphalt mixture samples with and without capsules (WO/C), and (b) stiffness modulus results of all test specimens versus air voids content.

With the aim of evaluating the influence of the capsule distribution on the stiffness of mixtures, Figure 6.10 shows the relationship between all the stiffness modulus values on the test specimens in the longitudinal (Y-Y') and cross (X-X') directions. In this Figure, it can be observed that regardless of the mixing order, Stage, and temperature evaluated, the stiffness modulus values were very similar in both directions (X and Y), for most of the asphalt specimens tested. This proved that asphalt mixtures with capsules did not present an anisotropic mechanical behavior for the plane orthogonal to the coaxial axis of the specimens, which can directly affect the average stiffness modulus.

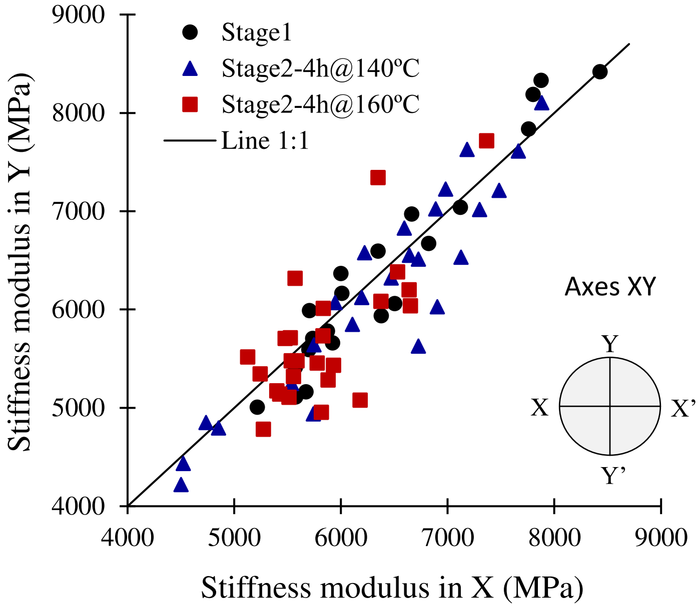

Figure 6.10. Relationship between stiffness modulus of the test specimens measured in longitudinal (Y) and cross (X) directions.

Additionally, previous results can also indirectly prove that the capsule distribution inside the asphalt mixtures can be considered as uniform, not presenting a negative influence on the stiffness modulus value. This result can be verified by observing the CT-Scans reconstructions shown in Figure 6.11. In this Figure, it is shown that the capsules presented a good distribution inside the mixture, with some damaged capsules due to the mixing and compaction processes. Overall, it can be concluded that capsules added in a percentage of 0.5 did not improve the stiffness modulus of asphalt mixtures respect to the mixtures without capsules.

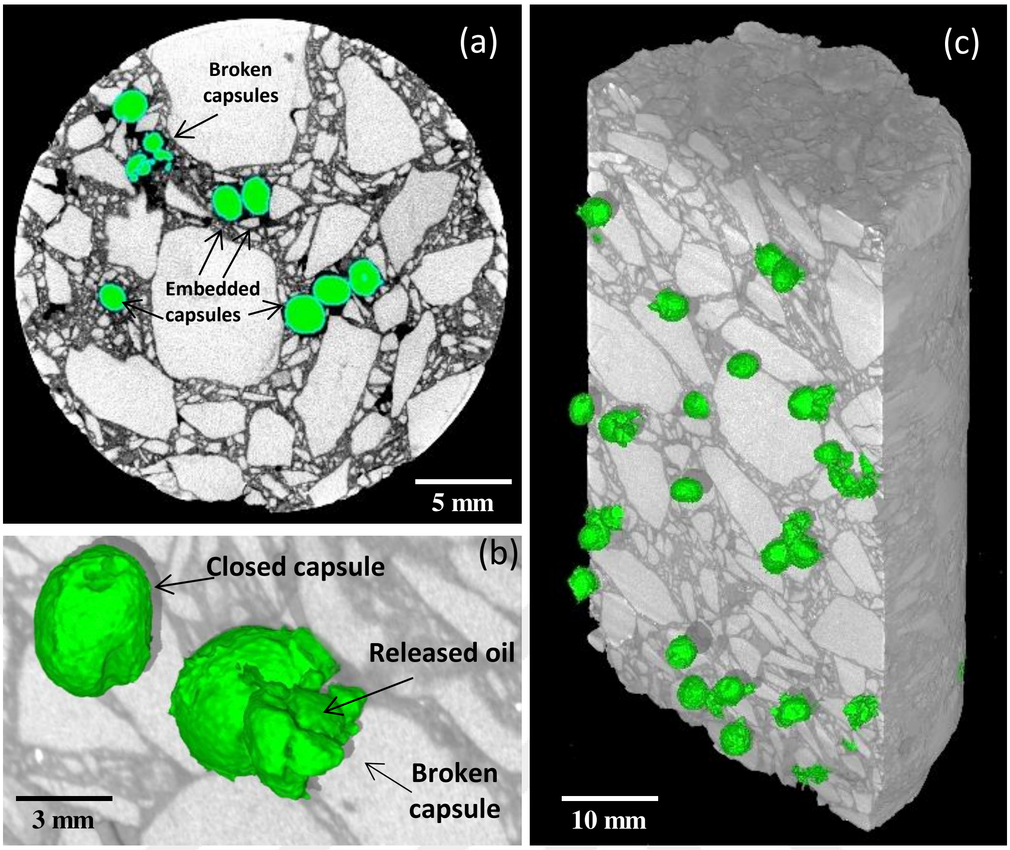

Figure 6.11. CT-Scans reconstructions of the asphalt mixture M4 with capsules highlighted in green color: (a) 2D cross-section image of sample with capsules, (b) 3D reconstruction of the embedded capsules in asphalt, and (c) 3D reconstruction of the capsule spatial distribution inside of the asphalt sample.

Furthermore, Figure 6.12 shows the results of the maximum force resisted by the semi-circular bending samples evaluated at different aging times. It can be observed that 1) flexural strength slightly increased with the aging time, and 2) mixtures without capsules (WO/C) resisted, in general, higher flexural forces than mixtures with capsules (M1-M4). This result can be attributed to the hardening of the bitumen because of aging, which increased the stiffness of asphalt mixtures. In fact, Figure 6.13(a) shows how the maximum flexural force resisted by asphalt samples without capsules increases with the viscosity of bitumen because of the aging time. Additionally, comparing the results for the mixtures evaluated according to Stage 2 at 140ºC and 160ºC, see Figure 6.12(a) and (b), it can be observed that these results were similar, regardless of the experimental Stage evaluated. In this way, it can be concluded that the addition of capsules did not improve the flexural strength of asphalt mixtures for the different aging times.

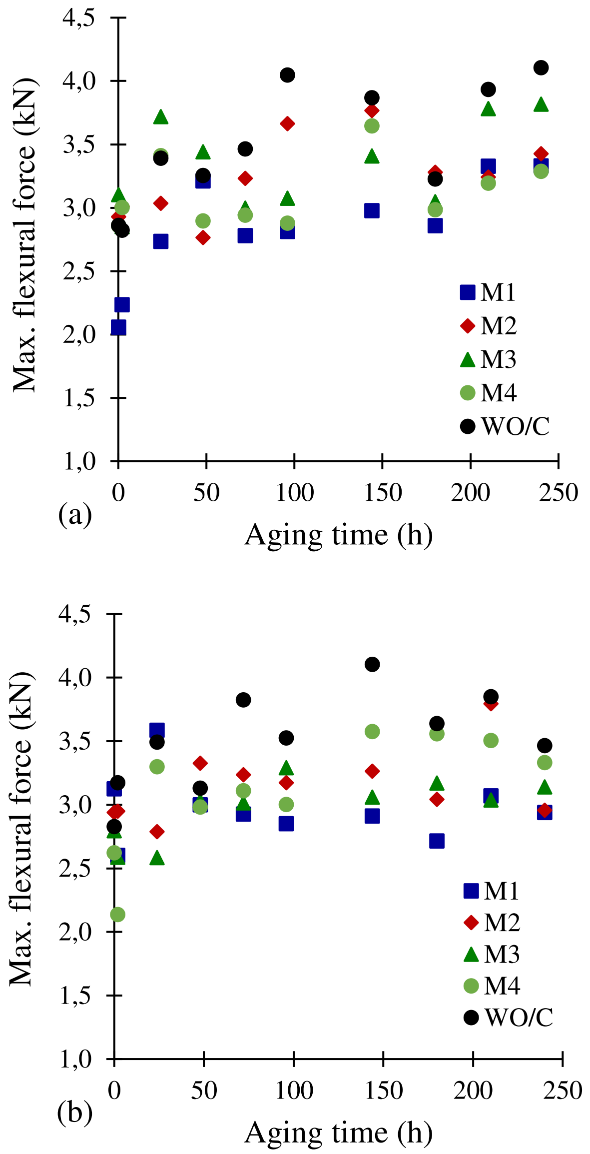

Figure 6.12. Variation of the maximum flexural forces versus aging times for all the asphalt test samples measured under (a) stage 2@140ºC, and (b) stage 2@160ºC.

In order to prove that the capsules did not have a significant influence on the flexural strength of asphalt mixtures, a ratio between the maximum flexural force of all the test specimens with capsules and that of the mixture without capsules (WO/C) tested at the same aging time was calculated, regardless of the mixing order and aging time. For reasons of simplicity, these data have not been presented in the paper. Nevertheless, to prove that the difference between them is due to the scatter (see dispersion of results in Figure 6.12), the Normal Probability of these values has been calculated and presented against the data percentiles in Figure 6.13(b). Results showed that all data can be aligned in a straight line with a 1:1 slope, regardless of the experimental Stage evaluated. This means that the differences in the flexural strength between tests specimens with, and without, capsules were due to statistical variations, and that the mixing order and aging time did not have a significant influence on the flexural strength reached by the mixtures. 3PB post-test view of aged samples is shown in Figure 14.4.

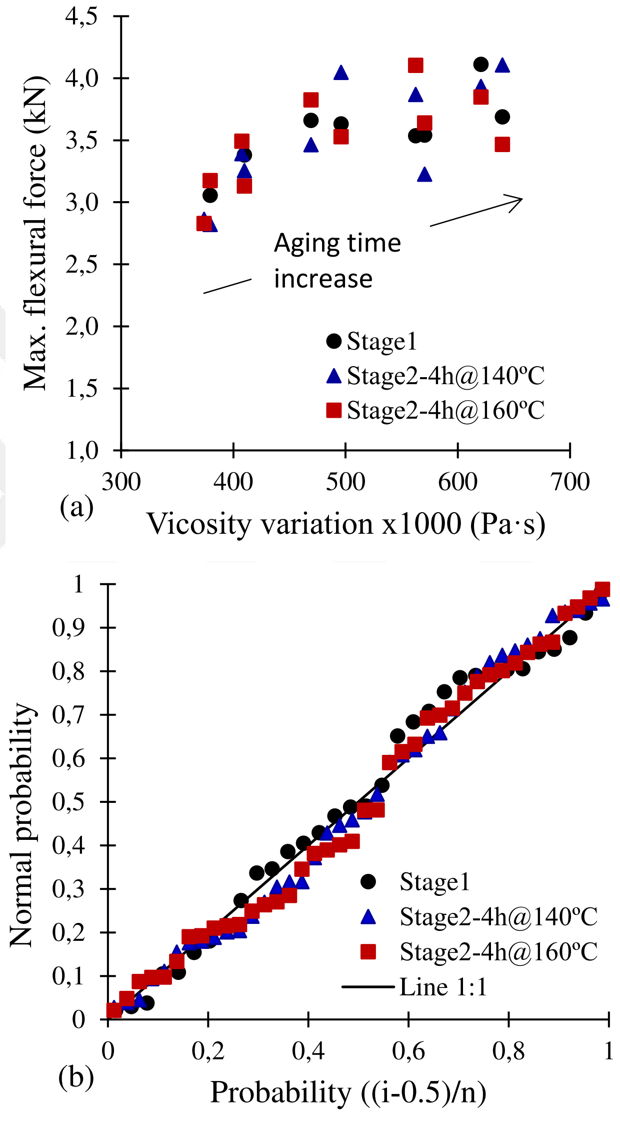

Figure 6.13. (a) Relation between the maximum flexural forces resisted by samples without capsules versus viscosity variation of bitumen with the aging time. (b) Normal probability-probability plot of the ratio between the flexural force of the test samples with (W/C) and without (WO/C) capsules at different aging times.

Figure 6.14. 3PB post-test appearance of aged samples.

6.7. Effect of mixing and aging on the healing properties of asphalt mixtures

The results of the healing levels depending on the asphalt mixtures with, and without, aging evaluated for a healing (rest) time of 120 h are presented in Figure 6.15(a). In this Figure, it can be observed that: 1) the healing level reached by the mixtures was different depending on the mixing order, and 2) healing levels of mixtures without aging were higher than those of mixtures submitted to aging process. In this study, it was proven that aging the mixtures in an oven at 85ºC for 240 h caused an increase in the viscosity of bitumen and oil of 71.09% and 65.84%, respectively (see Table 6.1), which causes a reduction of the healing properties of mixtures.

Additionally, in Figure 6.15(a) it can be observed that the mixtures with capsules with, and without, aging presented, on average, higher healing levels than mixtures without capsules (WO/C). Overall, mixtures with capsules presented a similar trend in the average healing levels, regardless of the aging state, see error bars in Figure 6.15(a). For example, in the case of mixtures without aging, M2-mixture with capsules presented the highest healing level with an average value of 53.16%, followed by mixtures M3, M1 and M4, with average healing levels of 47.82%, 44.11% and 32.86%, respectively, while the healing level in the reference asphalt mixture without aging was 29.40%.

These healing level results directly depended on the percentage of broken capsules in the mixtures Figure 6.15(b) shows the percentage of broken capsules inside the different asphalt mixtures after applying external compressive loads, see also Figure 6.11(b). Thus, mixtures with higher percentages of broken capsules presented, in general, higher average healing levels in Figure 6.15(a). The fact that mixtures with aging present lower values of oil-release was due to the increase of the oil viscosity with the aging time, see Table 6.1. In this study, the oil inside the designed capsules is stored inside small cavities of the calcium-alginate structure. Therefore, when the capsule is activated by an external compression load, the oil is released from the cavities into the bitumen in small volumes, thus avoiding the saturation of the bitumen with oil. Hence, if the viscosity of the encapsulated oil increases, the oil release from the capsules is more difficult, thus reducing the healing levels in the mixtures with aging, see Figure 6.15(a).

Table 6.1. Average viscosity and aging indices for the bitumen and sunflower oil at different aging times.

Aging time (h) in oven @85ºC	Viscosity value (Pa·s)		Aging index (%)	
	Bitumen	Sunflower oil	Bitumen	Sunflower oil
0	373900	0.073	--	--
2	379260	0.074	1.43	2.04
24	407400	0.075	8.96	3.29
48	409700	0.086	9.57	17.28
72	469100	0.090	25.46	23.87
96	496000	0.091	32.66	24.69
144	562500	0.100	50.44	36.63
180	570300	0.101	52.53	37.86
210	620500	0.109	65.95	49.79
240	639700	0.121	71.09	65.84

Furthermore, with the aim of verifying the efficiency of the capsules in the healing process of cracked asphalt beams, the viscosity of different bitumen samples (with, and without, aging) mixed with oil without aging, was measured. The amount of oil added to the bitumen samples was calculated using the percentage of broken capsules in the mixtures, based on Figure 6.15(b). The samples' viscosity was measured at 20ºC using the same procedure described in section 5.1 for bitumen samples without oil. Table 2 presents the average results of viscosity for the different mixture types evaluated, from M1 to M4. In this Table, it can be observed that all bitumen samples with oil presented lower viscosity values than the reference values at 0 and 240 h, shown in Table 6.2, for asphalt mixtures without, and with, aging, respectively. Additionally, it can be observed in Table 6.2 that the viscosity reduction in samples with aging was higher than that in samples without aging, see values of the viscosity reduction indexes in Table 6.2, which can be interpreted as a measurement to quantify the efficiency of the capsules in asphalt mixtures healing. In this way, the results obtained for the viscosity reduction indexes demonstrated that the addition of capsules with oil inside aged mixtures can help the bitumen to rejuvenate by between 19.55% and 26.33%, depending on the mixing order of the capsules.

Table 6.2. Average viscosity values and viscosity reduction indices of the oil-release asphalt samples with and without aging.

Mixture type	Broken capsules in mix (%)		Viscosity value (Pa.s)		Viscosity reduction index (%)	
	Without aging	With aging	Without aging	With aging	Without aging	With aging
M1	38.96	26.68	349847	486985	6.43	23.87
M2	45.30	32.24	332340	471278	11.12	26.33
M3	31.34	21.20	366700	514650	1.93	19.55
M4	36.40	25.94	365510	494949	2.24	22.63

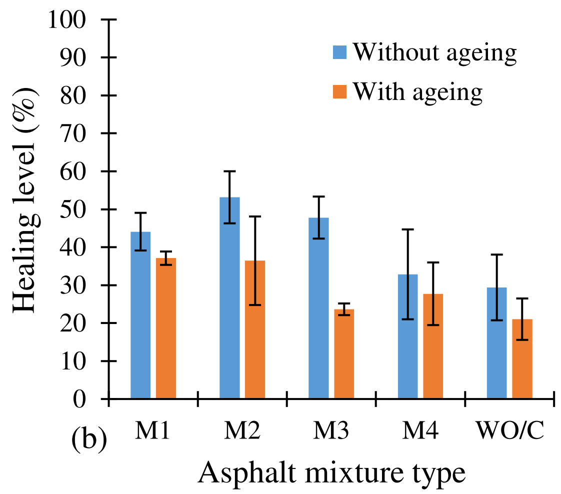

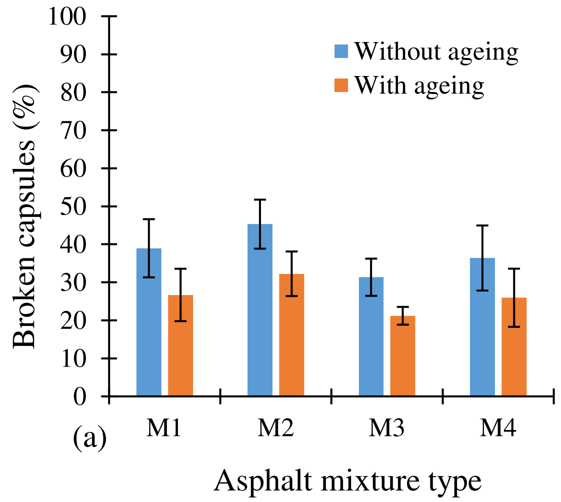

Figure 6.15. Results of the (a) healing levels for the different asphalt mixture types, and (b) percentage of broken capsules inside the different asphalt mixtures evaluated at healing time of 120h.

7. MECHANICAL PROPERTIES AND SELF-HEALING ABILITY OF STONE MASTIC ASPHALT CONTAINING POLYMERIC CAPSULES

7.1. Introductıon

Stone Mastic Asphalt (SMA) mixture is a road construction material widely used in many countries around the world [132]. It is a composite material formed by a coarse aggregate skeleton and a high binder content [133]. The coarse aggregate skeleton provides the mixture with stone-on-stone contact, giving it strength, while the high binder content grout enhances durability [134]. SMA mixtures should be designed and installed ensuring a strong coarse aggregate skeleton, because the high concentration of aggregate particles will make the mixture more resistant to wear [135].

Nevertheless, environmental conditions combined with dynamic traffic loads contribute to premature deterioration of SMA pavements, reducing their mechanical strength and durability over time [46]. The main environmental factors affecting durability of SMA mixtures are [136]: rutting, water damage, thermal cracking, fatigue and aging. These factors mainly depend on the bituminous binders used, because the aging damage of bitumen has a negative influence on the stiffness of SMA mixtures. The aging of bitumen is caused by the oxidation and the loss of volatiles from bitumen composition [137]. Aged bitumen has higher viscosity and is stiffer than fresh bitumen, presenting recognizable changes in its chemical composition [125]. These changes in the bitumen lead to raveling and cracking in the pavement surface, especially reflective cracking [138], that occur as bitumen becomes aged and more brittle [127].

One recent technique to solve the problem of the maintenance of aged asphalt pavements is the use of encapsulated rejuvenators to renovate the properties of the bitumen through self-healing methods [58,65,68,128]. A rejuvenator is a low-viscosity oil, or a healing agent used to recover the original properties of the aged bitumen. Polymeric capsules containing rejuvenator agents have been included in the asphalt [128]. The principle behind this approach is that these capsules containing rejuvenators will remain inactive in the road for several years until an external damage happens to the asphalt pavement [58,65,68,128].

Hence, when a microcrack starts to occur in the asphalt pavements, the crack reaches a capsule and breaks the capsule's shell at the appropriate time, leading to the release of the rejuvenator into the asphalt pavement, which will diffuse and reduce the bitumen viscosity allowing it to easily flow into the open cracks [68]. This concept is supported by the fact that bitumen is a self-healing material with the ability to close microcracks by itself.

Several experimental methods have been used to prepare capsules and microcapsules containing rejuvenator agents with asphalt self-healing purposes. In the research of Garcia et al. [53] different capsule types were manufactured by encapsulating rejuvenators using saturated porous aggregates with rejuvenators and sealing them with a shell made of epoxy-cement matrix and cement. Garcia et al. [59] encapsulated four different types of rejuvenators and their effect on the properties of the capsules was studied. Otherwise, Li et al. [139] designed microcapsules containing urea-formaldehyde resin as a core material based on an in-situ polymerization method, and Su and Schlangen [55] prepared microcapsules containing rejuvenator droplets by in-situ polymerization of urea-formaldehyde, making a methanol-melamine-formaldehyde (MMF) prepolymer as a shell. Furthermore, previous works had studied the use of heavy aromatic oils [67] and sunflower oil [69] as encapsulated rejuvenators in asphalt mixtures. Based on the work of Garcia et al. [68] it was concluded that heavy aromatic oils usage may present risks in terms of human health if they are not perfectly encapsulated, while sunflower oil can be used without human health risk, proving to have a positive effect on bitumen rejuvenation.

Authors like Al-Mansoori et al. have recently published studies where polymeric capsules with sunflower oil as the encapsulated agent were prepared to be evaluated in dense asphalt mixtures [78] and asphalt mastic [85]. These capsules were made by the ionotropic gelation of sodium alginate in the presence of calcium chloride solution. Overall, the works of Al-Mansoori et al. demonstrated that the calcium-alginate capsules with sunflower oil are resistant to asphalt mastic/mixture manufacture and release the rejuvenator agent by the action of external loading. Also, they have a positive effect on the physical and mechanical properties of aged and unaged bituminous materials. Likewise, these polymeric capsules proved the ability to self-heal open microcracks and rejuvenate aged asphalt mixture, although these studies did not evaluate the effect of the addition of capsules with sunflower oil in Stone Mastic Asphalts.

This study the use of calcium-alginate capsules containing sunflower oil as rejuvenator on the mechanical performance and self-healing ability of SMA mixtures. With this purpose, several physical and mechanical properties of SMA mixtures with, and without, capsules have been evaluated by measuring the stiffness modulus, indirect tensile strength and fatigue resistance, water sensitivity and skid resistance. Furthermore, the self-healing ability of SMA at different healing times (from 5 to 216h) was quantified through three-point bending tests on cracked SMA beams with, and without, capsules. Finally, the spatial distribution and the integrity of the calcium-alginate capsules inside the SMA samples were evaluated using X-ray computed tomography tests.

The materials and experimental program followed in this study. Figure 7.1 shows the different test methods used on the Stone Mastic Asphalt specimens with, and without, calcium-alginate capsules.

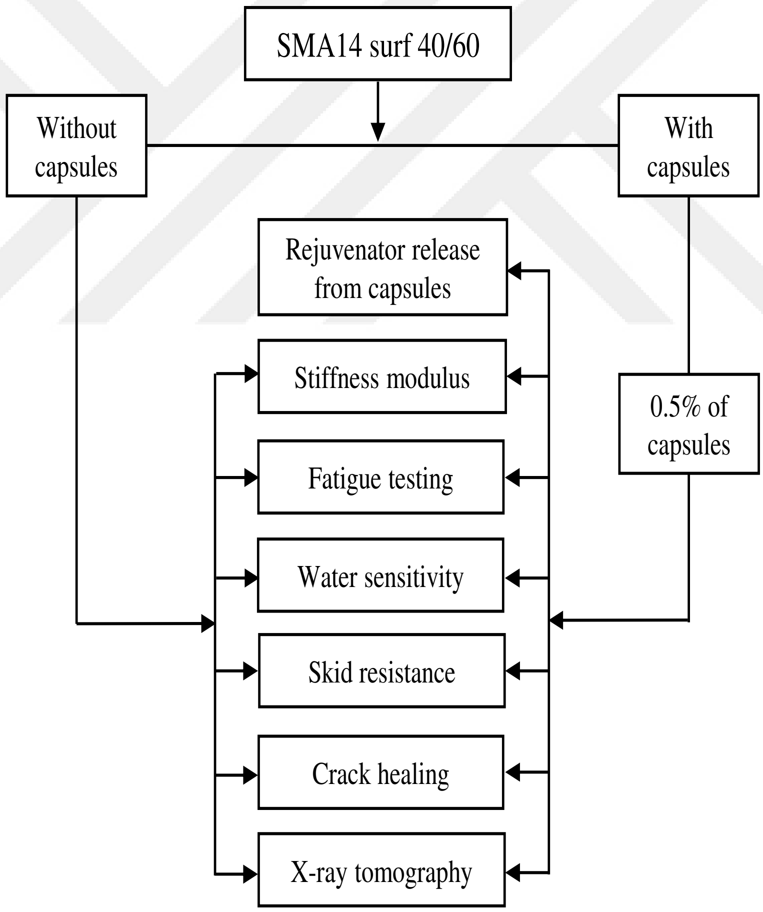

Figure 7.1. Experimental programme used in this study.

7.1. Manufacturing of SMA specimen

Prismatic and cylindrical SMA specimens with, and without, calcium-alginate capsules were manufactured in this study. A capsule content of 0.5% by total mass of the Stone Mastic

Asphalt was added to the specimens. This amount provides an approximate oil-to-bitumen content of 5.23% by mass of bitumen, which is set with the oil-to-bitumen content recommended by Ji et al. [129] with the aim of recovering the aged bitumen properties. SMA mixtures were manufactured in the laboratory in batches of approximately 14 kg, using a laboratory mixer equipped with a helical horizontal mixing shaft. SMA mixtures with, and without, capsules can be described as follows:

(1) <u>SMA with capsules (W/C)</u>: the aggregates and bitumen were pre-heated at 160ºC for 12 h and 4 h, respectively, while the capsules were left to defrost for two hours at 20ºC before mixing. Aggregates and bitumen were mixed for 2 minutes at 125 rpm at 160ºC, ensuring an adequate dispersion. After that, the capsules were added to the SMA mixture, and mixed for 20 additional seconds to obtain their uniform distribution in the asphalt.
(2) <u>SMA without capsules (WO/C)</u>: the aggregates and bitumen were pre-heated at 160ºC for 12 h and 4 h, respectively. Then, the raw materials were mixed for 2 minutes at 125 rpm at 160ºC, ensuring an adequate dispersion.

After that, the SMA mixtures were transferred to the steel molds for their compaction. Prismatic samples of approximately 150×100×60 mm, were cut from 306×306×60 mm SMA mixture slabs, compacted using a roller slab compactor to reach the design value for air voids, see Table3.2. Likewise, to facilitate the creation of a single crack surface on the prismatic samples during crack-healing tests, a transverse notch of 5×5 mm was made at the mid-point on the bottom surface of the beams. Furthermore, cylindrical test specimens, with 100 mm diameter and approximately 60 mm height, were compacted by using a gyratory compactor with an inclination angle of 2º and 650 kPa of static pressure. A maximum of 250 gyrations were applied during compaction. Finally, different SMA cylindrical cores of 3.5 cm diameter and 60 mm height were extracted from asphalt cylindrical specimens with capsules for the X-ray computed tomography tests.

7.2. Tensile strength and water damage of SMA mixtures

Figure 7.2(a) shows the average results of the Indirect Tensile Strength (ITS) of the SMA specimens with, and without, capsules after dry and wet conditioning at the test temperatures, 20ºC and 25ºC. Likewise, Figure 7.2(b) presents the results of the relationship between the ITS values (strength ratio, ITSR) measured on the specimens under dry and wet conditions, also at the test temperatures, 20ºC and 25ºC.

In Figure 7.2(a) it can be observed that the Indirect Tensile Strength of the SMA specimens reduced with the increase of the temperature and that the SMA specimens evaluated in wet conditions presented lower values of tensile strength than specimens tested in dry conditions, for both test temperatures. Overall, SMA mixtures with capsules tested in dry conditions showed slightly higher average ITS values compared with the specimens without capsules, see Figure 7.2(a). This increase was of 4.86% and 4.42% for test temperatures of 20ºC and 25ºC, respectively.

In addition, in contrast with specimens in dry conditions, specimens with, and without, capsules evaluated under wet conditions presented similar ITS values for both test temperatures, which shows that, under conditions of moisture damage, SMA mixtures can show a similar mechanical performance, see Figure 7.2(a). This result proved that the capsules manufactured in this study showed a positive influence on the tensile strength of SMA mixtures. Based on the study recently published by Micaelo et al. [69], this result can be mainly due to strong adhesion of the calcium-alginate capsules in the bituminous mastic matrix and to their good interlocking with the aggregate skeleton.

Moreover, in Figure 7.2(b) it can be observed that SMA specimens with capsules presented lower average values of ITSR than the specimens without capsules. Nevertheless, based on the dispersion of the ITS and ITSR values measured in the SMA specimens with capsules (see standard deviation bars in Figure 7.2(a) and (b)) it can be concluded that the capsules did not significantly affect the tensile strength of the SMA mixture. Consequently, the reduction of the tensile strength of the SMA specimens was mainly associated with the increase of the test temperature and not with the environmental test conditions or with the content of capsules. This result can be better observed in the values of stiffness modulus measured by indirect tensile tests at different temperatures.

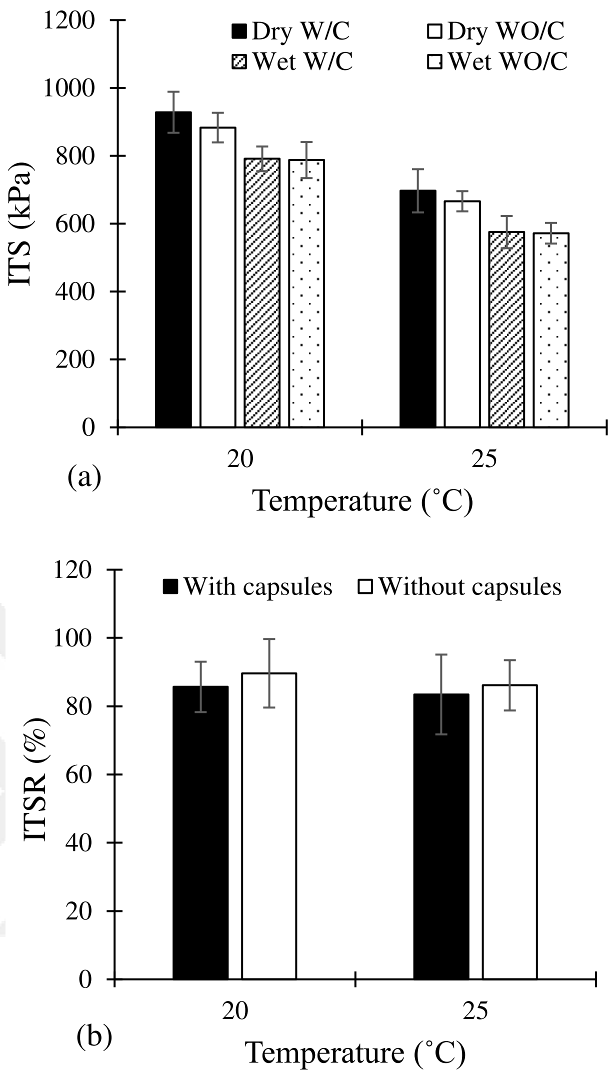

Figure 7.2. Average values and standard deviation bars of the: (a) Indirect Tensile Strength (ITS) of the SMA specimens with (W/C), and without (WO/C), capsules after dry and wet conditioning evaluated at two different test temperatures, and (b) Indirect Tensile Strength Ratio (ITSR).

7.3. Stiffness modulus and resistance to fatigue of SMA mixtures

Examples of ITSM are shown in Figure 7.3. The stiffness modulus results for the SMA mixtures with, and without, capsules measured at four different temperatures are presented in Figure 7.4(a). It can be observed that the stiffness modulus reached by the SMA specimens decreased with the increase of the test temperature, from 5ºC to 30ºC, and that overall, the average values of stiffness modulus were similar for specimens with, and without, capsules regardless of the test temperature, see Figure 7.4(a).

At low test temperatures (5°C), it can be observed that the addition of capsules positively affects the stiffness modulus of SMA mixtures with respect to the reference SMA mixtures without capsules, registering values of 9801 MPa and 9772 MPa for specimens with, and without, capsules, respectively. However, when the test temperature increased, their stiffness modulus significantly reduced, see Figure 7.4(a). For example, test specimens tested at 30ºC showed modulus values of 1102 MPa and 1119 MPa for mixtures with, and without, capsules, respectively, which represents a reduction of approximately 90% in the stiffness modulus. This result can be explained due to the viscoelastic behavior of bitumen, which undergoes a loss of stiffness when the temperature increases [78], thus resulting in a decrease in the viscosity of SMA mixture and the consequent reduction of the stiffness modulus.

Moreover, Figure 7.4(b) shows the relationship between all the stiffness modulus values measured by the indirect tensile test on the SMA specimens in the longitudinal (A-A') and cross (B-B') directions. It can be observed that, independent of the type of mixture tested, with or without capsules, and of the test temperature, the stiffness modulus measured in both directions was very similar, see line 1:1 in Figure 7.4 (b). This result proved that SMA mixtures with 0.5% of capsules did not present an anisotropic mechanical behavior in the orthogonal plane to the coaxial axis of the specimens, which can directly affect the average stiffness modulus. This result also proved that capsules did not negatively affect the stiffness of SMA mixtures, with respect to the mixtures without capsules.

Figure 7.3. Appearance of SMA ITSM test specimens.

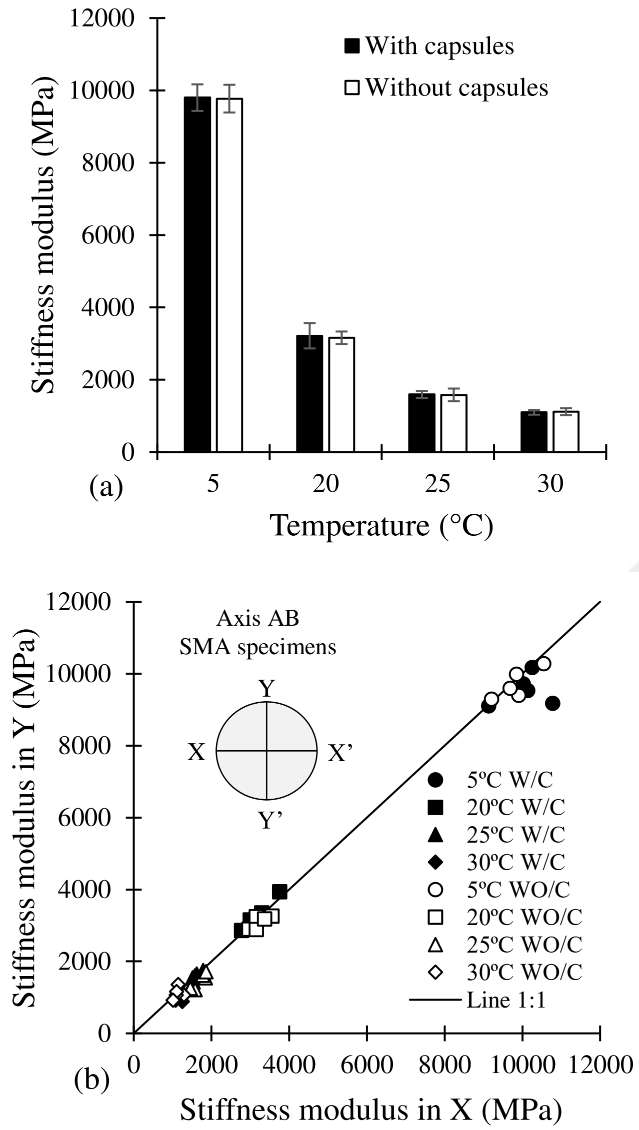

Figure 7.4. Average values and standard deviation bars of the: (a) stiffness modulus of SMA specimens with (W/C), and without (WO/C), capsules versus test temperature, and (b) relationship between stiffness modulus of the SMA specimens measured in longitudinal (Y) and cross (X) directions.

Furthermore, the number of cycles until fatigue failure of SMA mixtures with, and without, capsules is presented in Figure for the different tensile stresses applied on the specimens, from 200 to 400 kPa. In addition, the number of cycles to failure shown in Figure have been plotted versus the initial maximum horizontal tensile strain obtained by using the Equation (5.6) from section 5.3.2. In this Figure, it can be observed that the number of cycles to failure decreased with the increase of the stress level applied, and that the maximum horizontal tensile strain of the specimens increased with the increase of the stress level applied, see Figure7.5. These results were similar regardless of the type of mixture tested (with, or without, capsules), which proved that the addition of capsules in the SMA mixtures tested did not have an influence on the fatigue life of the specimens. Besides, the linear trend of the results, shown in Figure 7.5, suggest that the capsules did not produce a decrease of the fatigue resistance of SMA mixtures, and that the similarity of results of number of cycles to failure obtained by the specimens with, and without, capsules was mainly due to the equivalence of values between the stiffness modulus reached by the SMA specimens with, and without capsules, see Figure 7.4.

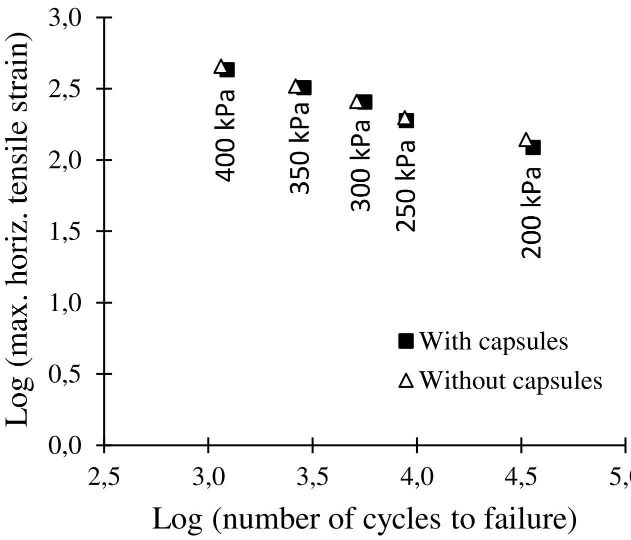

Figure 7.5. Maximum horizontal tensile strain average results versus the number of cycles to failure reached by the SMA specimens with, and without, capsules measured by indirect tensile fatigue tests.

Figure 7.6. Appearance of samples after fatigue test.

Moreover, the results shown in Figure 7.4(b) and Figure7.5 can also indirectly prove that the embedded capsules inside the SMA mixtures can be considered as uniformly distributed not presenting a negative influence on the stiffness modulus values and fatigue resistance of the SMA mixtures. This result can be verified observing the CT-Scan reconstruction results in Figure 7.7. In this Figure, it is shown that the capsules presented a good spatial distribution inside the SMA specimens, with some damaged capsules due to the mixing and compaction processes. Additionally, it was found that the physical properties of SMA mixtures with, or without, capsules were very similar registering non-significant differences for the bulk density and air void content values, see Table 7.1. Hence, this result proved that the capsules did not affect the volumetric properties of SMA mixtures.

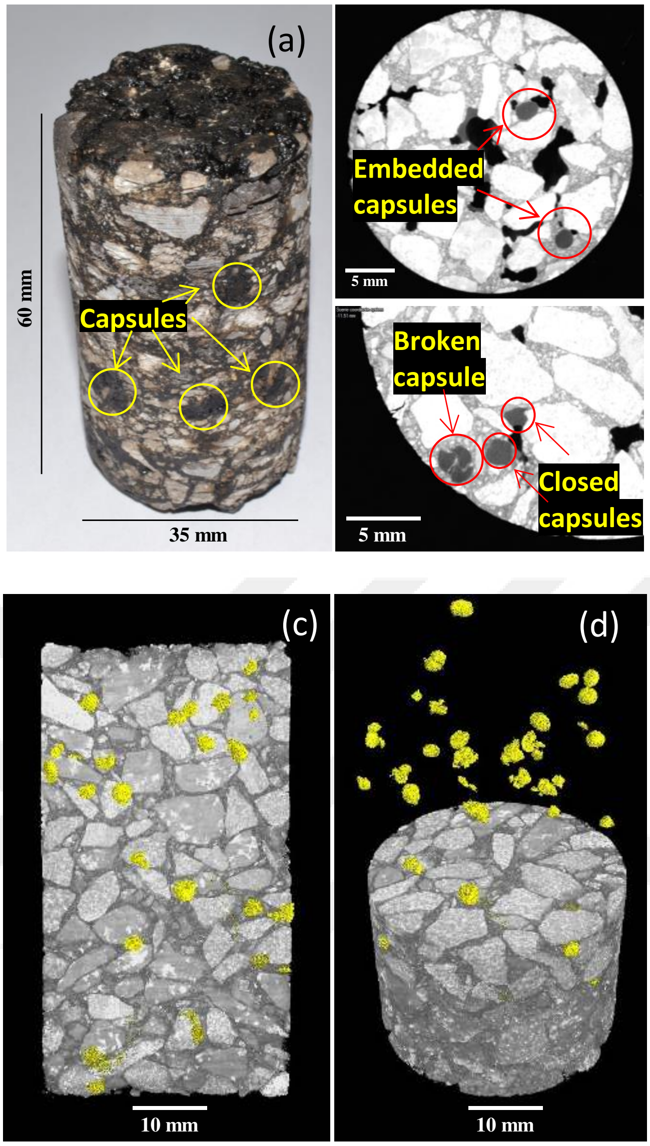

Figure 7.7. CT-Scans reconstructions of the SMA mixture with 0.5% of capsules: (a) SMA mixture core extracted from a cylindrical Marshall specimen, (b) 2D cross-section images of the sample with embedded capsules inside, (c-d) 3D reconstruction of the capsule spatial distribution inside the SMA sample, capsules have been highlighted in yellow color.

Table 7.1. Physical properties of the SMA mixtures with, and without, capsules: Average (Std. deviation) values.

Property	Unit	With capsules	Without capsules
Bulk density	g/cm^3	2.229 (0.011)	2.230 (0.011)
Air void content	%	5.969 (0.453)	5.899 (0.480)
Skid resistance	BPN	48.1 (1.893)	51.5 (2.334)

7.4. Crack-healing properties of SMA mixtures with, and without, addition of capsules

Crack healing test specimens are given in Figure 7.8. Figure7.9 (a) presents the results of the crack healing levels of SMA mixtures with, and without, capsules evaluated after different healing (rest) time ranging from 5 to 216 h. In this Figure, it can be observed that: i) the crack healing levels in the SMA mixture beams with capsules were higher than in beams without capsules, and ii) the crack healing level of mixtures with, and without, capsules increased with the healing time until a maximum value, and then the healing level remained constant. Micaelo et al. [78] indicated that after the maximum healing value, a new state of physical equilibrium usually is attained at the crack surface of the asphalt beams, which causes the healing level to remain constant. Based on the results, the maximum healing level value was reached at 96 h and remained mostly constant until 216 h.

Figure 7.8. Crack healing test samples.

In this way, crack healing level values registered for the SMA beams evaluated between the healing times of 5 and 72 h increased linearly, see Figure 7.9(a), reaching healing growth rates of 0.32 %/h and 0.41 %/h for mixtures with, and without, capsules, respectively. Moreover, the average healing results reached in the maximum healing level for SMA mixtures with, and without, capsules were 55.04% and 43.56%, respectively. These results proved that the capsules in the SMA mixtures resulted in higher healing levels for all the healing times studied, because the encapsulated rejuvenator released from the capsules to the bitumen improved the natural self-healing properties of the SMA mixtures. Therefore, the crack healing level results were directly dependent on the percentage of broken capsules inside the SMA mixtures.

In this context, Figure 7.9(b) shows the percentage of broken capsules inside the different SMA specimens after applying compressive loads. From this Figure, it can be proven that some capsules can be broken due to the mixing and compaction processes, see CT-Scan image in Figure 7.7(b), registering a content of broken capsules of 3.73%. However, the amount of broken capsules after applying an external compression force of approximately 75 kN on the SMA beams and healing test was 49.39%, which is equivalent to 13 times the percentage of broken capsules before healing.

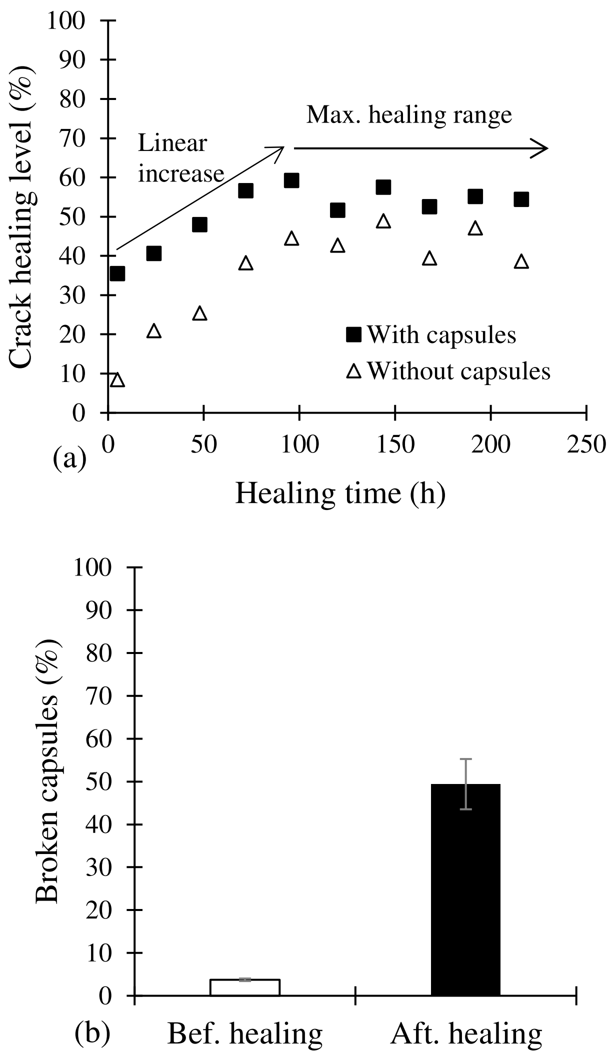

Figure 7.9. Results of the: (a) healing levels for the SMA specimens with (W/C), and without (WO/C), capsules versus healing period, and (b) percentage of broken capsules inside the different SMA mixtures before, and after, healing process.

Likewise, the oil released by the capsules could produce the risk of skid on the surface of the SMA mixtures. To provide evidence, Table 7.2 presents the average results of the skid resistance measured on the SMA beams with, and without, capsules. In this sense, the results of BPN suggested that the capsules slightly reduced the skid resistance of the SMA pavements, however, considering the variation of the results for the tested mixtures with, and without, capsules this reduction was not significant. Therefore, the oil released by the capsules did not produce risk of skid on the surface of the SMA asphalt pavement compared with SMA mixtures without capsules, which is a guarantee for its installation in real conditions.

Table 7.2. Physical properties of the SMA mixtures with, and without, capsules: Average (Std. deviation) values.

Property	Unit	With capsules	Without capsules
Bulk density	g/cm^3	2.229 (0.011)	2.230 (0.011)
Air void content	%	5.969 (0.453)	5.899 (0.480)
Skid resistance	BPN	48.1 (1.893)	51.5 (2.334)

8. EFFECT OF THE ACTIVATION FORCE ON THE HEALING LEVEL OF ASPHALT MIXTURE WITH EMBEDDED CAPSULES

8.1. Introductıon

Asphalt mixture is the most used material to build road pavements worldwide. The capacity of road pavements to carry loads depends on the bond between aggregate particles provided by the bitumen. Nevertheless, this bond degrades over time due the most significant issue that bitumen faces, which is the damage from aging [124]. Aging results from oxidation and loss of the volatiles from bitumen composition, which causes stiffness and an increase in viscosity. This leads to the appearance of microcracks which evolve to form macrocracks and the detachment or raveling of aggregates [125]. One recently used technique to resolve the problem of the maintenance of aging pavement is the use of encapsulated rejuvenators to restore the original properties of the bitumen via self-healing processes [55,78,128]. This technique is supported by the fact that bitumen is a self- healing material with the ability to close microcracks by itself [128]. The principle behind this approach is that these capsules containing rejuvenators will remain inactive in the asphalt road for several years until external damage happens to the asphalt pavement [78]. Then, cracks will break the capsule shells at the appropriate time, leading to the release of the rejuvenator into the asphalt, which will diffuse and reduce the bitumen viscosity to allow it to easily flow into the open cracks [53]. With this objective, different methods have been used to manufacture microcapsules, or capsules with encapsulated rejuvenators, for asphalt self-healing. Su et al. [55] prepared microcapsules containing rejuvenator droplets by in-situ polymerization of urea-formaldehyde making a methanol-melamine-formaldehyde (MMF) prepolymer as a shell. Furthermore, Garcia et al. [53] prepared capsules of a larger size by saturating porous sand with sunflower oil as rejuvenator material and protected by a hard shell of cement and epoxy resin. Details of another type of polymeric capsule were published by Al-Mansoori et al. [78] and Micaelo et al. [69]. These capsules were made by the ionotropic gelation of sodium alginate in the presence of calcium chloride solution. In these capsules, the encapsulated material was also sunflower oil and their size was a few millimeters. Broadly, these studies demonstrated that the capsules are resistant to asphalt fabrication and release the rejuvenators only when broken, but they did not show the effect on the asphalt self-healing properties for capsule content greater than 0.5% by total weight of mixture.

In this chapter, novel polymeric capsules for asphalt self-healing have been designed and tested in asphalt mixtures. These capsules have a greater amount of calcium-alginate structure where the oil is stored, which also improves their mechanical behavior. As a result, of the polymeric capsules mechanical characteristics investigated. Then, the effect of capsule content on the crack- healing properties of asphalt mixtures was quantified at different healing times (from 5 to 216h) and loads (from 0 to 85kN) by using a novel mechanical test.

8.2. Manufacturing of asphalt mixture specimens

Asphalt mixture beams with, and without, capsules were manufactured. In the asphalt mixture with capsules of 0.5% by total mass of the asphalt mixture was added to the specimens. This amount provides an approximate oil-to-bitumen content of 6.89% by mass of bitumen. The asphalt mixture was produced in the laboratory in batches of approximately 14 kg, using a lab mixer equipped with a helical horizontal mixing shaft. The aggregates and bitumen were pre-heated at 160ºC for 12 h and 4 h, respectively, while the capsules were left to defrost for two hours at 20ºC prior to the mixing process. The materials were mixed for 2 minutes at 125 rpm at 160ºC, ensuring an adequate dispersion. Then, capsules were added to the drum and mixed for 20 seconds to obtain their uniform dispersion. Then, the mixture was poured into the molds and compacted to the design for air voids (see section 3.3.1) by using a roller slab compactor to produce an asphalt slab with dimensions of 306 × 306 × 60 mm. Each slab was cut into six identical asphalt beam samples of 150 × 100 × 60 mm. Likewise, to facilitate the creation of a single crack surface during crack-healing tests, a transverse notch of 5 × 5 mm was carved at the mid-point, on the bottom surface of the beams.

8.3. Influence of loads on the healing properties

Figure 8.1 shows the relationship between displacement and compressive force in asphalt mixtures. As can be seen in the figure, as the static force increases, the displacement value of the asphalt mixture increases. The maximum displacement value (5 mm) is approached at the static load of 85 kN. Figure 8.2 shows the healing level results for all asphalt mixture beams without capsules tested at three different healing loads (Figure 8.2(a)) and with capsules tested at nine different healing loads (Figure 8.2(b)), in the healing time range from 5 to 216 h. Results of Figure 8.2 show that the healing level of asphalt increased with the time until a maximum value where it remained constant. As can be seen in Figure 8.2 (a), the healing level remains constant after the healing level of asphalt mixtures without capsules at three different loads increase linearly up to 120h. In Figure 8.2 (b), the level of healing for the other loadings applied is linearly increasing from 5 to 216 h, although the maximum healing level of the asphalt mixtures with capsules is about 96 h for three different loads (65, 75 and 85 kN). The mean maximum healing levels for mixtures with capsules varied from 31.59% to 34.54%, 35.13%, 45.23%, 47.35%, 55.17%, 44.52%, 53.42% and 57.70% for the loads between 0 kN and 85 kN, respectively. The difference was due to higher loads that reduce the mastic viscosity and allow the bitumen to flow and fill the surrounding micro-cracks. Therefore, the flow of bitumen to the crack is easier and faster. This can be observed in Figure 8.6 where a higher percentage of oil release from broken capsules is reached at the highest loads (85 kN), which improves the healing process in the cracked asphalt mixture. In this figure, it appears that the healing levels in such asphalt samples with capsules are higher than those of samples without capsules.

In summary, from Figure 8.2 it can be observed that 1) there is a proportional increase in the level of healing when there is a load increase of 65 kN in the asphalt mixture samples with or without capsules 2) the healing level at 65, 75 and 85 kN loads is stable after 96h 3) there is a proportional relationship between the healing level results of asphalt mixture with and without capsules, independent of the load and time evaluated.

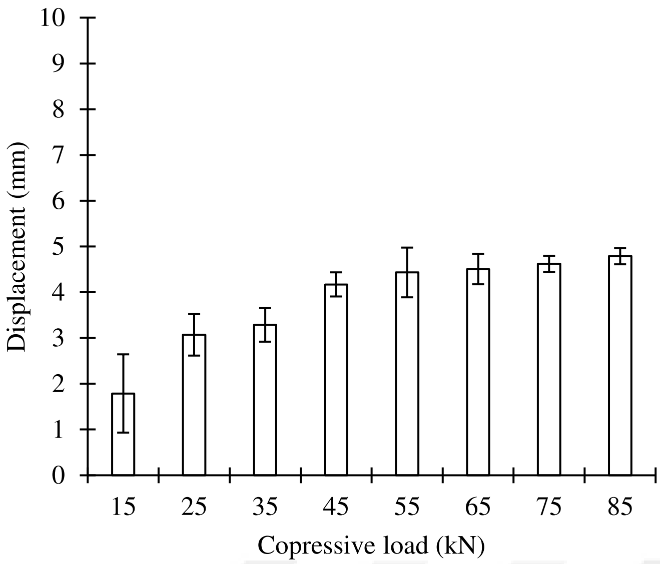

Figure 8.1. Compressive load-displacement different healing loads for a sample with capsules.

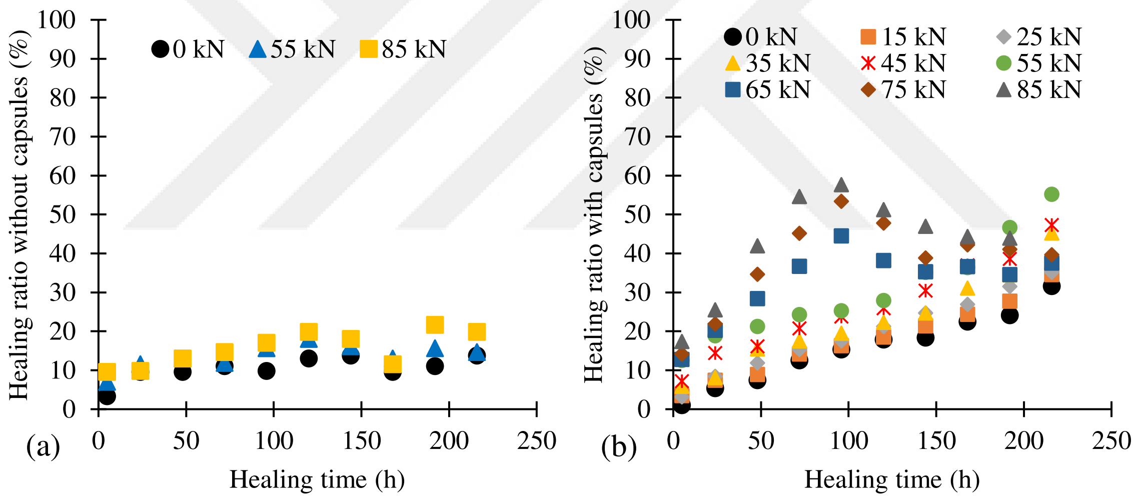

Figure 8.2. Healing level results of asphalt mixture a) without and b) with capsules different healing loads.

Figure 8.3 (a) shows the healing level results for all asphalt mixture samples with or without capsules tested at a recovery temperature of 20 ° C and a recovery time of 5 to 216 h. In this figure, it is seen that 1) the healing levels of the asphalt samples with capsules increases as the applied load increases 2) the healing level of the asphalt samples with capsule remains constant later. Based on the results, this maximum healing level value was generally reached at 96 hours and remained stable until 216 hours. In Figure 8.3 (b), the average healing results are shown as 38.80%, 43.83% and 48.69% for the asphalt mixture samples with capsules of 65 kN, 75 kN and 85 kN, respectively. These results show that 1) as the static load ratio applied increases, the asphalt mixture with capsules has higher crack-healing levels and 2) that the asphalt is a self-healing material by its nature. It is hypothesized that the healing level reached by cracked asphalt mastic samples with capsules, can be directly related to the amount of oil released from the capsules and diffused into the bitumen. As the amount of load applied increases, the amount of oil released from the capsules increases. This, in turn, increases the rate of healing in asphalt mixtures. To prove this hypothesis, Figure 8.6 shows the results of the amount of broken capsules as a percentage of the total capsules used for the asphalt samples containing capsules and tested at healing temperature of 20 ºC.

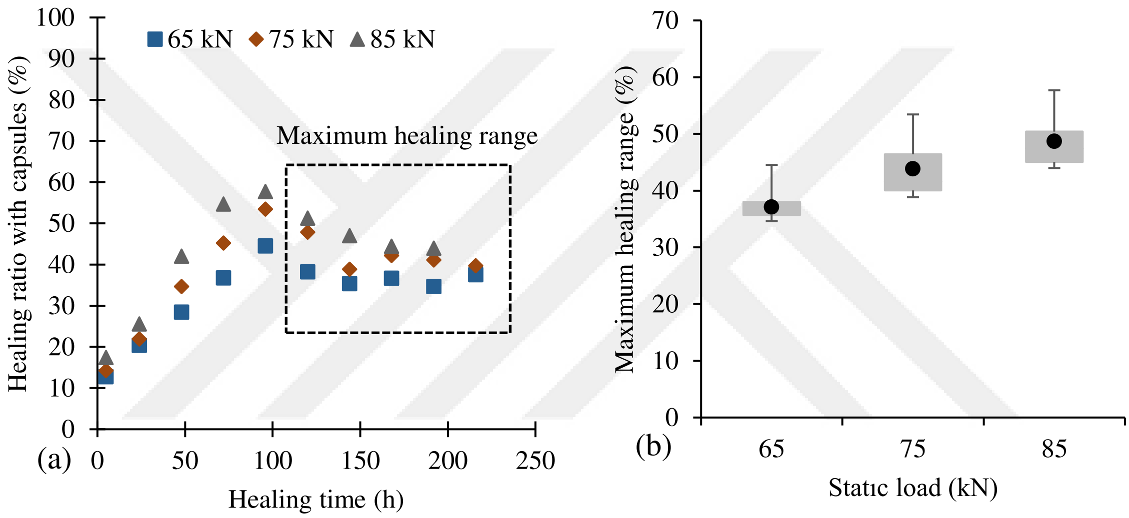

Figure 8.3. Self-healing results for asphalt mixture samples with capsules: a) healing level with healing time and b) box plots of the maximum healing range.

Figure 8.4 shows the rates of healing between the asphalt mixture samples with and without capsules under three static loads selected to evaluate the effect of the capsule distribution on the healing of the asphalt mixtures. A linear increase is seen in the rate of healing as the load applied to the asphalt mixtures tested in this way increases. As seen in the figure, the healing rate of the mixtures with capsules was determined to be higher than that of the samples without capsules. While the healing rate of the asphalt mixture samples without capsules is between 0-20%, the healing rate of the asphalt mixture samples with capsules is between 0-60%. This change seems to depend on the amount of static load applied.

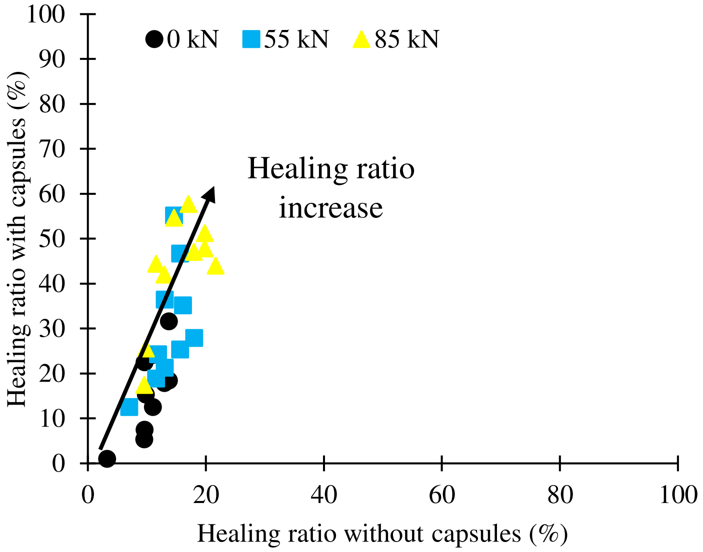

Figure 8.4. Comparison of healing rates of asphalt mixtures with and without capsules under different loads.

A Force Effect Ratio (FER) has been defined in this study as the quotient between the i-th rest time value (FER_i) reached by a mortar sample with capsules for 0 kN ($FER_{i-0\ kN\ with/without\ capsules}$), and the healing level value reached of the equivalent mortar sample with ($FER_{i-with/without\ capsules}$), evaluated at a certain loads and time, as follows:

$$FER = \frac{FER_{i-\ with/without\ capsules}}{FER_{i-0\ kN\ with/without\ capsules}} \tag{8.1}$$

Figure 8.5 shows the change in the force effect ratio over time for both samples with and without capsules. As can be seen in Figure 8.5 (a), the FER healing changes over time. As the applied static load and the healing time increase, there is not much change in the FER. The FER is approximately similar under the applied loads of 55 and 85 kN. In Figure 8.5 (b), however, the FER changes at various healing times of the asphalt mixtures with capsules are being investigated. As the static load value applied to the asphalt mixtures increases, there is no significant increase in the FER value. However, the healing time increases about 48 h and then decreases down to 216h. The FER values at 48h varied by 1.20, 1.60, 2.08, 2.17, 2.86, 3.81, 4.65 and 4.65, respectively. As the static charge applied to the encapsulated mixtures increased depending on the healing time, no significant change was observed in the FER values. The FER values were found to be approximately close to each other.

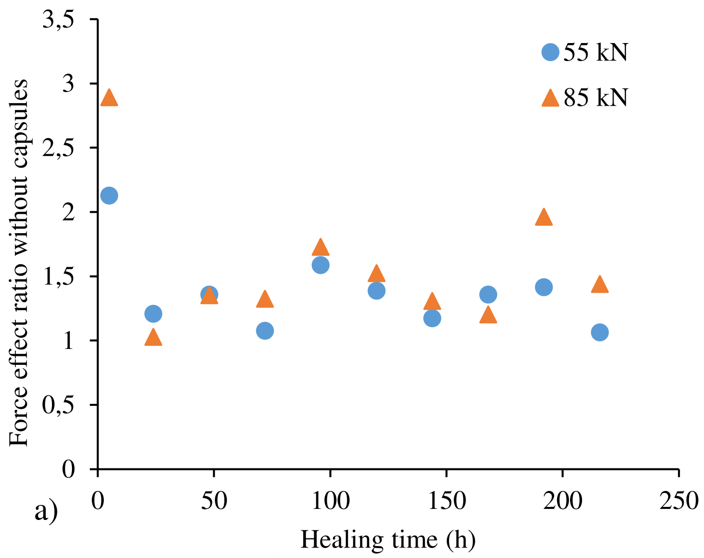

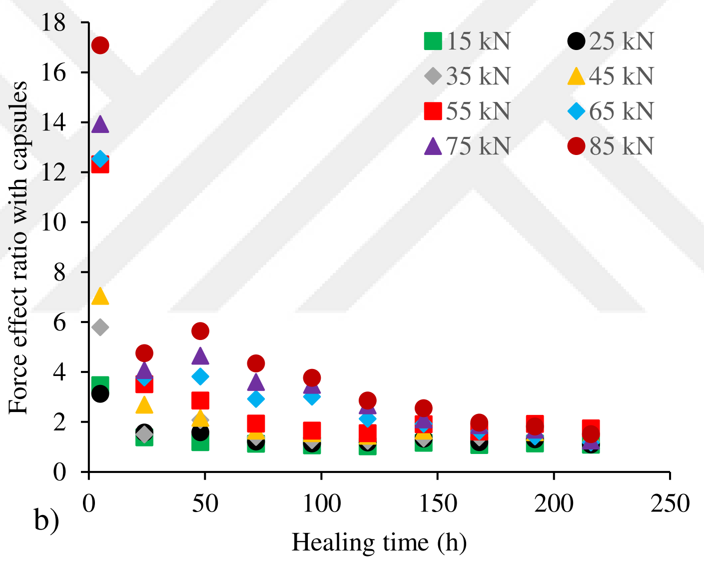

Figure 8.5. Force Effect Ratio results for all asphalt mixture beams (a) without and (b) with capsules tested at different healing loads.

8.4. Amount of rejuvenator in the bitumen and broken capsules

In this chapter, Fourier Transform Infrared spectroscopy (FTIR) tests were used to assess the modification of bitumen in asphalt mastic when the capsules release their content. Figure 8.6 presents the results of the number of broken capsules as a percentage of the total capsules used for asphalt mixtures with 0.5% capsule content and tested at healing temperature of 20ºC. The results of broken capsules were represented only after the external compression load. As seen in Figure 8.6, as the amount of static load applied to the asphalt mixtures increases, the breakage ratios of the capsules found in the asphalt mixtures increase. The amounts of breakage of the capsules in the asphalt mixtures under static loads varied from 2.8% to 7.7%, 17.9%, 30.2%, 35.6%, 43.6%, 56.0%, 60.8% and 65.4% for the loads between 0 kN and 85 kN, respectively. As seen in the figure, static loads have a great effect on the breakage of the capsules. As the ratio of the broken capsules increases, the diffusion of the oil contained in the capsules as the rejuvenator increases. Therefore, the rate of healing also increases. As shown in Figure 8.7, the maximum healing rate increases as the ratio of broken capsules increases. This proves the theory of healing. As the static load applied to the asphalt mixtures increases, both the maximum healing rate and the percentage of fractures of the capsules in the asphalt mixtures increase. The maximum healing rate varies between 30% and 60% depending on the applied load, while the percentage of broken capsules in asphalt mixtures ranges from 0% to 70%. As can be seen in Figure 8.7, as the percentage of broken capsule content increases, the maximum healing rate also increases. This depends on the amount of oil that is emitted during breakage. This figure clearly shows the relationship between the rate of healing and the number of broken capsules.

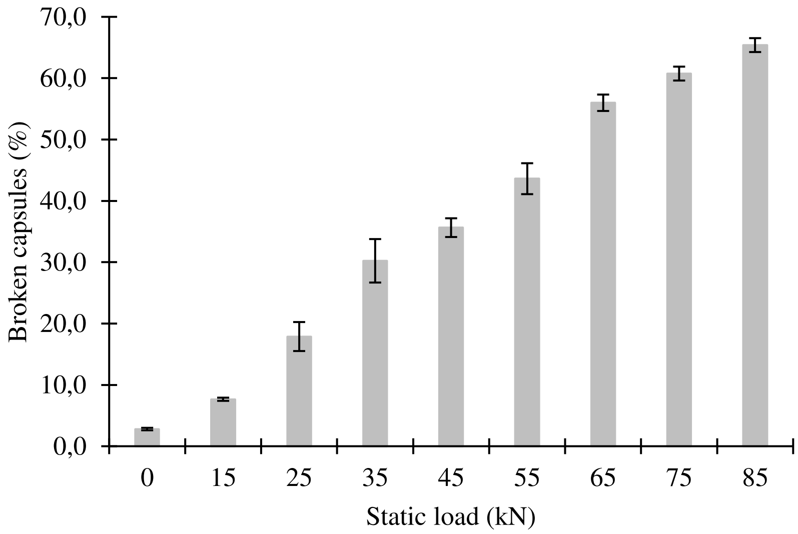

Figure 8.6. Percentage of broken capsules for asphalt mixture samples with different loads after compression at 20ºC.

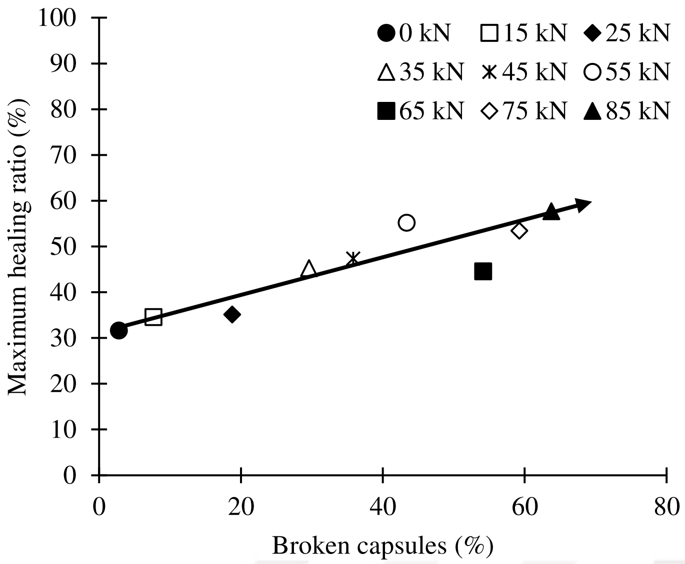

Figure 8.7. Broken capsules for maximum healing ratio.

9. SELF-HEALING CAPABILITY OF ASPHALT MIXTURES USING ENCAPSULATED REJUVENATORS: AN EXPERIMENTAL BY FATIGUE AND WHEEL TRACKING TESTS

9.1. Introductıon

Asphalt mixture is the most used material to build road pavements worldwide, and mainly consists of aggregates and bitumen. The capacity of asphalt pavements to carry vehicle loads decreases over time as a result of oxidation and loss of volatiles in a process called aging [124]. Therefore, it is a challenge for road agencies and engineers to maintain pavements' original properties and overcome aging during their service life, which is achieved by applying several maintenance strategies. In this context, the most recent solution to restore the original properties of aged pavements involves the acceleration of the self-healing property of asphalt, which is an intrinsic healing potential of asphalt mixtures [22].

Researchers have proposed two ways to increase the self-healing capability in asphalt [16]: induction and microwave heating [140,147] and encapsulated rejuvenating agents [53,55,78]. Although using the induction and microwave heating can soften the bitumen to close cracks and repair the damage, they are not a solution for the aging of binder.

To overcome the issues of asphalt aging by induction and microwave heating, researchers have proposed the use of microcapsules containing rejuvenating agents to promote the autonomic self-healing processes inside the aged asphalt mixtures [54,55,69,84,85]. The concept of this approach is to deliver the healing agent to the damaged site and rejuvenate the aged bitumen. In addition, these capsules containing rejuvenators will remain inactive in the asphalt road for several years until external damage happens to the asphalt pavement [78].

Numerous encapsulation methods have been used to manufacture capsules/microcapsules for asphalt self-healing. For instance, [55] prepared a melamine-formaldehyde (MMF) modified by methanol to encapsulate rejuvenators. The prepared capsules had an average size from 2 to 100µm, controlled by the stirring rate. García et al. [53] prepared porous sand capsules containing sunflower oil as the healing agent, protected by a hard shell of cement and epoxy resin. The average size of these capsules was 1.6 mm containing on average

20.9% of rejuvenator by the volume of the capsule. Additionally, other types of calcium-alginate capsules have recently been published [78]. These capsules were made by the ionotropic gelation of sodium alginate in the presence of a calcium chloride solution. These capsules contain sunflower oil as rejuvenating agent and their sizes were a few millimeters. These capsules were strong enough to resist mixing and compaction of asphalt mixture and break when an external damage is applied to the asphalt pavement. Furthermore, results showed that the addition of the capsules had a positive effect on the durability and safety of asphalt mixtures and their ability to self-heal aged bitumen and rejuvenate aged asphalt mixture was proved [69,78,84,85].

This chapter evaluates the self-healing capability of asphalt mixtures containing a new type of capsules designed [141]. These polymeric capsules are stronger than other calcium-alginate capsules presented in the literature, in terms of mechanical strength. The wheel tracking test evaluation in dense asphalt mixtures are presented in the paper. Additionally, the diffusion capacity of the rejuvenating agent inside of bitumen samples, and the healing level of the cracked asphalt mixtures with capsules have been evaluated by Fourier Transform Infrared Spectroscopy (FTIR) and fatigue tests, respectively. Finally, X-ray computed tomography has been used in this study to evaluate the internal structure of the capsules, and their integrity inside the different asphalt mixture samples.

9.2. Manufacturing of asphalt mixture specimens

Asphalt mixture beams with, and without, capsules were manufactured. In the asphalt mixture with capsules, three different capsule contents, as a percentage of the total mixture, were used: 0.5%, 0.75% and 1.0%. These contents provided an oil-to-bitumen content by mass in bitumen of approximately 6.97%, 10.46% and 13.95%, respectively. The capsule content for the fatigue test was only 0.5%. The asphalt mixture was produced in the laboratory in batches of approximately 14 kg, using a lab mixer equipped with a helical horizontal mixing shaft. The aggregates and bitumen were pre-heated at 160ºC for 12 h and 4 h, respectively, while the capsules were left to defrost for two hours at 20ºC prior to the mixing process. The materials were mixed for 2 minutes at 125 rpm at 160ºC, ensuring an adequate dispersion. Then, capsules were added to the drum and mixed for 20 seconds to obtain their uniform dispersion. Then, the mixture was poured into the molds and compacted to the design for air voids (see section 3.3.1) by using a roller slab compactor to produce an asphalt slab with dimensions of 306 × 306 × 60 mm. For the fatigue test, each plate was cut into eight identical asphalt bins of 150 × 75 × 60 mm and six identical asphalt beams of 150 × 100 × 60 mm for the crack-healing test.

9.3. Influence of capsule contents on the crack-healing properties of asphalt mixtures

Figure 9.1(b) presents self-healing results of asphalt beams containing different percentages of capsules 0.5%, 0.75% and 1.00% by total weight of the mixture. Figure 9.1(b) shows the healing levels reached for all the asphalt beams with, and without, capsules (WO/C), at different healing times ranging from 5 to 216 h. It can be observed that the healing levels in the asphalt beams with capsules were higher than in beams without capsules, and that the healing level of asphalt mixtures with, and without, capsules increased with the healing time until a maximum value, and then remained constant. Based on the results, maximum healing level value was reached, in general, at 96 h and remained mostly constant until 216 h, see box in Figure 9.1(b).

The average maximum healing levels were: 49.04%, 54.32% and 54.86% for asphalt mixtures with capsule content of 0.5%, 0.75% and 1.00%, respectively. Likewise, asphalt mixtures without capsules presented an average maximum healing level of 20.44%. These results proved that higher capsule contents in the mixture resulted in higher healing levels for all the healing times studied. This is because higher capsule contents increase the probability of breaking more capsules as a result of external damage, which increases the potential released oil in the mixture. In this study, the percentage of broken capsules measured by FTIR tests after the external compression load were: 35.45%, 45.02% and 60.93% for capsule content of 0.5%, 0.75% and 1.00%, respectively.

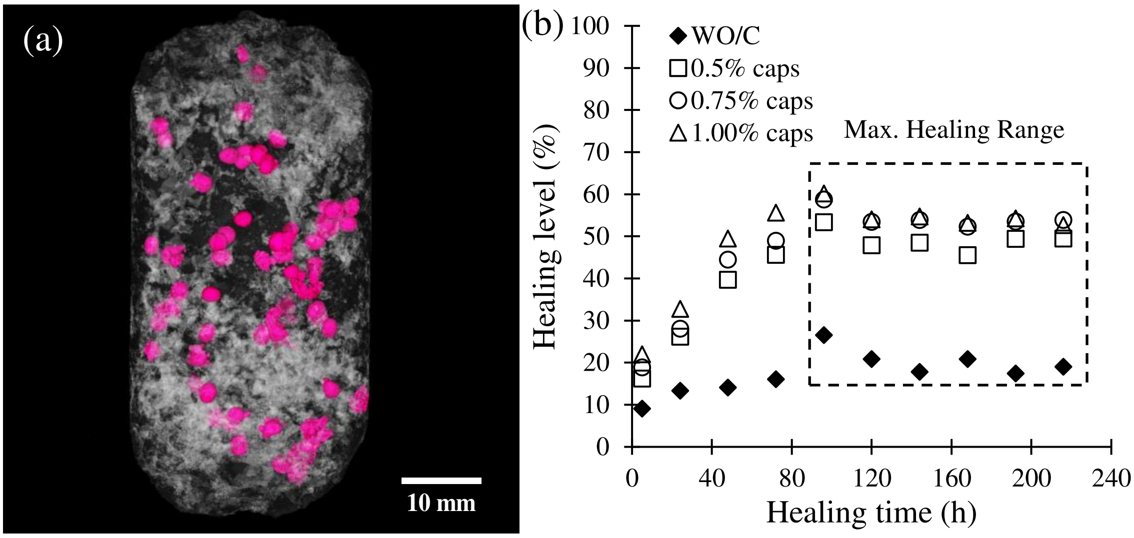

Figure 9.1. (a) CT Scan 3D image of the capsule spatial distribution inside a cylindrical sample of mixture with 0.5% capsule content, (b) healing level depending on healing time.

Furthermore, Figure 9.1(b) also shows that capsule contents higher than 0.5% did not present a significant increase in the maximum healing levels, see results of 0.75 and 1.00% in the maximum healing range. So, although higher contents of capsules increase the healing level of the mixtures, a rejuvenating excess, i.e., oil-to-bitumen content greater than 7.0% by mass, can be detrimental to the properties of the mixture, affecting the rheological properties of bitumen [89]. Therefore, based on the results of this chapter, 0.5% of capsules was considered as the optimal percentage for asphalt self-healing without affecting the rheological properties of asphalt mixture.

9.4. Evaluation of rejuvenator diffusion capacity over time and temperature

Figure 9.2(a) shows the dimensionless absorbance index results for the rejuvenator inside bitumen samples measured at different times and temperatures. This absorbance index can be interpreted as the concentration of diffused rejuvenator inside of bitumen over time and at a certain temperature. From these results, it can be observed that the rejuvenator concentration inside the bitumen samples increases with the time and the temperature until the moment when the concentration reaches a maximum value, which is independent of temperature (Figure 9.2(a)). For the first four test hours, more than 40% of maximum concentration of rejuvenator is obtained for the samples at 50ºC, while that value decreases to approximately 25% for samples tested at 20ºC. This phenomenon is due to the logarithmic trend of the results, which could be adjusted to a diffusion model based on the Fick's second law. However, a greater number of data would be necessary to obtain a good fit to model and so to calculate the diffusion coefficients. Additionally, from Figure 9.2(a) the influence of temperature in the diffusion can be detected for the rest of the times, existing a significant difference between the results at 20ºC and 50ºC. Nevertheless, it can be observed for the last sample tested at 114h that the dimensionless concentrations are practically the same for the two temperatures and that the value is very close to the maximum concentration. This result means that in that point the bitumen is almost saturated of rejuvenating agent and hence the tests could have reached a steady-state condition.

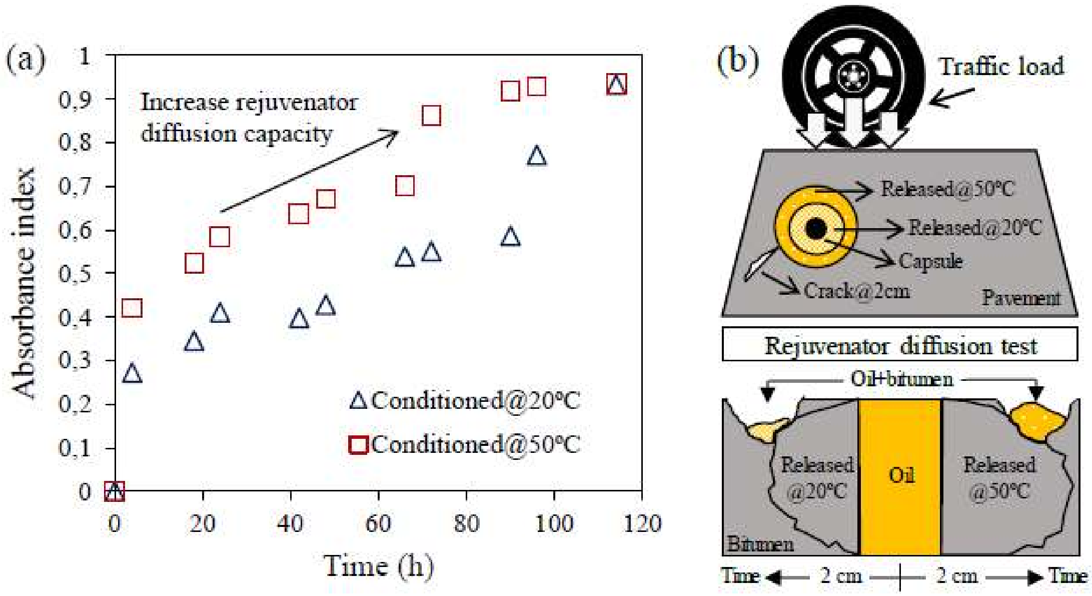

Figure 9.2. (a) Relationship between the dimensionless absorbance index of rejuvenator and the time inside bitumen at two different temperatures, and (b) representative scheme of the diffusion of the rejuvenator (into capsule and test) as a function of time and temperature.

From a practical approach, the results of the Figure 9.2(a) can be interpreted as the capacity of the rejuvenator released inside the pavement to heal a crack located 2 cm away, once the capsules release oil (i.e., compressed/broken capsule) because of the traffic load (Figure 9.2(b)). In this way, a larger absorbance area obtained in FTIR tests represents a higher concentration of rejuvenator inside the bitumen, and the diffusion of rejuvenator is quicker at higher temperatures, which means that a crack located at 2 cm from a broken capsule could be healed quicker at 50ºC than at 20ºC.

9.5. Effect of capsules on the self-healing properties of asphalt mixtures

As it can be seen in Figure 9.3(a), the number of cycles necessary to reach a given percentage of broken capsules reduced with the increase of the applied load, according to a power function. Hence, 30% of capsules were broken after 85480 cycles when 1.75kN were applied but after 8880 cycles, 2990 cycles and 1060 cycles, when 2.75kN, 3.75kN and 4.75kN were applied, respectively. Additionally, the percentage of broken capsules exponentially increased with the number of cycles producing a sharp increase when a critical value was exceeded. An example of the broken capsules inside asphalt mixtures can be observed in the Figure 9.5(a). From Figure 9.5(a) it can also be seen that the capsules can successfully resist the mixing and compaction process, being able to break later, due to the applied fatigue loads. However, in Figure 9.3(a) it was observed that the percentage of broken capsules decreased with the increase of load according to a power function, reaching 58449, 4251, 1286 and 825 cycles when 1.75kN, 2.75kN, 3.75kN and 4.75kN were applied, respectively.

Furthermore, the results of the fatigue test without resting period can be seen in Table 9.1. Similarly to the previous results, the number of cycles with 0.5 probability of breaking the material ($N_{0.5}$) reduces when the applied load increases, according to a power function. Hence, while samples resisted more than 55000 cycles when 1.75kN were applied, they resisted less than 1000 cycles when 4.75kN were applied. By taking these values as reference, the healing index was obtained for each sample by stopping the test at a different number of cycles and applying a resting period, see Figure 9.3(b). It can also be observed that the optimal Healing Index increased with the increase of average broken capsules in the asphalt mixture (see Figure 9.4).

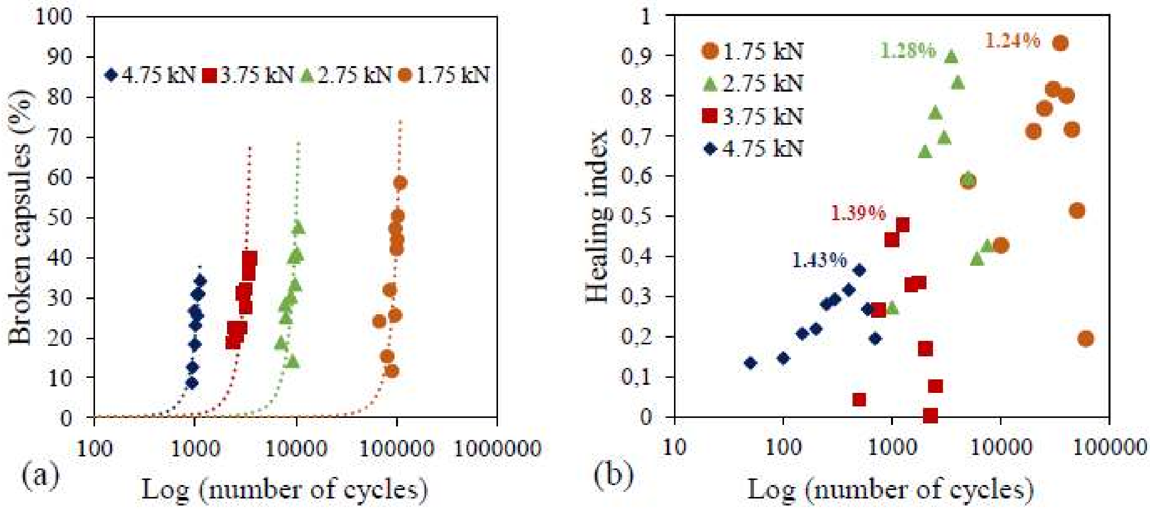

Figure 9.3. (a) Percentage of broken capsules over loading cycles, and (b) healing index obtained when applying a resting time at different number of cycles. The shown values represent the percentage of broken capsules at the number of cycles when the healing is optimum.

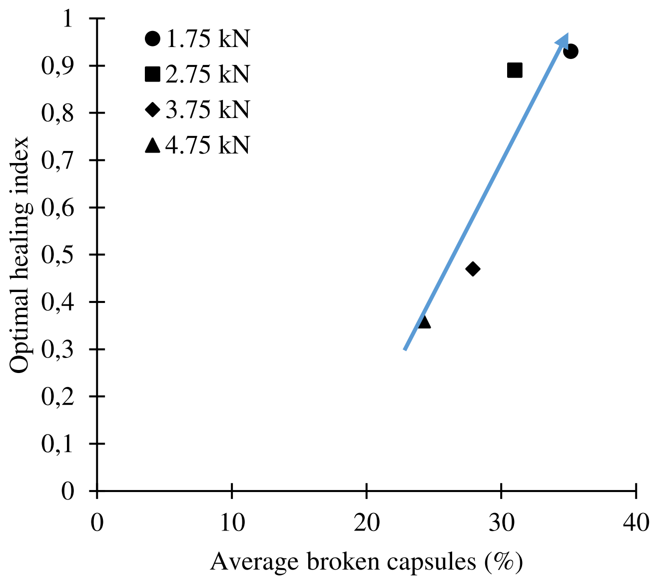

Figure 9.4. Results of healing indexes for the different loads.

As it can be seen in Figure 9.3(b), for all loads (from 1.75 to 4.75kN), the results presented a bell shape, which indicates that there is an optimum number of cycles to apply the resting period, at which the obtained life extension is maximum. This optimum number of cycles could be related to one of the following factors:

1) Optimum crack width. When the healing is applied too early, there are practically no cracks to heal and the life extension is negligible (values close to zero). On the contrary, when the healing is applied too late, the cracks are so wide that the healing is not effective, and

2) Optimum amount of oil released in the mixture. When the healing is applied too early, there are no broken capsules (i.e., released rejuvenator) enough to heal the cracks, as shown in Figure 9.2(a) for the results at 20ºC. On the contrary, an excessive amount of oil in the mix might reduce the mechanical performance reducing the fatigue life of the material.

Table 9.1. Number of cycles with 0.5 probability of breaking the material depending on the applied load by using fatigue tests.

Load (kN)	Number of cycles
1.75	56440
2.75	5560
3.75	2360
4.75	820

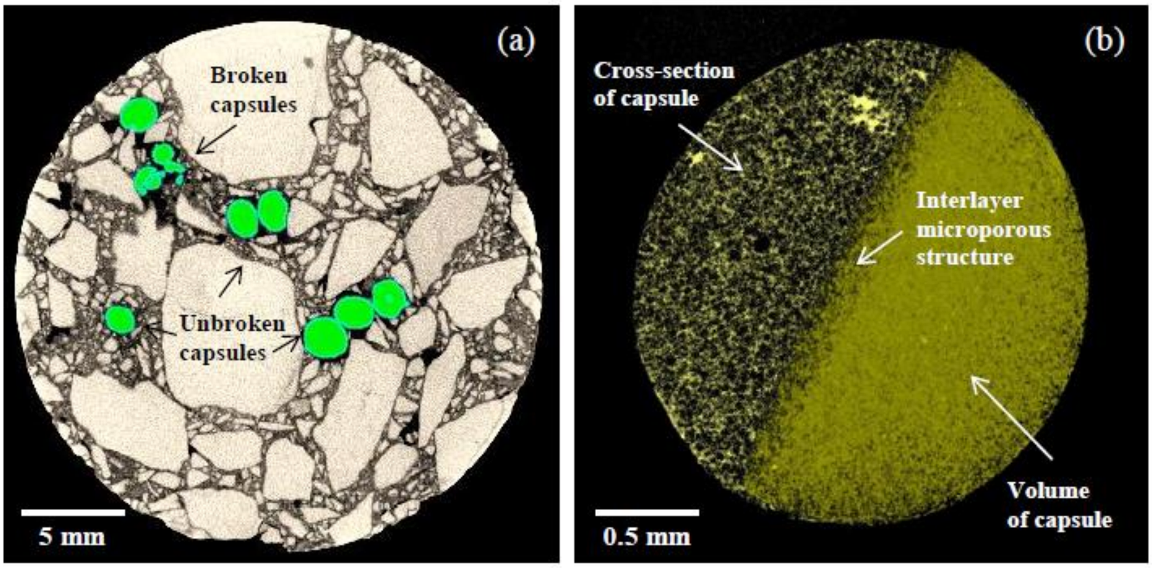

Figure 9.5. CT-Scans reconstructions of the (a) asphalt mixture with capsules highlighted in green colour (modified from Norambuena-Contreras et al., 2018), and (b) 3D reconstruction of an individual polymeric (calcium-alginate) capsule.

In this case, it was observed that the optimum number of cycles to apply the healing treatment decreased when the load increased, see Figure 9.3(b). Thus, it resulted in 35000, 3500, 1250 and 500 cycles when 1.75kN, 2.75kN, 3.75kN and 4.75kN were applied. In all cases, these values oscillate around 50-60% of the reference fatigue life ($N_{0.5}$). At these cycles, the percentage of broken capsules was significantly low for all the loads: 1.24% (1.75kN), 1.28% (2.75kN), 1.39% (3.75kN) and 1.43% (4.75kN). This means that contents of oil in the mix higher than these would be detrimental or, more likely due to the low values, that the cracks' width at 60% of fatigue life are the optimum to be healed. In addition, this result suggests that only a small portion of capsules close to the crack break and, consequently, the design of the calcium-alginate capsules in the form of microbeads can be considered very appropriate. Figure 9.5(b) shows the internal microstructure of an individual calcium-alginate capsule obtained through X-ray computed tomography characterization. From this Figure, it can be observed that the designed microbeads can break under load inside the mixture releasing the encapsulated oil in small volumes, due to its alveolar porous microstructure where the rejuvenating agent was encapsulated. Finally, in Figure 9.3(b) it can be also observed that the healing index (fatigue life extension) increased when the load reduced. This means that although the cracks are healed because of a greater number of broken capsules (Figure 9.3(a)) at low load, the new bonding capacity is not as strong as the original and high loads can reopen the cracks in fewer cycles. The sample used in this test are shown in Figure 9.6.

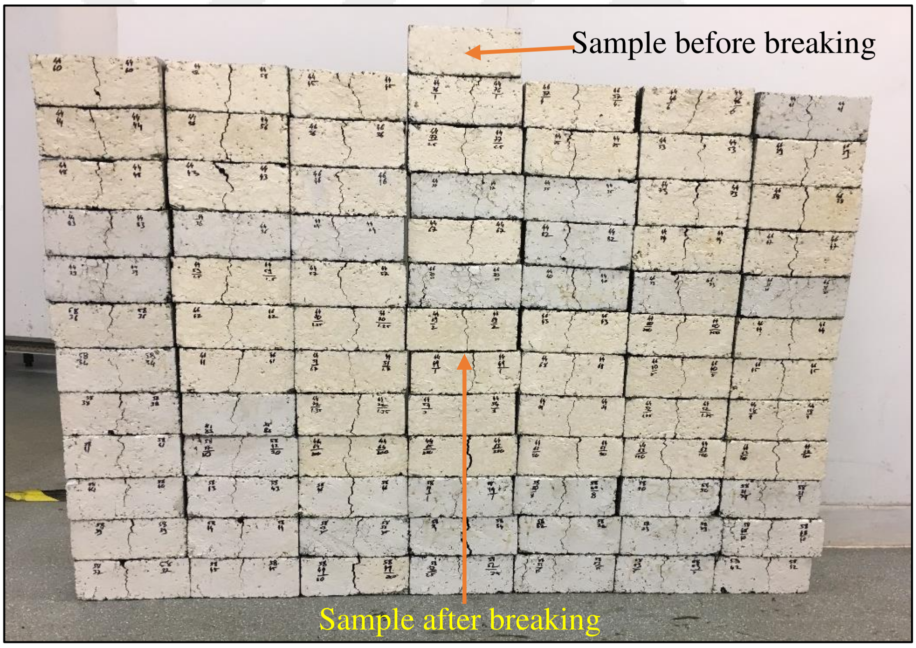

Figure 9.6. 3PB fatigue test samples.

9.6. Results of Rutting Test

In the study, the rutting test was both conducted in a dry environment according to the EN 12697-22 standards and inside water according to the AASHTO T324 standards. Dense graded asphalt samples were tested in the dry environment while the stone mastic asphalt samples were tested inside water. The rutting tests were conducted at 5 different temperatures (20, 30, 40, 50 and 60 ˚C) on mixtures that consisted of a control sample and samples with 3 distinct amounts of capsules (0.5%, 0.75% and 1%). The mixtures were subjected to 20.000 load repetitions in accordance with the standards. The deformation-number of load repetition graph obtained from the rutting test conducted at 60 ˚C in a dry environment was presented as an example in Figure 9.7.

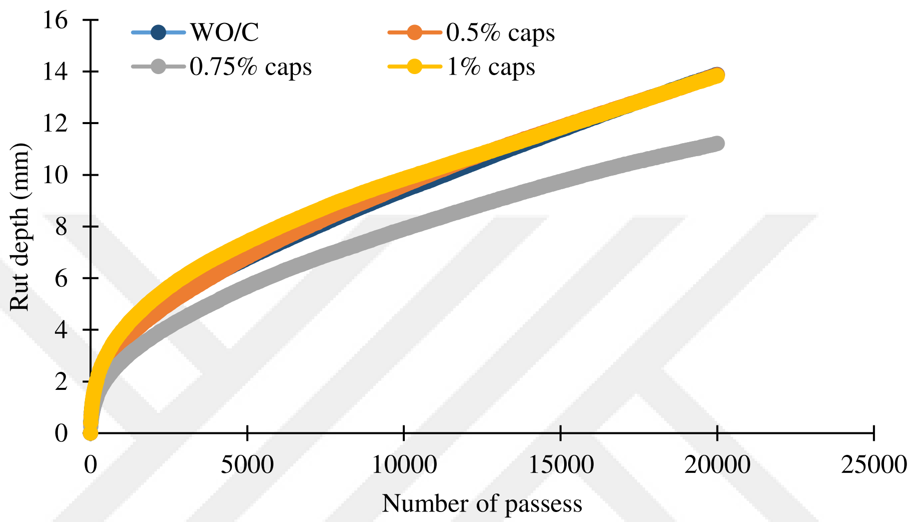

Figure 9.7. The relationship between deformation-number of load repetition obtained from the rutting test conducted at 60 ˚C in a dry environment.

The test results conducted in a dry environment in accordance with the EN 12697-22 standards were presented in Figure 9.8.

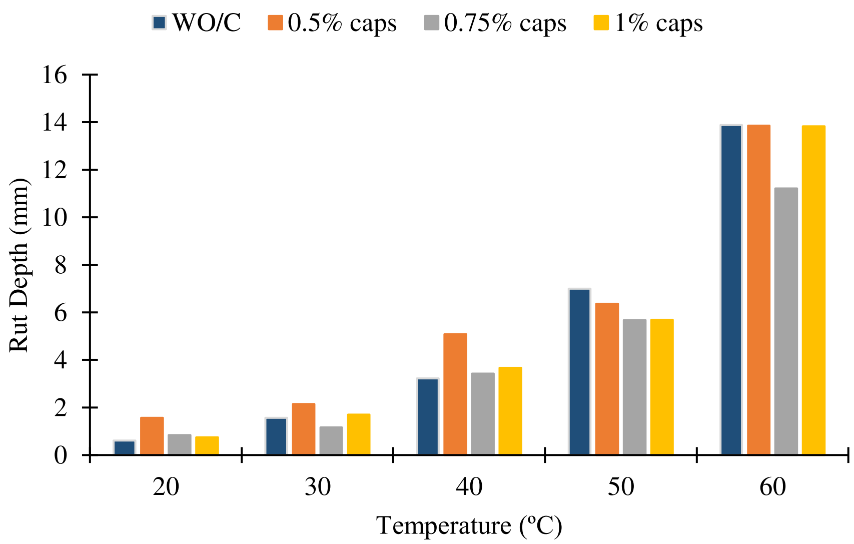

Figure 9.8. Results of the rutting test conducted in a dry environment.

As it can be observed in Figure 9.9, the rutting value increased with the increased temperature as expected. The formation of the rut especially occurred at 60 ˚C. It was determined that the highest rut depth was of the mixture containing 0.5% capsule at 20, 30 and 40 ˚C temperature while the pure mixture had the highest rut depth at 50 ˚C temperature. At 60 ˚C temperature, it was observed that the mixtures containing 0.5% and 1% capsules had similar rut depths. It was also observed that the lowest rut depth was those of pure mixtures at 20 ˚C temperature while the mixtures with 0.75% capsules had the lowest rut depth at 30 and 60 ˚C temperatures. Additionally, the pure mixtures and the mixtures with 0.75% capsules had the lowest rut depth at 40 ˚C while the mixtures with 0.75% and 1% had the lowest mixtures at 50 ˚C temperature. All the mixtures met the test standards and did not reach the 20 mm maximum rut depth following the 20.000 load repetitions. The results of the rutting test conducted on the stone mastic asphalt samples inside water were presented in Figure 9.9.

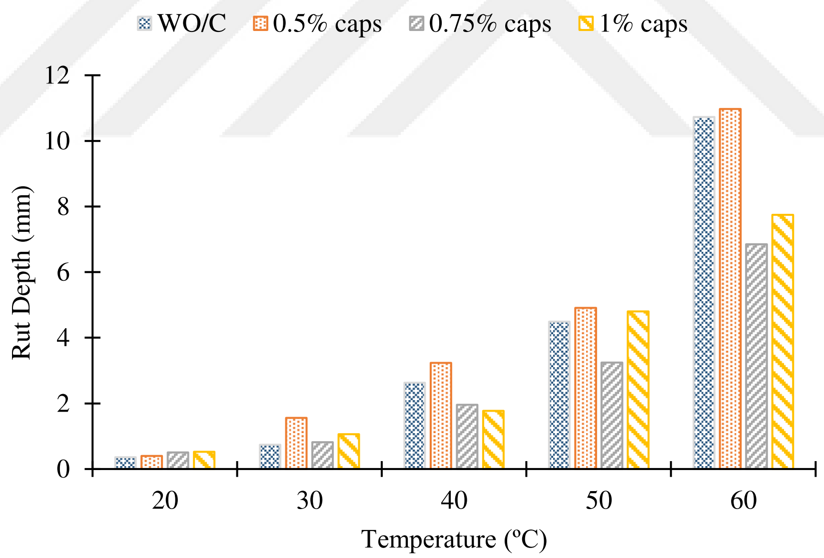

Figure 9.9. The relationship between deformation-number of load repetition obtained from the rutting test conducted at 60 ˚C temperature inside water.

As a result of the rutting test conducted on the stone mastic asphalt mixtures inside water and the examination of the rut depths following the 20.000 load repetition, it was determined that this value increased with increased temperature and the 20 mm maximum value was not exceeded even at the highest temperature, 60 ˚C temperature. It was observed that the rutting values of all mixtures were similar to each other at 20 ˚C temperature. At 30, 40, 50 and 60

˚C temperatures, it was determined that the mixtures containing 0.5% capsules had the highest rutting. At 40, 50 and 60 ˚C temperatures, the lowest rutting was those of mixtures containing 0.75% capsules.

The rutting test implemented in the study was conducted with the aim of determining whether capsule use created a negative effect in terms of rutting formation. As a result of all the tests conducted on different types of mixtures (dense and SMA) , in different conditions(on air/in a dry environment) and in water) , at different temperatures (20, 30, 40, 50 and 60 ˚C) and with different capsule contents (0, 0.5%, 0.75% and 1%), it was determined that none of the mixtures exceed 20 mm rut depth, which is the limit of the standards and there was no significant increase in the rutting formation with increased capsule content.

Figure 9.10 presents the results of the number of broken capsules as a percentage of the total capsules used for asphalt mixtures with 0.5% capsule content and tested at healing different temperature. The results of broken capsules were represented only after wheel tracking tests. Figure 9.10 shows the number of broken capsules as a percentage of the total capsules used for the asphalt mixture samples containing capsules with different oil contents and tested at different temperatures, ranging from 20 to 60 ºC. As seen in Figure 9.10, as the temperature applied to the asphalt mixtures increases, the fracture rate of the capsules found in the asphalt mixtures decreases. The rates of broken capsules in the asphalt mixtures at different temperatures between 20 ºC and 60 ºC vary from 15.75% to 16.53%, 16.24, 15.95, and 12.89%, respectively.

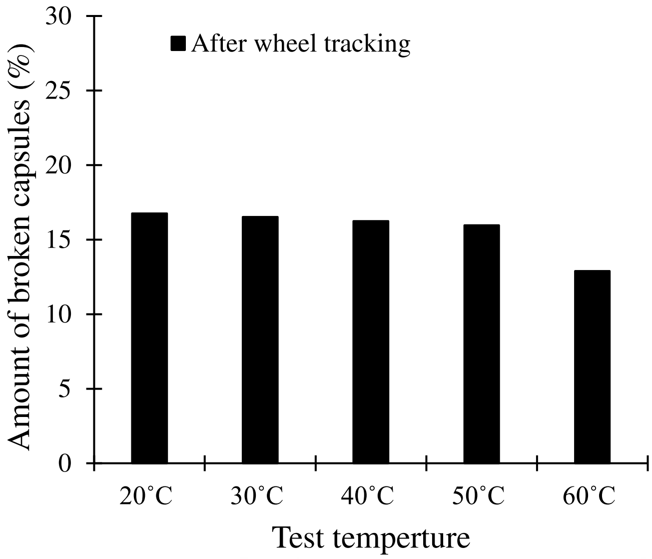

Figure 9.10. Percentage of broken capsules for mixture samples with capsules after wheel tracking tests at different healing temperatures.

Figure 9.11. Samples after wheel tracking test.

10. CONCLUSIONS AND RECOMMENDATIONS

10.1. Conclusion

It was determined that sunflower oil solves the aging problem of bitumen used in the asphalt coating. The sunflower oil used reacts with the bitumen and reduces the bitumen viscosity, leading to the reprocessing of the bitumen by renewing it. The capsules in the asphalt mixtures are broken under load, and the oil within the capsules meet the bitumen surrounding the aggregates to fill the cracks. In this way, small cracks on the roads heal without getting bigger.

This study aims to develop and characterize a self-healing asphalt coating that can recover and rejuvenate at ambient temperatures. One of the different aspects of this study is to produce a capsule containing new type of rejuvenator (sunflower oil). This capsule type has more oil and is easier to produce compared to other capsules. Moreover, the production of this capsule is cheaper, and it does not cause to any health problems. The physical, thermal and mechanical properties of the capsules produced were investigated. These capsules were then added into asphalt mixtures at specific ratios and the durability and mechanical properties of the mixtures with capsules were determined and compared with that of the asphalt mixtures without capsules. These properties have also been studied for two different asphalt mixtures: dense asphalt and SMA. Finally, the effect of capsules containing a new healing agent on the self-healing properties was examined. In this evaluation, the healing of the cracks in the asphalt mixtures containing the capsules was investigated. Different static loads and healing times were applied to determine the most effective healing period and load.

In the following sections, a detailed review of the main findings and conclusions are presented after the in-depth investigation and analysis conducted in this study:

10.1.1. Capsule properties

New capsuled were produced. The healing agent (rejuvenator) used was sunflower oil, encapsulated by ionotropic gelation of sodium alginate in the presence of calcium. Based on the results, the following conclusions have been obtained:

- The encapsulation method used in this study allowed the preparation of capsules with an average diameter of 2.5 mm and composed 1:3 of calcium-alginate polymer/rejuvenator.
- Density and compressive strength of the capsules decreased with the increase of temperature. In addition, thermal stability results proved that the capsules suffered only a minor mass loss, caused by the degradation of calcium-alginate polymer and water evaporation.
- CT-Scan results proved that the distribution of capsules inside the asphalt mixtures was uniform, not affecting their integrity during the asphalt mixture manufacturing.
- Density and compressive strength of the capsules decreased with temperature, not affecting their mechanical resistance to mixing, and compaction processes during the asphalt mixture manufacturing.

10.1.2. Capsules effect on dense asphalt and SMA performance

This result has evaluated the use of calcium-alginate capsules containing rejuvenator (sunflower oil) on the mechanical performance and self-healing ability of dense asphalt and SMA composite mixtures. For that, aging time, physical, mechanical and crack-healing properties of dense asphalt SMA test specimens with, and without, capsules were evaluated using several experimental tests. Based on the results, the following conclusions have been obtained:

- The encapsulation procedure presented in this study allowed the preparation of capsules with an average diameter of 2.5 mm and composed of 75% vol. of sunflower oil and 25% vol. of calcium-alginate polymer. The oil was encapsulated inside a complex microporous structure made of calcium-alginate.
- It was proved that the polymeric capsules can resist the mixing and compaction conditions and break inside the mixture releasing the encapsulated oil in small volumes. Nevertheless, when the capsules are exposed to high temperatures for long pre-heating periods, they can suffer peroxidation of the encapsulated sunflower oil.
- Density and compressive strength of the polymeric capsules decreased with the temperature, not affecting their mechanical resistance to mixing and compaction processes during the asphalt mixture manufacturing.

- It was demonstrated that the 4h-waiting time before compaction at high temperatures can affect the physical properties of the asphalt mixtures with, and without, capsules. This variation was attributed to the order of addition of capsules and to the aging damage of bitumen.
- In addition, it was proved that addition of capsules did not improve the stiffness modulus of asphalt mixtures compared to mixtures without capsules, and that the mixing order and the aging time did not have a significant influence on the flexural strength reached by the asphalt mixtures.
- Moreover, it was observed by X-ray computed tomography tests that the capsules' distribution inside the asphalt mixtures can be considered as uniform, not presenting a negative influence on the mechanical properties evaluated.
- The healing levels obtained by the asphalt mixtures varied depending on the order of addition of the capsules, and mixtures with capsules showed higher healing levels than mixtures without capsules. Besides, the healing levels for the mixtures without aging were greater than those of mixtures after aging process.
- Moreover, the viscosity reduction indices demonstrated that the addition of capsules to aged mixtures can help the bitumen to rejuvenate by between 19.55% and 26.33%, depending on the mixing order.
- Based on the results of the physical, mechanical and self-healing properties of asphalt mixtures containing capsules, the authors recommend adding and mixing the capsules with the hot asphalt mixture at the end of the mixing process, without the need to heat the capsules over 20ºC prior to the mixing process.
- Physical, thermal and mechanical properties of the calcium-alginate capsules manufactured in this study, have allowed the capsules to resist the mixing and compaction processes and to break inside the mixture releasing the encapsulated oil in small volumes.
- In addition, SMA specimens containing calcium-alginate capsules presented similar values of density and air void content to SMA specimens without capsules, which proved that that a capsule content of 0.5% did not adversely affect the physical properties of the SMA mixtures.
- The stiffness modulus, tensile strength and fatigue resistance, and water sensitivity of SMA specimens containing calcium-alginate capsules presented similar results to

SMA without capsules. This result evidenced that a capsule content of 0.5% did not significantly affect the mechanical properties of the SMA mixtures.

- Moreover, it was observed by X-ray computed tomography results that the spatial distribution of the calcium-alginate capsules inside the SMA mixtures can be considered as uniform, not presenting a negative influence on the physical and mechanical properties evaluated.
- SMA beams containing calcium-alginate capsules reached higher crack-healing levels than SMA beams without capsules for all the healing times studied, from 5 to 216 h. This result proved that the encapsulated oil released from capsules to bitumen improved the natural self-healing properties of the SMA mixtures. Hence, the healing level results directly depended on the percentage of broken capsules inside the mixtures.
- Finally, the oil released by the capsules did not produce risk of skid on the surface of the SMA mixtures, compared with SMA mixtures without capsules, which is a guarantee for its installation in real conditions.

10.1.3. Effect of the capsule on static loads

The effect of asphalt mixtures with capsules on self-healing properties under different static loads was investigated. Based on the results, the following conclusions have been obtained:

- As the load applied on the asphalt samples with capsules increases, the level of healing increases. It appears that the level of healing of the asphalt samples with capsules remained stable afterwards. Based on the results obtained, it was determined that the maximum level of healing was generally reached at 96 hours, which remained constant for up to 216 hours.
- As the load applied to the tested asphalt mixture samples increases, a linear increase is seen in the rate of healing. The healing rate of the mixtures with capsules was determined to be higher than that of the samples without capsules.
- As the static load and the healing time increases, there is no significant increase in the FER value. As the static load applied to the asphalt mixtures increases, the FER value increases. However, the healing time increases about 48 h and then decreases down to 216h.

- As the static load applied to the asphalt mixtures increases, the rate of fracture of the capsules in asphalt mixtures increases. The maximum healing rate increases as the ratio of broken capsules increases. This proves the theory of healing. As the static load applied to the asphalt mixtures increases, both the maximum healing rate and the percentage of fractures of the capsules in the asphalt mixtures increase.

10.1.4. The effect of the capsule on fatigue and wheel tracing experiments

This results has evaluated the use of calcium-alginate capsules containing sunflower oil on the self-healing capacity of dense asphalt mixtures by means of fatigue tests at different loading levels and number of cycles. In addition, fracture healing and wheel tracking test results were evaluated in capsules at different ratios. Based on the results, the following conclusions have been obtained:

- Capsules resisted the mixture manufacturing and, consequently, they can keep their oil content until they break inside the asphalt mixture beams under the effect of loading. Additionally, capsules showed a good spatial distribution inside the mixture.
- Healing levels in the asphalt mixtures with capsules were greater than in mixtures without capsules, and healing levels of asphalt samples with, and without, capsules increased with the healing time until a maximum value where the healing levels remained constant.
- Higher capsule contents in the mixture resulted in higher healing levels for all the healing times studied. Finally, a capsule content of 0.5% by total mass of asphalt mixture was considered as the optimal percentage for asphalt self-healing without affecting the properties of the mixture.
- FTIR absorbance index results proved that the rejuvenator concentration inside the bitumen samples increased with the time and the temperature until the moment when the concentration reaches a maximum value that is independent of temperature. This result was interpreted as the point where the bitumen is almost saturated of rejuvenating agent and hence a steady-state condition was reached.
- Fatigue healing results of asphalt mixture beams with capsules proved that: 1) the number of cycles necessary to reach a given percentage of broken capsules reduced when the applied load increased, 2) for the evaluated fatigue loading levels (from 1.75 to 4.75kN), the results of healing index presented an optimum number of cycles

to apply the resting period, at which the obtained life extension was maximum, and 3) this optimum number of cycles to apply the healing treatment decreased when the load increased but it was always between 50%-60% of the number of cycles whose probability of breaking the material is 0.5.

- CT-Scan results proved that the microstructure of the capsules corresponds to that of a microbead, where the rejuvenating agent can be encapsulated in small volumes inside of calcium-alginate micropores. In addition, CT-Scans reconstructions have shown that the capsules can successfully resist the mixing and compaction process of the asphalt mixtures.
- As the temperature increased, the wheel tracking values increased. It was determined that the mixture containing 0.5% capsule had the highest wheel tracking depth and the pure mixture had it at 50˚C.
- As a result of the applied tests applied on different mixtures (dense and SMA), different conditions (in air and water), different temperatures (20, 30, 40, 50 and 60° C), and mixtures with different capsule contents (0, 0.5%, 0.75% and 1%), no mixture exceeded the specification limit of 20 mm and the increase in capsule content did not lead to a significant increase in wheel tracking formation.

10.2. Recommendations for future research

This section presents suggestions for jobs that are not included in the present study due to lack of time and resources. These recommendations are important for a better understanding of the use of capsules in asphalt self-healing to accurately estimate their performances and take them to further levels.

- The size of capsules produced in this study is between 2-5 mm. It is recommended to produce small size capsules for a better capsule distribution and performance in asphalt mixtures.
- The capsules produced may break during mixing or compaction of asphalt mixtures. A variety of materials can be used to minimize this. The substances found can be used at various rates instead of calcium-alginate. The purpose is to have optimum mechanical properties of the produced capsules and minimize the breaking of the capsules during the mixing and compaction procedures.

- Attention should be paid to storage of the capsules produced at room temperature. Capsules produced at room temperature are very likely to become unusable. This effect can be studied. The storage life of the capsules should be studied.
- Self-healing times of asphalt mixtures with capsules should be investigated. Because capsules heal a crack in the asphalt mixture and cannot heal a second crack in the same area. The broken capsule can only heal the crack in an asphalt mixture once. Therefore, the effect of self-healing of capsules in asphalt mixtures should be investigated.
- A future goal might be to investigate the maximum width of a crack that can be cured by the effect of capsules in an asphalt coating. CT cracks can be investigated by measuring different crack widths and assessing the healing levels of these cracks. It may be necessary to examine the breaking of capsules and the rejuvenator released. This is important to investigate how the mechanism is affected by the capsules and crack properties.
- Asphalt mixtures should also be subjected to tests other than mechanical tests and the results should be compared. The mechanical tests such as 4 Pb or 2Pb can be applied.
- The characteristics of the asphalt mixtures with capsules should be investigated on a road that is exposed to continuous traffic. Because laboratory studies are conducted under any load during rest periods. But in real roads, asphalt mixtures are exposed to loads during rest periods. Therefore, it is necessary to examine the effect of these loads on the self-healing by applying different loads to asphalt mixtures with capsules during the rest period.
- The aim of this research was to produce a self-healing asphalt pavement by using the capsules and this objective has almost been accomplished within this study. However, further economic investigation is highly recommended for future studies to ensure the feasibility of capsules as a significant replacement for normal pavement maintenance. The economic study can include the life cycle assessment and fatigue life of asphalt pavement with and without capsules.

REFERENCES

1. **OECD,** 2013. Road traffic, vehicles and networks, In: Environment at a glance 2013: OECD indicators. OECD, Paris.

2. **European Union Road Federation,** 2012. European road statistics, European Union Road Federation (ERF), Brussels.

3. **Janoo, V.C. and Korhonen, C.,** 1999. Performance Testing of Hot-Mix Asphalt Aggregates, US Army Corps of Engineering Project, 99-20.

4. **Roque, R., Birgisson, B., Drakos, C. and Sholar, G.,** 2005. Guidelines for Use of Modified Binders, Florida Department of Transportation Project, 4910-4504-964-12.

5. **White, S.R., Sottos, N.R., Geubelle, P.H., Moore, J.S., Kessler, M.R., Sriram, S.R., Brown, E.N. and Viswanathan, S.,** 2001. Autonomic healing of polymer composites. Nature 409, 794-797.

6. **Fisher, H.,** 2010. Self repairing materials— a dream or a reality, Natural Science 2(8), 873–901.

7. **Amir, E., Schlangen, E.,** 2015. Self-Healing Technology for Asphalt Pavements. Advanced Polymer Science, DOI: 10.1007/12_2015_335.

8. **Little, D.N. and Bhasin, A.,** 2007. Exploring mechanisms of healing in asphalt mixtures and quantifying its impact, Self Healing Materials an Alternative Approach to 20 Centuries of Materials Science, Springer Series in Materials Science 100, 205-218.

9. **Bhasin, A., Little, D.N., Bommavaram, R. and Vasconcelos, K.L**., 2008. A framework to quantify the effect of healing in bituminous materials using material properties, International Journal of Road Materials and Pavement Design 8, 219–242.

10. **Self healing materials,** 2010. Concept and applications, NL Agency, Publication 3ISHM1001.

11. **Van der Zwaag, S.,** 2007. Self healing materials: an alternative approach to 20 centuries of materials science, Dordrecht, Springer Verlag.

12. **Craven, J.M.,** 1966. Cross linked thermally reversible polymers produced from condensation poly-mers with pendant furan groups cross-linked with maleimides, US patent 3,3435,003.

13. **Yalcin, E., Norambuena-Contreras, J., Garcia, A. and Yılmaz, M.,** 2018. Self-healing methods used in asphalt mixtures, 20th International Conference on Pavement Engineering, Paris, France, March 1219-1225.

14. **Francken,** L., 1979. Fatigue performance of a bituminous road mix under realistic best conditions. Transportation Research Record, 712:30-4.

15. **Van Dijk, W., Moreaud, H., Quedeville, A., and Uge, P.,** 1972. The fatigue of bitumen and bituminous mixes. 3rd int. Conference on the Structural Design of Asphalt Pavements. Ann Arbor, Michigan, USA.

16. **Hager, M. D., Greil, P., Leyens, C., Van Der Zwaag, S. and Schubert, U.S.,** 2010. Self-Healing Materials, Advanced Materials, 22**,** 5424-5430.

17. **Bazin, P. and Saunier, J., 1967**. Deformability, fatigue and healing properties of asphalt mixes. Intl Conf Struct Design Asphalt Pvmts.

18. **Raithby, K.D. and Sterling, A.B.,** 1970. The effect of rest periods on the fatigue performance of a hot-rolled asphalt under repeated loading. Journal of Association of Asphalt Paving Technologists, 39:134-52.

19. **Garcia, A., Bueno, M., Norambuena-Contreras, J. and Partl, M.N., 2013.** Induction healing of dense asphalt concrete, Construction and Building Materials, 49**,** 1-7.

20. **Boyer, R.E.,** 2000. Asphalt Rejuvenators Fact, or Fable, Transportation Systems 2000 (TS2K) Workshop San Antonio, Texas.

21. **Chiu, C. and Lee, M.,** 2006. Effectiveness of seal rejuvenators for bituminous pavement surfaces, Journal of Testing and Evaluation, 34**,** 390.

22. **Liu, Q.,** 2012. Induction healing of porous asphalt concrete. Ph.D. thesis, Faculty of Civil Engineering and Geosciences, TU Delft, Netherlands.

23. **Garcia, A., Schlangen, E., Van De Ven, M. and Van Liet, D.,** 2011c. Induction heating of mastic containing conductive fibres and fillers, Materials and structures, 44**,** 499-508.

24. **Minsk, L.D.,** 1968. Electrically conductive asphalt for control of snow and ice accumulation, Transportation Research Board, 227:57–63.

25. **Garcia, A., Schlangen, E., Van De Ven, M. and Liu, Q., 2012a**. A simple model to define induction heating in asphalt mastic, Construction and Building Materials, 31, 38-46.

26. **Garcia, A., Schlangen, E., Van De Ven, M. and Van Vliet, D.,** 2011b. Crack repair of asphalt concrete with induction energy, Heron, 56, 33-43.

27. **Liu, Q., Yu, W., Schlangen, E., Bochove, G.,** 2014. Unravelling porous asphalt concrete with induction heating, Construction and Building Materials, 71, 152-157.

28. **Obaidi, H., Gomez-Meijide, B. and Garcia, A.,** 2017. A fast pothole repair method using asphalt tiles and induction heating, Construction and Building Materials, 131, 592-599.

29. **Liu, Q., Wu, S. and Schlangen, E.,** 2013. Induction heating of asphalt mastic for crack control, Construction and Building Materials, 41, 345-351.

30. **Su, J.F., Schlangen E. and Qiu J.,** 2013. Design and construction of microcapsules containing rejuvenator for asphalt, Powder Technology, 235, 563–571.

31. **Gomez-Meijide, B., Ajam, H., Lastra-Gonzalez, P. and Garcia, A.,** 2016. Effect of air voids content on asphalt self-healing via induction and infrared heating, Construction and Building Materials, 126, 957-966.

32. **Garcia, A., Schlangen, E., Ven, M. and Vliet, D., 2011.** Crack repair of asphalt concrete with induction energy, Delft University of Technology, 56, 264-272.

33. **Garcia A., Schlangen E., Ven M. and Bochove G.,** 2012. Optimization of composition and mixing process of a self-healing porous asphalt, Construction and Building Materials, 30, 59–65.

34. **Liu, Q., Schlangen, E., Ven M., Bochove, G. and Montfort, J.,** 2012. Evaluation of the induction healing effect of porous asphalt concrete through four point bending fatigue test, Construction and Building Materials, 29, 403–409.

35. **Menozzi, A., Garcia, G., Partl, M. N.,Tebaldi, G. and Schuetz, P.,** 2015. Induction healing of fatigue damage in asphalt test samples, Construction and Building Materials, 74, 162–168.

36. **Liu, Q., Schlangen, E., Garcia, A. and van de Ven, M.,** 2010. Induction heating of electrically conductive porous asphalt concrete, Construction and Building Materials 24:1207–1213.

37. **Wu, S., Zhang, Y. and Chen, M**., 2010. Research on mechanical characteristics of conductive asphalt concrete by indirect tensile test, In: Proceedings of the 4th international conference on experimental mechanics, Proc. SPIE 7522: 752265. doi:10.1117/12.851473.

38. **Liu, X. and Wu, S**., 2011. Study on the graphite and carbon fiber modified asphalt concrete, Construction and Building Materials 25(4):1807–1811.

39. **Belanger, J.M.R., Paré, J.R.J., Poon, O., Fairbridge, C., Ng, S. and Mutyala, S.,** 2008. Remarks on various applications of microwave energy, The Journal of Microwave Power and Electromagnetic Energy 4:24–44.

40. **Hill, J.M. and Marchant, T.R.,** 1996. Modelling microwave heating, Applied Mathematical Modelling 20:3–15.

41. **Castaneda, N.F., Santos Rojas, J.K. and Carreno Cabra, D**., 2007. Utilizacion Del Secado Con Horno Microondas Para La Caracterizacion De Suelos Finos En Bogotà. Revista Epsilon, Università di La Salle Bogotá, Colombia 9. p. 129–40.

42. **Hagerty, D.J., Ullrich, C.R. and Denton, M.M.,** 1990. Microwave drying of soils. Geotechnical Testing Journal 13:138–41.

43. **Gallego, J., del Val Miguel, A., Contreras, V. and Paez, A.,** 2013. Heating asphalt concrete with microwaves to promote self-healing, Construction and Building Materials 42: 1–4.

44. **Benedetto, A. and Calvi, A.,** 2013. A pilot study on microwave heating for production and recycling of road pavement materials, Construction and Building Materials 44, 351-359.

45. **Yihan, S., Quantao, L., Shaopeng, W.U. and Fei, S.,** 2014. Microwave Heating of Steel Slag Asphalt Mixture, Key Engineering Material, 599, 193-197.

46. **Norambuena-Contreras, J., Serpell, R., Valdés Vidal, G., González, A. and Schlangen, E.,** 2016. Effect of fibres addition on the physical and mechanical properties of asphalt mixtures with crack-healing purposes by microwave radiation, Construction and Building Materials, 127: 369-382.

47. **Norambuena-Contreras, J. and Garcia, A.,** 2016. Self-healing of asphalt mixture by microwave and induction heating, Materials and Design, 106, 404-414.

48. **Norambuena-Contreras, J. and Gonzalez-Torre, I.,** 2017. Influence of the Microwave Heating Time on the Self-Healing Properties of Asphalt Mixtures, Applied Sciences, 7, 1076.

49. **Gallego, J., Val, M. A., Contrera,s V. and Paez, A.,** 2013. Heating asphalt mixtures with microwaves to promote self-healing, Construction and Building Materials, 42, 1–4.

50. **Karimi, M.M., Quantao, L., Shaopeng, W. and Fei, S.,** 2018. Induced heating-healing characterization of activated carbon modified asphalt concrete under microwave radiation, Construction and Building Materials, 178, 254–271

51. **Gonz_alez, A.,** Jahanbakhsh**, H.,** Jahangiri **B. and** Nejad**, F.M.,** 2018. Self-healing properties of recycled asphalt mixtures containing metal waste: An approach through microwave radiation heating, Journal of Environmental Management, 214, 242-251.

52. **Tabakovic´A. and Schlangen, E.,** 2015. Self-Healing Technology for Asphalt Pavements, Self-healing Materials, 285-306.

53. **Garcia, A., Schlangen, E., Van De Ven, M. and Sierra-Beltran, G.,** 2010b. Preparation of capsules containing rejuvenators for their use in asphalt concrete, Journal of Hazardous Materials, 184, 603-611.

54. **Garcia, A., Jelfs, J. and Austin, C.J.,** 2015. Internal asphalt mixture rejuvenation using capsules, Construction and Building Materials, 101, 309-316.

55. **Su, J. and Schlangen, E.,** 2012. Synthesis and physicochemical properties of high compact microcapsules containing rejuvenator applied in asphalt, Chemical Engineering Journal, 198, 289-300.

56. **Su, J., Qiu, J. and Schlangen, H**., 2013c. Self-healing bitumen by microcapsules containing rejuvenator, ICSHM 2013: Proceedings of the 4th International Conference on Self-Healing Materials, Ghent, Belgium, June 16-20, Ghent University; Delft University of Technology.

57. **Su, J.-F., Qiu, J., Schlangen, E. and Wang, Y.,** 2014. Experimental investigation of self-healing behaviour of bitumen/microcapsule composites by a modified beam on elastic foundation method. Materials and Structures, 1-10.

58. **Su, J., Qiu, J. and Schlangen, E.,** 2013a. Stability investigation of self-healing microcapsules containing rejuvenator for bitumen. Polymer Degradation and Stability, 98, 1205-1215.

59. **Garcia, A., Schlangen, E. and Ven, M.,** 2011. Properties of capsules containing rejuvenators for their use in asphalt concrete, Fuel, 90, 583–591.

60. **Qiu, J., Ven M., Wu, S., Yu, J. and Molenaar, A., 2011**. Evaluating Self Healing Capability of Bituminous Mastics, Experimental Mechanics, 52. 1163-1171.

61. **Asli, H., Ahmadinia, E., Zargar, M. and Karim, M.R.,** 2012. Investigation on physical properties of waste cooking oil – Rejuvenated bitumen binder, Construction and Building Materials, 37, 398–405

62. **Garcia A.,** 2012. Self-healing of open cracks in asphalt mastic, Fuel, 93, 264–272.

63. **Su, J.F., Wang, X.Y. and Dong, H.,** 2012. Micromechanical properties of melamine–formaldehyde microcapsules by nanoindentation: Effect of size and shell thickness, Materials Letters, 89, 1–4.

64. **Li, R., Zhou, T. and Pei, J**., 2015. Design, preparation and properties of microcapsules containing rejuvenator for asphalt, Construction and Building Materials, 99, 143–149.

65. **Chung, K., Lee, S., Park, M., Yoo, P. and Hong, Y.,** 2015. Preparation and characterization of microcapsule-containing self-healing asphalt, Journal of Industrial and Engineering Chemistry, 29, 330–337.

66. **Su, J.F., Qui, J., Schlangen, E. and Wang, Y.Y.,** 2015a. Investigation the possibility of a new approach of using microcapsules containing waste cooking oil: In situ rejuvenation for aged bitumen, Construction and Building Materials, 74, 83-92.

67. **Su, J.F., Schlangen, E. and Wang, Y.Y.,** 2015b. Investigation the self-healing mechanism of aged bitumen using microcapsules containing rejuvenator, Construction and Building Materials, 85, 49-56.

68. **Garcia, A., Austin, C. J. and Jelf, J.,** 2016. Mechanical properties of asphalt mixture containing sunflower oil capsules, Journal of Cleaner Production, 118, 124-132.

69. **Micaelo, R., Al-Mansoori, T. and Garcia,** A., 2016. Study of the mechanical properties and self-healing ability of asphalt mixture containing calcium-alginate capsules, Construction and Building Materials, 123, 734–744.

70. **Gray, A., Egan, S., Bakalis, S. and Zhang, Z.,** 2016. Determination of microcapsule physicochemical, structural, and mechanical properties , Particuology, 24, 32–43.

71. **Shirzad, S., Hassan, M.M., Aguirre, M.A., Mohammad, L.N., and Daly, W.H.,** 2016. Evaluation of Sunflower Oil as a Rejuvenator and Its Microencapsulation as a Healing Agent, Journal of Materials in Civil Engineering, 28(11): 04016116.

72. **Su, J.F., Yang, P., Wang, Y.Y., Han, H., Han, N.X. and Li W.,** 2016. Investigation of the Self-Healing Behaviors of Microcapsules/Bitumen Composites by a Repetitive Direct Tension Test , Materials, 9, 600; doi:10.3390/ma9070600.

73. **Aguirre, M.A., Hassan, M.M., Shirzad, S., Daly, V.H. and Mohammad, L.N.,** 2016. Micro-encapsulation of asphalt rejuvenators using melamine-formaldehyde, Construction and Building Materials, 114, 29–39.

74. **Lv, L., Schlangen, E., Yang, Z. and Xing, F.,** 2016. Micromechanical Properties of a New Polymeric Microcapsule for Self-Healing Cementitious Materials, Materials, 9, 1025; doi:10.3390/ma9121025.

75. **Wang, Y.Y., Su, J.F., Schlangen, E., Han, N.X., Han, H. and Li W.,** 2016. Fabrication and characterization of self-healing microcapsules containing bituminous rejuvenator by a nano-inorganic/organic hybrid method, Construction and Building Materials 121, 471–482.

76. **Su, J.F., Wang, Y.Y., Han, N.X., Yang, P. and Han, S.,** 2016. Experimental investigation and mechanism analysis of novel multi-self-healing behaviors of bitumen using microcapsules containing rejuvenator, Construction and Building Materials 106, 317–329.

77. **Lv, L., Yang, Z., Chen, G., Zhu, G., Han, N., Schlangen, E. and Xing F.,** 2016. Synthesis and characterization of a new polymeric microcapsule and feasibility investigation in self-healing cementitious materials, Construction and Building Materials 105, 487–495.

78. **Al-Mansoori, T., Micaelo, R., Artamendi, L., Norambuena-Contreras, J. and Garcia A.,** 2017. Microcapsules for self-healing of asphalt mixture without compromisi mechanical performance, Construction and Building Materials 155, 1091–1100.

79. **Xue, B., Wang, H., Pei, J., Li, R., Zhang, J. and Fan, Z.,** 2017. Study on self-healing microcapsule containing rejuvenator for asphalt , Construction and Building Materials, 135, 641–649.

80. **Su, J.F., Han, S., Wang, Y.Y., Schlangen, E., Han, N.X., Liu, B., Hang, X.L., Yang P. and Li, W.,** 2017. Experimental observation of the self-healing microcapsules containing rejuvenator states in asphalt binder, Construction and Building Materials 147, 533–542.

81. **Aguirre, M.A., Hassan, M.M., Shirzad, S., Mohammad, L.N., Cooper, S. and** Negulescu, L.L., 2017. Laboratory Testing of Self-Healing Microcapsules in Asphalt Mixtures Prepared with Recycled Asphalt Shingles, Journal of Materials in Civil Engineering29(9): 04017099.

82. **Sun, D., Li, B., Ye, F., Zhu, X., Lu, T. and Tian, Y.,** 2018. Fatigue behavior of microcapsule-induced self-healing asphalt concrete, Journal of Cleaner Production 188, 466e476.

83. **Sun, D., Lu, T., Zhu, X., Li, B. and Tian, Y.,** 2018. Optimization of synthesis technology to improve the design of asphalt self-healing microcapsules, Construction and Building Materials 175, 88–103.

84. **Al-Mansoori, T., Norambuena-Contreras, J. and Garcia, A.,** 2018. Effect of capsule addition and healing temperature on the self-healing potential of asphalt mixtures, Materials and Structures, 51:53.

85. **Al-Mansoori, T., Norambuena-Contreras, J., Micaelor, R. and Garcia, A.,** 2018. Self-healing of asphalt mastic by the action of polymeric capsules containing rejuvenators, Construction and Building Materials 161, 330–339.

86. **BSI, BS EN 13108-1,** 2016. Bituminous mixtures — Material specifications Part 1: Asphalt Concrete, British Standard Institute (BSI), 2016.

87. **BSI, BS EN 13108-5,** 2016. Bituminous mixtures — Material specifications Part 5: Stone Mastic Asphalt, British Standard Institute (BSI), 2016.

88. **Usama H.,** 2018. Effect of the repeated recycling on hot mix asphalt properties , PhD thesis, University of Nottingham, NOTTİNGHAM.

89. **Zargar, M, Ahmadinia, E, Asli, H. and Karim, M.R.,** 2012. Investigation of the possibility of using waste cooking oil as a rejuvenating agent for aged bitumen, Journal of Hazardous Materials, 233-234:254-258.

90. **Mookhoek, S.D., Fischer, H.R. and Van der Zwaag S.,** 2012. Alginate fibres containing discrete liquid filled vacuoles for controlled delivery of healing agents in fibre reinforced composites, Composites Part A Applied Science, 43(12):2176-2182.

91. **Thu, B., Bruheim, P., Espevik, T., Smidsrod, O., Soon-Shiong, P. and Skjak-Braek, G.,** 1996. Alginate polycation microcapsules: I. Interaction between alginate and polycation, Biomaterials, 17, 1031-1040.

92. **Peniche, C., Howland, I., Carrillo, O., Zaldivar, C. and Arguelles-Monal, W.,** 2004. Formation and stability of shark liver oil loaded chitosan/calcium alginate capsules, Food Hydrocolloids, 18, 865-871.

93. **Sengöz, B.,** 2003. Asfalt Film Kalınlığının Bitümlü Karısımların Yaşlanmasına ve Suya Duyarlılığına Etkisi, Doktora Tezi, İTÜ, Fen Bilimleri Enstitüsü, İstanbul.

94. **Whiteoak, D. and Read, J.,** 2003. The Shell Bitumen Handbook, London, Thomas Telford Ltd., 464 p.

95. **Vallerga, B.A.,** 1981. Pavement Deficiencies Related to Asphalt Durability, Proceedings, Association of Asphalt Paving Technologists, 50, 481-491.

96. **Traxler, R.N.,** 1963. Durability of Asphalt Cements, Proceedings, Association of Asphalt Paving Technologists, 32, 44-58.

97. **Bell, C.A. and Sosnovske, D.,** 1994. Aging: Binder Validation, Strategic Highway Research Program, SHRP-A-384, National Research Council, Washington D.C.

98. **Bell, C.A., Wahab, A.Y., Cristi, M.E. and Sosnovske, D.,** 1994(a). Selection of Laboratory Aging Procedures for Asphalt-Aggregate Mixtures, Strategic Highway Research Program, SHRP-A-383, National Research Council, Washington D.C.

99. **Bell, C.A., Wieder, J.A. and Fellin, J.M.,** 1994(b). Laboratory Aging of Asphalt-Aggregate Mixtures, Strategic Highway Research Program, SHRP-A-390, National Research Council, Washington D.C.

100. **Harigan, E.T., Leahy, R.B. and Youtcheff, J.S.,** 1994. The Superpave Mix Design System Manual of Specifications, Test Methods, and Practices, Strategic HighwayResearch Program, SHRP-A-379, National Research Council, Washington D.C.

101. **Dow, A.W.,** 1903. Asphalt Experiments at Washington, Engineering News Record, 47, 18-25.

102. **Juan, J. and Xiaoning, Z.,** 2005. Modification of the Rolling Thin Film Oven Test for Modified Asphalt, Proceedings of the 24th Southern African Transport Conference (SATC 2005), Pretoria, South Africa, July 11-13, 979-986.

103. **Raghavendra, S., Zapata, C.E., Houston, M.W.N., Witczak, M. and Mirza, M.W.,** 2006. Verification of the Rate of Asphalt Mix Aging Simulated by AASHTO PP2-99 Protocol, Seventh International Congress on Advances in Civil Engineering, Istanbul, Turkey, October, 11-13, 10 p.

104. Marsac, P., Pierard, N., Porot, L., Grenfell, J., Mouillet, V., Pouget, S., Besamusca, J., Farcas, F., Gabet, T. and Hugener, M., 2014 Potential and limits of FTIR methods for reclaimed asphalt characterisation, Materials and Structures, 47:1273-1286.

105. Liang, P., Want,.H., Chen, C., Ge, F., Liu, D., Li, S., Han, B., Xiong, X. and Zhao, S., 2013. The use of Fourier Transform Infrared Spectroscopy for quantification of adulteration in virgin walnut oil. Journal of Spectroscopy.

106. Kök, B.V., 2007. Bitümlü Sıcak Karışımların Üretiminde Yeni bir Karıştırma Yönteminin Araştırılması, Doktora Tezi, Fırat Üniversitesi, Fen Bilimleri Enstitüsü, Elazığ.

107. Zoorob, S.E. and Suparma, L.B., 2000. Laboratory Design and Investigation of the Properties of Continuously Graded Asphaltic Concrete Containing Recycled Plastics Aggregate Replacement (Plastiphalt), Cement&Concrete Composites, 22, 233-242.

108. BSI, BS EN 12697-26, 2004. Bituminous mixtures - Test methods for hot mix asphalt - Part 26: Stiffness, British Standards Institution, London.

109. Karim H.A., 2015. Foamed bitumen stabilised sandstone aggregates, PhD thesis, University of Nottingham, NOTTİNGHAM.

110. Francken, L., 1998. Bituminous Binders and Mixes, Rilem Reports, E & FN Spon, 352 p. London and New York.

111. Ghile, D.B., 2006. Effects of Nanoclay Modification on Rheology of Bitumen and on Performance of Asphalt Mixtures, MSc Thesis, Delfth University of Technology, Delfth.

112. Molenaar, A.A.A. and Medani, T.O., 2000. Rational Testing Methods for PerformanceBased Specifications, Proceedings of the 1st International Conference World of Asphalt Pavements, Sydney, Australia, July 7-10, 484-500.

113. Simms, S.A., 1998. Use of Coal Fly Ash in Asphalt Concrete Mixes, MSc Thesis, Dalhousie University, Daltech, Canada.

114. BSI, BS DD ABF, 2003. Method for the Determination of the Fatigue Characteristics of Bituminous Mixtures Using Indirect tensile Fatigue, British Standards Institution, London.

115. Chibuzor K.O., 2015. The design and optimisation of cold asphalt emulsion mixtures, PhD thesis, University of Nottingham, Nottingham

116. Vreeker, R., Li, L., Fang, Y., Appelqvist, I. and Mendes, E., 2008. Drying and Rehydration of Calcium Alginate Gels, Food Biophys, 3: 361-369.

117. BSI, BS EN 12697-12, 2008. Bituminous mixtures - Test methods for hot mix asphalt - Part 12: Determination of the water sensitivity of bituminous specimens, British Standards Institution, London.

118. BSI, BS EN 12697-23, 2003. Bituminous Mixtures - Test Methods for Hot Mix Asphalt - Part 23: Determination of the Indirect Tensile Strength of Bituminous Specimens, British Standards Institution, London.

119. BSI, BS EN 12697-32, 2003. Bituminous mixtures — Test methods for hot mix asphalt — Part 32: Laboratory compaction of bituminous mixtures by vibratory compactor, British Standards Institution, London.

120. BSI, BS EN 12697-33, 2003. Bituminous mixtures — Test methods for hot mix asphalt — Part 33: Specimen prepared by roller compactor, British Standards Institution, London.

121. BSI, BS EN12697-22, 2003. Bituminous mixtures — Test methods for hot mix asphalt — Part 22: Wheel tracking, British Standards Institution, London.

122. BSI, BS EN 13036-4, 2011. Road and airfield surface characteristics - Test methods Part 4: Method for measurement of slip/skid resistance of a surface: The pendulum test, British Standards Institution, London.

123. Valdes, G., Calabi, F.A., Miró R.R. and Norambuena-Contreras J., 2015. Mechanical behaviour of asphalt mixtures with different aggregate type, Construction and Building Materials, 101:474-481.

124. Airey, G., 2003. State of the art report on aging test methods for bituminous pavement materials, International Journal of Pavement Engineering, 4(3):165-176.

125. Lu, X. and Isacsson U., 1998. Chemical and rheological evaluation of aging properties of SBS polymer modified bitumens, Fuel, 77(9):961-972.

126. Burningham, S. and Stankevich, N., 2005. Why road maintenance is important and how to get it done, Transport Notes Series; No. TRN 4, World Bank, Washington, DC.

127. Holleran, G., Wieringa, T. and Tailby, T., 2006. Rejuvenation treatments for aged pavements, Transit New Zealand and New Zealand Institute of Highway Technology (NZIHT), 8th Annual Conference, Auckland, New Zealand.

128. Garcia, A., Schlangen E. and Van de Ven, M., 2010. Two ways of closing cracks on asphalt concrete pavements: microcapsules and induction heating, Key Engineering Materials, 417-418:573-576.

129. Ji, J., Yao, H., Suo,. Z, You, Z., Li, H., Xu, S. and Sun, L., 2016.Effectiveness of vegetable oils as rejuvenators for aged asphalt binders, Journal of Materials in Civil Engineering, 29(3).

130. Garcia, A., Norambuena-Contreras, J. and Partl, M.N., 2014. A parametric study on the influence of steel wool fibers in dense asphalt concrete, Materials and Structures, 47(9):1559-1571.

131. **Siriwardhana, N. and Jeon, Y.J.,** 2004 Antioxidative effect of cactus pear fruit (Opuntia ficus-indica) extract on lipid peroxidation inhibition in oils and emulsion model systems, European Food Research Technology, 219(4):369-376.

132. **Wu, S., Xue, Y., Ye, Q. and Chen, Y.,** 2017. Utilization of steel slag as aggregates for stone mastic asphalt (SMA) mixtures, Build Environ, 42(7): 2580-2585.

133. **Woodward, D., Millar, P., Lantieri, C., Sangiorgi, C. and Vignali, V.,** 2016. The wear of Stone Mastic Asphalt due to slow speed high stress simulated laboratory trafficking, Construction and Building Materials, 110: 270-277.

134. **Ahmadinia, E., Zargar, M., Karim, M.R., Abdelaziz, M. and Shafigh, P.,** 2011. Using waste plastic bottles as additive for stone mastic asphalt. Materials and Design, 32(10): 4844-4849.

135. **Vaiana, R., Praticò, F.G., Iuele, T., Gallelli, V. and Minani, V.,** 2013. Effect of asphalt mix properties on surface texture: an experimental study, Applied Mechanics and Materials, 368-370: 1056-1060.

136. **Praticò, F.G. and Vaiana, R.,** 2015. A study on the relationship between mean texture depth and mean profile depth of asphalt pavements, Construction and Building Materials, 101: 72-79.

137. **Yılmaz, M., Kök, B. and Kuloğlu, N.,** 2013. Investigation of mechanical properties of short-term and long-term aged asphaltite modified asphalt mixtures, Journal of Materials in Civil Engineering, 25: 563-572.

138. **Norambuena-Contreras, J. and Gonzalez-Torre, I.,** 2015. Influence of geosynthetic type on retarding cracking in asphalt pavements, Construction and Building Materials, 78: 421-429.

139. **Li, R., Zhou, T. and Pei, J.,** 2015. Design preparation and properties of microcapsules containing rejuvenator for asphalt, Construction and Building Materials, 99: 143-149.

140. **Liu, Q., García, A., Schlangen, E., and van de Ven, M.,** 2011. Induction healing of asphalt mastic and porous asphalt concrete, Construction and Building Materials*, 25(9)*, 3746-3752.

141. **Norambuena-Contreras, J., Yalcin, E., Garcia, A., Al-Mansoori, T., Yilmaz, M., and Hudson-Griffiths, R.,** 2018. Effect of mixing and aging on the mechanical and self-healing properties of asphalt mixtures containing polymeric capsules, Construction and Building Materials, 175, 254-266.

BACKGROUND

Erkut YALÇIN was born in 1989, Elazığ. He finished his primary, secondary and high school educations in Elazığ. He was enrolled in Fırat University, Faculty of Engineering, the Department of Geological Engineering in 2007, graduating from the department in 2011, and also enrolled in Fırat University, Faculty of Engineering, the Department of Civil Engineering in 2009, graduating from the department in 2012. He completed his Master's Degree at Fırat University, Faculty of Engineering, the Department of Geological Engineering, the Field of Applied Geology in 2013. He was enrolled in the Master's Degree in Fırat University, Faculty of Engineering, the Department of Civil Engineering, the Field of Transportation Engineering in 2012, graduating from the department in 2014. He started his PhD education in the same department and conducted his laboratory studies at the University of Nottingham, Nottingham Transportation Engineering Center in 2017. He was appointed to the department of Transportation Engineering of The Faculty of Engineering in Fırat University as a research assistant in 2014 and he still serves there.